This is to certify that the

dissertation entitled

REDUCTION OF PAVEMENT
RUTTING AND FATIGUE CRACKING

presented by

Hamid Mukhtar

has been accepted towards fulfillment
of the requirements for

Doctor of Philosophy degree in Civil Engineering

Gilbert Baladi
Gilbert Baladi
Major professor

Date 11/17/93

REDUCTION OF PAVEMENT RUTTING AND FATIGUE CRACKING

By

Hamid Mukhtar

A DISSERTATION

Submitted to
Michigan State University
in partial fulfillment of the requirements for the degree of

DOCTOR OF PHILOSOPHY

Department of Civil and Environmental Engineering

1993

ABSTRACT

REDUCTION OF RUTTING AND FATIGUE CRACKING

by

Hamid Mukhtar

Flexible pavements are typically designed to provide a good ride quality and to resist rutting and fatigue cracking. The two types of distress are mainly caused by wheel loads and are accelerated by material and environmental factors. Although all the pavement layers (base, subbase and roadbed soil) contribute to rutting and fatigue cracking, the contribution of the asphalt concrete (AC) layer alone could be very significant.

The pavement network in the State of Michigan is experiencing premature rutting and fatigue cracking problems. The main objective of this study is to identify the AC mix factors that affect pavement rutting and fatigue cracking.

Based on predetermined priority factors, forty-nine flexible and fifteen composite pavement sections were selected from a large pool of pavements. For each selected pavement section, rut and fatigue cracking measurements were made and for 13 sections, full depth pavement cores were obtained. The cores were subjected to various laboratory tests and the resilient, plastic, and fatigue life characteristics of the asphalt-aggregate mixes were determined.

A multivariate regression analysis were performed to determine the relationship of rut depth and laboratory fatigue life to the AC mix properties. The results showed that high percent content of coarse angular aggregates (crushed on 3 or 4 sides), air voids contents between 4 to 6 percent, and low amount of fine content can provide significant improvement in the rut and fatigue cracking resistance of the AC mixes.

Based on the analysis, shift factors between the fatigue lives of asphalt pavements and the laboratory fatigue lives of the AC cores were developed and verified. Finally, changes are recommended in the existing asphalt mix design and manufacturing processes in the State of Michigan to reduce pavement rutting and fatigue cracking potential.

To my wife, children, parents, sister and brothers and to all peace loving humans.

ACKNOWLEDGEMENT

Thanks to Allah Almighty for providing me with the opportunity to undertake and complete this task. The writer wishes to express his appreciation to his major professor, Dr. Gilbert Y. Baladi for his constant guidance and encouragement during the research. Thanks also to members of the writer's doctoral committee:

Dr. W.C.Taylor, Professor;

Dr. R.S. Harichandran, Associate Professor; and

Dr. R.V. Erickson, Professor.

Thanks are also extended to the Pakistan Military Engineering Services for partly sponsoring my study program and to the Michigan Department of Transportation and the University of Michigan Transportation Research Institute for sponsoring this study. Thanks to the Technical Advisory Committee for this project from Michigan Department of Transportation, including Dave Smiley, Jack DeFoe, Jerry Sweeny, and Ishvarlal Patel, also deserve special thanks for their guidance and comments. The dedicated effort of Kurt Bancroft in conducting the falling weight deflection tests and supervising coring operation is also recognized and appreciated. Help and guidance provided by Leo Defrain in programming is also appreciated.

Efforts of S. Stuart, Bill E., Guy N., John A., Erich T., and others in data acquisition and reduction is appreciated.

TABLE OF CONTENTS

APPENDICES

LIST OF TABLES

LIST OF FIGURES

CHAPTER 1

INTRODUCTION

1.1 GENERAL

The structural design of flexible highway pavements and bituminous overlays has been an evolutionary processes based primarily on the experience and judgement of highway engineers, expanded by empirical relationships developed through research and field observations. The proper design of asphalt concrete pavements and asphalt overlays requires the consideration of several complex and interrelated factors. Recent efforts considering the interaction of these factors have resulted in the development of rational new design models using the elastic and visco-elastic theories. Today, design methods for flexible pavements and bituminous overlays could be divided into two groups: empirical approaches, and mechanistic-empirical approaches. The main design considerations in both groups are to limit the compressive strains induced at the top of the subgrade to control permanent deformation (roadbed rutting), and to limit the tensile strain induced at the bottom of the asphalt layer to minimize fatigue cracking. Both approaches have their advantages and disadvantages. Empirical procedures are relatively easy to use, are mainly derived from experience (they lack theoretical background), and are often custom designed, thus, limiting their applications. Mechanistic-empirical design approaches are based and supported by theory. However, they are unable to model the interaction of different factors (e,g., environmental, drainage etc.) which cause pavement distress.

Rutting of flexible pavements and bituminous overlays is defined as accumulation of permanent deformation in the wheel path whereas, fatigue cracks are load induced cracks that can be found in both wheel paths and are accelerated by environmental factors. Both rutting and fatigue cracking are load related distresses. Rutting and fatigue cracking potentials are affected by traffic volume and load, material properties, construction quality, layer thicknesses, and the environment. Therefore, any methodology solely based on empirical or mechanistic approach, will fail to model the pavement behavior efficiently.

1.2 PROBLEM STATEMENT

A good portion of the pavement network in the State of Michigan is experiencing premature rutting and fatigue cracking problem. The two types of distresses are caused by several factors including:

1. Heavy vehicle loads and high number of multi-axle trailers.
2. The existing asphalt mix design practices.
3. The pavement design process.
4. Existing construction and quality control practices.

Hence, the need to determine the asphalt mix properties and asphalt mix design factors that affect the two distresses have been recognized.

1.3 RESEARCH OBJECTIVE

The objectives of this research study are to:

1. Determine the asphalt mix properties (i,e. percent aggregate, sand and fine, aggregate angularity, binder type and content, and percent air content) that affect pavement rutting and fatigue cracking.
2. Model the rut and fatigue cracks as functions of the asphalt mix properties, traffic load and volume, and the pavement cross-section.
3. Recommend changes in the existing asphalt mix design, and construction practices to decrease rut and fatigue cracking potentials.

To this end, this dissertation is organized into six chapters and two appendices as follows:

1. Chapter 2 - Literature review.
2. Chapter 3 - Research plan.
3. Chapter 4 - Field and laboratory investigation.
4. Chapter 5 - Analysis and discussion.
5. Chapter 6 - Conclusions.
6. Appendix A - Data acquisition and reduction software for indirect tensile test.
7. Appendix B - Pavement cross-section and deflection data for 564 pavement locations.

CHAPTER 2

LITERATURE REVIEW

2.1 GENERAL

The load carrying capacity of flexible pavements is brought about by the load-distributing characteristics of their layered systems. In general, flexible pavements consist of a series of layers with the highest quality material placed at or near the surface. Hence, their strengths are the result of building up thick layers and thereby distributing the load over the roadbed soil (1). Two types of load related distress can be found in flexible pavements:

1. **Rut** - Rut can be defined as the sum of the plastic (permanent) deformations in the AC, base, subbase, and roadbed soil. Rut is mainly caused by wheel loads and is accelerated by environmental factors. In general, rut can be minimized by using stiff materials in all layers and by proper pavement design and construction practices.
2. **Fatigue cracking** - Fatigue or Alligator cracking is a series of interconnecting cracks caused by fatigue failure of the asphalt concrete surface (or stabilized base) under repeated traffic loading. It is a load associated distress that can be found in both wheel paths and are accelerated by environmental factors. Fatigue cracking potential of any pavement can be minimized by using the appropriate pavement materials, proper design procedure, and good construction practices.

It should be noted that the contribution of the AC layer to the total pavement rutting due to densification is negligible since, this layer is typically compacted to near its theoretical maximum density during construction. Permanent deformation in the AC layer is mainly the results of lateral distortion due to repeated shear deformation (5).

The tensile stresses or strains induced at the bottom of the AC layer due to a wheel load cause fatigue cracking. In general, fatigue cracks start at the bottom of the

AC layer and they propagate upwards towards the surface. Hence, fatigue cracks may exist in a pavement structure for several years before they can be observed. Consequently, there is no universally adopted standard definition of fatigue failure of asphalt pavements.

In the laboratory, the fatigue life of a compacted asphalt specimen is defined by the number of load applications that causes fatigue failure of the specimen. The definition of fatigue failure, however, varies from one researcher to another. For example, Santucci and Schmidt (2) defined laboratory fatigue failure as the number of load applications required to reduce the stiffness of the specimen by 60 percent of its initial stiffness measured at 200 load applications. Baladi (3), on the other hand, defined the fatigue life (of a laboratory compacted Marshall size specimen tested by using the indirect tensile cyclic load test) as the number of load applications at which the cumulative horizontal plastic deformation (measured along the horizontal diameter of the specimen) reaches a value equal to 95 percent of the total horizontal deformation of a duplicate specimen tested to failure in the indirect tensile test mode.

Rut and fatigue cracking potentials of pavement can be minimized by taking balanced engineering steps during the material design (asphalt mix design), pavement design process and during construction. These include:

1. Engineered asphalt mix design that can withstand the expected traffic loading without plastic yielding, resists the induced tensile stress without cracking, and resists low temperature cracking.
2. Balanced pavement design process that provides adequate layer thicknesses to reduce the induced compressive stresses at the top of the base and subbase layers and at the top of the roadbed soil, which causes plastic deformation (rut) of these layers, and minimizes the tensile stress and strain induced at the bottom of the AC thereby, increasing the fatigue life of the asphalt layer (see Figure 2.1).
3. Good construction practices that deliver adequate and uniform compaction of the

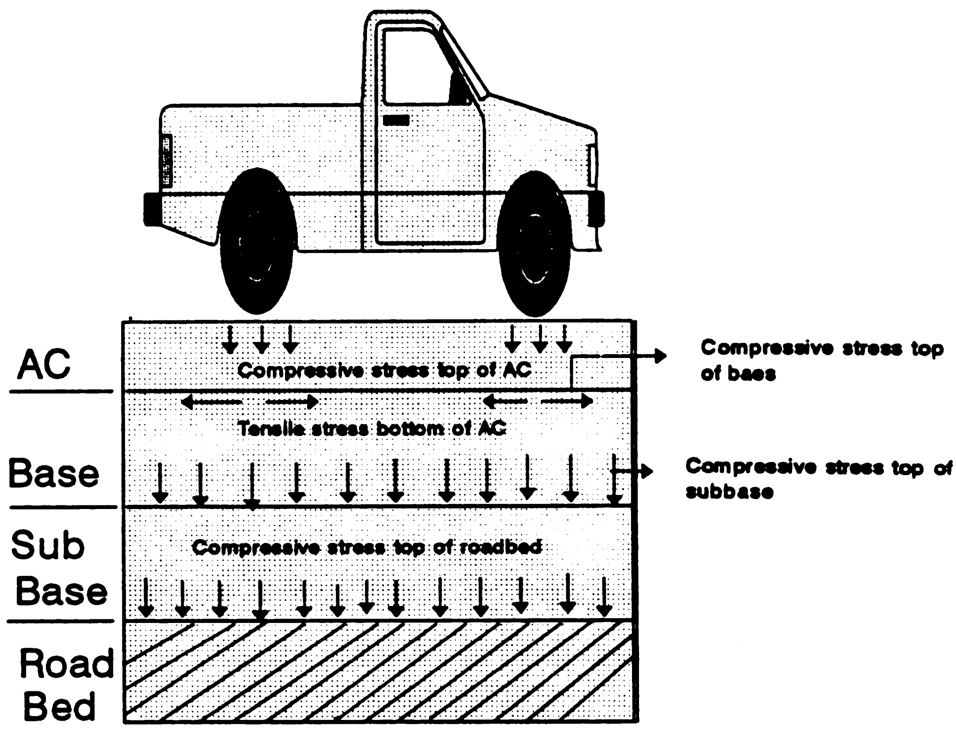

Figure 2.1 : Illustration of critical stress/strain locations in a typical pavement structure.

various pavement layers.

Existing flexible pavement design methods can be divided into two categories; empirical and mechanistic-empirical. Most empirical design methods are based on statistical equations derived from field observations of pavement rutting and surface roughness. Mechanistic-empirical design methods, on the other hand, are mainly based on two criteria:

1. Minimizing the rut potential of each pavement layer by limiting the magnitude of the compressive stress induced at the top of that layer by a moving wheel load.
2. Maximizing the fatigue life of the AC layer by minimizing the induced tensile stress at the bottom of the layer due to a moving wheel load.

Regardless of the pavement design method (empirical or mechanistic-empirical) employed in the design of flexible pavements, the design process involves two major steps as follows:

1. The design of the asphalt mix which involves the proportioning of the different ingredients (coarse and fine aggregates, mineral fillers, and asphalt cement) in the mix and the compaction effort.
2. The thickness design of the AC course and the other pavement layers (base and subbase), which involves the evaluation of the behavior of these layers under the anticipated traffic load and environmental conditions.

Since the outcomes of the asphalt mix design process (step 1) affect the engineering properties of the mix, the thickness design of the pavement, and the pavement performance, the two steps (mix design and thickness design) and construction practices must be considered in a comprehensive way so that the desired pavement performance is assured.

2.2 MECHANICS OF PERMANENT DEFORMATION AND FATIGUE CRACKING

2.2.1 Permanent Deformation (Rut)

Permanent deformation in flexible pavements manifest itself as rutting in the wheel paths thereby, causing permanent distortion in the transverse profile. In addition, pavement uplift may occur along the sides of the rut. In many instances, ruts are noticeable only after a rainfall, when the wheel paths are filled with water. Nevertheless, permanent deformation of the pavement surface is the result of rutting of the roadbed soil, the subbase and base layers, and the AC surface. Pavement rutting is mainly caused by densification or lateral distortion due to traffic loading, hence, rut is a load related distress. Several other factors affect the magnitude of rut and its time rate of accumulation. These include:

1. Construction factors including inadequate compaction (either low compaction effort or compaction at lower temperatures than those specified).
2. Asphalt mix factors that include soft (low viscosity or high penetration) asphalt cement, high air voids, rounded aggregate, and excess sand in the mix.
3. Environmental factors that include high temperatures which soften the AC layers, and high moisture content or saturation of the lower layers (base and subbase) due to inadequate drainage.
4. Tire factors such as studded tires and high tire pressures.

As stated earlier, pavement rutting is the sum of the rut in the AC, base and subbase layers and in the roadbed soil. Figure 2.2 shows the results of a study of the transverse profile of loops 4 and 6 of the AASHO Road Test (4). It can be seen that rutting has taken place in all pavement layers and in the roadbed soil. The contribution of each layer to the total pavement rut varies from one pavement to another. For example, the average rut in each layer as a percent of the total pavement rut of section

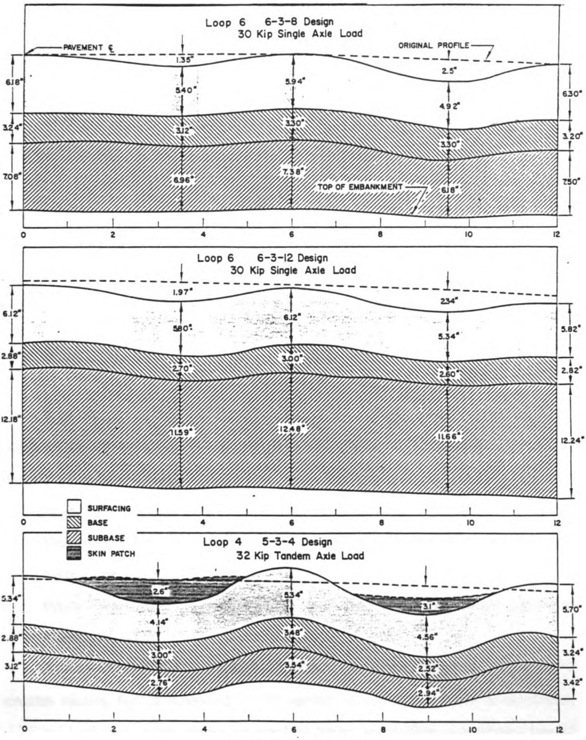

Figure 2.2 : Trench study of the transverse profile of loops 4 and 6 of the AASHO ROAD TEST (4).

51 of the AASHO Road Test, is shown in Table 2.1.

Table 2.2 provides a list of the relative percentages of the permanent deformation of section 51 of the AASHO Road Test that are attributable to distortion alone. It can be seen that, in general, permanent deformation is largely due to lateral distortion.

Based on laboratory data, Morris (5) concluded that densification and lateral distortion in compacted asphalt concrete specimens are largely a function of the test conditions. He added that, in the field, asphalt pavements are subjected to densification in the compression zone and to lateral distortion in the tension zone. Tests on asphalt concrete used at the Brampton Test Road (6), confirmed the above observations. It was noted that the rut potential in the tension zone in asphalt concrete pavements is higher than that in the compression zone because of distortion.

2.2.2 Fatigue Life

With the passage of each wheel load, a cyclic tensile stress is induced at the bottom of the AC layer which causes cyclic tensile strains. This strain is composed of three components as follows:

1. Elastic strain which is recoverable upon the removal of the load.
2. Viscoelastic strain which is recoverable after the load has been removed for a certain time period.
3. Plastic strain which is permanent in nature and causes the asphalt cement to stretch and crack.

As the number of load applications increases, the cumulative plastic tensile strains increases causing further stretching of the asphalt cement until a crack is developed. Additional load applications causes the crack to widen and to propagate upward toward the pavement surface where it manifest itself as alligator (fatigue) cracks. Hence, the plastic strain is the sole cause of the fatigue cracking. A perfectly elastic material

Table 2.1 : Average rut (percent of total rut) in each layer of section 51 of the AASHO Road Test (5).

Percent of the total rut.			
AC	Base	Subbase	Roadbed soil
32	14	45	9

Table 2.2 : Percent rutting in various layers due to distortion, section 51 of AASHO Road Test, 1960, (5).

MATERIAL	% Rutting due to distortion during a given season			AVERAGE
	SPRING	SUMMER	FALL	
A/C SURFACE	82	82	76	80
BASE	0	70	NO MEASUR.	Figs.inconsistent
SUBBASE	97	96	NO MEASUR.	95.5

will never develop fatigue cracking (3).

It should be noted that as the fatigue crack initiates at the bottom of the AC, the tensile strength of the AC is reduced and hence its resistance to tensile cracking decreases. Therefore, the rate of tensile cracks propagation increases as the width and length of the crack increases.

Over the last 30-year period, large quantities of laboratory fatigue life data for compacted asphalt mixtures have been obtained. Traditionally, the data are presented as stress or strain amplitude versus the number of load repetitions to failure. The resulting curves are known as the S-N curves. Like metals and other engineering materials, the fatigue life of compacted asphalt mixtures steadily increases with decreasing stress or strain amplitude until the stress or strain level of the fatigue limit is reached, below which the fatigue life becomes infinitely long. In general, tensile stresses at or below the fatigue limit causes only elastic strains. Based on laboratory fatigue tests conducted by using indirect tensile and flexural beam tests, Baladi (3) concluded that the fatigue limit of compacted asphalt mixtures is reached when the tensile stress is about 35 percent of the indirect tensile strength of those mixtures.

2.3 FACTORS AFFECTING RUTTING AND FATIGUE CRACKING OF ASPHALT SURFACED PAVEMENTS

2.3.1 Tire Inflation And Tire-Pavement Contact Pressures

In the U.S.A. asphalt surfaced pavements are experiencing premature rutting and fatigue cracking due to increased traffic volume, loads and/or increased truck tire pressure. Surveys in the States of Illinois and Texas indicate that the tire pressures have increased substantially over the last few decades. An average tire pressure of 96 psi with a maximum of 130 psi were recorded in the Illinois survey. The Texas survey showed an average tire pressure of 110 psi with a maximum pressure of 155 psi (7).

Typically, the rut potential of asphalt pavements has been evaluated on the basis of the magnitude of the compressive stresses induced at the top of the base layer and roadbed soil due to an 18-kip single axle load and a constant tire pressures (typically 85 psi). Experimental studies conducted by GoodYear tires and Rubber Company indicate that (8):

1. For a constant tire load, increasing the tire inflation pressure causes a shift in the point of maximum contact pressure to the center region of the contact area between the tire and the pavement surface.
2. For a constant tire pressure, increasing tire loads causes a shift of the point of maximum contact pressure towards the perimeter of the contact area between the tire and the pavement surface.
3. Regardless of the tire load and tire pressure, the tire-pavement contact pressure is not uniform within the tire-pavement contact area. The distribution of the contact pressure is a function of the tire type and design. For example, contact pressures as high as twice the tire inflation pressure were measured for three tire types as shown in Table 2.3.

Smith and Bonquist (9) studied the influence of tire type and tire inflation pressure on pavement performance. They conducted full-scale pavement tests using the Federal Highway Administration (FHWA) Accelerated Loading Facility (ALF) located at Turner Fairbank Highway Research Center in Mclean, Virginia. The study examined the effects of tire pressure, tire load, pavement cross-section, and environmental conditions on pavement response (stresses and strains) and on pavement performance (rut potential and fatigue life). They made the following conclusions:

1. The effect of wheel load on pavement responses is greater than the effect of tire pressure. The measured pavement responses (stresses and strains) doubled for an increase in load from 9,400 pounds to 19,000 pounds, while increasing the tire inflation pressure from 76 psi to 140 psi resulted in a less than 10 percent

Table 2.3 : Effect of tire type and tire inflation pressure on the maximum tire -pavement contact pressure, (8).

Tire type and load	Tire-inflation pressure (TIP) (psi)	Max. contact. Pressure (MCP). (psi)	Ratio(MCP/TIP)
11-24.5	65	117	1.8
4250 lbs.	75	114	1.5
	95	118	1.2
11r24.5	75	122	1.6
4250 lbs	95	152	1.6
	115	182	1.6
385/65R22.5	100	200	2.0
	120	226	1.9
	140	252	1.8

increase in the measured response. This conclusion support the results of mechanistic analysis of flexible pavement structures. For example, Baladi (unpublished data) used MICHPAVE (a linear/nonlinear finite element computer program) to analyze the stresses and strains induced in the pavement layers due to various wheel loads and tire inflation pressures. He reported that the effects of increasing tire pressure on the induced stresses and strains in the pavement are much smaller than those due to increasing wheel load.

2. Increasing tire pressure from 76 psi to 140 psi causes less than 30 percent increase in the expected fatigue damage. Increasing the wheel load from 9,400 pounds to 14,100 pounds, on the other hand, causes an increase in the expected fatigue damage by 350 to 650 percent. Based on mechanistic analysis of flexible pavements and the rut and fatigue prediction models embedded in MICHPAVE, similar conclusion was also made by Baladi (unpublished data). He reported that an increase in the wheel load by 50 percent causes an increase in the pavement rut by a factor of 1.4 to 3 and a decreases in the fatigue life by a factor of 5 to 10 depending on the layer thicknesses and material quality. He added that increasing the tire pressure by a factor of 2, on the other hand, decreases the fatigue life by a factor of 1.2 to 2 depending on the layer thicknesses and material quality.

3. The effects of tire pressure and/or wheel load on pavement rutting are much higher for thin pavement sections (less than 2-inch AC surface) than for typical or thick sections (more than 4-inch thick AC surface). Further, higher temperatures cause higher rut potential. Hence, the combinations of high tire pressure, high wheel load, high temperatures, and thin pavement sections are extremely damaging to flexible pavements.

Although, the average truck tire inflation pressure has increased by about 20 psi over the last thirty-year period, the above findings suggest that this increase has an insignificant effect on pavement rutting and a moderate effect on fatigue life. On the other hand, the reported increase in wheel load (e.g., the average wheel-load in Michigan has increased by 4000 pounds over the last twenty-year period) has significant effect on both the rut potential and the fatigue life of flexible pavements.

Chen (10) employed the three dimensional Texas Grain Analysis (TEXGAP-3D) program (a 3-D linear finite element computer program) to study the effects of various wheel loads, nonuniform tire pressures, and nonuniform tire-pavement contact pressures on the induced stresses and strains and the resulting damage in asphalt concrete pavements. Results of the analysis were also compared with those of the ELSYM5 computer program which uses a circular contact area with uniform contact pressure distribution. Chen used two field fatigue distress models developed by Finn et al (one model is applicable to 10 percent or less of fatigue cracks per area of wheel path and the other for 45 percent or more). Chen used the two models to analyze the effect of tire pressure and load on fatigue life. He also utilized a rutting model developed from the AASHO Road Test data to analyze pavement rutting. He made the following observations:

1. For a constant load of 4500 pounds, a variation of the tire inflation pressures from 75 to 110 psi have more influence on the strains at the bottom of a thin pavement surface layer than on a thick one (see Figure 2.3).
2. For a thin surface course, higher loads consistently produce higher tensile strains even at a distance of 6-inch from the tire centerline as shown in Figure 2.4.
3. For a constant axle load of 4500 pounds, a 47 percent increase in the tire inflation pressure produces less than 2 percent increase in the compressive strain developed at the top of the subgrade as shown in Figure 2.5.
4. For a constant inflation pressure, a 20 percent increase in the axle load produces approximately a 20 percent increase in the subgrade compressive strain at the top of the subgrade as shown in Figure 2.6.

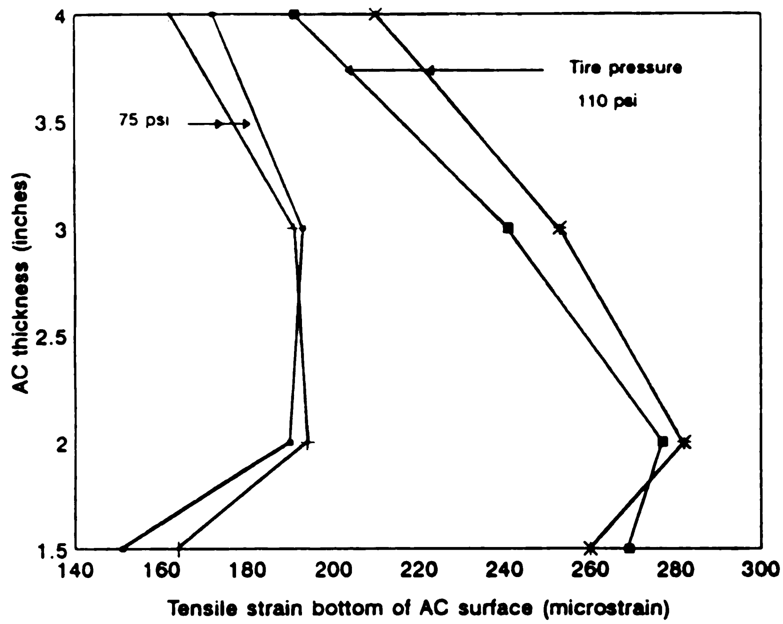

Figure 2.3 : Variation of tensile strain at the bottom of the AC surface for different AC thicknesses and two tire inflation pressures (10).

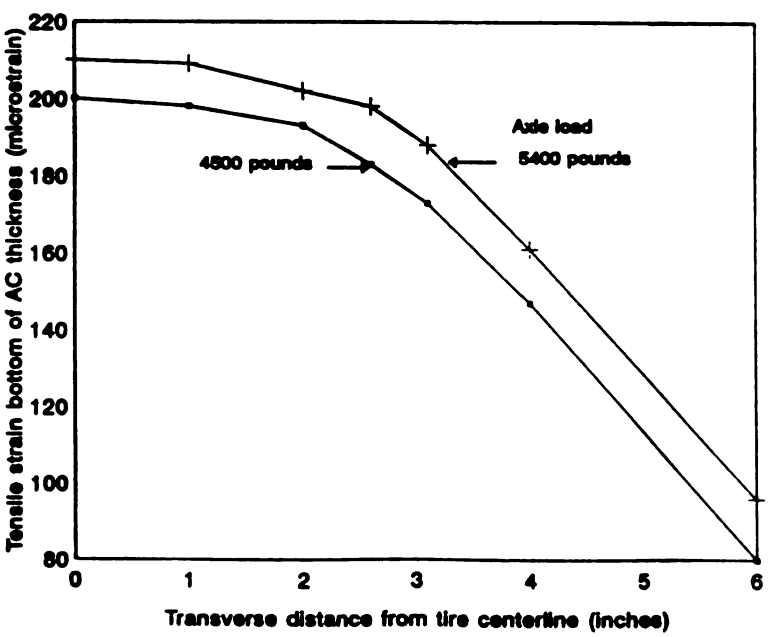

Figure 2.4 : Variation of tensile strain at the bottom of a 2-in. thick surface pavement with lateral distance from the center of the tire, treated tire with 90 psi pressure (10).

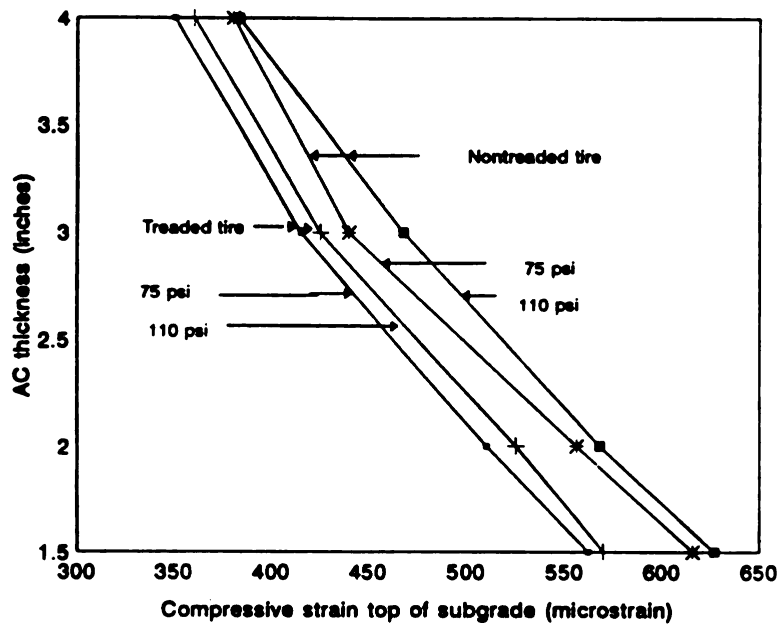

Figure 2.5 : Variation of compressive strain at the top of the subgrade for different thickness and tire pressure (10).

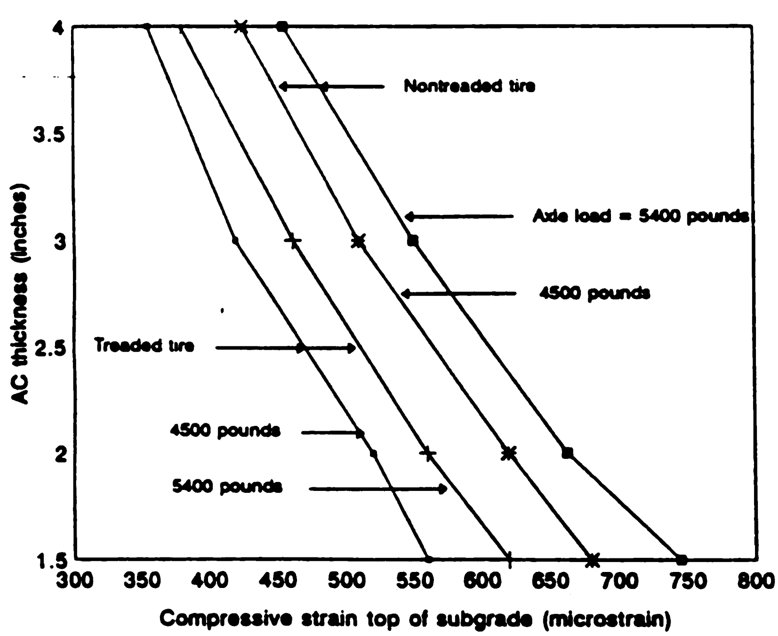

Figure 2.6 : Variation of compressive strain at the top of the subgrade for different AC thicknesses and two Axle loads (10).

5. For a 2-inch thick AC surface pavement and a constant axle load, a 47 percent increase in the tire inflation pressure results in a 48 percent reduction in fatigue life using the 10 percent fatigue model as shown in Figure 2.7. whereas, for a 4-inch thick AC surface pavement and a constant tire inflation pressure, a 20 percent increase in axle load causes a 36 percent reduction in fatigue life for both the 10 percent and the 45 percent fatigue models as shown in Figure 2.8.
6. For the same tire inflation pressure, increase in axle load from 4500 pounds to 5400 pounds results in a 50 percent reduction in pavement life based on subgrade compressive strain as shown in Figure 2.9.

Based on these observations Chen et al. made the following conclusions:

1. High inflation pressure and heavy load causes higher tensile strains at the bottom of the asphalt concrete and a significant reduction in the pavement fatigue life.
2. The axial load not the inflation pressure has a major influence on subgrade rutting.

2.3.2 Consolidation And Field Compaction

Proper specifications and quality assurance regarding asphalt mixture composition and compaction decrease the rutting potential due to densification and offers a benefit in terms of increased fatigue life.

Barksdale (11) conducted laboratory study on compacted asphalt mixes composed of AC-20 asphalt cement and crushed granitic genesis aggregate. He concluded, that for a range of asphalt content from about 4 to 5.5 percent, the fatigue life of all specimens compacted by using 75 blows Marshall compaction is higher than those compacted at 50 blows as shown in Figure 2.10. He added that, the benefits of higher compaction efforts decrease as the percent asphalt cement content increases from about 4 to 5.5 percent. Barksdale also cited the work of Raithby, Epps and Acott, and reported that asphalt

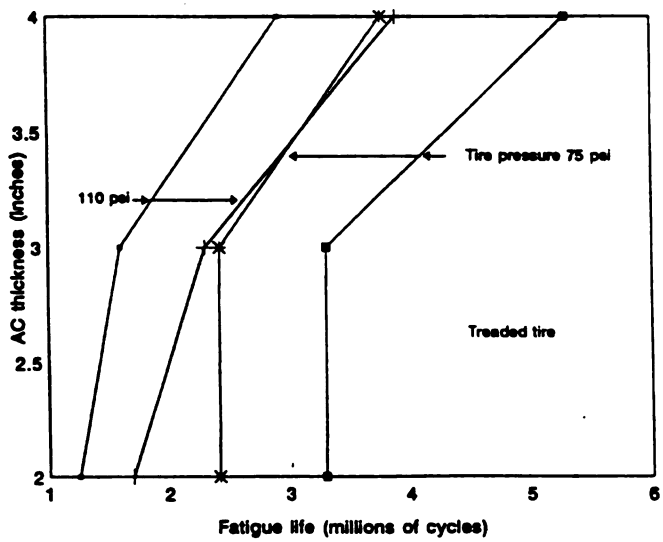

Figure 2.7 : Fatigue life variation for different AC thicknesses and tire inflation pressures (10).

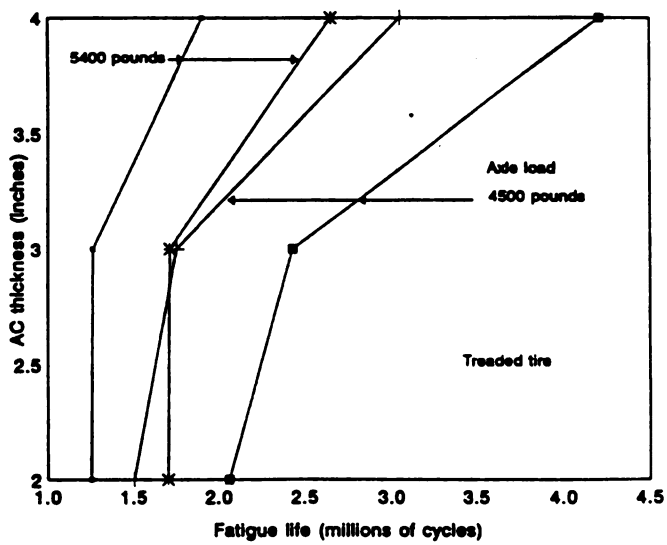

Figure 2.8 : Fatigue life variation for different thickness and tire loads (10).

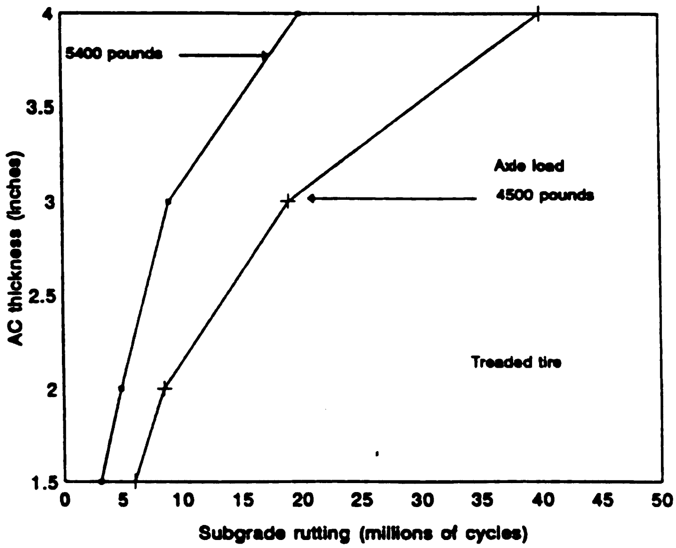

Figure 2.9 : Pavement subgrade rutting damage life for different thickness and loads (10).

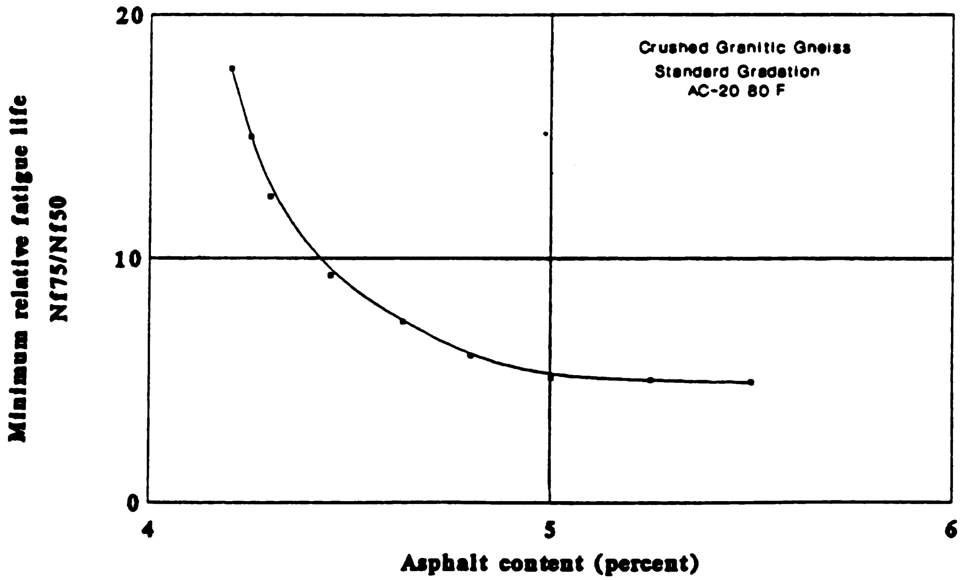

Figure 2.10 : Fatigue life ratio of two asphalt mixes compacted at 50 and 75 blows Marshall compaction versus the asphalt content (11).

mixes placed in the field at a compaction level equal to the 50 blows Marshall compaction experienced gradual compaction and densification due to traffic loading.

Several other researchers (12-16) have shown that the fatigue life of asphalt cement is reduced by about 10 to 30 percent for each 1 percent increase in air voids over the normal range of 4 to 7 percent. Finn and Epps (13) evaluated two flexible pavements with AC thicknesses of 4 and 6-inch. He reported that, when the percent air voids (due to compaction) is increased from a desirable level of 7 percent to a very poor compaction level of 12 percent, the 4-inch thick AC layer effectively lasts only as long as the 2-inch thick layer. Likewise, the life of the 6-inch AC layer is reduced to that of the 4-inch thick layer. Similarly, Epps and Monismith (17) reported that asphalt mixes placed at higher percent air voids due to inadequate field compaction experienced shorter fatigue life and densification under traffic loading. They added that the changes in the fatigue life due to variations in air void contents cannot be entirely explained by changes in the mixture stiffness produced by the same variation in air void contents. That is higher percent air voids produces softer mix and shorter fatigue life. The implication of their findings is that stiffness alone cannot be used to model the fatigue life of AC mixes. Higher AC mix stiffness could be produced by higher compaction efforts, higher viscosity asphalt cement in the mix, and different arrangements of the aggregate matrix in the mix. Increasing mix stiffness due to compaction is beneficial and it tends to extend the fatigue life of the mix. On the other hand, increasing the mix stiffness by using higher viscosity asphalt cement reduces the fatigue life of the mix. Similar findings were also reported by Baladi (3).

Huges and Maupin (7) monitored the rut depth of asphalt pavements made by using different asphalt mixes (see Figure 2.11). They measured the rut depth right after construction, six months, and one year after construction. They reported that mix 1 with the highest initial voids in the total mix (VTM) has rutted more quickly than Mix 4 which had the lowest initial VTM. This supports the widely held belief that improving

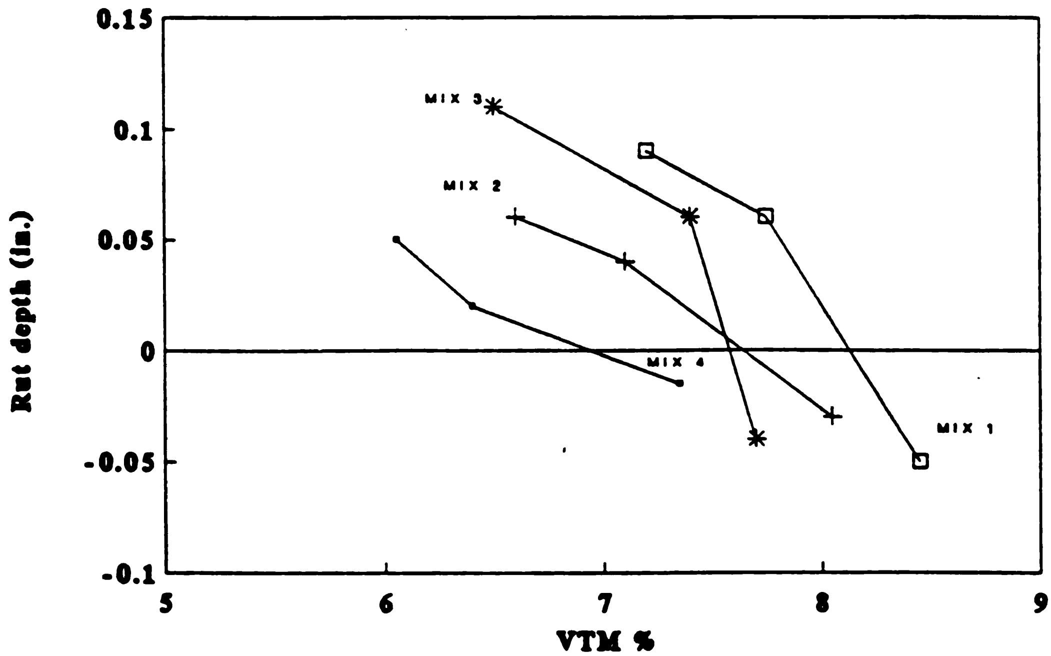

Figure 2.11 : **Rutting as a fuction of the voids in the total mix (VTM),(7).**

density during construction reduces rut depth.

Miller (16), based on results obtained from 24 test sites in Arkansas, stated that asphalt mixtures placed and compacted at air voids between 2.5 to 5 percent provide an acceptable level of rutting. He added that pavements with deep rutting have air void contents of less than 1.0 percent. Brown (18) stated that in place air void contents above 3 percent are needed to decrease the probability of premature rutting throughout the life of the pavement, whereas, air voids of less than 3 percent greatly increase the probability of premature rutting. Huber and Heiman (19) reached similar conclusion and suggested that asphalt mixes should be compacted above a threshold value of 4 percent air voids.

2.3.3 Aggregates

The performance of asphalt mixes depend on providing adequate aggregate interlock for resisting and distributing the wheel load rather than on the shear strength of the asphalt cement. Therefore, the size, shape and angularity, and quality of the aggregates play an important role in the performance of the AC mix. Hence, every precaution should be taken to insure that a face to face aggregate contact and aggregate interlocking are provided for the high quality AC mixes.

The maximum aggregate size, aggregate shape, and angularity, and the percent aggregate content in the mix influence the rut and the fatigue life of asphalt pavements and Marshall stability and flow of the asphalt mix. Higher aggregate angularity produces higher Marshall stability, lower flow, and lower pavement rutting (16,19,21,22). Figure 2-12 depicts the rut depth as a function of Marshall stability. Larger top size aggregate in the asphalt mix, on the other hand, produces higher stability, higher resilient modulus, higher compressive strength and lower rut potential (24,25).

Herrin and Goetz (26) studied the effects of the percent aggregate in the mix and aggregate shape on the stability of the mix. They observed that as the percent aggregate

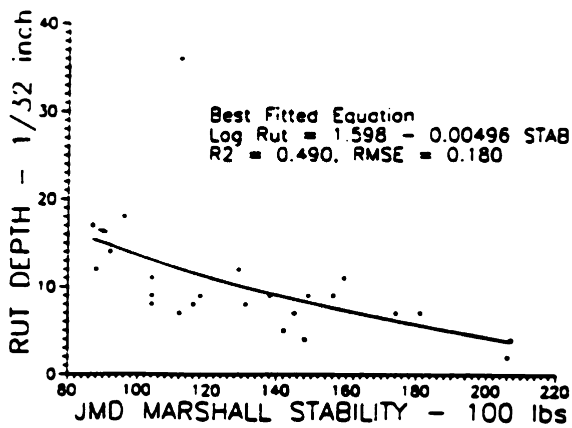

Figure 2-12 : Relationship between rut depth and stability (16).

in the mix decreases, its influence on the stability of the mix decreases. This may be explained by the fact that as the percent aggregate decreases and the percent sand increases, face to face aggregate contact is lost producing a ball bearing effect. That is higher percent sand contents cause the aggregate particles to float in the sand matrix thereby, reducing friction and stability. Indeed the European Stone Mastic Asphalt (SMA) mix consists of 70 to 80 percent crushed aggregate. The SMA is well known for its low rutting potential. In addition for a constant asphalt content, large size aggregates causes an increase in the density of the compacted asphalt mixtures (27). The increase in density is more pronounced when the aggregate top size is increased from 3/4 to 2-inch as it can be seen from Table 2.4. Further, increasing the aggregate top size in a mix causes an increase in the percent air void and in the percent void in the mineral aggregates (VMA) as shown in Figure 2.13 and 2.14 (27).

Similarly, based on literature review conducted by Button at el. (28), he concluded that the rutting problem can be addressed by using large top size aggregates (1 to 1½-inch), increasing the percent void in mineral aggregate requirements (14 to 15 percent minimum), replacing most or all the natural sand in the mix with manufactured angular particles, increasing the minimum allowable air void in the laboratory compacted mix to

4 percent and limiting the ratio by weight of mineral filler to bitumen to about 1.2. Epps and Monismith (17) reported that crushed (angular) aggregates produce AC mixtures with high rut and fatigue resistance. Typical requirement for crushed coarse aggregate are:

1. A minimum of 75 percent of particles with two crushed faces.
2. A minimum of 90 percent of particles with one crushed face.

Table 2.4 : Summary of mix densities (lbs/c.ft),(27).

Asphalt Content	Aggregate Top Size				
	¾"	1"	1½"	2"	2½"
3%	--	--	--	148.77	150.00
4%	143.71	145.50	148.19	151.30	151.38
5%	144.14	148.02	149.68	150.25	149.65
6%	142.96	145.88	148.98	--	--

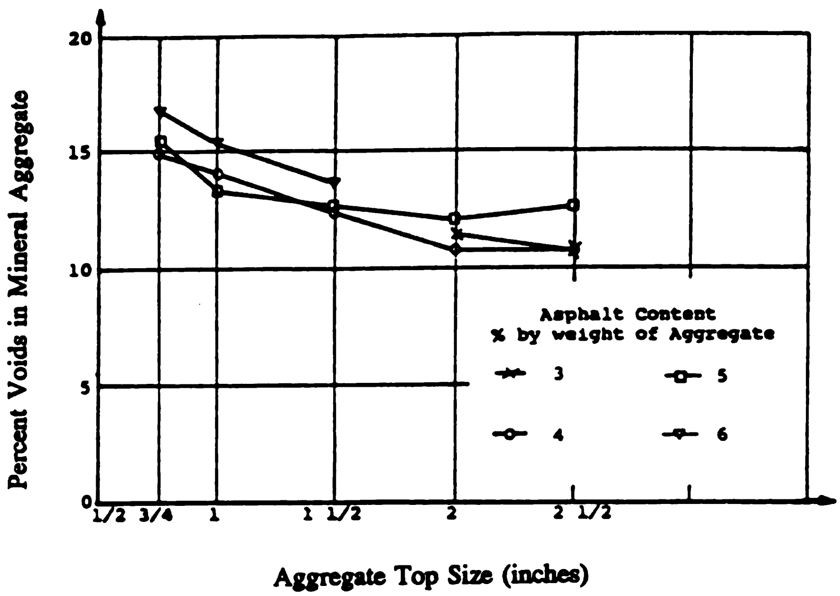

Figure 2.13 : **Effect of aggregate top size upon the percent voids in mineral aggregate (27).**

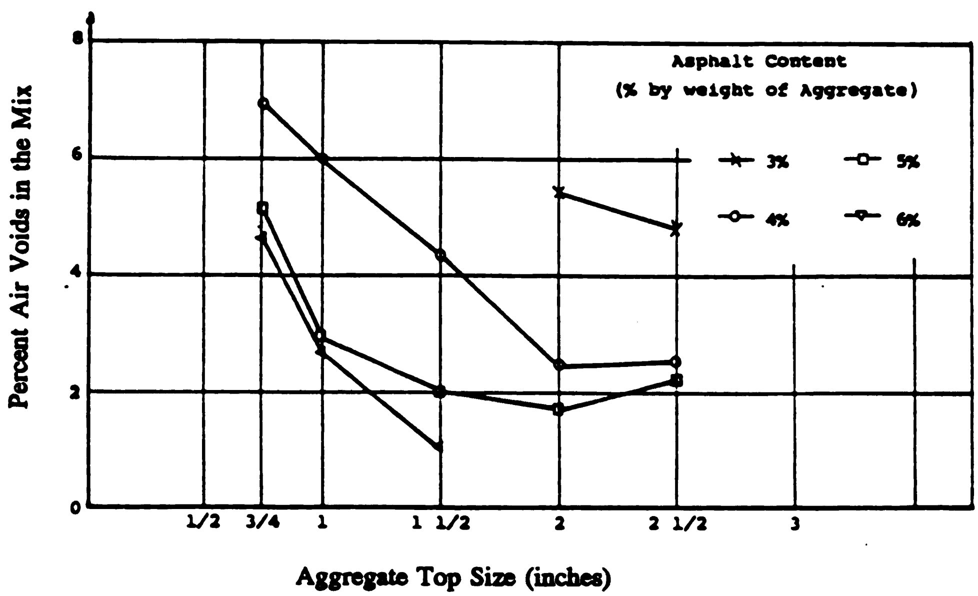

Figure 2.14 : **Effect of aggregate top size on the percent air voids in the mix (27).**

2.3.4 Sand and Mineral Filler

The angularity and shape of the sand particles, the percent sand content in the AC mix, and the type of mineral filler influence the rut and fatigue life performance of asphalt pavements. The Federal Highway Administration (FHWA) recommends that natural sand (rounded sand particles) be limited to 15 to 20 percent of the total weight of aggregates for high volume roads and to 20 to 25 percent for medium and low volume roads (29). Similarly, Button et al. (28) suggested that for high traffic volume roads limiting the natural (uncrushed) sand particle content of the asphalt mixes to about 10 to 15 percent reduces rut and fatigue cracking potentials. Young (30) cited Barksdale and Hicks, and reported a significant increase in pavement rutting due to an increase in the percent sand contents.

Barksdale (11) studied the effect of three types of mineral filler (the dust produced from crushing aggregates, fly ash and portland cement) on the fatigue properties of asphalt pavements. He reported that the use of fly ash as mineral filler resulted in a lower fatigue life than the other two types of fillers.

2.3.5 Asphalt Type And Content

The type of the asphalt cement and its content in an asphalt mix impact the rut and fatigue life of the asphalt mixes. Typically, the type of asphalt cement used in an asphalt mix depends on the environmental conditions. Higher temperature regions require harder (higher viscosity or lower penetration) asphalts. On the contrary, softer asphalts are used in the construction of asphalt pavements in cold regions. The asphalt cement hardness or viscosity affects three types of distress.

1. Fatigue life which is affected by the AC viscosity at inservice temperatures.
2. Rutting- Softer asphalt tends to cause higher rutting potential. Hence, rut is affected by the AC viscosity at high temperatures.

3. Cold temperature cracking- Stiff asphalt cements tends to harden at lower temperatures and loose its flexibility. Thus, cold temperature cracking is affected by the AC viscosity at low temperatures.

The effects of the asphalt binder on the various distress modes vary. For example, a study conducted by the National Research council, Strategic Highway Research Program (SHRP), found that the binder contribution to the rut potential of the asphalt course is about 40 percent as shown in Figure 2.15. The other 60 percent is attributed to the other ingredients in the mix (aggregate, sand and mineral filler) and their proportions and to the construction practices. Also shown in the Figure is that the binder contribution to the fatigue life of the asphalt layer is about 60 percent. The other 40 percent is related to the pavement layer thicknesses and properties. Finally, the asphalt binder contribution to the low temperature cracking potential is about 80 percent.

Traditionally, asphalt binders are classified and specified according to their viscosities at a given temperature. Two AC binders of the same grade (e,g., AC-20) may have the same viscosity at the specified temperature. However, their viscosities at higher or lower temperatures may differ substantially and so their behaviors. This fact has been recognized in the new SHRP binder specifications which consider three types of distress: permanent deformation, thermal cracking and fatigue cracking. These distresses are related to the rheological properties of the binder at high, low, and intermediate temperatures, respectively.

Huber and Heiman (19) stated that penetration and viscosity of the AC binder do not possess a significant effect on rutting rate because an asphalt grade typically produces a similar penetration and viscosity after mixing. They attributed the rutting performance to air voids, voids filled with asphalt and asphalt content. Huges and Maupin (7) on the other hand, stated that binder type is not as important as aggregate gradation in minimizing early pavement rutting. Kruts (31) evaluated the impact of moisture on rutting potential of polymer modified mixtures. He reported that moisture

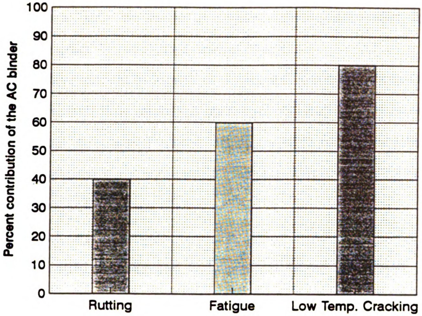

Figure 2.15 : Binder contribution to different distresses.

conditioning of laboratory specimens before determining their permanent deformation potential yielded a fairly consistent permanent deformation results for all mixtures regardless of the grade of the asphalt cement binder.

An excessive amount of asphalt or a very soft grade asphalt can often produce a mix with high Marshall flow values. A maximum Marshall flow of 16 is often specified for mix design and construction control. Brown and Cross (32) reported that Marshall flow is a good indicator of rutting potential. Higher amount of rutting is associated with mixes having flow values above 10.

Mixes with large aggregates have less asphalt requirement to coat the aggregate. Case studies of rutted pavements in Oklahoma conducted by Hensley and Leahy (33) showed that missing intermediate fines in stone-filled mixtures make them less sensitive to asphalt content. This is due to the fact that intermediate fines increase the surface area to be coated with asphalt cement and increase their ball bearings effects. Thus, their absence not only reduces the asphalt requirement but also reduces the sensitivity of the mix to increased asphalt contents.

Decker and Goodrich (34) ranked five asphalt cement factors relative to their effects on asphalt pavement distresses. They used a ranking scale from 0 to 5. A ranking of 0 indicates no effect whereas 5 indicates significant affect. Since, asphalt cement properties are mainly governed by the source of the crude, they found that the refining process has a very minor effect on rutting and fatigue cracking. Decker and Goodrich studied and ranked the physical properties (such as stiffness, temperature susceptibility) and rheology of the AC binders (see Table 2.5). They made the following conclusions:

1. Increasing the viscosity of the AC binder causes an increase in the stiffness of the AC mix which in turn improves the rut resistance.
2. For a thick pavement section, fatigue resistance can be increased by increasing the binder stiffness. Whereas, softer mixes provide a better resistance for thin

Table 2.5 : Effect of asphalt cement factors on pavement distress (34).

ASPHALT FACTORS	PAVEMENT PERFORMANCE			
	THERMAL CRACKING	FATIGUE CRACKING	RUTTING	MOISTURE DAMAGE
REFINING TECHNIQUE	1	1	1	0
PHYSICAL PROPERTIES	4	3	2	1.5
CHEMICAL PROPERTIES	2	2	2	2
AGING	1	3	1	1.5
MODIFICATION	2.5	2.5	2.5	2.5

pavement sections. The reason for this is that aging of the binder causes the AC mix to stiffen and to loose its flexibility to contract due to low temperatures. For thin AC pavements, the aged binder may influence the tension zone in the AC layer thereby, causing less resistance to fatigue cracking. For thick AC pavements, on the other hand, the aging process affect the upper part of the AC layer causing higher stiffness in the compression zone and lower tensile stress in the tension zone. Hence, the fatigue life is increased.

Epps and Monismith (17) conducted tests to determine the effects of mixture variables on the flexural fatigue properties of asphalt mixes and reported an asphalt content of 6.7 percent reduces fatigue cracking (see Figure 2.16). They argued the fact that increased viscosity or decreased penetration should increase the stiffness of the AC mix, which in turn should increase the fatigue life at a particular stress level as shown in Figure 2.17. They cited Jimenez and Heukelom and Klomp for reaching similar conclusion.

Kim et al. (35) used indirect tensile test to determined the significance of the asphalt content on fatigue life of the sample. They reported a significant improvement in the fatigue resistance of the AC mixes when asphalt content of 0.6 percent above the optimum asphalt content at 32° F (not at 68° F) is used.

2.3.6 Environmental Factors

Exposure to environment causes the bituminous material to harden over time. With the passage of time, the bituminous binder becomes so brittle that it can no longer sustain the strains affiliated with daily temperature changes and with traffic loads. The rate of hardening is a function of the oxidation-resistance of the binder, temperature, and thickness of the asphalt film. Therefore, the rate of hardening vary with the binder type, climate and material design. It should be noted that most of the asphalt hardening takes

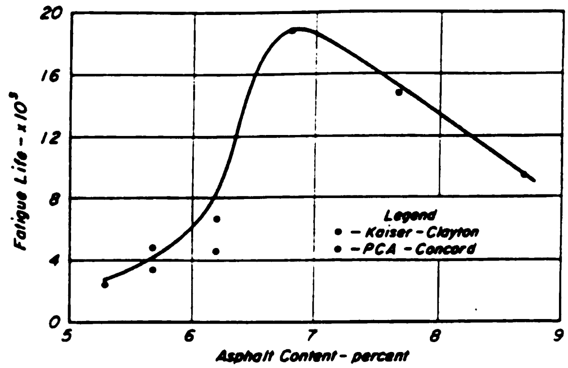

Figure 2.16 : **Effect of asphalt cement on fatigue life- California medium grading, Basalt aggregate, 60-70 penetration asphalt (17).**

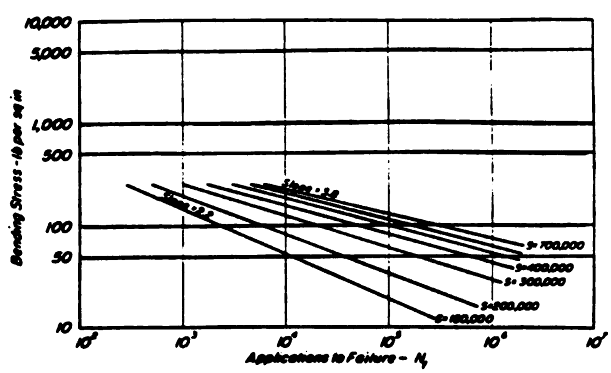

Figure 2.17 : **Bending stress vs. application to failure , for mixes of different stiffness-California graded mixes, granite aggregate, 85-100, 60-70 and 40-50 penetration asphalt, 6 percent asphalt (17).**

place during mixing, agitating, transporting, and construction.

Asphalt durability can be defined as its resistance to change in its original properties during mixing, construction, and service life. Durability of the asphalt is not a factor that effects rutting directly. In fact the embrittlement of the asphalt due to aging can cause increases in both the cohesion and the stiffness of the binder, which result in a greater resistance to permanent deformation under loading. Asphalt hardening on the other hand, adversely affects its fatigue life and low temperature cracking.

Huges and Maupin (7) reported that early pavement rutting is a function of the temperature of the pavements when it is opened to traffic. They suggested pavement temperatures of less than 150 °F lead to a stable asphalt mix under traffic.

Vallerga et al. (36) evaluated the effect of asphalt aging (they used the Rolling Thin Film Oven to produce an aged asphalt) on the fatigue performance of AC mixes. They reported that for a particular stiffness modulus, the aged asphalt resulted in a greater number of load repetitions to failure. However, it is conceivable that continued embrittlement of the asphalt through aging beyond some point, adversely affect the fatigue cracking of the AC pavement.

Paterson (37) reported that bituminous binder hardens due to environmental exposure, which substantially reduces the fatigue life of thin to medium thick asphalt pavements. Whereas, the fatigue life of thick asphalt pavements is less effected due to aging because they behave according to controlled-stress conditions. He suggested that the timing of fracture is governed by three mechanisms, which are effected by the interaction of aging and traffic as shown in Figure 2.18. These mechanisms are:

1. Aging mechanism - After construction, the aging of the asphalt course is almost uniform across its thickness. Because of exposure to the environment, the top side of the asphalt course will age more rapidly than the bottom side. Therefore, since the fatigue life is dependent on aging, the available fatigue life at the top of the AC course decreases more rapidly than that at the bottom side as it is shown

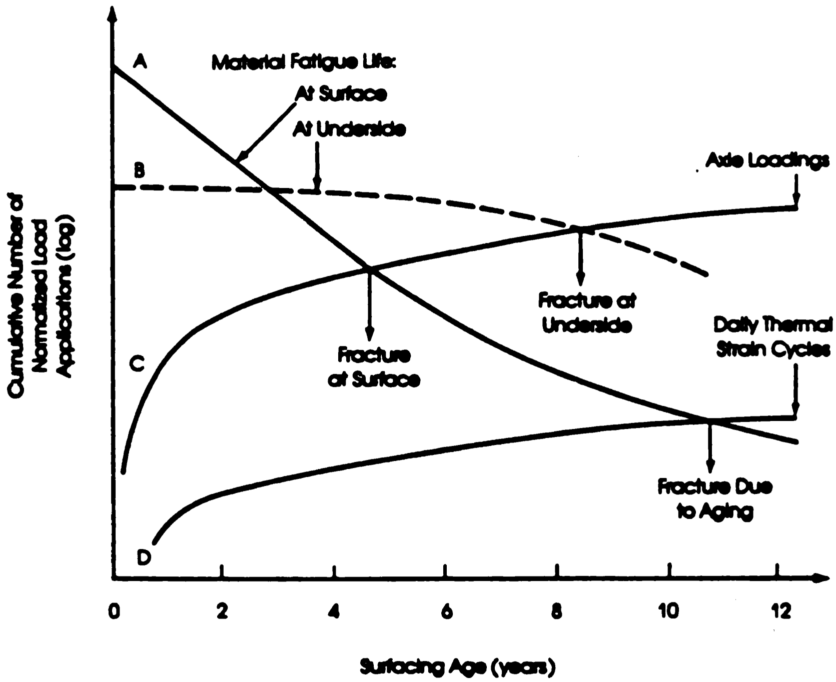

Figure 2.18 : **Interaction between traffic related and aging related fatigue cracking in bituminous surfacing (37).**

by curves "A" and "B" of Figure 2.18.

2. Load induced strains - When the cumulative plastic strain due to repeated load application reaches the available fatigue life, the AC will fatigue crack. For thin pavements (high tensile strains at the top of the AC), the top side of the AC surface will crack first as shown by curve "C" of Figure 2.18. For thick pavements, on the other hand, the bottom side of the AC surface will crack first.

3. Thermal strain - Due to temperature changes, plastic strain will accumulate at the top and bottom sides of the AC layer. This thermal plastic strain is much higher at the top of the AC than at the bottom because of the temperature variation throughout the AC thickness. Hence, the top side will experience low temperature cracking first, as it is shown by curve "D" of Figure 2.18.

It should be noted that the relative location of curves "C" and "D" (load induced or thermal strain induced cracking) depends on the traffic volume and the environmental conditions of the region.

2.3.7 AAMAS Mixture Properties Related to Pavement Performance

A comprehensive study of the effects of asphalt mixture variables on the performance of flexible pavements and on the engineering properties of the mixtures was sponsored by the National Cooperative Highway Research Program (NCHRP). The title of the project is Asphalt Aggregate Mixture Analysis System (AAMAS). The asphalt mix design factors included in this study are: compaction, resilient and creep modulus, indirect tensile strength and strain at failure and the compressive strength. Each factor was ranked on a scale from 0 to 5. A ranking of 0 indicates that the factor has no effect on the pavement performance. A ranking of 5 indicates significant effects (38).

Two static creep and repeated load tests were used in the AAMAS study, the uniaxial compression and the indirect tensile. The values of the resilient modulus obtained from the first test were used to evaluate the rut potential of the compacted asphalt mixes. The values obtained from the second test were used to assess the fatigue cracking potential.

Table 2.6 provides a list of the ranking of the various test outputs. It can be seen that:

1. The resilient modulus of asphalt mixtures possesses a significant effect on the fatigue cracking potential, a moderate effect on rut and thermal cracking potentials, and a minor effect on the moisture damage potential.
2. The creep modulus of the AC mixture has significant effect on the rut and thermal cracking potentials, a moderate effect on fatigue cracking, and a minor effect on moisture damage potential.
3. The tensile strength at failure and the indirect tensile strength have significant effects on both the thermal and fatigue cracking potentials and minor effects on rut and moisture damage potentials.
4. The compressive strength has a moderate effect on rut potential, a minor effect on moisture damage, and no effects on the fatigue and thermal cracking potentials of the mixes.

Other mix factors such as aggregate particles orientation, which is affected by the compaction method (the gyratory compaction technique was recommended by the AAMAS study), the slope and intercept of the creep-time curve (also known as the alpha and gnu parameters), the tensile stress to tensile strength ratio, and the compressive stress to compressive strength ratio were also included in the AAMAS study. Their respective ratings are listed in Table 2.6.

The AAMAS findings and conclusions tend to confirm those reported earlier by Baladi (3), who also provided correlations of the test factors to some of the basic properties of the mix. For example, Baladi stated that the indirect tensile strain at failure decreases with increasing the kinematic viscosity of the asphalt binder. The tensile

Table 2.6 : Summary of ranking of mixture properties related to pavement performance, (38).

FACTORS	DISTRESS MANIFESTATIONS			
Fundamental Engineering Properties:	Permanent Deformation	Thermal Cracking	Fatigue Cracking	Moisture Damage
Resilient Modulus	3	3	5	1
Creep Modulus	5	5	3	1
Tensile Strain At Failure	1	4	5	1
Indirect Tensile Strength	3	0	0	1
Other Properties & Factors:				
Particle Orientation	3	3	3	0
Alpha and Gnu	5	1	2	0
Tensile Strength Ratio	2	0	3	5
Resilient Modulus Ratio	3	0	2	4
Compressive Strength Ratio	2	0	0	2

strength, on the other hand, was related to the test temperature, air voids in the mix, the aggregate angularity, and the kinematic viscosity of the asphalt. He stated that higher indirect tensile strength implies higher fatigue life and higher resilient modulus of the AC mix. The higher tensile strength can be obtained by using a lower air void in the mix, higher aggregate angularity, higher kinematic viscosity of the AC binder, lower temperatures, or by combination thereof. It should be noted that aggregate angularity was qualified relative to three descriptive terms: rounded, a mix of 50 percent by weight crushed and 50 percent rounded, and 100 percent crushed. No attempt was made to differentiate between those aggregates that were crushed on 1, 2, 3, or 4 faces.

2.3.8 Effects of Mix Manufacturing and Field Placement on AC Mix Performance

The objectives of the asphalt concrete mix design include the determination of the aggregate gradation that meets the required specifications in terms of percent voids in mineral aggregates (VMA), percent air voids, density, and stability. Any change from the specifications will affect both the rut and the fatigue life of the AC mix. The rut and fatigue potentials of AC mix are significantly affected by the compacted density of the mix. Hence, factors related to manufacturing, laying, and compacting asphalt mixes that affect the density will also affect the pavement rut and fatigue cracking potentials. Further, most of the aging of the AC binder takes place during the mix manufacturing and transporting, and during pavement construction. Hence, these factors affects the fatigue and low temperature cracking potentials.

Scherocman and Acott (39) studied the affect of AC mix manufacturing, transportation, and placement on pavement performance and reported that:

1. **Manufacturing**- A number of factors can affect the quality of the aggregate during mix production. The most important one is the proportion of each aggregate delivered from the cold feed bins of asphalt plant. Secondary factors

are segregation and contamination with foreign material and dust. The handling of the asphalt cement during the production of the asphalt concrete mixture can affect the properties of the produced mix in a number of ways. A reduction in the stiffness of the asphalt concrete mix (caused by a variation in the asphalt content) can greatly change the characteristics of the mix. The second most significant factor is the aging or hardening of the binder during production. Proper storage of the AC binder in the asphalt plant tank, will not cause appreciable hardening of AC binder. On the other hand, if the material is overheated, excessive hardening of the binder asphalt cement can occur.

2. **Placement** - Ambient temperature, wind velocity, and rain at the time of mix placement affect the ability of the paver to properly distribute the asphalt mixture across the roadway and to compact them. The ambient temperature will affect the rate of cooling of the mix and thus, its change in stiffness. Although, environmental conditions during placement does not directly affect the rut and fatigue cracking potentials, they affect the compaction process which in turn influences the mix performance. Further, inadequate placing can produce a teared and rough surface causing increase in the air void contents. The higher air contents affect both the rutting and fatigue cracking potentials of the AC mix.

3. **Compaction** - The primary effect of environmental conditions on the compaction of an asphalt concrete mix is on the time available for compaction. Higher air temperatures, cause a lower rate of cooling and provide a longer time period for compaction (typical minimum compaction temperature is 175°F). Three types of compaction equipment are normally used to compact asphalt concrete mixtures: static steel wheel rollers, pneumatic tire rollers, and vibratory rollers. Each type of roller exerts its own compaction efforts. Compaction equipment which is capable of densifying the mix more quickly produces lower air voids in the mix. In general, vibratory rollers are able to impart a greater degree of density per

pass to the mix than are pneumatic tire rollers and static rollers. All roller types however, can achieve the same level of density in the mix if enough time is available for proper compaction.

2.4 PERMANENT DEFORMATION PREDICTION MODELS

The proper pavement design and pavement management systems must be capable of predicting the pavement performance with time, the service life, and the remaining service life of the pavement structures. Rut is one type of distress that must be predicted during the pavement design and the pavement evaluation processes. In several countries, an overlay is applied when the rut depth of the pavement is of the order of 20 to 30 mm. In the U.S.A., the maximum acceptable rut varies from one State Highway Agency (SHA) to another and it depends on the pavement class (interstate versus farm to market roads).

Current rut prediction models can be divided, in general, into two groups: mechanistic and mechanistic/empirical. The mechanistic models are based either on the theory of elasticity, theory of plasticity, or the viscoelastic theory.

Barksdale (40,41), Heukelon and Klomp (42), Romain (43) and others have suggested that layered elastic theory can be used to calculate the induced stresses and strains in the pavement due to traffic. The plastic strain can be assumed to be proportional to the elastic strain and the number of load repetitions. In this type of analysis, the relationship between the plastic strain and the applied stress for each pavement component can be obtained from laboratory repeated load test along with either linear or nonlinear elastic theory. Nonlinear theory should provide more accurate results, but its use has been limited because of its complex nature. Rut prediction cannot be made directly from plastic stress-strain relationship although, it provides a considerable insight regarding material behavior.

Barksdale and Leonards (44) suggested that rutting can be estimated by assuming that the pavement can be represented as a viscoelastic layered system. The plastic strain can then be predicted by using the material characteristics obtained in the laboratory from the creep tests. Elliot and Moavenzadeh (45) suggested the use of the linear rather than the nonlinear viscoelastic theory due to its mathematical complexities for predicting structural response.

Morris (5) cited Kenis and a study conducted at Washington State University Test Track and reported that the rut prediction obtained by using linear viscoelastic theory were substantially lower than the actual measured rut depth. For the test track, after 247,000 load repetitions, the linear viscoelastic theory predicted rut depth in the order of 5 to 10 percent of the actual measured ones.

The complexities involved with the theoretical prediction models tempted the researchers to develop mechanistic/empirical models to predict rutting. Some of these models are presented below.

Leahy and Witczak (46) assessed the influence of repeated triaxial test conditions and mix parameters on the permanent deformation characteristics of asphalt concrete and presented a statistical model of the form:

$$\log_{10} \epsilon_p = -15.83 + 7.132 \times \log_{10}(T) + 1.105 \times \log_{10}(S) - 0.118 \times \log_{10}(V) + 2.155 \times \log_{10}(EAC) + 1.117 \times \log_{10}(VOL) + 0.986 \times (TTEMP^{-0.102} \times VMA^{-0.198}) \times \log_{10}(LN) \tag{2.1}$$

$$R^2 = 0.82$$

Where;

ϵ_p = permanent deformation;

T = test temperature (°F);

S = deviator stress (lb/in^2);

V = viscosity at 70° F (10^6 poise);

EAC = effective asphalt content (percent by volume);

VOL = percent air void;

TTEMP = test temperature (°F);

VMA = percent void in mineral aggregates; and

LN = load repetition.

A sensitivity analysis of the above equation showed that the temperature is by far the most significant variable. The model is less sensitive to loading conditions, material type and mix parameters (46).

Based on laboratory test data Morris et al. (6) presented the following regression equation, to predict pavement rutting:

$$\epsilon_p = f(\sigma_1, \sigma_2, T, N) \pm E \quad (2.2)$$

Where

ϵ_p = amount of permanent strain;

σ_1 = vertical stress;

σ_2 = horizontal stress;

T = temperature;

N = number of load applications; and

E = The estimate of error associated with any attempt to predict ϵ_p as a function of the other four factors.

The laboratory developed model was used to predict the observed rutting at the Barmpton Road Test. Although the model does not account for the effect of the AC thickness, the binder type, and the percent air voids, the overall predicted and observed values were comparable as shown in Figure 2.19.

Baladi (47) correlated AC mix and other pavement layers properties to predict the rut depth in the AC layer. He presented an equation of the form:

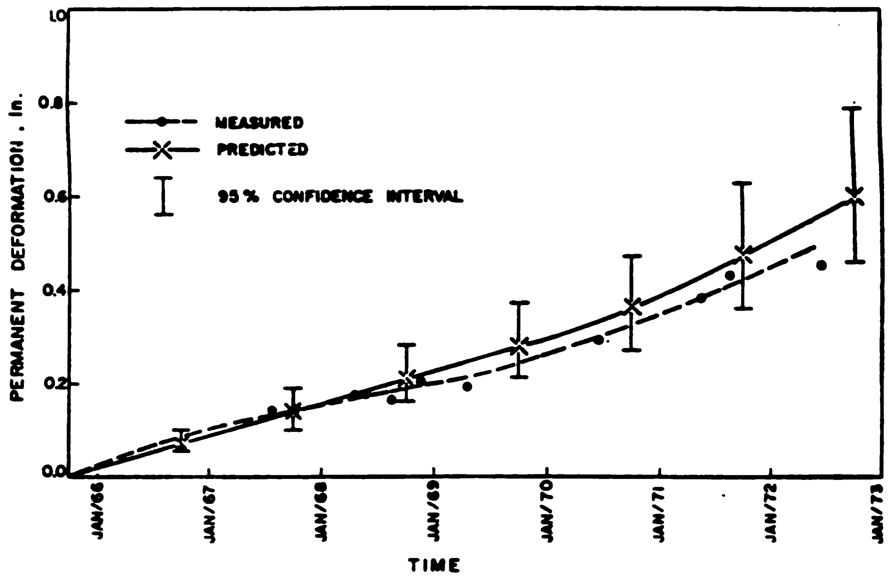

Figure 2.19 : **Permanent deformation as a function of time (Brampton Road Test section 3), (6).**

$$\begin{aligned} LOG(RD) = \; & -1.6 + 0.067\times(AV) - 1.4\times(\log(TAC)) + 0.07\times(AAT) \\ & - 0.000434\times(KV) + 0.15\times(\log(ESAL)) - 0.4\times(\log(MR_{RB}) \\ & - 0.50\times(\log(MR_{B}) + 0.1\times(\log(SD)) + 0.01\times(\log(CS)) \\ & - 0.7\times(\log(TB_{EQ})) + 0.09\times(\log(50-(TAC + TB_{EQ}))) \end{aligned} \tag{2.3}$$

where

LOG = natural log;

RD = rut depth (inch);

AV = the percent air void in the mix;

TAC = thickness of AC layer (inch);

AAT = average annual temperature (°F);

KV = kinematic viscosity at 275 °F (AASHTO T-201) (centistrokes);

ESAL = the number of 18-Kip ESALs at which the rut depth is being calculated;

MR_{RB} = resilient modulus of roadbed soil (psi);

MR_B = resilient modulus of the base material (psi);

SD = pavement surface deflection (inch);

CS = compressive strain at the bottom of the AC layer; and

TB_{EQ} = equivalent thickness of base material (inch), which is the actual thickness of the base layer plus the equivalent thickness of the subbase layer; equivalent thickness of the subbase layer is equal to the actual thickness of the subbase layer reduced by the ratio of the modulus of the subbase to that of the base material.

Baladi, concluded that air voids is the most important factor affecting rut and higher air voids lead to higher rut potential.

2.5 LABORATORY FATIGUE CRACKING MODELS

Several Phenomenological and mechanistic models have been suggested to represent fatigue cracking. Phenomenological models are based on Miner's law. They express "internal damage" in terms of crack geometry, stress, strain and the energy in the vicinity of the damaged region irrespective of the molecular mechanisms involved. The main drawbacks of these models are that they do not satisfactorily account for the influence of pavement geometry and material heterogeneities and they do not provide a quantitative measure of the extent of cracking in pavements. Mechanistic models are complex, impractical to use, although they do provide quantitative description of the degree of cracking in pavements (48).

Pell and Cooper (49) studied the effects of AC mix factors on the laboratory fatigue life of asphalt mixes. Mix variables were correlated to the laboratory fatigue life and the following regression equation with a correlation coefficient of $R^2 = 0.877$ was reported.

$$\log N = 4.13 \times \log(V_B) + 6.95 \times \log(T_{R,B}) - 11.13 \qquad (2.4)$$

where

N	=	laboratory fatigue life;
V_B	=	volume of binder(percent of total volume); and
$T_{R\&B}$	=	ring and ball temperature.

To make use of laboratory results they didn't suggested any shift factor. Based on their study they concluded that asphalt content is the most important variable affecting the fatigue life.

Baladi (3) used the results of stress-controlled indirect tensile tests on Marshall size specimens, to develop a fatigue model using statistical methods. His model is presented below:

$$LOG(N_f) = 36.631 - 0.1402 \times (TT) - 2.300 \times LOG(CL) - .5095 \times (AV) - .001306 \times (KV) + .06403 \times (ANG) \qquad (2.5)$$

where

LOG	=	natural log;
N_f	=	laboratory fatigue life;
TT	=	test temperature (°F);
CL	=	cyclic load (pounds);
AV	=	air void (percent);
KV	=	kinematic viscosity (centistoke);
ANG	=	aggregate angularity.

Based on limited field observations of in-service flexible pavements in Michigan and Indiana, Baladi reported that the predicted laboratory fatigue life of asphalt samples were 20 times less than the fatigue life of the observed pavements.

Irrespective of the procedure used, fatigue life of a pavement cannot be predicted with a reasonable accuracy due to the following reasons:

1. Fatigue life is dependent upon the stress distribution in the materials and other environmental and material factors.
2. The stress distribution in a pavement system depends upon the thickness and the characteristics of the different pavement layers.

2.6 MATERIAL ALTERATION

Rutting and Fatigue cracking are the primary load related distresses in flexible and composite pavements. Efforts are being made to overcome this problem by changing the design methodology, altering the material properties and by use of additives. Various asphalt additives are being promoted to increase the stability of asphalt mixes and to improve their performance. For example, the use of large size aggregates and little fines is often arbitrary recommended to optimize the interaction and contact among the coarse aggregate particles in the mixes and to overcome the problem of rutting. Brown et al

(24) evaluated the performance of different aggregate gradations using aggregate maximum nominal size of 1½ to ½-inch (see Table 2-7). They observed significant increases in the creep performance, resilient modulus and tensile strength as the maximum nominal size increases: whereas, the maximum nominal size has no significant effect on Marshall stability. Other researchers (25, 28, 50) also recommended the use of larger size crushed aggregates with low angular sand content to improve the resistance of asphalt mixes to rutting and fatigue cracking.

Recent development in Europe produced AC mixes that consist of high percent contents of coarse aggregate, asphalt binder, and low percent content of sand-size particles (the mix is called Stone Mastic Asphalt ,SMA) (51). SMA mixtures are being used in the U.S.A and in the State of Michigan. Comparison of the aggregate gradation for SMA and Michigan 20AAA rut resistance mix are shown in Figure 2.20. Due to an increase amount of crushed aggregate, which provides face to face aggregate contacts and interlocking, the SMA gradation provides a better guard against rutting. Presently, the Federal Highway Administration is in the process of evaluating the SMA's feasibility for its implementation in the U.S.A.

To improve the performance of asphalt concrete, a variety of materials have been promoted over the years as asphalt binder modifiers. For a modifier to be successful, the benefits offered by its use should offset the increase in the cost of production of the asphalt mix. Binder modifiers can be classified into 6 generic types as shown in Table 2.8. The most common modifiers used by State Highway Agencies are polymers. Polymer modified asphalts have the following potential benefits over straight asphalts:

1. Increasing the viscosity of the binder at high temperature.
2. Reducing the thermal susceptibility of the binder.
3. Increasing the cohesion of the bitumen.
4. Increasing the resistance to permanent deformation.

Table 2.7 : Gradation ranges for asphalt concrete mixes, (24).

	Grading Designation				
Sieve Designation	A	B	C	D	E
2 inch	100	--	--	--	--
1 ½ inch	97-100	100	--	--	--
1 inch	--	97-100	100	--	--
¾ inch	66-80	--	97-100	100	--
½ inch	--	--	76-88	97-100	--
⅜ inch	48-60	53-70	--	--	100
No. 4	33-45	40-52	49-59	57-69	97-100
No. 8	25-33	25-39	36-45	57-69	62-81
No. 40	9-17	10-19	14-22	14-22	22-37
No. 200	3-8	3-8	3-7	3-8	7-16
(Federal Highway Administration)					

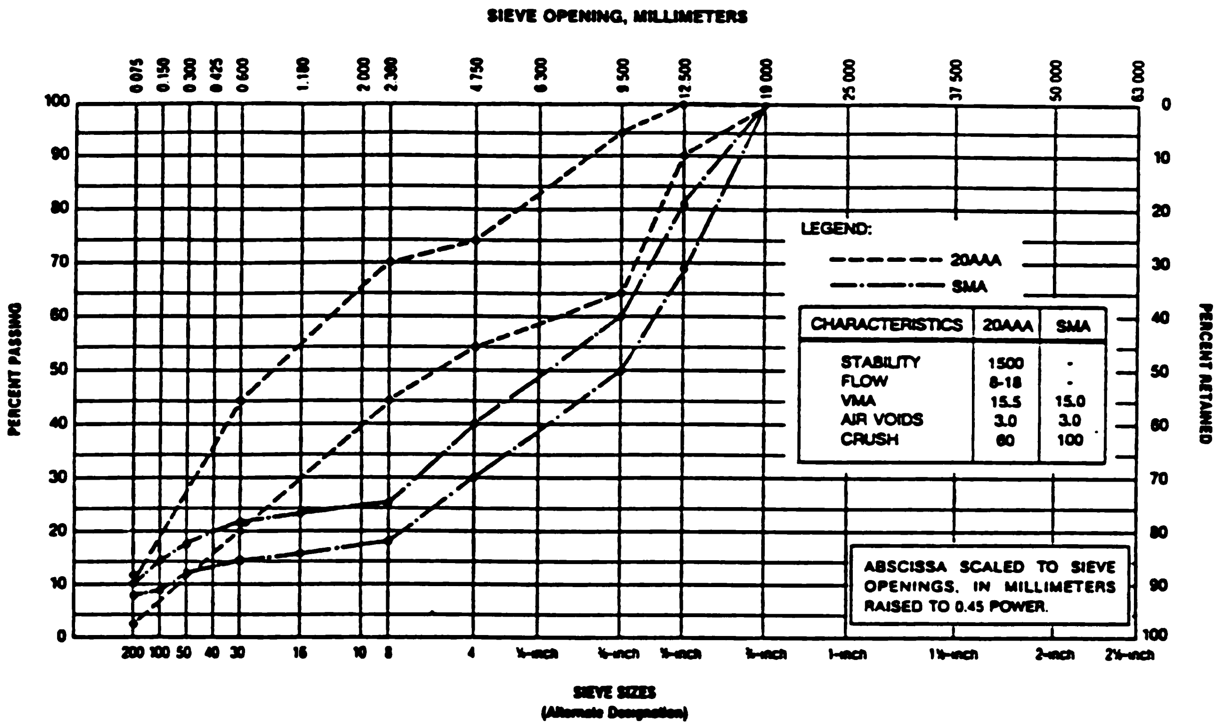

Figure 2.20 : **Aggregate gradation curves and mix design criteria: SMA compared with MDOT 20AAA (51).**

Table 2.8 : Different binder modifiers.

Modifier Type	Modifiers Encountered	Most Promising Modifiers
Dispersed Thermoplastics	Polyethylene (PE), Ethylene acrylic copolymer Atactic polypropylene (APP), Polypropylene Wax (PPW), Ethylene acrylic copolymers, Hydroxylterminated Polybutadiene (HTPB)	PE
Network Thermoplastics	Neoprene, Styrene-butadiene-styrene (SBS), Styrene-ethylene-butadine-styrene (SEBS), Styrene-butadiene copolymer (SBR), Styrene-butadiene latex, Ethylene-vinyl acetate (EVA)	SBS/SEBS,SBR
Reacting Polymers	Epoxy, Elvaloy, AM, Furfural, Maleic anhydride (MAH), Chromium trioxide (CrO_3)	Epoxy
Fiber	Cellulose fiber, Mineral fiber, Glass fiber, Polyester fiber.	Cellulose fiber
Rubber	Microfil 8, Crumb rubber modifiers (CRM) from passenger car and truck tires	Microfil 8, CRM
Others		

Collins et al. (53) reported that an AC mix containing 6 percent by weight of Thermo Block Copolymers (TBC) lead to a 7.5-fold increase in rut resistance. Based on a comprehensive series of laboratory tests using polymer additives, Carpenter and Vandam (54) concluded that polymer modified asphalt cement, particularly at high temperatures, slightly increased the fatigue resistance of bituminous mixtures and significant improved rutting at 100 °F.

Under the SHRP program (52), 38 asphalt modifiers were evaluated by surveying various State Highway (SHA) and binder manufacturers. Based on the results of the survey, the following conclusions were made:

1. Polymers were identified to be the best suited against permanent deformation (see Figure 2.21, 2.22 and Table 2.9,2.10).
2. Polymer and reclaimed rubber improve the asphalt mix resistance against fatigue cracking.

Higgins (55) suggested the use of liquid modifiers and reported that Manganese-based modifiers improve the strength and reduce the deflection of full-depth asphalt concrete so that heavy loads may be supported over an extended time period.

Today, a number of asphalt additives are sold in the market with the claims of improving the asphalt mix resistance against key distresses. These additives usually add significantly to project cost, therefore, it is important to determine their effectiveness under field conditions and to evaluate the cost effectiveness of their use.

2.7 MATERIAL CHARACTERIZATION

2.7.1 State of Stress

Under a static load uniformly applied to a circular area at the top of a full depth asphalt, the elements immediately below the center of the loaded area are subjected to principal stresses vertical "σ_1" and horizontal "σ_3" . Figure 2.23 shows the distribution

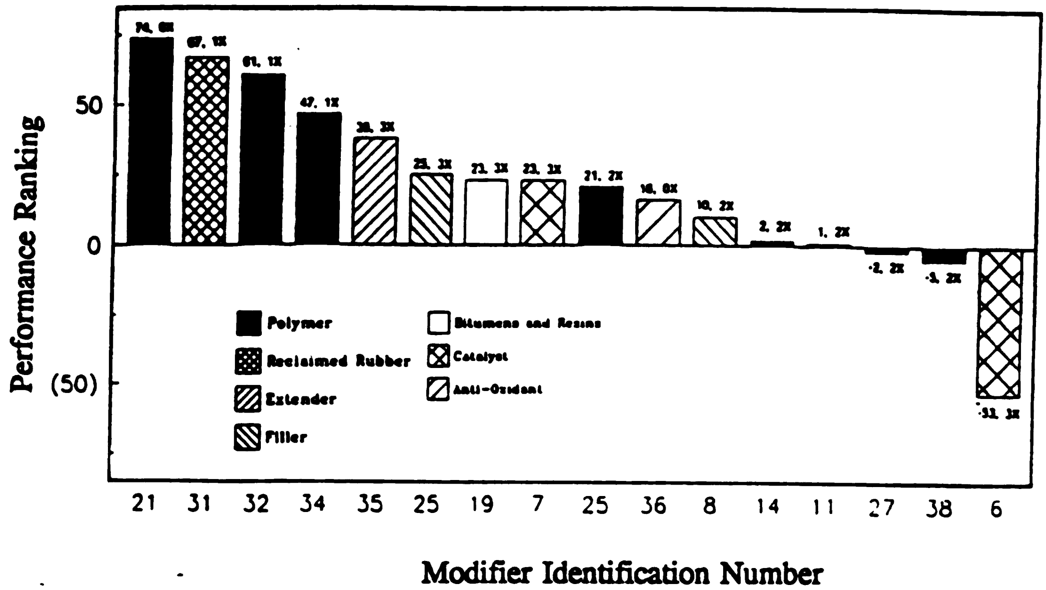

Figure 2.21 : **Modifier ranking bar chart for fatigue cracking (52).**

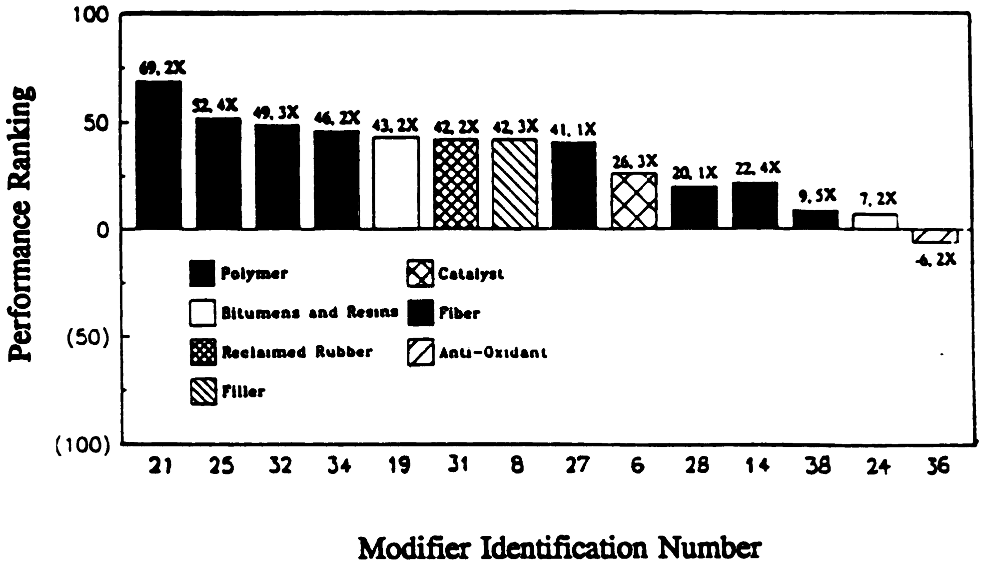

Figure 2.22 : **Modifier ranking bar chart for permanent deformation (52).**

Table 2.9 : Analysis of SHA questionnaire: Modifiers most commonly used (52).

Responses	
Modifiers	(Percent)
A. Polymers	86
B. Anti-Stripping Agents	77
C. Fillers/Fibers/Extenders	59
D. Recycling Agents	43
E. Catalyst	25
F. Aging Inhibitors	16
G. Others:	
Ground Tire Rubber	36
Gilsonite	9
Trinidad Lake Asphalt	7

Table 2.10 : Analysis of SHA questionnaire: Primary targeted pavement distress (52).

Responses	
Distress	(Percent)
A. Permanent deformation	24
B. Fatigue Cracking	20
C. Moisture Susceptibility	21
D. Low Temperature Cracking	20
E. Aging	15

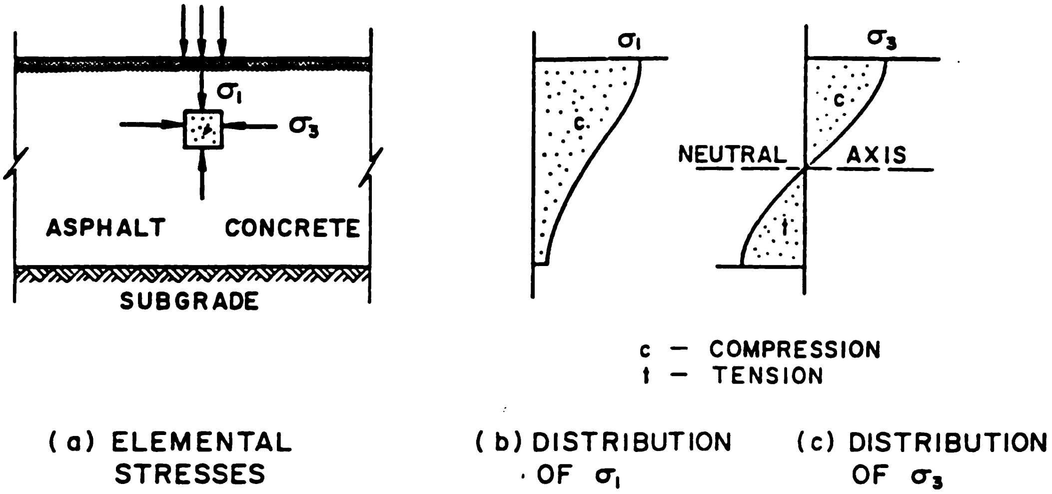

Figure 2.23 : Typical pavement stress distribution under static loading.

of σ_1 and σ_3 with depth. Different state of stress are induced in asphalt concrete pavements due to a wheel load as shown in Figure 2.24. These states of stress and their relative locations are:

1. Compression at the surface and immediately underneath the wheel.
2. Lateral tension combined with vertical compression at the bottom of the AC layer and immediately underneath the load.
3. Lateral tension at the surface at some distance from the load.
4. Lateral compression at the bottom of the AC layer at some distance from the load.

These state of stresses cannot be duplicated in the laboratory. Consequently, different tests are needed to represent different stress states. To evaluate the asphalt mix properties, several tests are presently being used. The Marshall, Hveem and Hubbard tests are used to determine the proportioning of the different components in the mix. Triaxial, indirect tensile and flexural tests are used to determine structural properties needed as input to mechanistic and mechanistic-empirical pavement design methods. Presently, the only laboratory technique that can be used to closely duplicate the field stress conditions is the wheel tracking test. A scaled model of the pavement section representing field condition is constructed in the laboratory and traffic loading is simulated by a loading wheel mechanism capable of applying different load intensities. The wheel tracking test however, is not available in most of the research facilities. Hence, researchers often utilize conventional testing techniques.

Asphalt mix tests (e,g,. Marshall) provide information relative to proportioning of different components in the mix. However, they do not provide any information

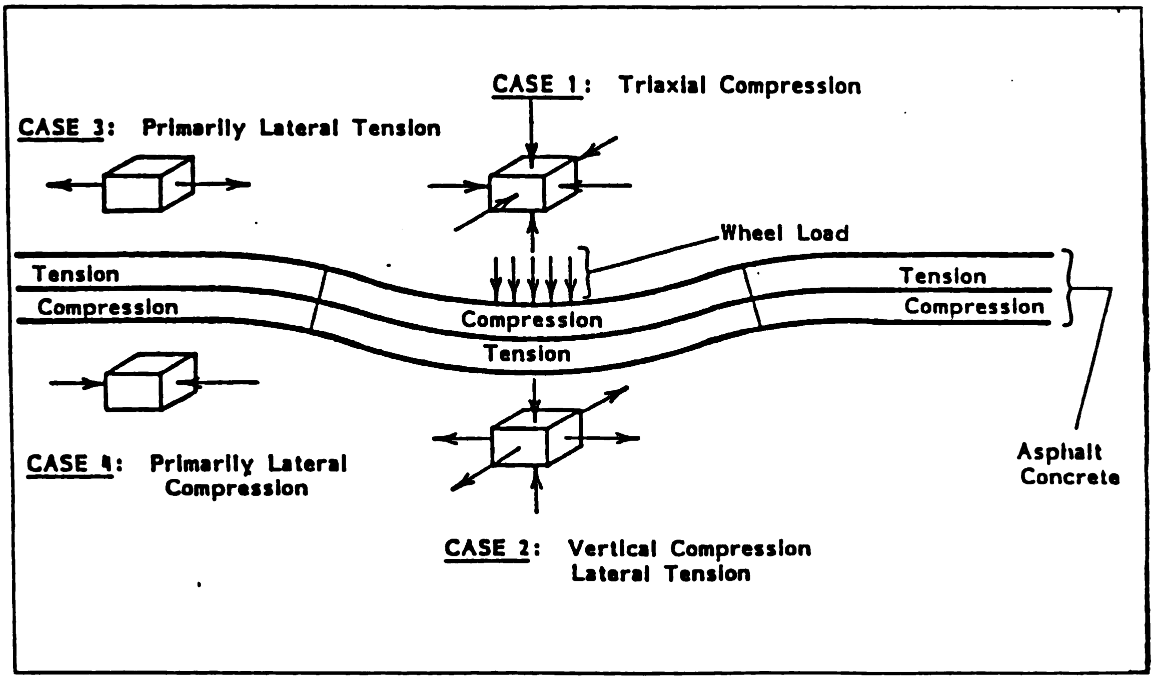

Figure 2.24: Typical stress states in the asphalt concrete layer with wheel load applied.

regarding the structural properties (e.g, permanent deformation, fatigue life) which are needed for the design of the pavement structure (3). Hence, a second group of tests (triaxial, indirect and flexure) are used to determine the structural properties of the mixes.

Triaxial test was recommended and used by researchers (6,56,57,58) for material characterization due to its low cost and relatively accurate estimates of material properties. In this test, cylindrical samples are used to determine the stress-strain behavior. The samples may be subjected to a lateral confining stress and an axial stress is applied to the ends of the sample. In a conventional triaxial test, the axial load is steadily increased and the sample deformation is monitored until failure. In the triaxial cyclic load test, the sample is subjected to a constant or a pulsating confining pressure, and a cyclic axle load (simulating a moving load). The main limitations of triaxial tests are (30,59):

1. The presence of end friction between the specimen's cap and the loading mechanism which restricts lateral deformations.
2. Lack of capability to apply shear stresses to simulate a moving load.

Recall that the critical location for fatigue cracking and rutting (due to lateral distortion in the tension zone) of the asphalt layer is located at the bottom of the layer (see Figure 2.1), where tensile stresses can be found along with vertical compression. This configuration of stresses can be simulated in the indirect tensile test.

Several researchers recommended (6,60,61) the use of tensile test to characterize the pavement deformations. Reynaldo (62) cited Roque and Ruth and reported that modulus values determined using strain gauge measurements obtained in the vicinity of the center of the face of an indirect tension specimen resulted in admirable predictions of the strain and deflections measured on full scale pavements at low in-service temperatures. Baladi (63), pointed out the problems with the existing indirect tensile test apparatus (Schmidt's apparatus). He devised a new indirect tensile test apparatus and after testing 412 Marshall size test samples using the new apparatus reported that:

1. The test results were consistent and very reasonable.
2. Maximum of only seven percent difference was observed between results for any triplicate.
3. Poisson's ratio was found to be a function of the mix variable and its value varied from 0.2 to 0.42 for all specimens. For any triplicate specimen, the values were almost the same.
4. More meaningful, reasonable and consistent fatigue lives were obtained for all test specimen as compared to flexural cyclic load tests.
5. The plastic deformation can be analyzed both in compression and tension modes and the test results were more consistent than those obtained from cyclic load triaxial tests.

The indirect cyclic tensile test procedure recommended for the Baladi's apparatus is practically the same as that found in the ASTM D-4123 with the exception that deformations can be measured in all three directions. The indirect tensile testing mode seems to be both practical and versatile for determining the properties of asphalt concrete and it was employed in this research.

2.8 TEST PARAMETERS

In order to predict the behavior of inservice pavement from the results of laboratory tests on different pavement components, it is essential to perform the testing in a way to simulate field conditions. Hence, the test parameters must be chosen to closely represent the most realistic field conditions. The effects of test parameters on the test results are discussed in the following subsections.

2.8.1 Pulse Shape

Barksdale (64) noted that, in the field, the form of the stress pulse changes with depth. He reported that vertical stress pulse varies from a near sinusoidal near the top of the pavement structure to a more triangular shape at the lower portion of the base course. Allan and Thompson (65) described the vertical stress pulse as generally sinusoidal with a sharper peak near the surface and a flatter top in deeper portions of the base course. In general, sinusoidal wave form simulates traffic loading better than any other wave form and it was adopted in this study.

2.8.2 Pulse Duration and Rest Period

The stress pulse applied by a moving wheel loads (under actual in-service conditions) lasts about 0.01 to 0.1 of a second (30). This duration time is mainly dependent upon the speed of the vehicle and the position of the element under consideration within the pavement structure. The speed of a vehicle is inversely related to the load duration. That is, the load duration decreases with the increase in the velocity of the vehicle.

Maclean (cited by Morris (5)) reported that (for a limited number of load applications) the rest period is an important factor affecting permanent deformation. Snaith (cited by Morris (5)) conducted his testing with and without rest periods for higher number of load repetitions. He concluded that the rest period is not a significant variable. Bonnaure et al. (66), tested 9 by 1.2 by 0.8-inch rectangular beam specimens in the stress and strain controlled modes and reported the effects of the rest period upon the fatigue characteristics of asphalt concrete mixes. They observed higher number of load cycles to failure for longer rest periods. They concluded that the most beneficial rest period is equal to 25 times the loading period. Young (30) reported insignificant effects of the rest period on the resilient modulus of a bituminous mixture for the conditions of short stress duration and low temperature. However, it has significant effects at higher temperatures when the behavior of the asphalt mixes is nonlinear. Baladi (3) and Roque (67) used a rest period of 0.4 seconds for their studies. In general, conflicting data exists on the effects of stress duration and rest period. For the purpose of this study a load duration period of 0.1 second and a rest period of 0.4 second were selected. These two periods, simulate the loading time of one axle load and the time delay at a point between two consecutive axles of a vehicle travelling at 55 miles per hour.

Brown and Snaith (56) reported an increase in the permanent strain with a decrease in the frequency of the applied vertical stress. They added that permanent strain is time dependent for frequencies of more than 1 cycle per second. Terrel and Awad (68) reported similar findings to those of Brown and Snaith. Monismith et al. (69) studied the effects of load frequency and stress reversal on the fatigue properties of asphalt mixtures. They used a frequency range from 3 to 30 cycles per minute. They concluded that, for a given load level, higher frequencies causes lower strain and that the test frequency has no effect upon the mix behavior in repeated flexure. Many researchers (56,63,68) have employed 0.1 second loading time and 0.4 second relaxation period which are considered to appropriately simulate traffic loading.

2.9 SUMMARY

Rutting and fatigue cracking of asphalt surfaced pavement structures are load-related distresses that are affected by several factors including:

1. The asphalt mix properties.
2. Inadequate construction practices (e.g., compaction, segregation).
3. Softening of the asphalt binder due to high temperatures.
4. Strength and type of the materials used in the various pavement layers.

5. Softening of the base, subbase, and roadbed materials due to moisture infiltration and freeze-thaw cycles.

6. Heavy multi-axle vehicles.

Although all the pavement layers (AC, base, subbase and roadbed soil) contribute to rutting and fatigue cracking, the contribution of the asphalt concrete (AC) layer alone could be very significant. Adequate asphalt mix design, manufacturing, and construction practices, increase the resistance of the AC layer to rut and fatigue cracking. The AC mix variables that affects rutting and fatigue cracking potentials include:

1. The percent coarse aggregates and sand contents in the mix.
2. The aggregate angularity.
3. The percent asphalt content.
4. The asphalt grade (viscosity or penetration).
5. The percent air voids.

Numerous statistical fatigue cracking and rut depth models for AC surfaced pavements have been developed. Generally, the models are based on laboratory data (laboratory prepared samples) and are extended to predict field rut and fatigue cracking by using a transfer or a shift function. These models are either based, solely on the material properties or they take into account the effect of 18-kip ESAL. Further, existing shift factors are generalized for all pavement sections.

The use of laboratory prepared samples to evaluate AC mixes have some drawbacks. For example, the laboratory prepared samples may or may not represent the actual conditions in the field such as the level of compaction. Hence, the use of core samples eliminates this problem.

The significance of the AC mix variables affecting rut and fatigue cracking potentials using laboratory prepared samples is affected by the test conditions and the range of the values of the variable in question. For example, a low percent contents of coarse aggregate has an insignificant impact on the rut and fatigue cracking resistance of the AC mix. However, investigating the coarse aggregate at high contents will have a significant affect on the rut and fatigue cracking resistance as the aggregate interlocking is mobilized due to aggregate face to face contact (26, 51).

The effect of the aggregate angularity on rut and fatigue cracking potential is often evaluated in terms of the percent contents of angular (crushed) and rounded (uncrushed such as river gravel) particles without considering the number of the crushed faces (3). For example, aggregates crushed on one face only would not have the same effects as those crushed on 3 or 4 faces.

The objectives of the asphalt concrete mix design include the determination of the aggregate gradation that meets the required specifications in terms of the percent voids in mineral aggregates, the percent air voids in the mix, density, and stability. Any change from the specifications will affect rut and fatigue life of the AC mix. Hence, manufacturing, laying, and compacting asphalt mix practices that cause appreciable variation in the properties of the compacted AC mix would impact the pavement rut and fatigue cracking potentials.

To this end, the objectives of this study are to:

1. Select test sections that are representative of the various pavement sections encountered throughout the State of Michigan and are subjected to various levels of traffic load and volume.
2. Obtain representative core samples.
3. Test the pavement cores to determine their physical and engineering properties.
4. For each cored pavement section, determine the variability of the material and layer thicknesses along the section. This information can be used to calibrate the construction practices and to enhance the existing quality control.
5. Develop a test procedure to characterize aggregate angularity in terms of the number of crushed faces.
6. Determine the combined effects of traffic and material properties on pavement

rutting.

7. Asses the laboratory fatigue life of the pavement cores and develop a relationship between the fatigue life and the asphalt mix properties.

8. Develop shift factors relating the laboratory and field fatigue lives.

CHAPTER 3

RESEARCH PLAN

3.1 INTRODUCTION

The research plan for this study has evolved around the policy, practices, and acceptance specifications of the Michigan Department of Transportation (MDOT) regarding the asphalt mix design procedure. Thus, for completion, the MDOT policy and standard specifications are addressed below.

As is the case for most State Highway Agencies (SHA), the MDOT policy and standard specifications for asphalt mix design have changed over time. Three sets of specifications that belong to three time periods can be identified as follows:

1. AC mixes made prior to 1979 (see Table 3.1).
2. AC mixes made between 1979 and 1992 (see Table 3.2).
3. AC mixes made after 1992 (see Table 3.3).

As it can be seen from Tables 3.1 and 3.2, the basic features of, and differences between, the early (prior to 1979) AC mixes and those made between 1979 and 1992 are:

1. The specifications and tolerance limits for the AC, base and binder courses are the same in both sets of specifications. For the base course, the percent passing of six sieves (1.5", 1", 3/8", No. 8, No. 30, and No. 200) are specified. For the binder course, on the other hand, the percent passing of 4 sieves are specified. The maximum possible percent sand (passing the number 8 sieve) contents for the base and binder courses are 65 and 45 percent, respectively.
2. For the two sets of AC mixes number 4.09 and 4.11; and 4.13 and 4.22; the specifications and tolerance limits in both sets are the same.
3. For the AC mix number 4.12, the earlier specifications have been enhanced by adding tolerance limits for sieve number 4 and modifying the percent passing for

Table 3.1 : MDOT specifications and tolerance limits for various AC courses (prior to 1979).

Bituminous Mixture	Usage	Aggregate	Total Percent Passing Designated Sieves									Bitumen % in Mix
			1½-in	1-in.	¾-in.	½-in.	⅜-in.	No.5	No.8	No.30	No.200	
3.05	Base Course	20C	100	80-100			55-90		30-65	15-45	0-12	3-6
4.09	Bit.Agg.	20AA			100	95-100	65-90		45-70	20-45	2-10	4-8
	Surface	20A			100		60-90		40-65	20-40	2-10	4-8
	Course	20B			100		60-95		40-70	20-45	2-12	4-8
4.11	Bit.Agg.	20AA			100	95-100	65-90		45-70	20-45	3-10	5-7
	Pavement	20A			100		60-90		40-65	20-40	3-10	5-7
4.12	Binder	9A,3CS,3FS	100	98-100					25-45		0-5	4-8
	Leveling	25A,3CS,3FS			100	98-100			25-45		0-5	4-8
	Leveling	31A,3CS,3FS				100	98-100		25-45		0-5	4-8
	Wear.Ty.C	25A,3CS,3FS			100	98-100			45-70		4-8	5-8
	Wear.Ty.CM	25A,3CS,3FS			100	98-100			55-65		3-8	5-8
	Wear.Ty.M	31A,3CS,3FS				100	98-100		50-70		4-9	5-9
	Wear.Ty.F	31A,3CS,3FS				100	98-100		70-90		5-10	5-10
4.13	Sand Asphalt	3CS,3FS						100			4-10	5.5-8.0
	Pre-Coated Sand	3CS,3FS						100				0.5-1.5
4.22	Sand Asphalt	25A,3CS,3FS			100	98-100			55-70		7-15*	6.5-9.0
	Pre-Coated Sand	31A,3CS,3FS				100	98-100		55-70		7-15*	6.5-9.0

When asbestos fiber or powdered asphalt additives are used, the Engineer may specify other limits for Passing No. 200 sieve.

Table 3.2 : MDOT specification and tolerance limits for various AC courses (1979-1992).

Bituminous Mixture		Usage	Aggregate	Total Percent Passing Designated Sieves										Bitumen
Former	New			1½ in.	1 in.	¾ in.	½ in.	⅜ in.	No.4	No.5	No.8	No.30	No.200	%in Mix
3.05	No.5	Base Course	20C	100	80-100			55-90			30-65	15-45	0-12	3-6
4.09	No.9,20AA	Bit.Agg.	20AA			100	95-100	65-95			45-70	20-45	2-10	5-8**
	No.9,20A	Surface	20A			100		60-90			40-65	20-40	2-10	5-8**
	No.9,20B	Course	20B			100		60-95			40-70	20-45	2-12	5-8**
4.11	No.11,20AA	Bit.Agg.	20AA			100	95-100	65-90			45-70	20-45	3-10	5-7**
	No.11,20A	Pavement	20A			100		60-90			40-65	20-40	3-10	5-7**
4.12	No.12B	Binder	A,3CS,3FS	100	98-100						25-45		0-5	4-8
	No.12LC	Leveling	25A,3CS,3FS			100	98-100		30-60		25-45	15-35	0-5	4-8
	No.12LF	Leveling	31A,3CS,3FS				100	98-100	30-60		25-45	15-35	0-5	4-8
	No.12WC	Wear.Ty.C	25A,3CS,3FS			100	98-100		55-75		45-70	25-45	4-8	5-8
	No.12WCM	Wear.Ty.CM	25A,3CS,3FS			100	98-100		55-75		55-65	25-45	3-8	5-8
	No.12WM	Wear.Ty.M	31A,3CS,3FS				100	98-100	60-85		50-70	25-45	4-9	5-9
	No.12WF	Wear.Ty.F	31A,3CS,3FS				100	98-100			70-90		5-10	5-10
4.13	No.13	Sand Asphalt	3CS,3FS							100			4-10	5.5-8.0
	PreC.Sand	Pre-Coated Sand	3CS,3FS							100				0.5-1.5
4.22	No.22	Sand Asphalt	25A,3CS,3FS			100	98-100				55-70		7-15*	6.5-9.0
		Pre-Coated Sand	31A,3CS,3FS				100	98-100			55-70		7-15*	6.5-9.0

* When asbestos fiber or powdered asphalt additives are used, the Engineer may specify other limits for Passing No. 200 sieve.
** When these mixtures are placed in 2 courses, the bitumen content of the first course placed will be designed to have upto .5 percent less bitumen than the optimum specified for the top course.

Table 3.3 : MDOT AC mix design criteria (1992).

MIXTURE NO.	2		3		4						
MIXTURE TYPE	C	B	C	B	C	B	13A	13	11A	36A	36B
VMA MIN %	12.5	12.0	14.5	14.0	15.5	15.0	14.5	14.0	12.0	16.0	15.5
AIR VOIDS %TARGET	3.0	3.0	3.0	3.0	3.0	3.0	3.0	3.0	3.0	3.0	3.0
FINES/ASPHALT RATIO MAX	1.2	1.2	1.2	1.2	1.2	1.2	1.2	1.2	1.2	1.2	1.2
FLOW HUNDERTHS OF AN INCH	8-16	8-16	8-16	8-16	8-16	8-16	8-16	8-16	8-16	8-16	8-16
L. A. ABRASION MAX. % LOSS	40	40	40	40	40	40	40	40	50	40	40
SOFT PARTICLE MAX.(%by weight)	5.0	5.0	5.0	5.0	5.0	5.0	5.0	5.0	5.0	5.0	5.0
FINE AGG. ANGULARITY	4.0	3.0	4.0	3.0	4.0	3.0	2.5	2.0	2.5	3.0	2.5

sieve number 8.

4. The 1979-1992 specifications requires that (for AC mixes placed in two courses), the percent AC binder of the lower course be 0.5 percent lower than that of the upper course.

5. Both sets of specifications do not address the percent air voids in the mix or the percent voids in mineral aggregates.

The 1992 specifications (see Tables 3.3 through 3.6) are based on several criteria including:

1. The percent air voids in the AC mix and the percent voids in mineral aggregates.
2. The maximum ratio by weight of the fines to the AC binder.
3. The angularity of the fine aggregates (sand).
4. The Marshall flow.
5. Maximum losses by weight of 40 and 50 percent based on the Los Angeles abrasion tests.
6. One directional commercial average daily traffic (ADT).
7. Thickness of the AC layer.

The new specifications (1992) are more strict in terms of the percent passing through any particular sieve. For example, comparing the new base mixes 2C (see Table 3.4) and No. 5 base mix (see Table 3.2) it can be seen that, for the No. 5 mix the percent by weight in the mix of the aggregate larger than the ⅜-inch sieve, can be any where from 10 to 45. Whereas, for base mix 2C, the maximum percent passing the ⅜ sieve has been specified, thus, ensuring that the mix contain more of the coarser aggregate. Comparison between the new (1992) and the old (1979) specifications indicates that, in general, the new specifications calls for less amount of fine (minus #200 sieve) and higher percent of crushed aggregates (plus #4 sieve) depending on the one directional commercial ADT in the design lane (see Table 3.5). Table 3.6 presents the recommended placement thickness and usage of the mixes. The new specifications were

Table 3.4 : MDOT specifications and tolerance limits for AC mixes (1992).

MIXTURE NO.	2		3		4						
MIXTURE TYPE	C	B	C	B	C	B	13A	13	11A	36A	36B
BITUMEN %	3-6	3-6	4-7	4-7	5-8	5-8	5-8	5-8	4-6	5-8	5-8
SIEVE NO.	PERCENT PASSING THE INDICATED SIEVE										
1 ½ inch	-	-	-	-	-	-	-	-	100	-	-
1 inch	100	100	-	-	-	-	-	-	80-95	-	-
¾ inch	90 max	90 max	100	100	-	-	100	100	70-90	-	-
½ inch	78 max	78 max	90 max	90 max	100	100	75-95	75-95	60-80	100	100
⅜ inch	70 max	70 max	77 max	77 max	90 max	90 max	60-90	60-90	55-80	92-100	92-100
No. 4	52 max	52 max	57 max	57 max	67 max	67 max	45-80	45-80	35-75	65-90	65-90
No. 8	20-40	20-40	28-45	28-45	33-52	33-52	30-65	30-65	25-65	55-75	55-75
No. 16	10-30	10-30	18-33	18-33	20-37	20-37	20-50	20-50	20-50	-	-
No. 30	8-22	8-22	10-25	10-25	15-27	15-27	15-40	15-40	15-40	25-50	25-50
No. 50	5-17	5-17	5-19	5-19	10-20	10-20	10-25	10-25	8-25	-	-
No. 100	4-15	4-15	5-15	5-15	5-15	5-15	5-15	5-15	4-15	-	-
No. 200	3-6	3-6	4-6	4-6	4-6	4-6	3-6	3-6	3-6	4-10	4-10
Crushed Min %	95	50	95	50	95	50	25	0	25	60	40

Table 3.5 : MDOT AC mix selection criteria (1992).

One Way Commercial ADT	Mixture Type	Crushed Aggregate % by weight
0-99	13 or 11A	0 or 25
100-250	A	25
251-10000	B	50
1001-3500	C	95
Over 3500	Special Provision	

Table 3.6 : Recommended AC mix placement thickness (1992).

Mix Type	Course (lift)	Single Course Thickness (inch)
2B, 2C*	Base	2 to 2½
3B, 3C*	Base, Level	1¼ to 2½
4B, 4C	Top	1 to 1½
11A *	Base	2 to 3½
13, 13A*	Base, Level, Top	1¼ to 2½

* Use bituminous mixture-11A for any base course over 2½" total thickness (regardless of commercial ADT) except for rubbelized concrete projects. For rubbelized concrete projects use bituminous mixture-C or B for the base course regardless of the thickness. First layer over rubbelized concrete shall be a minimum of two inch.

adopted (April 1992) after the start of this study. Therefore, the new mixes are not included in this study.

3.2 RESEARCH PLAN

Over the last few decades, the number of heavy multi-axle trailers using Michigan roads has substantially increased. This resulted in higher rutting and fatigue cracking potentials. The resistance of the AC mixes to rut and fatigue cracks is a function of the AC mix properties (percent coarse and fine aggregate, angularity of the aggregate, and the asphalt binder content and viscosity), the pavement design process, construction practices and environmental factors. Recall that (see Chapter 2) one of the SHRP studies concluded that forty percent of rutting, sixty percent of fatigue cracking and eighty percent of thermal cracking potential may be attributable to the asphalt binder alone whereas, the remaining percentages of the respective distresses can be attributed to the other properties of the AC mix and to the overall design of the pavements. This suggests that rut and fatigue cracking resistance of AC mixes can be enhanced by changing the properties of the AC mixes to withstand the present day traffic conditions and to perform satisfactorily over the design life.

Research studies need to be conducted to establish the AC mix factors that enhance the resistance against rutting and fatigue cracking of the mix. Study of factors affecting the rut and fatigue cracking potentials of the AC mixes involves several steps including (see Figure 3.1):

1. Selection of existing pavement sections having various asphalt grades and percent asphalt contents, aggregate types and angularity, gradation, and various types of fines and percent fine contents, various AC thicknesses, different levels of traffic volume and load, and different service lives.
2. For each selected pavement section, the rut and fatigue cracking data are

measured and core samples are obtained. Because of economical reasons and time constraints, the number of cores have to be limited. Variations of the pavement properties along the pavement sections can be analyzed by using nondestructive deflection testing data. The deflection basins may also be used to analyze the rut potential of those pavements.

3. The cored samples are then brought to the laboratory for testing to determine the asphalt mix properties. These include the elastic, viscoelastic and plastic properties, gradation, the asphalt content, the air voids and the angularity of the aggregate.

4. A statistical study whereby the properties obtained in step 3 are related to the rut and fatigue cracking data of step 2.

5. A sensitivity analysis whereby the effects of the various parameters of the statistical models of step 4 on the rut and fatigue life are assessed.

Details of the pavement site selection and the field and laboratory investigations are presented in Chapter 4.

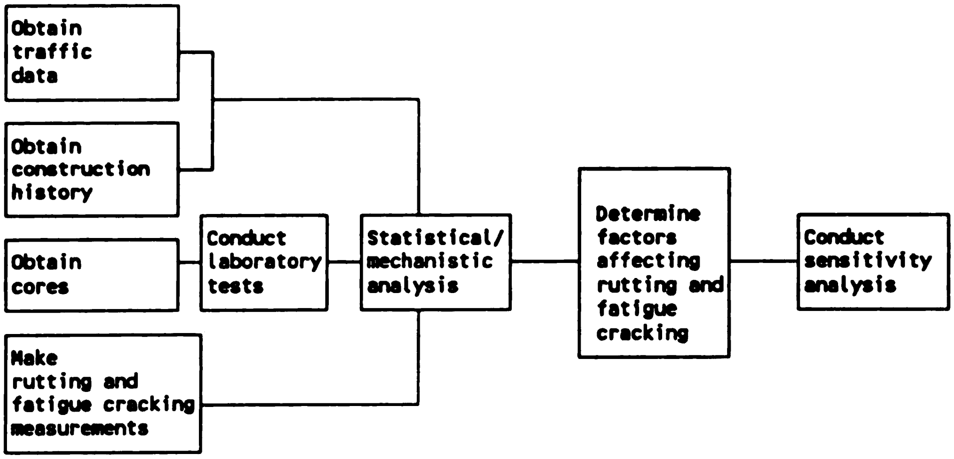

Figure 3.1 : Overall research plan.

CHAPTER 4

FIELD AND LABORATORY INVESTIGATION

4.1 PAVEMENT SELECTION

The pavement section selection was accomplished in consultation with personnel from the Michigan Department of Transportation (MDOT). The main criterion used in this selection is that the selected sections should represents the spectrum of pavement cross-sections, paving materials, and traffic volume and load found throughout the State of Michigan. In this regard, the following variables were identified and prioritized prior to the selection of the pavement sections.

1. Asphalt Course Thicknesses - Thin (less than 3-inch), moderately thick (3- to 6-inch), and thick (more than 6-inch) asphalt surface.
2. Traffic Volume and Load - Heavy, moderate, and light traffic loads and volumes in terms of the 18-kip equivalent single axle load (ESAL).
3. Pavement Types - flexible pavement without overlays, flexible pavements with overlays, and PCC pavements with overlays.
4. Cross-Sections - One layer (AC only), two layers (AC and base), and three layers (AC, base and subbase).
5. AC Mixes - Stability based and standard type mixes.
6. Roadbed Type - Cohesive and cohesionless soils.
7. Pavement Surface Age - Newly constructed and/or rehabilitated (less than 3-year old) and older pavement sections.
8. Distress Types - Rut and fatigue cracking.

Table 4.1 provides a list of the combination of variables used to prioritize the various flexible and composite pavement sections and the weight factors assigned to each variable. The values of the weight factors are based on the importance of the variable in

Table 4.1 : Criteria for finial section selection.

Flexible Pavements		Composite Pavements	
Factor	Weight	Factor	Weight
Traffic (ESAL)		Traffic (ESAL)	
Light	3	Light	3
Heavy	4	Heavy	4
Thickness (inch)		Thickness (inch)	
Thin < 3"	3	Thin < 3"	2
Medium 3 To 6"	2	Medium 3 To 6"	3
Thick > 6"	2	Thick > 6"	4
Cross Section		AC Overlay	
2 Layers	3	1 Course	2
3 layers	2	2 Course	2
4 layers	2	3 or more Courses	3
AC Courses (no overlay).		Number of Overlays	
Less than 3	1	1 Overlay	2
More than 3	1	2 or more Overlays	2
AC (overlay)	1	Overlay Age (years)	
		Less than 3	2
Roadbed Soil		New Mix	2
Sand	2	Old Mix	2
Clay	2		
Pavement Age (years)		Pavement Distress	
Less than 3	2	Fatigue	2
New Mix	2	Rut	2
Old Mix	2	fatigue and Rut	2
Pavement Distress			
Fatigue	2		
Rut	2		
Fatigue and Rut	4		

question to this study. For example, heavy traffic loads (high percent commercial vehicles travelling the pavement section) were assigned a weight factor of 4 while light traffic loads were assigned a weight factor of 3. Likewise, a weight factor of 2 was assigned to each of the following types of distress, fatigue cracking and rut. Hence, the weight factor of a pavement section showing either rut or fatigue cracking is 2 the weight factor for a pavement showing both fatigue cracking and rut is 4, and the weight factor of a pavement section with no fatigue cracks and/or rut is zero.

Based on the above criteria and the various variables, 200 pavement sections (150 flexible and 50 composite) of variable lengths (one to several miles) were initially selected. For each pavement section, the MDOT pavement management system data base and the MDOT 1987 sufficiency rating book were used to obtain the location reference point, construction and rehabilitation history, rut, fatigue cracking, stripping, other distress data, traffic volume and load, cross-sectional data (layer thicknesses and types), and other general information. The data was then tabulated in a spreadsheet.

For each of the 150 flexible and 50 composite pavement sections, a score (based on the variables and their weight factors) was then calculated. A pavement score consists of the sum of the weight factors assigned to each variable. The pavement section with the highest score was given the highest priority. Based on the pavement score (priority), the 49 flexible and 15 composite pavement sections with the highest priorities were chosen and they are included in this study. Tables 4.2 and 4.3 provide lists of the flexible and composite pavement sections chosen in this study. Other data such as pavement type, route number, direction (north, south, east, or west bound), district, control section number, and the beginning and ending mile post of each pavement section are also listed in the Tables.

For each of the 49 flexible and 15 composite pavement sections, the pavement condition data (obtained from MDOT data bank) was examined. It should be noted that the MDOT data bank does not identify fatigue cracking as a separate distress category.

Table 4.2 : Selected flexible sections.

Section No.	Pave ment Type	Route I =11 US=22 M =33	Dir. N=1 S=2 E=3 W=4	District	Control Section	Mile Post From	To
1	AC	3366	1	3	40031	2.00	13.00
2	AC	3350	3	8	23052	1.30	14.00
3	AC	3334	3	8	46041	1.50	11.20
4	AC	3372	3	3	40023	0.00	8.00
5	AC	3328	3	1	66022	3.00	14.40
6	AC	3350	4	5	34021	4.50	8.00
7	AC	22131	1	5	54014	8.00	11.10
8	AC	33138	3	6	79011	16.70	19.90
9	AC	3320	4	5	54022	0.00	0.60
10	AC	3328	3	1	31021	4.60	9.60
11	AC	3344	3	5	41051	4.20	5.20
12	AC	1196	3	5	61152	1.20	5.40
13	AC	2227	1	3	18034	1.31	1.80
14	AC	3377	1	2	75052	8.00	10.00
15	AC	2227	2	4	20016	0.00	6.30
16	AC	22131	1	3	83031	2.50	3.00
17	AC	22131	1	5	54013	0.50	8.41
18	AC	2227	1	4	20016	0.00	6.30
19	AC	1175	1	4	69013	0.00	6.00
20	AC	3366	1	5	59051	11.90	13.20
21	AC	3319	1	6	74032	0.00	10.00
22	AC	3382	4	5	62041	0.00	5.90
23	AC	3328	3	1	66023	6.60	11.00
24	AC	3399	1	8	33011	4.30	4.60
25	AC	22131	2	3	83031	3.00	2.00
26	AC	3357	3	6	25102	2.85	2.95
27	AC	1175	1	4	72061	7.00	13.40
28	AC	1175	1	4	16093	0.00	5.90
29	AC	3399	1	8	23092	2.20	7.30
30	AC	1175	1	4	69013	6.00	7.00
31	AC	3326	4	1	66051	0.00	4.00
32	AC	22131	1	5	59012	11.00	11.10
33	AC	22131	2	5	54014	8.50	8.60
34	AC	33129	1	2	17072	12.10	19.30
35	AC	1175	1	4	16091	0.00	1.50
36	AC	1175	2	4	72061	13.30	7.00
37	AC	1175	1	4	72061	19.00	23.66
38	AC	3366	1	3	57013	8.20	12.71
39	AC	222	3	2	21024	4.80	14.80
40	AC	1175	1	4	20015	4.10	9.10
41	AC	1175	1	4	20015	9.10	14.20
42	AC/RC	1194	3	7	11015	13.00	15.00
43	AC	1194	3	7	11015	3.00	7.00
44	AC	2223	1	4	71073	24.70	26.71
45	AC	1175	1	4	20015	0.00	1.00
46	AC	3366	1	3	40031	0.00	1.22
47	AC	3361	3	3	18041	8.65	8.92
48	AC	3349	1	8	30011	11.00	17.00
49	AC	1175	2	4	72061	16.80	17.50

Table 4.3 : Selected composite sections.

Section No.	Pavement Type	Route I =11 US=22 M =33	Dir. N=1 S=2 E=3 W=4	District	Control Section	Mile Post From	Mile Post To
1	Composite	1194	4	8	81104	5.60	7.90
2	Composite	1194	4	8	81104	1.90	5.60
3	Composite	3350	3	8	46081	1.10	3.00
4	Composite	22127	1	8	30071	0.00	4.90
5	Composite	2241	1	1	7023	8.48	14.01
6	Composite	22223	3	8	46061	2.80	3.60
7	Composite	22127	1	8	46011	4.50	5.18
8	Composite	3350	3	8	46081	8.30	13.20
9	Composite	2241	1	1	7013	0.00	3.10
10	Composite	3350	3	8	46081	3.00	8.30
11	Composite	3325	3	6	32012	12.00	19.90
12	Composite	3325	3	6	32012	19.90	27.90
13	Composite	22127	1	8	30071	9.80	10.30
14	Composite	22127	1	8	30071	4.90	9.80
15	Composite	1175	1	9	63173	9.25	9.50

Rather, it identifies the severity and extent of cracking (which includes all types of cracking). That is, when cracking data is found in the data base, it implies that the cracked pavement section may have edge cracking, temperature cracking, fatigue cracking, transverse cracking, or a combination thereof. Consequently, only the rut data in the MDOT data bank were considered accurate and relevant. Nevertheless, the rut data for each pavement section was examined and, within each section, several 100-feet long pavement sites showing rutting problem were identified and they were labeled as test sites. For some pavement sections, the test sites were adjacent to each others while for some others, they were separate.

During the Summer of 1991, four members of the Michigan State University (MSU) research team visited each test site. The purposes of the visit were to:

1. Verify the location reference point, pavement type, and general conditions.
2. Mark the test sites.
3. Inspect, measure, and record the extent and severity of rutting, fatigue cracking and other types of distress.
4. Identify those test sites to be cored by MDOT.
5. Mark locations for nondestructive deflection tests (NDT) within each test site.

The rut depth was measured by using a six foot straight-edge leveling rod, a graduated triangular wedge with an accuracy of 0.025-inch and a scale with accuracy of 0.06-inch. The rut was measured in the outer wheel path over each marked core location and at several other locations along the test site. The fatigue crack was recorded in terms of severity and the percent of the 100-feet long test site showing alligator cracking. Further, a total of 107 locations were designated for pavement coring. Each test site and NDT and core locations were given specific designation numbers. The coring method and the designation numbers are presented in the next section.

4.2 MARKING, CODING, CORING AND NDT

Each test site was designated by a two-number system. One number designates the pavement section and the other designates the test site. For example, a test site designation of 29-1 indicates the first test site of pavement section number 29. It should be noted that, for all pavement sections, the test site number increases from south to north and from west to east.

Some test sections were selected for coring (see Table 4.4). The cores were located either in the outer wheel path, between the wheel paths, or in the inner wheel path of the traffic lane. In addition, some cores were located over an existing longitudinal crack. Each core location was designated using a seven digit number. Starting at the left-most digit, the first two digits indicate pavement section number; the third digit indicates pavement type (1 for flexible and 2 for composite); the fourth digit designates the site number; the fifth and sixth digits indicate the distance of the core location from the beginning of the site; and the seventh digit indicates the core number within that site. For example, a core location designation of 2712402 indicates (left to right) that the test is conducted on section 27, flexible pavement, test site number 2, at 40 feet from the beginning of the site, and is the second core at the site.

The cores were obtained by using a power auger equipped with a 6-inch coring bit. A hand auger was preferred over a power auger to obtain disturbed samples from non-stabilized base, subbase and roadbed soil. The reason for this is that different layers can be easily identified. Most of the cores obtained from the wheel paths were utilized for resilient modulus and, extraction testing to determine material properties and fatigue life. The laboratory test procedures are presented in section 4.3 of this chapter.

Non-destructive deflection tests (NDT) using a falling weight deflectometer (FWD) were also conducted at several locations along each test site. The NDT tests were divided into two categories as follows.

Table 4.4 : List of cored sections.

Section No.	Proposed			
	Total AC Thickness	Concrete Thickness	Base Thickness	Subbase Thickness
	(inches)			
7F	7.2	0	4	18
10F	4.54	0	6	18
13F	4.17	0	8	32
14F	2.93	0	6	18
19F	3.75	0	8	8
29F	13.5	0	11	0
35F	7.25	0	8	28
43F	12.44	0	6	18
1C	10.5	8	0	0
4C	2.75	8	0	0
5C	5.9	8	0	0
8C	4.5	8	0	0
11C	4.09	8	0	0

1). Regular tests - Each test site (100' long) was subjected to five FWD tests (a test is 3 drops). The tests were conducted at equal intervals of 20' starting at the beginning of the test site.

2). Additional tests - For cored test sites, additional FWD tests were conducted over the core location.

Each FWD test is designated by using an eight digit number. Starting at the left most digit, the first two digits indicate pavement section number; the third digit indicates pavement type (1 for flexible and 2 for composite); the fourth digit designates the site number; the fifth and sixth digits indicate the distance of the test location from the beginning of the site; the seventh digit indicates the sequential drop number (drop number 1, 2 or 3); and the eighth (right most) digit indicates test location (0 indicates regular test in the outer wheel path, 1 for additional test in the outer wheel path, 2 for additional test at the center of the lane, 3 for additional test in the inner wheel path, 4 for a test at a joint in the outer wheel path, and 5 for a test at a joint in the inner wheel path). For example, an FWD test designation of 27124020 indicates (left to right) that the test is conducted on section 27, flexible pavement, test site number 2, at 40' from the beginning of the site, and is the second drop of a regular test in the wheel path.

4.3 LABORATORY INVESTIGATIONS

This section provides a summary of the laboratory test procedures used to determine the physical and engineering characteristics of the materials. Various laboratory tests were conducted to assess the properties of the core materials obtained from the various test sites. Since these tests are standards of the American Society for Testing and Material (ASTM), only the ASTM test designation numbers and the purpose of the tests are mentioned. For details of the test procedure, the reader is referred to the "Annual Book of ASTM Standards" Volume 4.03.

As noted earlier, all pavement cores were obtained by MDOT. The cores were then transported to the MSU laboratories and they were:

1. Inspected to document the possible existence of distress such as cracking and stripping, and to determine the thicknesses of the various AC courses.
2. Subjected to specific gravity tests to determine the bulk specific gravity (ASTM D-2726) before cutting and handling.
3. Cut by sawing to obtain 2.5-inch thick test samples.

The 2.5-inch thick, 6-inch diameter samples were then subjected to the following tests.

1. Bulk specific gravity (ASTM D-2726).
2. Indirect cyclic load test to determine the resilient modulus, fatigue life, and permanent deformation characteristics along the horizontal and vertical diameters of the samples.

After the completion of the indirect tensile tests, several test samples of similar AC courses and thicknesses were combined along with some of the untested cores. The combined materials were then subjected to extraction tests. The purpose of the extraction tests are to determine:

1. The percent asphalt, fine, sand, and coarse aggregate contents.
2. The penetration of the recovered asphalt cement.
3. The top size and gradation of the aggregates.
4. The coarse aggregate angularity.
5. The theoretical maximum specific gravity of the AC mix.

A brief description of each test procedure and data reduction are presented in the next sections.

4.3.1 Indirect Cyclic Load Tensile Test for Bituminous Mixtures

Several researchers recommended the use of indirect tensile test to characterize compacted asphalt mixes (6,59,60,61,62). Baladi (62,70,71), pointed out some of the problems associated with some existing indirect tensile test apparatus (e,g., the Schmidt's apparatus) and devised a new one. He concluded that tests conducted by using the new apparatus are:

1. Consistent and very reasonable.
2. Repeatable (a maximum of only seven percent difference was observed between results obtained from any triplicate specimens).
3. More meaningful, reasonable, and consistent fatigue lives were obtained for all test specimen as compared to flexural cyclic load tests.

Hence, the Baladi's new device (see Figure 4.1) along with an MTS closed loop servo-hydraulic system were used in this study. Details regarding the testing equipment can be found else where (72). The data acquisition software is contained in appendix "A". A modified version of the ASTM standard test procedure D-4123 was used to determine the resilient characteristics and fatigue lives of the asphalt mixes. Modifications of the D-4123 test procedure include:

1. A 50 pounds sustained load was used. The ASTM standard procedure does not specify any value for the sustained load.
2. The ASTM recommended cyclic load range is 10 to 50 percent of the tensile strength of the test sample. The older specifications recommended cyclic load of 25 pounds. A cyclic load of 300 pounds was used.

   The reasons for these modifications are:

   a). Under a 25 pounds cyclic load, the sample deformation along its thickness was within the accuracy of the measuring system (Linear variable differential transformers with .00001-inch accuracy).

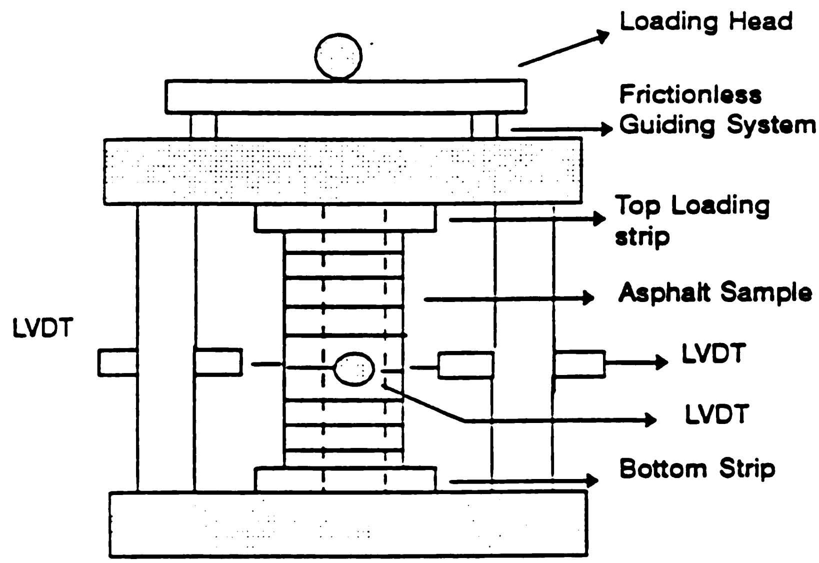

Figure 4.1 : Baladi indirect tensile test apparatus.

b). The test results obtained by using the 300 pounds cyclic load were more consistent than those using the 25 pounds cyclic load.

All the indirect cyclic load tensile tests were conducted to failure. During each test, the sample resilient and permanent deformations were collected along the vertical and horizontal diameters and along the thickness of the sample. Since only the deformation from any 2-directions are required to calculate the resilient modulus and Possion's ratio of the specimen, the least square technique was used such that the sum of the errors between the properties calculated by using the data from any 2-directions were minimized (3,62,70,71). This resulted in the following equations for resilient modulus and Possion's ratio of a 6-inch diameter sample (Harichandran, R. S., 1992, private communication, Department of Civil Engineering, Michigan State University, East Lansing):

$$D = 1.1045791\,(H^2+V^2+A^2) - (H - 0.0627461\,V + 0.319145\,A)^2 \tag{4.1}$$

$$MR = (0.253680\,H - 3.9702876\,V - 0.0142874\,A)/D \tag{4.2}$$

$$\nu = (0.225127\,H^2 - 0.269895\,V^2 - 0.086136\,AH - 3.570975\,HV - 1.145064\,AV)/D \tag{4.3}$$

where;

- H = $D_H\,L/P$;
- V = $D_V\,L/P$;
- A = $D_A\,/P$;
- D_H = the horizontal resilient or total deformation of the specimen along the horizontal diameter (inch);
- D_V = the vertical resilient or total deformation of the specimen along the vertical diameter (inch);
- D_A = the longitudinal resilient or total deformation along the longitudinal axis (thickness) of the specimen (inch);

P	=	the magnitude of the applied cyclic load (pounds);
M_R	=	the total or resilient modulus depending on the type of deformation used (psi);
L	=	the sample thickness (inch); and
υ	=	the total or resilient Possion's ratio.

The resilient modulus and Possion's ratio were calculated at load cycle number 500 by using equations 4.1 through 4.3. Further, the following protocol was used for all samples:

1. For each cored pavement section, 3 cores were used to obtain 6-inch diameter and 2.5-inch thick test samples. The bulk specific gravity of the sample was determined prior to the commencement of the cyclic test.
2. On the average, 2 test samples of 2.5-inch thick were obtained from each core. The location of each test sample within the core was a function of the thickness of the core and the thicknesses of the various asphalt courses within the core. Care was taken as not to include more than one asphalt course in one sample.
3. For all cores with an asphalt course thickness of more than 2.2-inch, a test sample was sawed from the core such that the sample consisted of only one asphalt course.
4. For all cores with an asphalt course thickness of less than the required minimum of 2.2-inch, the test sample was sawed from the core such that one test sample consisted of two or more courses. Hence, only the global behavior of the asphalt courses were determined.
5. No tests were conducted on any friction course.
6. For test samples with more than one asphalt course, the age of all courses within the sample were the same. Asphalt courses having different ages were not combined in one test sample.
7. For all pavement sections that were subjected to more than one rehabilitation

activity and historical rut and fatigue cracking data were not available, the test samples were obtained from those asphalt courses for which distress data was available.

8. A total of 78 samples were tested in the cyclic load indirect tensile test. This implies that at least 2 samples from each of three cores of the 13 cored test sections were tested.

Based on the above protocol, the test samples were sawed as close to the 2.5-inch thickness as possible. The samples were then marked using the respective code of the core with an extension of one more digit. For example, a test sample designation number of 29172711-1 indicates (left to right) that the test sample is from pavement section 29, flexible pavement, test site 7, at 27 feet from the beginning of the site, first core in the site, located in the wheelpath and the extension of 1 indicates that the sample was obtained from the top 2.5-inch portion of the core.

After sawing, the bulk specific gravity of each test sample was determined and the sample was left to dry for a 48-hour period at room temperature. After drying, each sample was inspected. Those samples that showed uneven and rough vertical surfaces were rejected.

The cyclic load indirect tensile tests were conducted at room temperature (about 75°F). First, the test sample was placed on the lower loading strip of the indirect tensile test apparatus such that its vertical diameter was parallel to the MTS actuator. Five LVDT's were then mounted and their initial (reference) readings were recorded. The sample was then preconditioned under 100 load cycles using 300 pounds cyclic load. During the preconditioning, the sample position on the lower loading strip was adjusted as to eliminate any measurable differential horizontal movement. After sample conditioning, the test was commenced and continued until failure. Throughout the test the 300 pounds cyclic load was applied at a frequency of 2 cycles per second. Each load cycle consisted of 0.1 second loading and unloading time, followed by a 0.4 second relaxation period.

4.3.2 Maximum Theoretical Specific gravity Tests

The maximum theoretical specific gravity (Gmm) of each AC course was determined by using the ASTM D 2041 standard test procedure. After the test, the percent air voids in the AC mix was calculated by using the following equation:

$$P_a = 100\left(\frac{G_{mm} - G_{mb}}{G_{mm}}\right) \tag{4.4}$$

Where

P_a = the air voids in the compacted asphalt mixture, percent of total volume;

G_{mm} = the maximum theoretical specific gravity of the paving mixture; and

G_{mb} = the bulk specific gravity of the compacted mixture.

The ASTM D-2726 standard test procedure defines bulk specific gravity as the ratio of the mass of a given volume of material at 25° C to the mass of an equal volume of water at the same temperature. This test method is only recommended for dense graded or practically non absorptive compacted mixtures. The bulk specific gravities of the entire core prior to cutting and of the indirect cyclic test samples were determined by using the above ASTM procedure. The core specific gravity data was used to determine the air voids of the entire core whereas, the test sample specific gravity of each test sample was used to determine its air voids content.

After failure of the test samples in the indirect tensile mode, they were sawed down to individual layers presenting different AC mixes. The bulk and maximum theoretical specific gravities were determined according to the ASTM D 2726 and D

2041 procedures. The maximum theoretical specific gravity procedure requires a minimum sample weight of 2000 grams for maximum aggregate size of ¾-inch. Whenever it was not possible to obtain enough material for the maximum theoretical specific gravity test, layers (same AC mix) from two different cores of the same section were combined to obtain enough material. The maximum theoretical specific gravities for different layers of 13 cored sections are presented in Table 4.5. Cores or test samples having more than one layer, the maximum theoretical specific gravity and the bulk specific gravity were calculated for each individual layer. Further, the weighted average (the sum of the products of the specific gravity of each layer and its respective thickness divided by the entire thickness of the core/test sample) specific gravity was also calculated.

4.3.3 Extraction Tests

After the determination of the maximum theoretical specific gravity, the samples were subjected to extraction test in accordance with the ASTM D 2172 standard test procedure. The tests were conducted to determine the AC mix composition. This test separates the asphalt cement in the AC mix from the aggregate. Thus, the AC mix composition such as, the percent asphalt, fine, sand and aggregate contents can be determined. It should be noted that, the test results may be affected by the age of the asphalt mix. Older mixes tend to yield slightly lower bitumen content due to aggregate absorption. It is difficult to remove all the asphalt when some aggregate types are used and some chlorides may remain within the mineral matter affecting the measured asphalt content. Nevertheless, trichloroethylene was used as solvent and bitumen content was established by difference from the mass of the extracted aggregate, moisture content, and mineral matter in the extract. The bitumen content (see Table 4.5) was expressed as percent by the weight of the moisture-free mixtures as follows:

Table 4.5 : Results of extraction, penetration and maximum theoretical specific gravity tests for all AC courses of the cored pavement sections.

Section No.	Prop. AC Thickness (inches)	Percent AC	Recovered Penetration	Coarse Agg. Angularity	Max. Th. Sp. Grty
7F					
Layer1	1.2	5	77	3.45	2.482
Layer2	1.5	4.4	39	1.79	2.525
Layer3	4.5	4.1	32	1.96	2.51
10F					
Layer1	1.18	7.7	48	3.427	2.451
Layer2	1.09	6.8	63	3.783	2.481
Layer3	2.27	3.6	13	3.82	2.583
13F					
Layer1	1.18	6	39	4.488	2.464
Layer2	1.18	5.4	45	5	2.504
Layer3	1.81	5.5	53	5	2.464
14F					
Layer1	0.75	5.7	62	3.11	2.468
Layer2	1.18	5.4	84	3.03	2.477
Layer3	1	7.4	185	3.45	2.81
19F					
Layer1	1	5.1	12	4.644	2.486
Layer2	1.25	5.9	70	2.885	2.456
Layer3	1.5	5.2	43	3.453	2.478
29F					
Layer1	1	5.5	38	4.407	2.466
Layer2	1.5	4.8	47	4.294	2.525
Layer3	11	4.6	43	1.476	2.512
35F					
Layer1	1	6.7	27	4.89	2.444
Layer2	1.25	5	25	4.68	2.5
Layer3	5	5.4	22	4.67	2.472
43F					
Layer1	1.36	6.1	85	2.813	2.467
Layer2	1.27	6.8	45	2.838	2.496
Layer3	0.81	5.1	40	4.162	2.519
Layer4	9	5.1	39	4.157	2.576
1C					
Layer1	1.25	5.8	50	4.654	2.485
Layer2	1.25	5.4	43	4.394	2.504
Layer3	2.25	4.8	36	3.813	2.529
Layer4	1.5	4.6	15	2.184	2.513
Layer5	1.5	5.9	32	4.412	2.465
Layer6	1.25	5.3	33	4.915	2.506
Layer7	1.5	4	36	4.981	2.556

Table 4.5 : Results of extraction, penetration and maximum theoretical specific gravity tests for all AC courses of the cored pavement sections, (continued).

Section No.	Prop. AC Thickness (inches)	Percent AC	Recovered Penetration	Coarse Agg. Angularity	Max. Th. Sp. Grty
4C					
Layer1	1.25	5.9	91	2.954	2.46
Layer2	1.5	5.9	39	2.994	2.45
5C					
Layer1	1.18	6.1	79	3.8135	2.483
Layer2	1.18	5.8	65	3.925	2.504
Layer3	1.27	5.6	36	4.125	2.496
Layer4	2.27	6	58	4.521	2.491
8C					
Layer1	1.25	6.2	33	4.654	2.538
Layer2	1.25	6	17	4.902	2.488
Layer3	2	5	31	4.9968	2.461
11C					
Layer1	1.25	6	59	3.095	2.421
Layer2	1.75	5.8	65	3.331	2.442
Layer3	1.09	5.4	27	4.513	2.454

$$AC = \left[\frac{(W_1 - W_2) - (W_3 + W_4)}{(W_1 - W_2)} \right] \times 100 \qquad (4.5)$$

Where,

AC	=	asphalt content (percent by total weight of mix);
W_1	=	mass of test portion;
W_2	=	mass of water in test portion;
W_3	=	mass of the extracted mineral aggregate; and
W_4	=	mass of the mineral matter in the extract.

After extraction of the bitumen from the AC mix, the recovered bitumen, the aggregate and the fine material were further tested to determine the recovered asphalt penetration and the gradation and angularity of the aggregate.

4.3.4 Recovered Asphalt Penetration

The ASTM D5-86 standard test procedure was used to measure the penetration (consistency) of the recovered bituminous material. Higher values of penetration indicate softer asphalt or lower viscosity. Penetration is defined as the consistency of a bituminous material expressed as the distance in tenths of a millimeter that a standard needle vertically penetrates a sample of the material under known conditions of loading, time, and temperature. The recovered asphalt penetrations are listed in Table 4.5.

4.3.5 Sieve Analysis

The particle size distribution of the aggregate and sand obtained from the extraction tests was determined by using sieve analysis in accordance with the ASTM C 136-84a standard test procedure. The tests were conducted by passing a weighed sample of dry aggregate through a series of sieves of progressively smaller openings. Table 4.6 lists the percent by weight of aggregate passing through each sieve.

4.3.6 Aggregate Angularity

Since, there is no standard test procedure for determining the coarse aggregate (retained on sieve number 4) angularity, the number of crushed faces of an individual aggregate particle was used as a measure of the angularity. Numbers ranging from 1 (rounded and subrounded) to 5 (crushed on all four faces) were assigned to the aggregates depending on the number of crushed faces. The test procedure consists of the following steps:

1. A 300 gram aggregate sample was obtained irrespective of the amount of the coarse aggregates in the AC mix.
2. The aggregates were then divided into different piles depending on the number of crushed faces. Each pile was inspected and an angularity number was assigned according to the number of crushed faces of the aggregates. For example, the pile which consists of aggregate particles crushed on only one face (one side) was given an angularity of 2. Likewise, the pile that consists of aggregate particles crushed on all four faces was assigned an angularity number of 5.
3. The weight of each pile as a percent by weight of the 300 grams sample was determined.
4. The angularity of the aggregate sample was then determined as the sum of the percent by weight of each aggregate pile times the assigned angularity of each pile and divided by the total weight of 300 grams.
5. For AC samples with more than one AC course, the angularity of the sample was determined by calculating the weighed average angularity of the aggregates in the various AC courses.

The above procedure implies that the angularity of the coarse aggregate is independent of the amount of the coarse aggregate in the AC mix. That is two samples with 20 and 50 percent coarse aggregate contents may yield the same angularity. The drawback of this procedure is that, asphalt mixes with low coarse aggregate contents may have the same aggregate angularity as those mixes made with high coarse aggregate contents. At low coarse aggregate contents, the aggregate particles float in the sand matrix which causes separation of the particles. Hence, the aggregate interlocking and friction are decreased. This scenario implies that care should be taken when analyzing the effects of the coarse aggregate angularity on the AC mix performance. The aggregate angularity must be considered in view of the percent aggregate contents in the mix. That is, higher coarse aggregate content in the mix leads to more mobilization of the aggregate angularity. Nevertheless, the test procedure and the method of calculating the angularity were adopted to minimize the dependency of the angularity on the percent aggregate or to minimize the collinearity between these two factors as discussed in chapter five. It should be that this test procedure represents a departure from those procedures used by other researchers. In their test method, the aggregate angularity is defined by three categories (rounded, subrounded, and angular). The sample angularity is calculated as the weighted average angularity of the three categories based on their weights. The method do not differentiate between aggregates crushed on 1, 2, 3, or 4 faces.

The angularity of sand size particles (passing standard sieve number 4 and retained on sieve number 200) can be determined by using the Michigan standard test method (MTM) 118-90. The test procedure however, requires a minimum sample size of 1500 grams which was not available in this study. Hence, the sand angularity was not determined and it is not considered in any further analysis.

Table 4.6 : Results of sieve analysis for each AC course.

Sieve Size											
Section No.	1 1/2	1	3/4	1/2	3/8	#4	#8	#16	#30	#50	#100	#200
Percent Passing												
7F												
Layer1	100	100	100	99.6	89.2	63.4	48.4	42.6	35.5	21.6	9.4	6.4
Layer2	100	100	97	83	73.6	56.5	47.2	41.8	36.6	17.8	5.3	3.6
Layer3	100	100	88.3	84.8	80.6	71.9	60.7	50.8	40.3	17.7	4.7	3.1
10F												
Layer1	100	100	100	97.7	88.6	66.1	56.2	49.3	41.3	23.2	9.6	5.3
Layer2	100	100	100	96.7	88.6	68.7	57.2	48.6	40.1	25	12.7	7.8
Layer3	100	100	100	94.3	89.4	72.4	57.2	45.9	34.9	22.1	13.8	10.3
13F												
Layer1	100	100	100	99.1	82.8	47.2	38.1	35.1	31.7	20.8	9.1	3.9
Layer2	100	100	100	98.2	86.3	60.4	48.3	43.1	38.3	23.1	12.4	7
Layer3	100	100	84.2	55.7	47.6	41.2	37.2	35.2	31.3	20.8	7.7	3.8
14F												
Layer1	100	100	98.1	87.4	76.5	62.1	51.5	42.7	34.7	21.4	10.8	7.2
Layer2	100	100	99.3	83.7	72.6	57.9	49.1	41.8	33.9	19.7	10.9	8.4
Layer3	100	100	100	100	93.3	55.1	33.3	26.4	20.2	12.3	6.8	4.6
19F												
Layer1	100	100	100	100	91.7	40.1	14.5	9.5	5.9	3.4	1.9	1.2
Layer2	100	100	100	98.8	89.1	63.9	50.2	43.6	36.9	18.6	8.6	6.5
Layer3	100	100	.100	97.5	87.2	62	49.3	43.2	37.1	19.2	8.8	6.6
29F												
Layer1	100	100	100	98.9	93.3	81.6	60.5	44.8	31.9	18.8	9.1	7.1
Layer2	100	100	100	97.4	79.3	48.6	30.9	22.2	15.6	9.1	3.8	2.5
Layer3	100	100	95.3	90.1	84.7	70.7	55.2	41.9	27.2	13.2	6.3	4.3
35F												
Layer1	100	100	100	98.6	91.1	73.6	56.6	44.9	31.9	15	8.3	6.2
Layer2	100	100	100	97.2	81.3	49.6	33.4	.26.7	20.1	10.4	6.2	5.1
Layer3	100	100	100	91.9	77.5	53.5	39.3	32.1	23.7	12.9	8.1	6.5
43F												
Layer1	100	100	100	98.4	91.4	65.5	51.3	41.8	33.3	20	9.7	6.9
Layer2	100	100	100	98.5	90.6	68.5	51.9	42.4	32.7	17.7	9.3	6.9
Layer3	100	100	98.6	87.6	78.6	61.4	46.5	37.2	29.1	17.4	9.4	7
Layer4	100	100	95	79.8	69.9	51.6	40.2	32.2	25.3	17.4	10.6	8.3
1C												
Layer1	100	100	100	97.2	84.8	63.9	47.4	36.7	26.7	16.1	9.5	6.9
Layer2	100	100	100	97.2	84.2	57.5	42.4	33.1	24.2	15.3	9.6	7.2
Layer3	100	100	99.1	95.5	81.2	57.4	42.2	33.1	25.3	16.4	9.8	7.1
Layer4	100	100	99	85	77.1	55.9	42	33.2	25	16.1	8.6	6.2
Layer5	100	100	100	97	80.6	61.4	48.4	35.9	26.4	14.5	7.4	5.6
Layer6	100	100	100	97.1	84	50.2	41.7	39.4	36.4	27.6	13.2	7.5
Layer7	100	100	75.9	47.8	38.6	30.4	28.1	26.4	24.2	17.8	7.6	3.5

Table 4.6 : Results of sieve analysis for each AC course, (continued).

	Sieve Size											
Section No.	1 1/2	1	3/4	1/2	3/8	#4	#8	#16	#30	#50	#100	#200
	Percent Passing											
4C												
Layer1	100	100	100	95.4	87.2	69.7	56.3	46.2	35.4	21.7	11.6	7.6
Layer2	100	100	100	100	94.9	56.4	43.7	37.4	29.6	16.8	7.4	4.6
5C												
Layer1	100	100	100	98	89	70	54.7	43.1	33.1	22	13.8	10
Layer2	100	100	100	96.9	87.3	67	52.4	41.8	32.5	21.9	13.1	9.2
Layer3	100	100	100	99	91.8	69.3	54.5	43.8	35.2	24	12.9	7.8
Layer4	100	100	100	98.6	90.2	65.1	48.3	37.1	27.3	17.6	11.2	8.3
8C												
Layer1	100	100	100	98.4	88.3	65.5	50.8	42.1	34.4	22	10.7	7.5
Layer2	100	100	100	99	88	54.8	44.2	41.1	38.7	27.1	14.6	7.5
Layer3	100	96.5	82.9	52	39.5	31.7	29.4	27.8	24.4	17	8.2	3.8
11C												
Layer1	100	100	100	95.8	87.4	67.1	51.4	43	33.1	20.8	11.4	6.9
Layer2	100	100	100	97	88.7	68.3	53.2	44.2	35.5	22.5	10.9	6.9
Layer3	100	100	100	97.7	82.1	56.2	42.4	35.1	28.9	18.5	9.8	6

CHAPTER 5
ANALYSIS AND DISCUSSION

5.1 General

A wheel load moving on a pavement structure causes three types of responses; elastic, viscoelastic, and plastic. Although the three responses are dependent on the material properties, the elastic one is time independent while the viscoelastic and plastic responses are time dependent. The plastic response of asphalt pavements manifests itself as rut (permanent deformation) and/or fatigue (alligator) cracks.

As is the case for most solids, asphalt concrete pavements exhibit a greater variety of mechanical behavior than liquid or gases. It is extremely difficult to arrive at a single set of equations that realistically describes or models the interplay of the elastic, viscoelastic, and plastic responses under a combined set of stresses and boundary conditions. Even if such equations could be developed, they would be far too complex for the practical analysis of stresses and strains induced in the pavement structure. To simplify the problem, in the early work on plastic solids, the yield condition and plastic flow rule were treated as independent ingredients of a theory of plasticity. For example, an experimental based yield condition was advanced by Tresca (73). Later, Saint Venant (74) and Levy (75) adopted Tresca's condition and developed a plastic flow rule whose form was inspired by the theory of elasticity. In his theory of plasticity, Von (76) retained the plastic flow rule and modified (for the purpose of mathematical convenience) the Tresca yield condition.

Recently, the plastic flow rule and yield condition for asphalt surfaced pavements were further simplified and fatigue and rut models were developed. Each model is based on a single variable, the radial strain for the fatigue model and the compressive strain for the rut model. Both radial and vertical compressive strains are calculated by using elastic layer theory. Examples of these models are those developed by the AASHTO/ARE (77) and Majidzadeh and Ilve (78). The main limitations of the models are that:

1. They are independent of the plastic properties of the paving materials.
2. They cannot be used to assess the effects of material properties on the fatigue life and rut potential of asphalt pavements.
3. Their accuracy is poor at best.

Numerous statistical fatigue cracking and rut depth models for AC surfaced pavements have also been developed. The models express the fatigue life and rut depth in terms of the asphalt-aggregate mix properties and compositions. These models are presented in Chapter 2 of this dissertation. It should be noted that the fatigue life and rut depth of asphalt pavements are functions of not only the AC layer properties but also the properties of the base and subbase layers, the characteristics of the roadbed soils, the traffic load and volume and the environmental factors.

As stated in Chapter 1, the objectives of this study are to determine the asphalt mix variables that affect the structural performance (rut and fatigue cracks) of flexible and composite pavements and to recommend changes in the existing asphalt mix design procedure and standard specifications. To accomplish these objectives, the outputs of this study must include relationships between pavement performance and asphalt mix variables such that the sensitivity of the pavement performance to the various asphalt mix variables can be assessed. Therefore, the data analysis procedure to be employed must account for the variability of the asphalt mix and must be capable of:

1. Providing a good description of the sensitivity of the response variables to the input parameters (independent variables).
2. Developing realistic models whereby the relationships between the dependent and independent variables are reasonable and have good engineering interpretations.
3. Predicting pavement responses in terms of rutting and fatigue cracking potentials for the range of the given variables.

Two types of analysis can be employed; mechanistic and statistical. The former is typically based on existing theory (e.g., elastic, plastic, viscoelastic) and it requires substantial inputs regarding material properties. Because of the limited resources, such inputs cannot be obtained. Further, the resulting mechanistic models are not practical and they cannot be used by State Highway Agencies. Consequently, a statistical type analysis was selected in this study. The inputs to the statistical models include the engineering and physical properties of the AC materials as well as traffic loading, volume and pavement service life (age).

The main advantage of the statistical analysis is its simplicity and low cost. The main disadvantage is that the resulting statistical models are applicable only within the range of data from which the models have been developed. This disadvantage can be minimized if the range of material properties used in developing the statistical model represents the spectrum of the properties used in the field. Therefore, the selection of the experiment is very crucial to the success of the analysis. The experiment should include:

1. A representative range of the properties and variability of the asphalt mixes used in the construction of various pavement sections that are:
   a) expected to experience light, medium, and heavy traffic;
   b) located in the various environmental regions;
   c) supported by different roadbed soils;
   d) constructed by using different base and subbase materials; and
   e) consisted of various cross-sections.
2. A representative range of the properties and variability of each of the materials used in the compacted asphalt mixes.

The details of the experiment in this study are presented in Chapter 3. The statistical package (computer program) used in the study is "Statistical Package for Social Sciences (SPSS)". The reasons for this selection include:

1. The simplicity and user friendliness of the program.

2. The various options that are embedded in the program which allow the users to examine the various statistical parameters of the output models.
3. Its graphic capability whereby each input and output variable can be plotted and examined for engineering interpretation.
4. The capability of the program to access the data through a common spreadsheet and/or data base.
5. The flexibility of the program which allows the users to input the desired form of equations relating the dependent and independent variables.

Most statistical procedures are generally based on the least squares criteria (minimization of the sum of the square of the differences between the predicted and the observed data). Again most procedures are simple and easy to use provided that the proper relationship between each independent variable and the dependent one is properly specified. The issues here are that the relationship must:

1. Have the proper engineering interpretations.
2. Be representative of the observed trend between the dependent and independent variables.
3. Model other data reported in the literature.

Several aspects relative to these issues and some specific comments regarding the statistical procedure used in this study are presented in the next section.

5.2 STATISTICAL ANALYSIS TECHNIQUES AND ISSUES

The most important issues regarding statistical analysis of engineering data include:

1. The number of variables to be included in the analysis, their significance level, and their collinearity if any.
2. The form of the equation(s) relating each independent variable and/or clusters of

independent variables to the dependent one.

3. The engineering interpretations of the final correlation equation.

If the only purpose of the statistical analysis is to express the behavior of the response (dependent) variable in terms of the independent variables and to minimize the residual sum of squares, then the best suited model is the one that include all the available independent variables regardless of whether or not the variables are causally related or the model is realistic. A model having fewer variables, on the other hand, has the appeal of simplicity, and economic advantage in terms of obtaining the necessary information. The elimination of some variables from the model, however, is obtained at the expense of biases and loss of predictability of the model. Thus, the exclusion of any variable with a significant correlation coefficient causes a bias penalty (79).

Regardless of the number of variables to be included in the final model, the results of any statistical analysis that is based solely on the least square technique reflect only the correlational structure of the data being analyzed. This structure may or may not be representative of the true engineering relationships between the dependent and independent variables. Another problematic aspect of variable selection is that the relative importance of a variable as manifested in the sample may not necessarily reflect its relative importance in the population. Important variables in a sample may appear unimportant in the population and vice versa. That is, the best set of variables in a sample might not be the best set in the population. The choice of variables in the final model depends on prior knowledge and experience and on the variable clusters used to model a behavior. Further, statistical correlations between independent variables (e,g., material properties), and the dependent variable (e,g., pavement performance in terms of rut and fatigue cracking) may lead to several possible outcomes including:

1. Certain material properties (e.g., air void) appear to have specific effects on pavement performance which can be related to certain observed patterns.

2. Certain material properties appear to have no effect on pavement performance.

That is, regardless of the range of the property and its variation, the pavement performance is more or less constant for the entire range of that property.

3. Variation in the values of the pavement performance appear to have similar pattern that can be related to variations in the material properties.

Nevertheless, in this study, the statistical analysis were conducted by using the SPSS computer program. The statistical models (regression equations) were developed by using four steps. A brief discussion of each of these steps is provided here and a detailed discussion is contained in the model development.

Step 1 Determination of a Simple Correlation Matrix

In this step, a simple correlation coefficient between the dependent and each of the independent variables was computed and tabulated in a matrix format. Each coefficient was then examined to determine the trend between the dependent and each of the independent variables and the significance of the latter on the former. The trends and the significant levels were also compared to field observations and experience. The simple correlation matrix also provides information regarding the degree of collinearity between any two independent variables (a situation when two or more independent variables are correlated among themselves). A higher degree of collinearity between any two independent variables, causes more difficulty in separating the effect of each independent variable on the response variable (80). Because of its importance, the degrees of collinearity between the independent variables were also examined in steps 2 and 3.

Step 2 Computation of Eigenvalues and Condition Indices

The eigenvalues of a symmetric (square) matrix "$A(n \times n)$" are a set of "n" non-negative scalars "λ_i^2" such that their product with n non-zero vectors "z_i, $i=1\ldots n$" of the matrix is the same as the product of the matrix with the z_i vectors. That is "$Az_i = \lambda_i^2 z_i$". The eigenvalues are typically used to examine the collinearity between the independent variables. In addition, the scaled uncentered cross-products matrix and the decomposition of the regression variance corresponding to these eigenvalues were computed. There is an indication of near dependency of variables, when there is a high proportion of the variance of two or more coefficients that are associated with the same eigenvalue (81). Hence, the condition index which is defined below can be calculated.

$$\text{Cond. Index} = [\text{eigenvalue}_{max} / \text{eigenvalue}_i]^{0.5} \tag{5.1}$$

The presence of collinearity results in small eigenvalues and consequently, larger condition index values. Furthermore, the number of large condition index values corresponds to the number of cases of collinearity between the independent variables.

Step 3 Computation of Variable Tolerance and Variance Inflation Factor (VIF)

Variable tolerance and variable inflection factors (VIF) are other measures of collinearity between the independent variables. The variable tolerance and the VIF are defined as (78):

$$\text{Tolerance} = (1-R_i^2) \tag{5.2}$$

$$\text{VIF} = [\,1/\,(1-R_i^2)] \tag{5.3}$$

where

R_i = the multiple correlation coefficient of the ith independent variable when it is predicted from other independent variables.

If the tolerance of an independent variable is small, or its VIF is high, then the variable is collinear with one or more independent variables.

Step 4 Variable Selection Methods

In this step, the independent variables to be included in the statistical model are selected. Several variable selection methods are available to the user of the SPSS program. In this study, the stepwise regression method is used. This method identifies a good (not necessarily the best) set of variables to be included in the development of the statistical model. The statistical model is constructed by considering one variable at a time that having the greatest or the least impact on the residual sum of squares of the model. Three stepwise techniques can be identified (76); forward selection, backward elimination and stepwise selection. These three techniques are addressed below.

Forward Selection - In the forward selection technique, the first independent variable to be considered in the development of the statistical model is that which accounts for the largest amount of variation in the dependent variable. At each successive step, the independent variable (from the independent variable pool) that causes the largest decrease in the residual sum of squares of the existing model is added. In the absence of any termination rule the process continues until all the variables are included in the model.

Backward Elimination - In the backward elimination technique, first the statistical model is developed by including all the independent variables in the pool. At each consequent step, a variable whose deletion causes the least increase in the residual sum of squares is dropped. If no termination rule is specified the deletion process continues until only one independent variable is left in the model.

Stepwise Selection - The stepwise selection technique is basically a forward selection process that at every step reexamines the significance of the previously added variables. If the partial sum of squares of any previously added variable does not meet a minimum specified criterion, the variable is dropped from the model and the selection process changes to backward elimination. The variable elimination process continues until all of the variables remaining in the model meet a minimum specified criterion after which the forward stepwise selection process is resumed. It should be noted that, at every step, the significance of all variables relative to the model is reexamined. Hence, any variable that has been deleted from the model in earlier steps may be added back to the model when it meets the minimum specified criterion.

Neither the forward selection nor the backward elimination techniques consider the impacts of adding or deleting a variable on the remaining variables in the model. A variable added to the model in the forward selection technique may become insignificant after other variables have been added. Similarly, the significance of a deleted variable may increase as other variables are deleted from or added to the model.

The stepwise selection technique was used in this study because the process allows a better chance of selecting the best independent variables relative to the other two techniques. Nevertheless, the forward selection and the backward elimination techniques were occasionally used to compare the resulting statistical models. For each statistical model, the null hypothesis of no relationship between the dependent and independent variables were tested. Finally, the residual analysis and the comparison of the predicted versus observed values were performed.

To this end, several technical terms relating to the pavement performance are used throughout the remaining parts of this thesis. These terms are defined in the next section.

5.3 DEFINITION OF TERMS

For the benefits of the readers, the following pavement performance terms are defined in this section.

1. **Design Life** - The design life of a pavement structure is defined as that period of time (typically in years) assumed during the pavement design process. Pavement design life could be greater, equal, or less than the actual pavement performance

period.

2. **Performance Period** - A pavement performance period is defined (see Figure 5.1) by the time period in years between construction and rehabilitation or between two rehabilitation activities during which the pavement was opened to traffic and its conditions were equal to or better than the specified threshold value.

3. **Service Life** - A pavement service life is defined by the time period in years between construction/rehabilitation and the present time as shown in Figure 5.2. Hence, a pavement service life is always shorter than the pavement performance period. However, the pavement service life could be longer, equal, or shorter than the pavement design life.

4. **Remaining Service Life** - The remaining service life (RSL) of a pavement structure is defined by the future (predicted) time period in years between the present time and that point in time where a pavement distress reaches its minimum specified threshold value as shown in Figure 5.3. Hence, for any pavement structure several RSL values could be calculated (one value for each type of distress). The RSL of the pavement structure could be assigned as the smallest of the RSL values or it could be calculated on the basis of the weighted average of all types of pavement distress.

5.4 ANALYSIS AND DISCUSSION OF FATIGUE LIFE

Recall that (see Chapter 2 - Literature Review) fatigue cracks are the results of the tensile strains induced at the bottom of the AC layer due to a moving wheel load. These tensile strains are the sum of three components; elastic, viscoelastic, and plastic. While the first two components are recoverable upon the removal of the load and with time, the plastic tensile strain is permanent in nature. The magnitude of the plastic

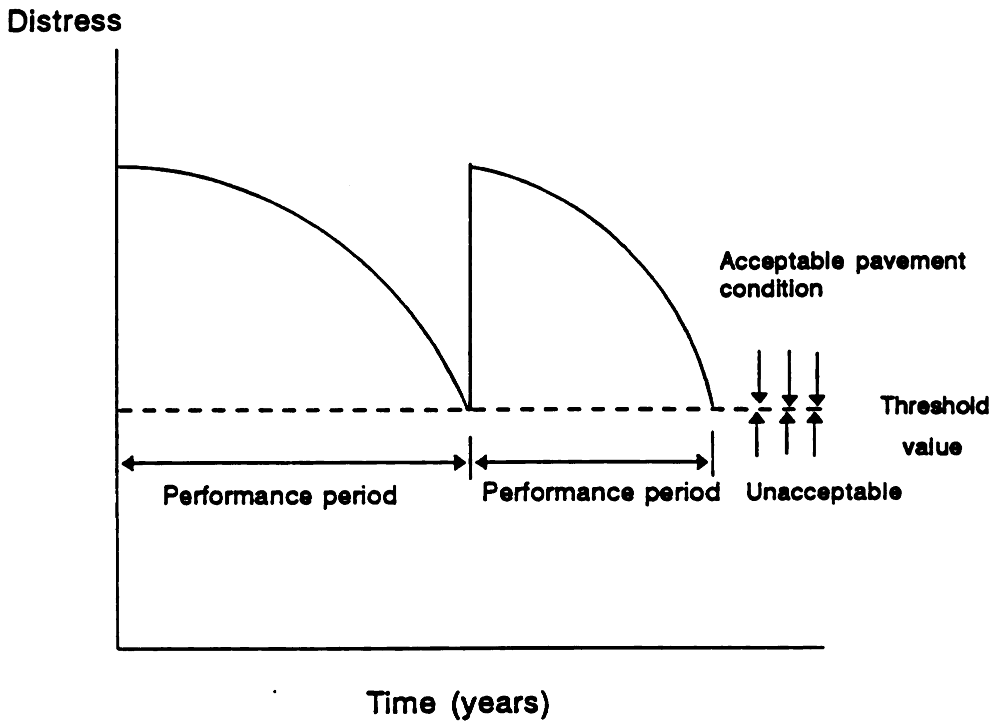

Figure 5.1 : Performance period of a pavement.

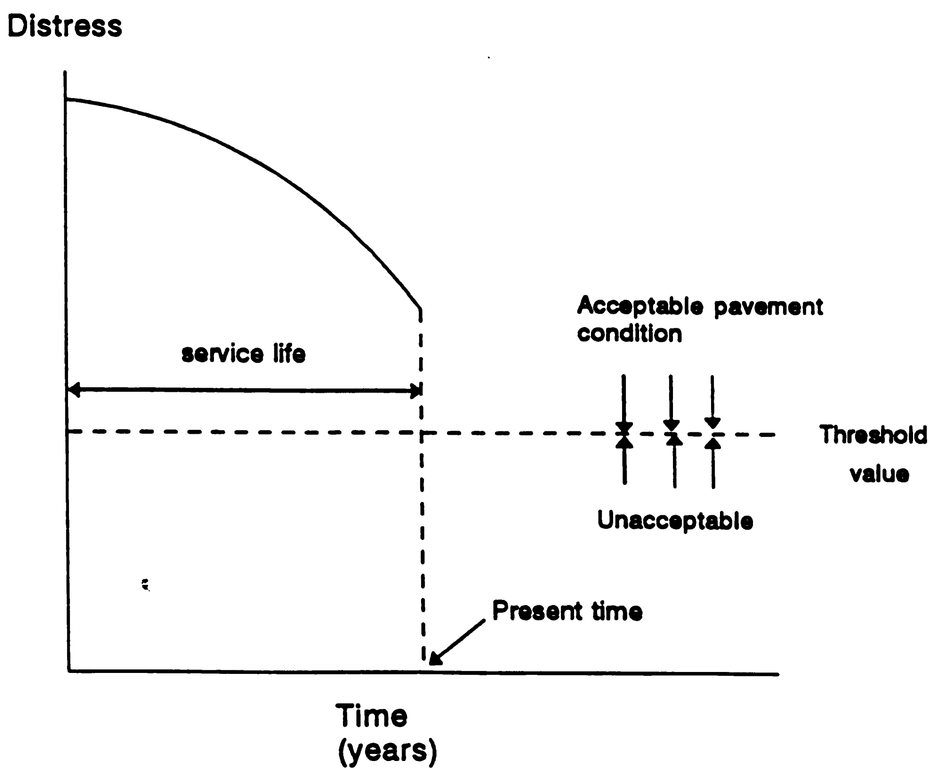

Figure 5.2 : Service life of a pavement.

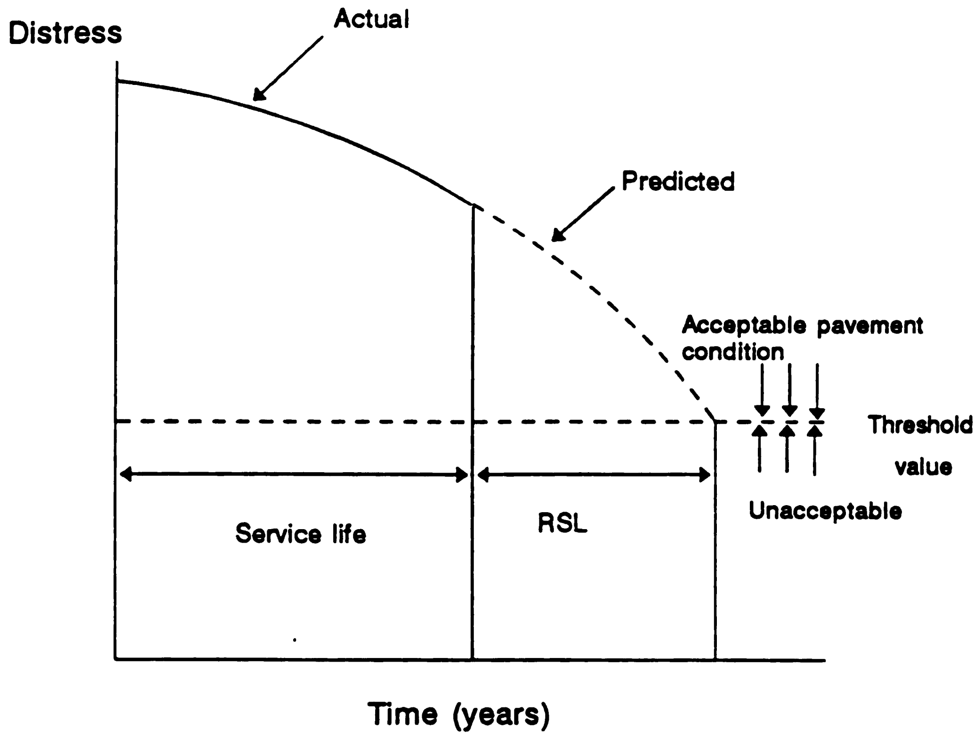

Figure 5.3 : Remaining service life (RSL) of a pavement.

tensile strain depends on the material properties and the magnitude of the wheel load. Higher loads cause higher strains. Further, as the number of wheel load applications increases, the cumulative plastic (permanent) strain increases until the asphalt cement cannot stretch any longer. Hence, cracks will develop and with further load applications, the cracks will propagate toward the pavement surface where they manifest themself as alligator or fatigue cracks.

Various fatigue cracking models for asphalt concrete pavements have been established by numerous investigators based on both field performance data and laboratory fatigue data. The laboratory based fatigue models generally predict failure much sooner than is observed in the field. The reason for this is that most laboratory models predict crack initiation. In the field, fatigue cracks start at the bottom of the AC layer and after some time (few months to few years depending on the pavement cross-section), they propagate upward toward the pavement surface. Hence, fatigue cracks in asphalt pavements may exist for a long time period before they can be detected at the surface of the pavements. Figure 5.4 illustrates a generalized fatigue cracking performance model for asphalt pavements. The scale on the vertical axis indicates the fatigue cracking index (FCI). An FCI value of 100 indicates no fatigue cracks can be seen on the pavement surface. An index value of less than 100, on the other hand, indicates the presence of fatigue cracks. As the severity and intensity of the fatigue cracks increase, the value of the FCI decreases. Three important observations can be made from Figure 5.4. These are:

1. An FCI value of 100 implies that no fatigue cracks can be seen on the pavement surface. This however, does not imply that the pavement is free from fatigue cracks. Indeed, the time of fatigue cracks initiation could be anywhere along the horizontal line ab as shown in Figure 5.4.
2. The time period between the first observation of fatigue cracks and failure of the pavement structure due to fatigue cracks is much shorter than the period between

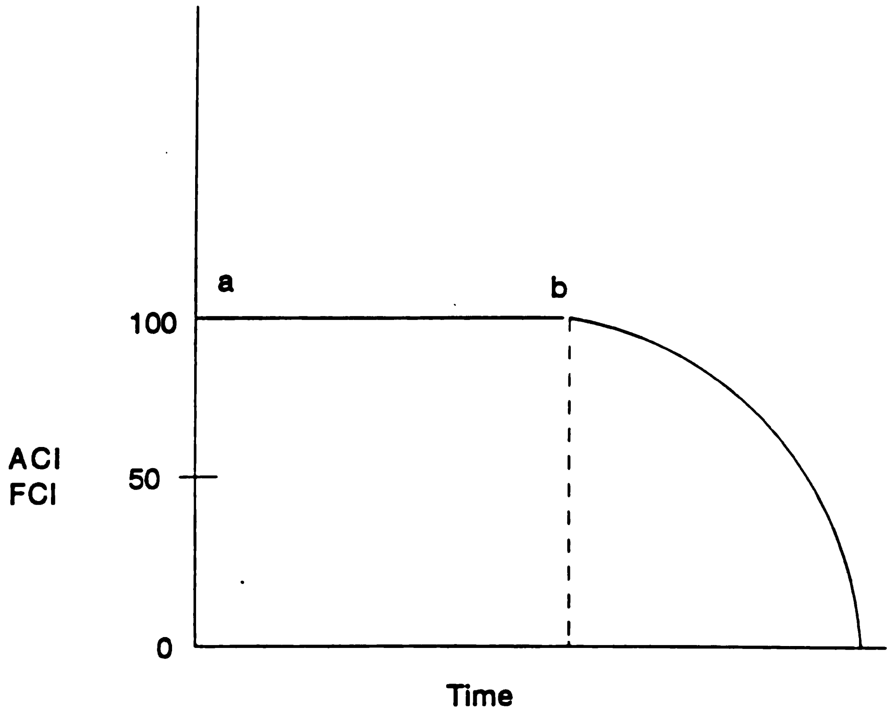

Figure 5.4 : Fatigue cracking index (FCI) as a function of time.

construction or rehabilitation and the first observation of fatigue cracks.

3. Because of the above two observations, no universal definition of fatigue crack failure has been adopted. Some State Highway Agencies (SHA) define fatigue failure in terms of the area of the cracked pavement. Some others, in terms of the percent of the pavement section that showing fatigue crack. Still others, define fatigue crack failure by the combination of the areas of the pavement that show low, medium, and high severity fatigue cracking.

To this end, and because accurate and historical filed fatigue cracking data were not available to this study, the results of laboratory tests are used to assess the effects of the properties and compositions of the asphalt-aggregate mixes on their fatigue lives. Hence, the following assumptions were made at the onset of this study.

1. If an asphalt-aggregate mix variable has an adverse or favorable effects on the laboratory determined fatigue life of the mixes then that variable has and adverse or favorable effects on the fatigue life of the AC layer in the field.
2. For the type and range of the variables included in this study, the order of significance each variable has on the laboratory determined fatigue life is the same as the order of significance in the field. That is, if variable "XX" is the most significant variable affecting the laboratory determined fatigue life then "XX" is also the most significant variable affecting the fatigue life of the pavements.

The above two assumptions are reasonable because of the following reasons:

1. The absence of accurate and historical field fatigue data and the absence of a definition of pavement fatigue life make it impossible to relate material properties to the fatigue life of the pavements.
2. The objective herein is not to quantify or predict the pavement fatigue life but to assess the effects of each mix variable on the pavement fatigue life.
3. The fatigue life of AC pavement is also affected by traffic load, volume and by

the thicknesses and stiffnesses of the other pavement layers and the roadbed soils. While for each pavement section included in the study, the traffic data is available, layer stiffnesses and the stiffness of the roadbed soil were not available. Nevertheless, as stated in Chapter 3, the laboratory samples were obtained from field cores and they were tested by using the indirect cyclic load (INCL) tests. Observations regarding the field cores, laboratory samples, and the INCL tests are presented in the next section.

5.4.1 Field Cores, Laboratory Samples, and the INCL Tests

Presently, different laboratory techniques are used to evaluate the fatigue potential of asphalt mixes in the laboratory. As noted in Chapter 2, the indirect cyclic load (INCL) tensile test has several advantages over other testing methods and it was used in this study. The INCL tests were conducted on core samples by using an MTS closed loop servo-hydraulic system and the Baladi's indirect tensile test (INTS) device (3). Initial tests were conducted by using a fixed and a hinged 0.5 inch loading strips. The test data indicated that, for test samples consisted of more than two courses (i,e. leveling and surface courses), the fixed loading strip delivered most of the load to the stiffer course. The resulting fatigue life was much shorter than that of compatible sample tested by using the hinged loading strip. Further, since all the test samples were obtained from field cores (the cores lacked smooth and vertical surface), the fixed loading strip did not make a full contact with the samples. Consequently, the hinged loading strip was used throughout the testing program.

The 6-inch diameter test samples were sawed from asphalt concrete cores that were obtained by MDOT from pavement sections selected for coring. The cores were composed of surface, leveling and base courses (see Table 4.5). The thicknesses of the various AC courses varied from one core to another. For example, the combined thicknesses of the surface and leveling courses varied from about 2 to about 3 inch. Whereas, the AC base course thickness varied from about 3 to about 9 inch. The INCL test samples were prepared by sawing about 2.5-inch thick portion from the 6-inch diameter cores (see sample preparation, Chapter 4). Because of the limited thicknesses of the surface and leveling courses, it was not possible to obtain 2.5-inch test sample from each course. Therefore, combinations of the surface and leveling courses and, occasionally the base course were included in the test samples. That is some of the test samples contained only surface and leveling courses while others contained surface, leveling and base courses. This implies that the test results reflect the global behavior of the combined courses rather than the individual course behavior. It should be noted that extreme care was taken as not to include any base course material in test samples made from the surface and leveling courses. For a few samples however, this was not possible and a minimum amount of the AC base course was included (a minimum sample thickness of 2.2-inch was specified in this study). The above scenario presented no problems for all test samples obtained from the base course (all cores contained more than 2.5-inch thick base coarse).

Trial INCL tests were also conducted by using a constant sustained load of 50 pounds and two cyclic load levels of 500 and 300 pounds. It was observed that some samples tested under the 500 pounds cyclic load were failing in shear (punching of the loading strip along the vertical diameter of the sample) rather than in fatigue. Therefore, a cyclic load of 300 pounds was selected and used throughout the testing program.

5.4.2 Test Results

A total of one-hundred and six full-depth 6-inch diameter cores were obtained from thirteen cored pavement sections. Each core was carefully examined and defects such as stripping, cracking, and smoothness of the core side were noted and the thicknesses of each AC course (surface, leveling, and base) were measured and recorded.

After examining the cores, one-hundred test samples (approximately 2.5-inch thick) were carefully sawed. Each test sample was then inspected for possible defects and the thickness of each AC course in the sample was measured and recorded. It was observed that the vertical sides of 43 test samples were highly uneven due to the coring process. Uneven sample side is known to cause a rocking motion in the sample during the application of cyclic load, hence, these samples were rejected. Thus, 55 test samples were accepted for testing. Prior to the commencement of the INCL tests, the bulk specific gravity of each of the 55 test samples were measured by using the ASTM D-2726 standard test procedure. The test results are listed in Table 5.1.

After the completion of the INCL tests, similar test samples (that have the same, leveling and/or base courses) and some of the 43 rejected samples were combined and asphalt extraction tests were conducted. The reason for combining several samples is to obtain adequate materials for the asphalt extraction tests. The extraction tests were conducted according to the ASTM D-2172 standard test procedure which specifies that a minimum material weight of 2000 grams be used. The extracted asphalt cement and the recovered aggregate were used to determine:

1. The recovered penetration of the AC cement.
2. The percentages by weight of the:
    a) coarse aggregate (plus number 4 standard sieve);
    b) fine aggregate (minus number 4 and plus number 200 standard sieves);
    c) fines (minus the number 200 sieve).
    d) asphalt cement.
3. The maximum theoretical specific gravity of the asphalt mix.
4. The weighted average angularity of the coarse aggregate.

Tables 5.1 and 5.2 summarize the test results. These include the sample designation number, thickness, specific gravity, the recovered penetration of the asphalt

Table 5.1 : Data for the 57 INCL test samples.

Line No.	Sample Designation Number	Sample Thick (inches	Sample Sp.Gty.	Rec. Pen.	Percent by weight AC	Sand	Fine	Agg	Angularity	Air Void	Cyclic Load (lbs)	Test Temp. (F)	Comp. Stress (psi)	Tensile Stress (psi)	Resilient Modulus (500)(psi)	Service Life (years)	Cum. ESAL (mill.)	Lab. Ftaigue Life
1	7112011 1	2.58	2.441	58	4.7	55	5	40	2.61	2.5	289	73.40	37	12	249871	7	1.25	6400
2	7122411 1	2.53	2.400	56	4.7	55	5	40	2.55	4.2	293	75.74	37	12	274045	7	1.25	5900
3	7122411 2	2.27	2.271	32	4.1	69	3	28	1.97	9.5	329	76.82	42	14	275982	7	1.25	8800
4	7127721 2	2.57	2.193	32	4.1	69	3	28	1.97	12.6	291	73.22	37	12	208436	7	1.25	3500
5	29172711 1	2.63	2.362	43	5.0	62	5	34	3.50	5.6	283	73.40	36	12	247754	11	0.76	9000
6	29117721 1	2.56	2.353	44	5.1	57	4	39	4.33	6.0	292	72.32	37	12	299678	11	0.76	6000
7	29183321 1	2.41	2.316	43	5.0	61	5	34	3.71	7.4	31,1	77.00	40	13	291162	11	0.76	5900
8	29146911 1	2.49	2.301	43	5.1	59	4	37	4.22	8.0	303	77.00	39	13	263544	11	0.76	5100
9	29117721 2	2.54	2.323	43	4.6	66	4	29	1.48	7.5	292	74.66	37	12	244897	11	0.76	2600
10	29172711 2	2.53	2.292	43	4.6	66	4	29	1.48	8.8	294	74.66	37	12	258849	11	0.76	1800
11	29186711 2	2.51	2.277	43	4.6	66	4	29	1.48	9.4	297	74.84	38	12	222358	11	0.76	1400
12	19118331 1	2.47	2.419	53	5.5	56	7	37	3.24	2.1	301	73.13	38	13	291540	11	1.58	3600
13	19158421 1	2.37	2.346	63	5.7	57	7	37	3.04	4.7	314	75.92	40	13	322706	11	1.58	2700
14	19141811 1	2.37	2.352	54	5.5	56	7	37	3.22	4.7	315	73.94	40	13	274495	11	1.58	1600
15	19121611 1	2.53	2.335	57	5.6	56	7	37	3.16	5.3	294	75.74	37	12	255384	11	1.58	3000
16	19148131 1	2.46	2.322	51	5.4	56	7	37	3.29	6.0	303	76.82	38	13	247165	11	1.58	870
17	11257021 1	2.48	2.386	62	5.9	61	7	32	3.22	1.9	301	74.30	38	13	224869	6	0.12	2100
18	11245021 1	2.41	2.361	62	5.9	61	7	32	3.22	2.9	309	75.20	39	13	240757	6	0.12	2100
19	11265911 1	2.32	2.350	62	5.9	61	7	32	3.23	3.4	322	75.20	41	14	256620	6	0.12	1700
20	43148341 1	2.61	2.387	61	6.4	60	7	32	2.79	2.5	274	77.90	35	12	183108	1	0.76	3800
21	43141611 1	2.51	2.402	62	6.5	60	7	33	2.83	3.2	296	81.14	38	12	217082	1	0.76	2700
22	43131911 1	2.62	2.385	60	6.5	60	7	33	2.83	4.0	283	80.24	36	12	188093	1	0.76	2600
23	43152311 1	2.48	2.357	61	6.5	60	7	33	2.83	5.1	300	81.86	38	13	157658	1	0.76	2000
24	43161411 1	2.48	2.347	64	6.5	60	7	33	2.83	5.4	300	77.36	38	13	233163	1	0.76	900
25	43121811 1	2.55	2.356	60	6.5	60	7	33	2.83	5.1	293	74.30	37	12	205504	1	0.76	1700
26	43148333 1	2.57	2.337	62	6.5	60	7	33	2.83	5.9	291	76.40	37	12	188558	1	0.76	870
27	43141611 2	2.56	2.402	39	5.1	43	8	48	4.16	6.1	289	80.42	37	12	259948	1	0.76	7800
28	35136221 1	2.56	2.361	26	5.9	56	6	38	4.79	4.6	291	76.22	37	12	213566	14	1.37	8000
29	35118931 1	2.54	2.325	26	5.9	57	6	37	4.80	6.0	295	80.96	38	12	215245	14	1.37	7200
30	35123311 1	2.54	2.301	26	5.9	57	6	37	4.80	6.9	295	78.44	38	12	213796	14	1.37	4000
31	35128321 1	2.52	2.281	26	5.9	56	6	38	4.79	7.8	295	74.66	38	12	233920	14	1.37	2900
32	35161411 1	2.52	2.256	26	6.1	59	6	35	4.82	8.6	296	78.08	38	12	249448	14	1.37	1900

Table 5.1 : Data for the 57 INCL test samples (continued).

Line No.	Sample Designation Number		Sample Thick (inches	Sample Sp.Gty.	Rec. Pen.	Percent by weight AC	Sand	Fine	Agg	Angularty	Air Void	Cyclic Load (lbs)	Test Temp. (F)	Comp. Stress (psi)	Tensile Stress (psi)	Resilient Modulus (500)(psi)	Service Life (years)	Cum. ESAL (mill.)	Lab. Ftaigue Life
33	35152311	1	2.54	2.293	26	6.0	58	6	36	4.81	7.2	294	77.00	37	12	217860	14	1.37	3000
34	10131011	1	2.43	2.396	55	7.3	61	6	33	3.59	2.8	262	74.84	33	11	186154	7	0.22	2800
35	10121711	1	2.31	2.392	56	7.2	61	7	33	3.61	3.0	321	74.03	41	13	218949	7	0.22	2000
36	10128121	1	2.65	2.373	57	7.2	61	7	32	3.63	3.9	280	78.80	36	12	218316	7	0.22	1500
37	8221011	1	2.38	2.357	25	5.9	47	7	46	4.84	5.3	312	81.32	40	13	352722	16	1.74	13000
38	8231511	1	2.54	2.342	25	5.9	47	7	46	4.83	5.9	293	82.87	37	12	271793	16	1.74	12000
39	8251811	1	2.38	2.323	25	6.0	49	7	43	4.81	6.4	313	79.88	40	13	286641	16	1.74	7000
40	5258321	1	2.50	2.459	68	5.9	59	9	31	3.90	1.4	301	78.80	38	13	198195	6	0.31	6100
41	5229221	1	2.45	2.409	71	5.9	59	10	32	3.88	3.5	304	77.00	39	13	175537	6	0.31	3000
42	5218631	1	2.59	2.334	71	5.9	59	10	32	3.88	6.5	290	76.28	37	12	186135	6	0.31	3800
43	1240411	1	2.56	2.418	45	5.5	52	7	40	4.48	3.2	292	77.18	37	12	225608	2	3.36	9500
44	1251611	1	2.47	2.403	47	5.6	54	7	39	4.53	3.7	305	75.50	39	13	235055	2	3.36	14000
45	1261611	1	2.60	2.406	45	5.5	53	7	40	4.40	3.7	287	81.68	36	12	219521	2	3.36	8500
46	1264221	1	2.64	2.369	44	5.4	53	7	40	4.33	5.3	283	75.65	36	12	227024	2	3.36	5000
47	14121713	1	2.38	2.375	90	5.8	52	7	41	3.12	5.8	317	78.80	40	13	138412	13	0.18	2000
48	14148233	1	2.45	2.372	97	5.9	52	7	41	3.15	6.8	308	79.70	39	13	149744	13	0.18	2000
49	13156621	1	2.56	2.442	45	5.7	45	7	50	4.84	1.5	292	77.00	37	12	283722	30	1.51	7000
50	13142311	1	2.58	2.414	46	5.6	45	7	50	4.83	2.6	292	78.80	37	12	213703	30	1.51	3200
51	13132911	1	2.65	2.372	46	5.6	44	6	51	4.84	4.2	281	73.94	36	12	228523	30	1.51	2500
52	13117121	1	2.66	2.371	42	5.7	48	8	47	4.78	4.7	279	74.66	35	12	278651	30	1.51	2300
53	13126311	1	2.51	2.348	46	5.7	44	7	51	4.86	5.3	295	74.66	38	12	249606	30	1.51	4000
54	13151511	1	2.49	2.450	45	5.7	45	7	50	4.84	1.2	300	77.90	38	13	308307	30	1.51	6800
55	13164311	1	2.55	2.440	45	5.7	45	7	50	4.83	1.6	296	76.10	38	12	251182	30	1.51	6600

Table 5.2 : Descriptive statistics of the properties of all test samples.

	Sample Thick (inches	Sample Sp.Gty.	Rec. Pen.	Percent by weight				Angul arity	Air Void	Cyclic Load (lbs)	Test Temp. (F)	Comp. Stress (psi)	Tensile Stress (psi)	Resilient Modulus (500)(psi)	Service Life (years)	Cum. ESAL (mill.)	Lab. Ftaigue Life
				AC	Sand	Fine	Agg										
Min.	2.27	2.193	26	4.1	44	4	28	1.48	1.2	279	72.32	33	11	138412	1	0.12	870
Max.	2.68	2.459	97	7.2	61	10	51	4.86	12.6	317	82.87	41	14	322706	30	3.36	14000
Avg.	2.51	2.36	49	5.7	56.2	6.39	38	3.68	5.07	297	76.79	37.73	12.50	236919	10.93	1.16	4510
Std.Dev.	0.09	0.05	16	0.7	6.5	1.35	6.5	1.00	2.32	12	2.55	1.56	0.52	42433	8.58	0.80	3123

cement, the percent by weight of the AC, fine, sand, and coarse aggregate in the asphalt mix, the angularity of the coarse aggregates, the percent air voids, the magnitude of the cyclic load, the INCL test temperature,the resilient modulus of the sample calculated at load application number 500, the maximum compressive and tensile stresses induced in the sample during the test, the service life of the pavement section (the period in year between construction or last rehabilitation and the time of coring), the cumulative 18-kip ESAL experienced by the pavement section in question during its service life, and the fatigue life of the sample.

For each sample, the test data were analyzed and several procedures were used to determine its fatigue life. These specify that the fatigue life of the sample corresponds to:

1. The number of load repetitions at which the value of the resilient modulus of the test sample is equal to half of its original value.
2. The number of load repetitions at which the rate of change (the slope) of the logarithmic value of the accumulated plastic and total deformation (along the vertical and horizontal diameters of the sample) relative to the logarithmic value of the total number of load applications increases significantly (see Figure 5.5a).
3. The number of load applications at which the rate of change of the plastic deformation ratio (the ratio of the accumulated plastic deformation along the horizontal diameter to that along the vertical diameter) relative to the logarithmic value of the number of load applications increases significantly as shown in Figure 5.6b.
4. The number of load applications at which a crack along the vertical diameter was observed. The width of the crack, however, varied from one sample to another.

The second method (the slope of the line representing the logarithmic values of the cumulative plastic deformation along the horizontal diameter of the sample versus the logarithmic values of the total number of load applications) produced good results.

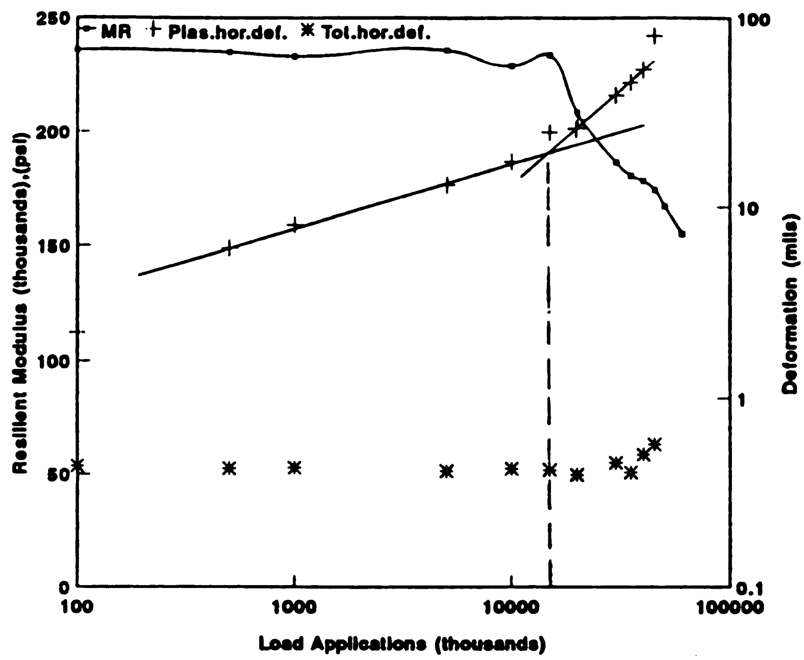

Figure 5.5a : **Resilient modulus, horizontal plastic and total deformation as a function of the number of load applications.**

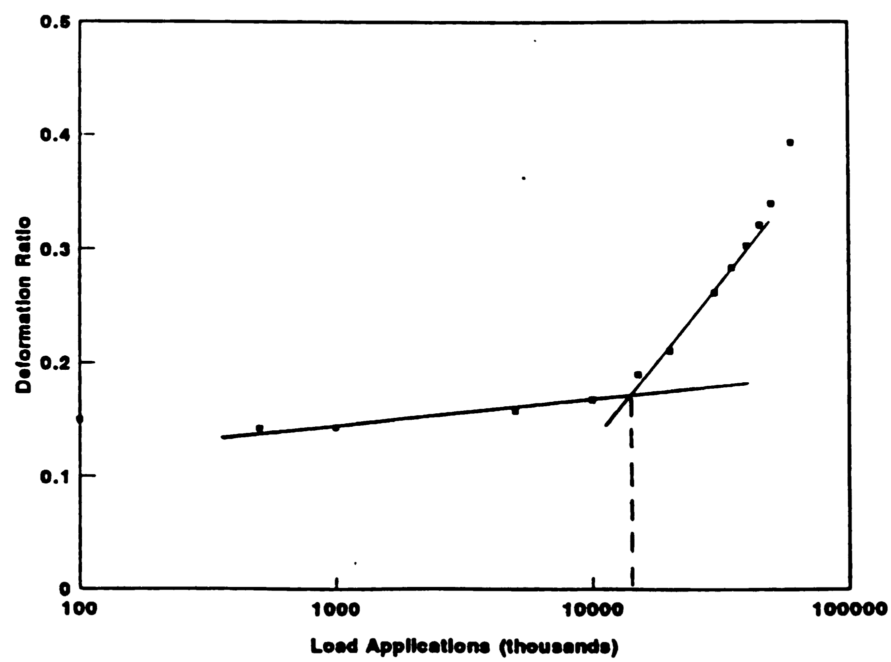

Figure 5.5b : **Deformation ratio (horizontal plastic/vertical plastic) as a function of the number of load applications.**

However, locating the point where the slope shows an increase was subjective in nature due to the nonlinear nature of the data at the higher numbers of load applications. The third procedure yielded more consistent results and hence, it was used for all the test samples. This procedure consisted of three steps as follows:

1. The ratios of the cumulative plastic deformation measured along the horizontal diameter to that measured along the vertical diameter were calculated at several number of load applications and plotted against the logarithmic values of the number of load applications as shown in Figure 5.6. It should be noted that the test data for the first 100 load applications was not included due to sample seating and/or sample conditioning.
2. Two best fit lines prescribing the data were then drawn and their intersection was found.
3. The laboratory fatigue life of the test sample was then defined by the number of load applications corresponding to the intersection of the two best fit lines.

Table 5.1 provides a list of the fatigue lives of the 55 test samples estimated by using the above procedure.

5.4.3 Analysis and Discussion of the Test Results

Statistical analyses were conducted to relate the fatigue life of the test samples to the test and the asphalt-aggregate mix variables. In the analysis, the fatigue life was assumed to be the dependent variable and the test and asphalt mix variables were assumed to be the independent ones. In reality, the test and mix variables are not truly independent variables. For example, the recovered asphalt penetration is a function of the asphalt cement aging process which, in turn, is a function of the original asphalt mixing process, storage time, the percent aggregate and sand in the mix, the service life of the pavements, and the environmental conditions. Likewise, the percent aggregate in the asphalt mix is a function of the 18-kip ESAL experienced by the pavement structure since construction. This is a direct result of the MDOT pavement design practices. For example, the asphalt course layer of a pavement structure expected to carry high number of 18-kip ESAL is typically designed to have higher percent aggregate, angular aggregate, and low percent sand. Hence, these three factors are not truly independent of the number of 18-kip ESAL. Consequently, extreme caution should be taken while conducting the statistical analysis and explaining the engineering interpretation of the statistical equations.

The above scenario implies that various degrees of collinearity (collinearity between two variables implies that the two variables are related) exist between the independent variables. This is evident from the correlation matrix where the coefficient of correlations between the dependent (the logarithmic value of the fatigue life) and the original values of the independent variables (asphalt mix properties and test parameters) and between the independent variables themselves are listed in Table 5.3. A coefficient correlation value of 0.0 implies no linear relationship or collinearity between the variables. A value of 1.0, on the other hand, implies 100 percent collinearity. Further, a positive value indicates a direct relationship (increasing value of one variable causes an increase in the value of the other variable) while a negative value marks an inverse relationship. It can be seen that the degrees of collinearity between the various independent variables vary from a negative 0.001 (between the tensile strain "TS" at failure and the aggregate angularity "AG"), an insignificant collinearity, to -0.976 (between the percent aggregate "AGG" and the percent sand "SAND" in the mix), which implies significant collinearity. Some of these collinearities can be eliminated. For example, the sand content can be expressed in terms of the aggregate and the percent fine content "FINE" as follows:

$$SAND = 100 - (AGG + FINE)$$

However, most other collinearities cannot be eliminated by substitution. For example,

Table 5.3 : Correlation matrix for fatigue life and independent variables.

	LOG(FL)	R.PEN	Percent by weight				ANG	SPGTY	CL	TT	MR	TS
			AC	SAND	FINE	AGG						
LOG(FL)	1.000											
R.PEN	-.424	1.000										
AC	-.308	.261	1.000									
SAND	-.365	.057	-.094	1.000								
FINE	-.076	.456	.570	-.452	1.000							
AGG.	.388	-.165	-.031	-.976	.262	1.000						
ANG	.470	-.429	.283	-.700	.347	.677	1.000					
SPGTY.	.203	.443	.272	-.504	.574	.418	.187	1.000				
C.L	-.058	.070	-.174	.110	-.057	-.111	-.121	-.130	1.000			
T.T	.205	-.041	.304	-.271	.345	.187	.246	.140	.067	1.000		
MR	.340	-.493	-.391	-.243	-.289	.332	.196	-.032	.276	-.158	1.000	
TS	-.169	.165	.022	.144	.371	-.195	-.001	.288	-.014	.146	-.196	1.000

LOG = natural log;
FL = laboratory fatigue life;
R.PEN = recovered asphalt penetration;
AC = asphalt content (percent by weight);
SAND = sand in AC mix (percent by weight);
FINE = fine in AC mix (percent by weight);
AGG = aggregate (plus #4) in AC mix (percent by weight);
ANG = angularity of aggregate (plus #4) particles in AC mix;
SPGTY = sample bulk specific gravity;
CL = average load (pounds);
TT = test temperature (°F);
MR = resilient modulus (psi);
TS = tensile strain at failure.

the coefficient of correlation between the specific gravity "SPGTY" of the samples and the recovered penetration "R.PEN" of the asphalt cement is 0.443 (see Table 5.3). This is reasonable (not coincidental) and it can be explained. That is, higher values of specific gravity indicate higher densities and lower air voids and hence, lower rates of oxidation of the asphalt cement which result in a higher recovered penetration. However, one term cannot be substituted by the other due to the lack of a proper transformation model (the rate of oxidation is affected by numerous other factors whose effects are not fully understood at this time).

The problem of collinearity between the independent variables can be partially resolved by several methods including:

1. Stratifying the data by grouping it such that only the value of one independent variable changes at one time. For the type and nature of the data of this study, this method is not practical and it cannot be applied. The reason is that, the experiment matrix will have to have a large number of entries. Stated differently, the size of the experiment and the number of the samples that needed to be tested make the cost of this study prohibitive.
2. Excluding those variables which show high collinearity to other variables from the statistical model. This solution can cause some bias in the resulting statistical model.
3. Creating clusters of variables whereby two or more independent and collinear variables are clustered together and the values of the cluster are used to represent the collective influence of the independent variables. Although this method is sound where the independent variables can be expressed through a transformation function or theoretical models, it is not applicable to this data.

Nevertheless, the values of the coefficient of correlation between the dependent and independent variables listed in Table 5.3 reflects the relationship between the logarithmic values of the fatigue life and the original (untransformed) values of the independent variables. Examination of the values of the coefficient of correlations leads to the following statistical observations:

1. The most significant variable (corresponding to the highest value of the coefficient of correlations of Table 5.3) affecting the fatigue life of the asphalt mixes is the aggregate angularity. Increasing aggregate angularity causes an increase in the fatigue life. This result is reasonable and it was expected. Higher aggregate angularity provides a better aggregate interlocking which causes a better stress distribution (i.e., lesser compressive and tensile stresses).

2. The second most important variable is the asphalt cement in the mix. In this regard, two factors adversely affect the fatigue life. In their order of significance, these two factors are the recovered penetration of the asphalt cement and the percent asphalt content. Increasing values of any of these two variables cause a decrease in the fatigue life. In reference to Table 5.3, two important observations can be made as follows:

    a) The recovered asphalt penetration shows some degrees of collinearity to the percent fine and to the aggregate angularity. Higher percentage of fine cause denser mixes and lower air voids. Hence, the rate of field oxidation decreases. On the other hand, using angular aggregates in the asphalt mix causes lower densities and higher air voids which increase the rate of oxidation in the field.

    b) The percent asphalt content shows a relatively high degree of collinearity to the percent fine and a relatively low one to the aggregate angularity. While the latter observation is not significant, the former one implies that higher percent fine content causes higher asphalt contents. Once again, this is reasonable because higher fine contents increases the total surface area that needs to be coated with asphalt. Hence, the effects of the asphalt content on the fatigue life cannot be assessed unless the percent fine is held constant and the percent asphalt content increased. While this solution is possible for laboratory compacted samples, it is not practical for core samples.

The two observations noted above implies that the values of the coefficient of correlations between the fatigue life, on one hand, and the percent asphalt content and the recovered penetration, on the other hand, should not be taken at their face values. The collinearity between these two variables and other independent variables should be addresses. In other words, the above observations are statistical in nature and they should not be taken at face values when considering their engineering interpretations. To illustrate, consider the value of the coefficient of correlation of the recovered asphalt penetration of "-.424" (see Table 5.3). This implies that if the values of the recovered asphalt penetration is truly an independent variable, then increasing values result in a shorter fatigue life. Recall that the recovered penetration of the asphalt cement is a function of the asphalt mix processing practice and temperature, storage time, age (service life) of the pavement, the air voids in the asphalt mix and the composition of the aggregate and sand in the AC mix. Hence, the coefficient of correlation of the recovered penetration (PEN) of "-.424" reflects the global effects of the above noted factors. Hence, this correlation cannot be taken at its face value. That is one cannot conclude that softer asphalts have a better ability to withstand plastic deformation without cracking than that of harder asphalt. Moreover, the correlation matrix of Table 5.3 provides information relative to the relationship between the fatigue life and the unprocessed (original) values of the independent variables. The values of the coefficient of correlation listed in the Table and the order of significance of the independent variables may change as their values are transformed. For example, if the value of the recovered asphalt penetration are expressed by an exponential function, then their coefficient of correlation to fatigue life and their order of significance will change.

Further, examination of the values of the coefficient of correlation of Table 5.3 indicates that the variables contributing the most to the fatigue life of the AC mix is the angularity of the coarse aggregate and the second one is the recovered asphalt penetration. This however, does not imply that the recovered penetration of the asphalt cement will be included as a variable in the final statistical equation. The reason for this is that the recovered penetration shows a certain degree of collinearity to the aggregate angularity and other variables. Indeed, the final statistical equation based on the untransformed values of the independent variables did not include the recovered asphalt penetration as a variable. The significance of this term was below the specified criterion. This criterion for variable inclusion in the final statistical model specifies that if the probability associated with the "F" statistics for the hypothesis that the coefficient of the variable is zero is equal to or less than five percent (0.05), then the variable is excluded from the model. In the SPSS computer program, this probability is designated by "FIN".

3. The percent aggregate, sand and fine contents affect the fatigue life of the asphalt mixes in the respective order of significance. Increasing the percent aggregate content cause an increase in the fatigue life. Whereas, increasing sand and fine contents leads to a decrease in the fatigue life. Once again, these results were expected and confirm the data reported in the literature. One point should be noted here is that, the aggregate in the asphalt mix affects the fatigue life in two ways, the aggregate content and the angularity of the aggregate. Further, the effects of the aggregate on fatigue life cannot be had unless the aggregates are not floating in the sand matrix. That is, a full contact between the aggregates is fully mobilized.

4. The effects of the other asphalt mix variables (such as the resilient modulus and

the specific gravity or air voids of the samples) on the fatigue life also confirm those reported in the literature (3, and 12 through 16). Increasing either the specific gravity (decreasing the air voids) or the resilient modulus cause an increase in the fatigue life.

5. The effects of the test variables (such as the temperature and the magnitude of the applied load) on the fatigue life are statistically insignificant. The reasons being are:
   a) All tests were conducted at room temperature where the measured temperature (see Table 5.1) varied from about 74 to about 82 °F. Most tests were conducted at about 75 °F.
   b) The cyclic load was carefully controlled to within the accuracy of the MTS system. Although the magnitude of the cyclic load varied from one sample to another, most samples were tested under a 300 pounds cyclic load.

The above observations concerning the effects of the independent variables on the independent one are only relevant to the untransformed values of the independent variables. These observations may be altered or totally changed when the values of each variable are transformed by using the proper transformation form based on the observation of the trend between the dependent and the independent variables. For example, the coefficient of correlation of the most contributing significant variable (the aggregate angularity) of 0.47 may not be the optimum value. That is if the value of the aggregate angularity are used in a transformed form then its coefficient of correlation will change. For this reason, several transformed forms of the independent variables were used. First the independent variable in question was plotted against the logarithmic values of the dependent variable (fatigue life). From the plot, several transformation forms that simulate the trend between the dependent and the independent variables were used and the forms that showed the highest coefficient of correlation and the least standard error were selected for the final analysis. These and other issues are presented in the next section "Regression Analysis".

5.4.4 Regression Analysis

The fatigue life of the asphalt mix core samples is a function of the asphalt mix variables, the test conditions and the previous loading history. Although, the test variables were kept constant throughout the testing program, some variations were observed in the applied cyclic load and the test temperature (see Table 5.1). Therefore, the test variables were considered as independent variables affecting the fatigue life of the samples. Further, since the test samples were obtained from pavement cores, the age (service life) of the pavement structure, the cumulative 18-kip ESAL that had travelled on the pavements were also included in the analysis. It should be noted that the service lives of the composite pavement sections were not included in the analysis. The reason for this is that due to the thickness and stiffness of the portland cement concrete (PCC) slab located beneath the AC layer, the neutral axis of the composite pavement is located below the AC overlay. That is, the AC surface was not subjected to tensile stress or strain due to traffic loading. The tensile strains induced in the AC layer due to the expansion and contraction of the concrete slab and the AC surface were neglected. Such strains cannot be calculated unless the state of cracks of the PCC slab is fully known.
As stated earlier, the criterion for excluding a variable from the statistical model specifies "FIN" value of 5 percent or better. Prior to the analysis, each independent variable was plotted against the logarithmic values of the fatigue life. The trend of the data was then modeled using several equation forms (e,g. logarithmic, cubical, polynomial). During the analysis, the various equation forms for each variable were analyzed. The form that yielded the lowest "FIN" value, highest coefficient of correlation, highest significance level, and lowest standard error in the presence of the other independent variables was

then selected for the final analysis.

Again, all the sample and test variables were included in the analysis. Variables that did not meet the specified "FIN" criterion were excluded from the model. Table 5.4 provides a list of the correlation matrix for those variables that satisfied the "FIN" criterion. It can be seen that only 5 variables are included in the final model. These variables are listed below in their order of explaining the observed variations in the fatigue life.

1. Aggregate angularity.
2. Asphalt content.
3. Specific gravity.
4. Percent fine.
5. Pavement age or service life.

Examination of the values of the coefficient of correlation matrix of Table 5.4 indicates that:

1. The coarse aggregate angularity has the highest correlation coefficient (the most significant variable) with the fatigue life. Increasing aggregate angularity causes an increase in the fatigue life. In addition, the aggregate angularity has a positive (direct) degree of collinearity with the service life. That is higher aggregate angularity is associated with higher service life. This collinearity can be directly attributed to the MDOT pavement and mix design practices. Typically, more angular aggregates are used for those pavements designed to have higher service life and higher traffic volumes.
2. The asphalt content (LOGAC) and the sample bulk specific gravity (SPGTY2) have some degrees of collinearity with the percent fine (LOGFINE). As stated earlier this was expected because higher amount of fines causes an increase in the surface area of the sample to be coated with asphalt thus, increasing the asphalt content in the AC mix. Further, fines fill the intermediate voids between the

Table 5.4 : Correlation matrix for the final variables.

	LOGFL	ANG3	LOGAC	SPGTY2	LOGFINE	SL
LOGFL	1.000					
ANG3	.490	1.000				
LOGAC	-.310	.204	1.000			
SPGTY2	.264	.142	.322	1.000		
LOGFINE	-.096	.281	.687	.603	1.000	
SL	-.001	.456	-.144	.064	-.134	1.000

LOG = base 10 logarithmic;
FL = laboratory fatigue life (thousands of load applications);
ANG3 = (angularity of the coarse particles (plus #4) in the AC mix)^3;
AC = asphalt content, (percent by weight);
SPGTY2= (sample bulk specific gravity)^2;
FINE = Fine, (percent by weight); and
SL = pavement service life from construction until coring.

larger aggregates thereby affecting the bulk specific gravity of the AC mix.

Nevertheless, the degree of collinearity between the independent variables listed in Table 5.4 were examined. Table 5.5 provides a list of the six eigenvalues and condition indices, and the variance proportion (the percent of the variance attributable to the eigenvalue) of each variable for each eigenvalue. It should be noted that, for each variable, the sum of the values of its variance proportion over the eight eigenvalues is equal to 1.0. That is, the variance of each variable has a different degree of proportionality to the various eigenvalues such that their sum is equal to 1.0. For example, a value of the variance proportion of the aggregate angularity (ANG) of 0.00564 implies that .564 percent of the variance of ANG is attributed to the first eigenvalue. Likewise, the ANG variance proportion of 0.01049 indicates that 1.05 percent of the variance of ANG is attributed to the 6th eigenvalue. Nonetheless, the values of the variance proportion and the eigenvalue indicate the degree of collinearity or multicollinearity of the variable in question to the other variables. Higher values of the variance proportion for the lowest eigenvalue implies a high degree of collinearity. For example, the two terms "SL" (service life) and "constant" have high variance proportion values of 0.87275 and 0.94560, respectively, for the minimum eigenvalue of 0.0. These values indicate, as it should be expected, a high degree of collinearity between the two terms. Since, the other variables have small variance proportion values for the 6th eigenvalue, they do not seem to have a significant multicollinearity. In addition the tolerance and the variance inflation factors (VIF) were calculated for each variable and are listed in Table 5.6. The low VIF values for the variables indicate that they are not collinear, and authenticate the previous finding based on eigenvalues and condition index. These diagnostics indicate that no significant degree of collinearity exists among the variables.

The results of the regression analysis are listed in Table 5.7. Once again, all the variables that are included in the resulting equation satisfy the specified criterion for the

Table 5.5 : **Collinearity diagnostics (eigenvalues, condition indices and the proportion of the variance attributable to the eigenvalue).**

		Cond	Percent of variance attributed to the eigenvalues					
Number	Eigenval	Index	Constant	ANG3	LOGAC	SPGTY2	SL	LOGFINE
1	5.32541	1.000	.00004	.00564	.00009	.00018	.00004	.00762
2	.48260	3.322	.00013	.02986	.00030	.00065	.00012	.50661
3	.18158	5.416	.00017	.81789	.00018	.00007	.00015	.32286
4	.00751	26.623	.04390	.12803	.00024	.45946	.00885	.11645
5	.00231	48.000	.01015	.00808	.77616	.09755	.11809	.02455
6	.00058	95.504	.94560	.01049	.22303	.44210	.87275	.02191

Table 5.6 : Collinearity diagnostics: TOL and VIF

Variable	Tolerance	VIF
ANG3	.655789	1.525
LOGAC	.512891	1.950
SL	.675476	1.480
SPGTY2	.588911	1.698
LOGFINE	.327870	3.050

variable inclusion. It can be seen from Table 5.7 that all the variables in the equation have a "T" significance values of less than 0.05. Hence, they are significant variables. The results of the regression analysis listed in Table 5.7 indicate that the standard error of the resulting model is 0.14923. The value of the coefficient of determination (R^2) is 0.78 and the adjusted R^2 is 0.75. The numbers listed under the column designated "B" are the regression constants for the indicated variables. The stepwise development of the model is addressed below.

Table 5.8 provides a list of the regression constants and the values of the R^2 and the standard error obtained from each step of the stepwise method of the SPSS computer program. It can be seen that the aggregate angularity "ANG" is the most significant variable and this term alone explains 24 percent of the variation of the logarithmic values of the fatigue life (the dependent variable) of the asphalt samples. This percentage increases, as it should be expected, with the inclusion of more variables in the model. The final model can be expressed as follows:

$$LOG(FL) = 2.1261 + .0068\,(ANG)^3 - 2.4266\,(LOG(AC)) - .0183\,(SL) + .7520\,(SPGTY)^2 - 1.484\,(LOG(FINE)) \quad (5.4)$$

$$R^2 = 0.781,\ SE = 0.149,\ F = 34.97,\ F_{(Sig)} = 0.000$$

where

LOG	=	base 10 logarithm;
FL	=	laboratory fatigue life (thousands of load applications);
ANG	=	angularity of the coarse aggregate particles in the AC mix (1=rounded, 5=crushed on all sides);
AC	=	asphalt content (percent by weight of the total AC mix);
SL	=	pavement service life from construction or last rehabilitation to coring (years);
SPGTY	=	sample bulk specific gravity;

Table 5.7 : Results of regression analysis.

Multiple R	.88380
R Square	.78110
Adjusted R Square	.75877
Standard Error	.14923

Analysis of Variance

	DF	Sum of Squares	Mean Square
Regression	5	3.89390	.77878
Residual	49	1.09122	.02227

F = 34.97017 Signif F = .0000

* * * * M U L T I P L E R E G R E S S I O N * * * *

Equation Number 1 Dependent Variable.. LOGFL

------------------ Variables in the Equation ------------------

Variable	B	SE B	Beta	T	Sig T
ANG3	.006869	6.35088E-04	.892749	10.817	.0000
LOGAC	-2.426645	.525708	-.430794	-4.616	.0000
SL	-.018319	.002592	-.574717	-7.067	.0000
SPGTY2	.752051	.106965	.612354	7.031	.0000
LOGFINE	-1.483891	.348211	-.497427	-4.261	.0001
(Constant)	2.126127	.575990		3.691	.0006

Table 5.8 : Regression matrix for laboratory fatigue life.

Laboratory Fatigue life LOG(FL)	Intercept	Regression coefficient of Independent variables						
		ANG3	LOGAC	SL	SPGTY2	LOGFINE	R.Sq.	S.E
	3.325366	.003773					.240	.267
	5.100313	.004444	-2.4114				.416	.236
	5.591363	.006169	-3.0284	-.01412			.560	.207
	3.442994	.006075	-3.7687	-.01535	.4890		.699	.173
	2.126127	.006869	-2.4266	-.01832	.7521	-1.4839	.781	.149

variables same as correlation matrix.

FINE = fine (percent by weight);

R^2 = coefficient of determination;

SE = standard error;

F = F statistic; and

$F_{(sig)}$= significance of F.

Based on the statistics of the model, the following two observations were made:

1. The null hypothesis of no linear relationship between the independent variables and the laboratory fatigue life was rejected and it was concluded that at a probability of F=0.000, 78 percent of the variation in the laboratory fatigue life is explained by the above listed independent variables.
2. The largest value of the "T" significance is 0.0001. This implies that all variables in the model are statistically significant.

In addition, the following statistics were calculated to study the residuals and the predicted values and are listed in Table 5.9.

1. PRED = the unstandardized predicted values;
2. RESID = the unstandardized residuals;
3. ZPRED = the standardized predicted values;
4. ZRESID = the standardized residuals; and
5. D.W.S = the Durbin-Watson statistics.

The Durbin-Watson statistics is a measure of the autocorrelation between the residuals. The regression analysis assumes that the residuals are uncorrelated, in which case the value for Durbin-Watson test should be close to 2. The calculated value of 2.14 for the model signifies a satisfactory lack of correlation between the residuals. Further, the maximum, minimum, mean and standard deviation of the unstandardized and standardized predicted values and the residuals are also presented in Table 5.9. Based on the values of the residuals and the standardized residuals the ten worst residuals are listed in Table 5.10.

Table 5.9 : Residual statistics of the data.

	Min	Max	Mean	Std Dev	N
*PRED	3.1525	4.0739	3.5532	.2685	55
*RESID	-.2916	.2848	.0000	.1422	55
*ZPRED	-1.4922	1.9391	.0000	1.0000	55
*ZRESID	-1.9538	1.9088	.0000	.9526	55
Durbin-Watson Test = 2.14477					

Table 5.10 : Ten worst Residual.

Case #	*RESID	*ZRESID
16	-.2916	-1.95378
42	.2848	1.90878
15	.2565	1.71892
24	-.2387	-1.59939
20	.2327	1.55961
3	.2315	1.55162
6	-.2254	-1.51032
13	.2205	1.47733
26	-.2129	-1.42690
5	.2128	1.42625

A histogram of the standardized residuals of equation 5.4 is presented in Figure 5.6. "N" represents the observed number of residuals in an interval whereas, "Exp N" indicates the expected number of residuals in that interval. The extreme interval labeled as "out" contain more than 3 standard deviations from the mean of the residuals. The expected frequency and the overlap between expected and observed are indicated by a period and a colon respectively. The presented histogram is fairly normal indicating that the statistical model has no significant bias.

To this end, the sensitivity of the statistical model to the various input parameters and comparison between the observed and predicted values are presented in the next section.

5.4.5 Sensitivity Analysis and Engineering Interpretation

The statistical model presented by equation 5.4 was used to predict the fatigue life of the test samples. Figure 5.7a depicts the values of the predicted fatigue life versus the laboratory observed one. The straight line in the Figure represents the locus of those points where the observed and predicted fatigue lives are equal. It can be seen that most predicted values are reasonably close to the observed ones. Figure 5.7b depicts the percent errors between the predicted and the observed fatigue life values. A negative percent error implies that the statistical model under predicts the fatigue life of the indicated sample. A positive error on the other hand, indicates an over prediction. Examination of the Figure indicates that the predicted fatigue lives of 89 percent of the samples (about 50 samples) are within 50 percent of the observed values. This indicates that the statistical model is relatively accurate.

One additional point should be made herein is that, the fatigue life of a pavement structure is a function of several variables including the stiffnesses and thicknesses of the various pavement layers, the properties of the materials in the AC mix, the traffic

```
N Exp N     (* = 1 Cases,     . : = Normal Curve)
0   .04   Out
0   .08  3.00
0   .21  2.67
0   .49  2.33
1  1.00  2.00 :
3  1.84  1.67 *:*
2  3.02  1.33 **.
5  4.44  1.00 ***:*
7  5.84   .67 *****:*
7  6.89   .33 ******:
6  7.28   .00 ******.
3  6.89  -.33 ***   .
9  5.84  -.67 *****:***
6  4.44 -1.00 ***:**
3  3.02 -1.33 **:
2  1.84 -1.67 *:
1  1.00 -2.00 :
0   .49 -2.33
0   .21 -2.67
0   .08 -3.00
0   .04   Out
```

Figure 5.6 : Histogram standardized residual

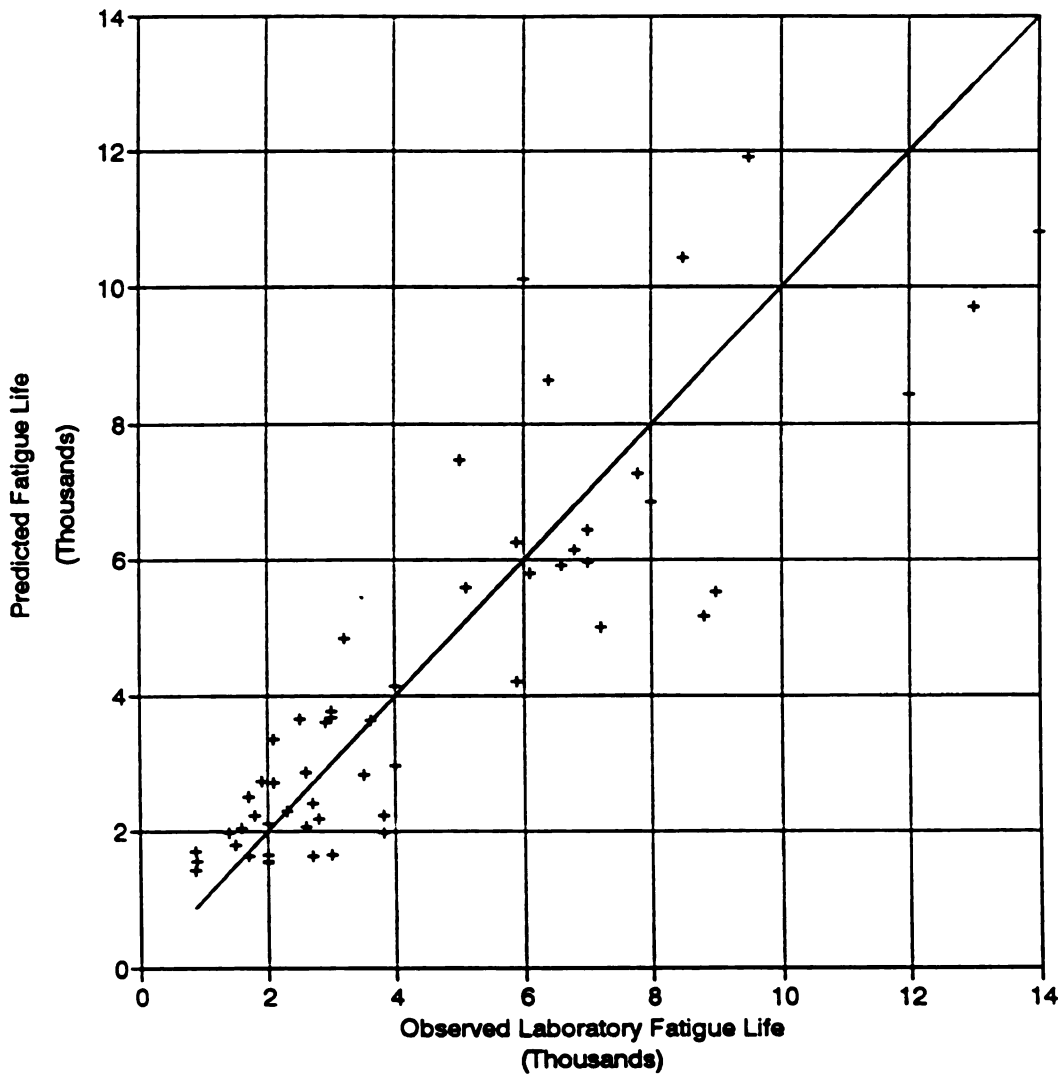

Figure 5.7a : **Observed versus the predicted laboratory fatigue lives of the 55 test samples.**

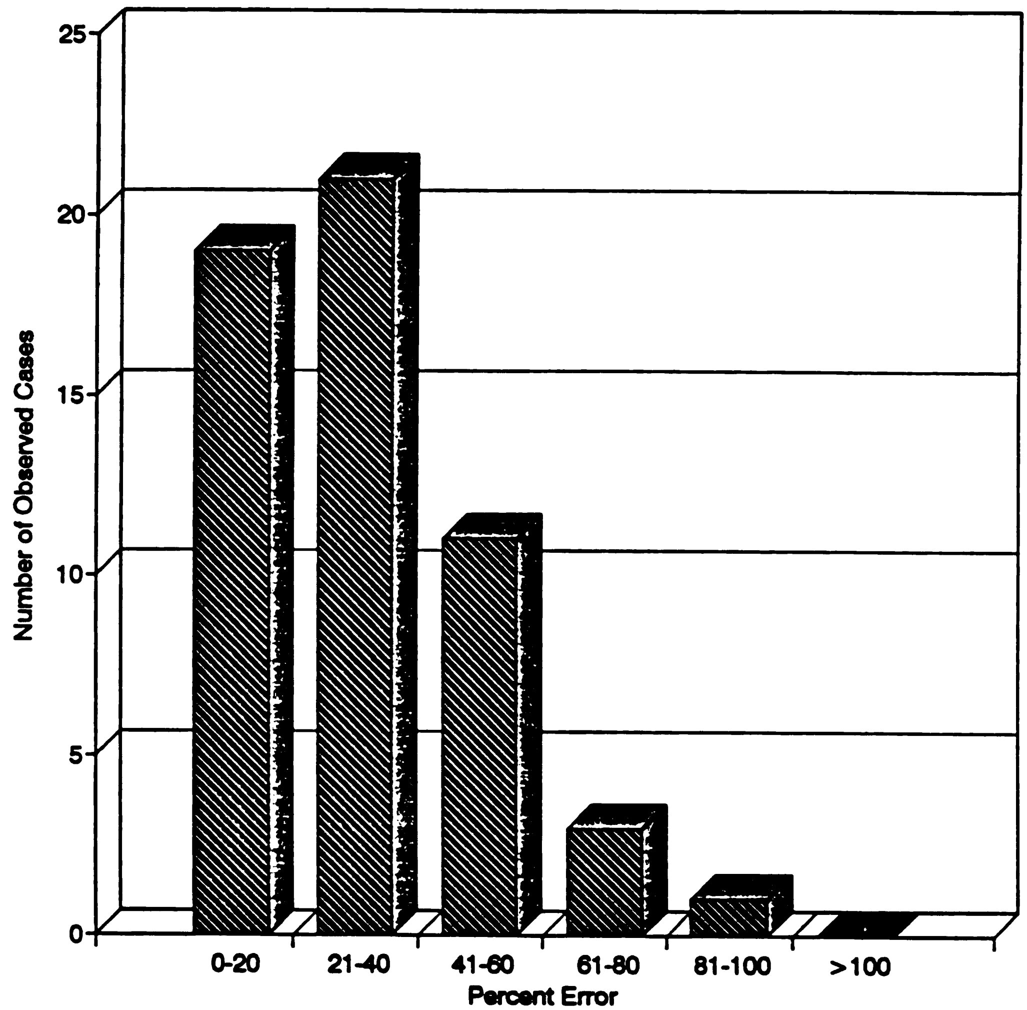

Figure 5.7b : **Percent difference between the observed and the predicted laboratory fatigue lives for the 55 test samples.**

volume, load, and environmental factors. In this study, only the asphalt mix properties and the traffic load and volume data are used. Since, all of the test samples were obtained from field cores, they were subjected to a history of stresses/strains that is a function of the above listed factors. Consequently, one should not expect the statistical model presented in equation 5.4 to fully explain the variations in the fatigue life.

In any event, the sensitivity of the statistical model to variations in each independent variable and the engineering interpretations of the model are presented in the next section.

Sensitivity analysis of equation 5.4 was performed to determine the effect of each variable in the equation on the predicted fatigue life of the test samples. The sensitivity of the model to each variable was analyzed such that:

1. The values of three variables in the equation were held constant.
2. The value of a fourth variable was changed from a low, to a medium, to a high value within the range of that variable.
3. The value of the variable in question was varied from one end of its range to the other.

Results of the sensitivity analysis are presented and discussed below.

Aggregate Angularity - Figure 5.8 depicts the sensitivity of the predicted fatigue life to the aggregate angularity for constant values of the asphalt and fine contents, and the specific gravity of the sample, and for three levels of service life (1, 15, and 20 years). Examination of the Figure indicates that:

1. Increasing aggregate angularity from 1 (rounded aggregate such as river gravel) to 5 (aggregate crushed on all sides) causes an increase in the fatigue life by a factor of about 7.
2. The rate of increase in the fatigue life varies from one value of the aggregate angularity to the other. For example, using aggregate crushed on only two sides (aggregate angularity of 3) causes the fatigue life of the

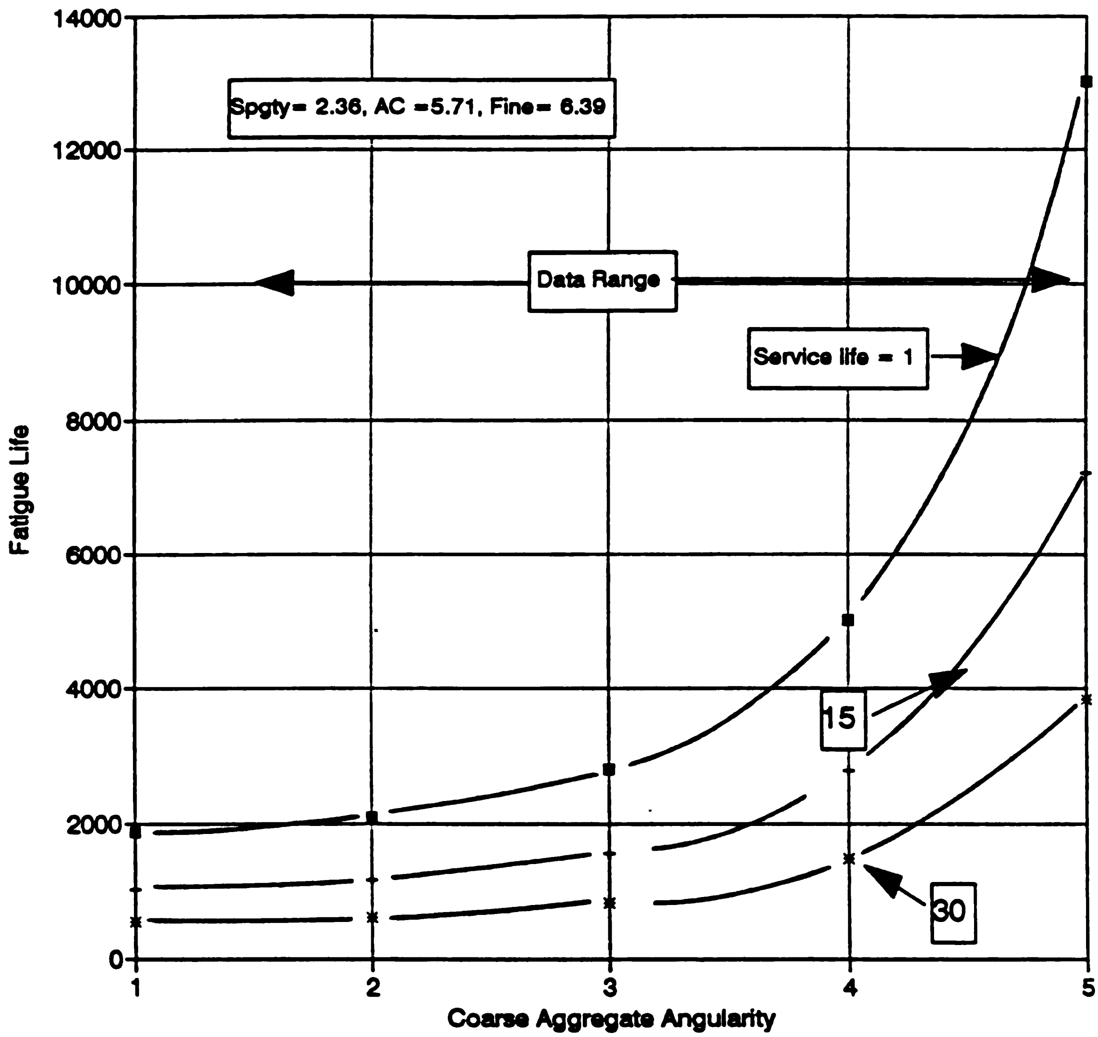

Figure 5.8 : Laboratory fatigue life as a function of aggregate angularity, for different levels of service life.

asphalt mixes to increase by a factor of only 1.5 relative to those made by using rounded aggregate. Given that the difference in cost between crushing the aggregate on one side and on all sides is not significant, the benefit to cost ratio will be maximized by using aggregate crushed on all sides.

3. For all values of the service life, the rate of increase in the predicted fatigue life is the same.

Service Life - Figure 5.9 shows the sensitivity of the predicted fatigue life to the service life of the pavement structure for constant values of the asphalt and fine contents, and the specific gravity of the sample, and for three levels of aggregate angularity (1, 3 and 5). Examination of the Figure indicates that:

1. Increasing the service life (older pavements) from zero (after construction) to 30 years causes a decrease in the predicted fatigue life by a factor of about 3.5. Recall that a longer service life of a pavement structure indicates that the pavement was subjected to a higher traffic volume. Higher traffic volumes cause higher accumulation of plastic (permanent) strain in the asphalt which is the main cause of fatigue cracking. Thus, the term "service life" herein represents the stress and/or strain history of the asphalt course. If the asphalt course was subjected to higher stress and/or strain levels during its service life then its remaining service life (RSL) should be expected to decrease.

2. The rate of increase in the fatigue life of the asphalt samples with respect to the service life of the pavement structure is almost constant (near linear relationship). This implies that the data can be used to obtain a shift factor whereby the laboratory measured/predicted fatigue life of an asphalt mix can be used to calculate the fatigue life of a pavement structure made by using the same asphalt mix. Such a shift factor will be constant for all

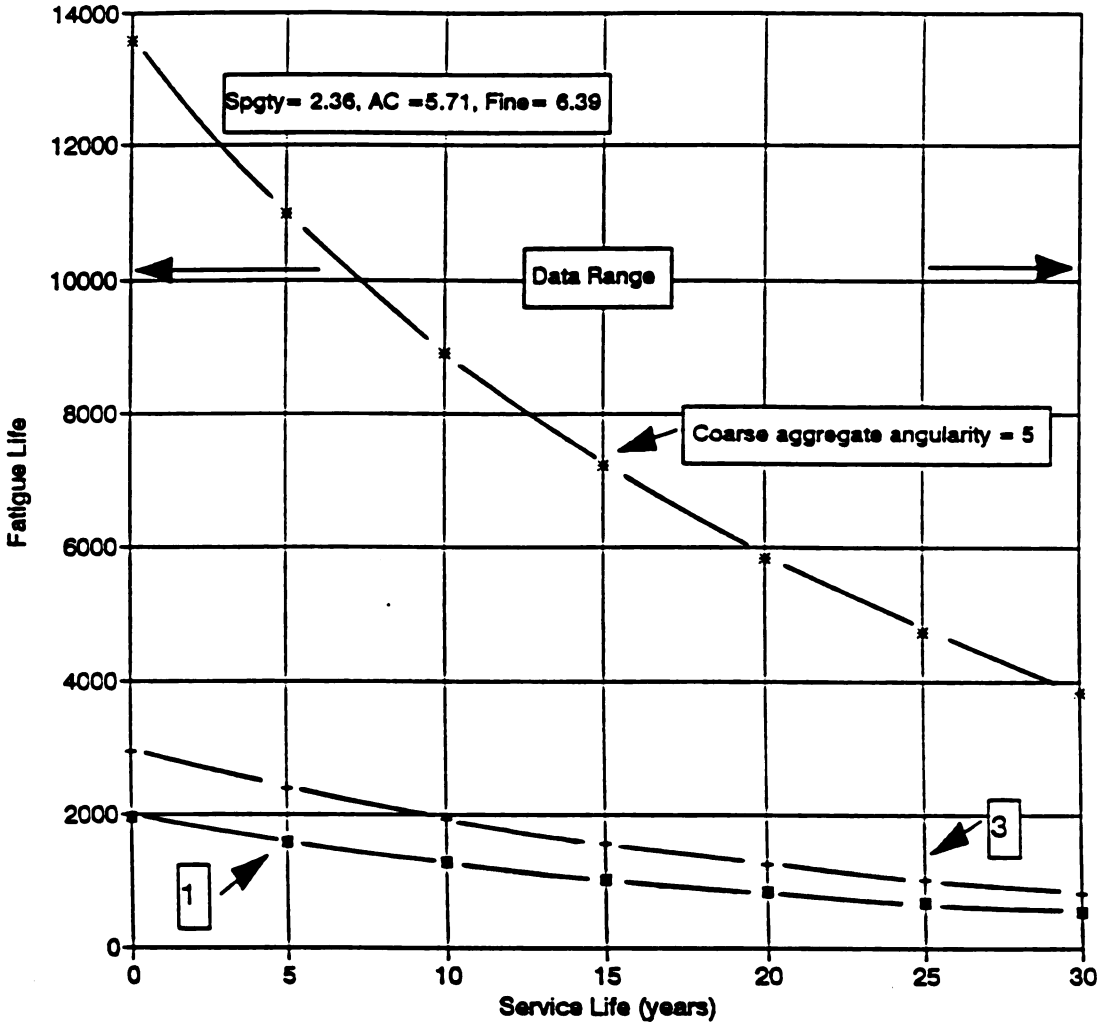

Figure 5.9 : **Laboratory fatigue life as a function of pavement service life, for different levels of coarse aggregate angularity.**

pavement structures provided that the service lives of the pavements are used. On the other hand, if one is interested to predict the fatigue life of the pavement structure in terms of the number of 18-kip ESAL, then the shift factor becomes site specific. In this regard, the number of 18-kip ESAL can be calculated by using the average daily traffic (ADT), the percent commercial, and the ESAL factor for the pavement in question. Table 5.11 provides a list of the values of the shift factors in terms of service life and the number of 18-kip ESAL for the flexible pavement sections included in this study. Verification of the shift factors is presented in section 5.7.

Bulk Specific Gravity - Figure 5.10 shows the predicted fatigue life as a function of the bulk specific gravity of the samples for constant values of the asphalt and fine contents and service life and for three levels of aggregate angularity of 1, 3 and 5. Examination of the Figure indicates that:

1. Increasing the sample bulk specific gravity from 2.2 to 2.5 causes an increase in the fatigue life by a factor of about 11.5. This observation however, should not be interpreted as higher bulk specific gravity causes a better pavement performance. Other types of pavement distress such as rut need to be evaluated before a decision can be made. The reason being is that higher bulk specific gravity values imply lower air voids. Although, lower air void values (lower than about 2 percent) cause higher fatigue life, percent air voids in the order of 2 or less causes distortion and rutting in the pavement structures. One other point should be noted herein is that very low bulk specific gravity values (lower than about 2.25) may cause bearing capacity failure of the pavement structure.

2. The rate of change in the fatigue life with respect to the bulk specific gravity increases at the higher values of the specific gravity. This implies

Table 5.11 : Shift factor for the flexible pavement sections.

Section No.	Avg. Material Properties				Service Life	Cum. ESAL	Lab. Fatigue Life	Lab. Fatigue Life for Zero S.L	Difference	Shift Factor
	AC	Fine	Ang.	Spgty	(years)	(millions)				
7F	4.4	4.0	2.3	2.326	7	1.25	4929	6622	1693	739
29F	4.8	4.4	2.9	2.318	11	0.76	3238	5150	1912	398
19F	5.5	6.6	3.2	2.355	11	1.58	2019	3210	1192	1324
43F	6.3	7.1	3.0	2.372	1	0.76	2080	2170	90	8464
35F	5.9	5.7	4.8	2.303	14	1.37	4159	7506	3348	408
10F	7.2	6.6	3.6	2.387	7	0.22	2025	2721	696	311
14F	5.9	7.3	3.1	2.374	13	0.18	1562	2703	1141	157
13F	5.7	6.9	4.8	2.405	30	1.51	4250	15063	10814	140

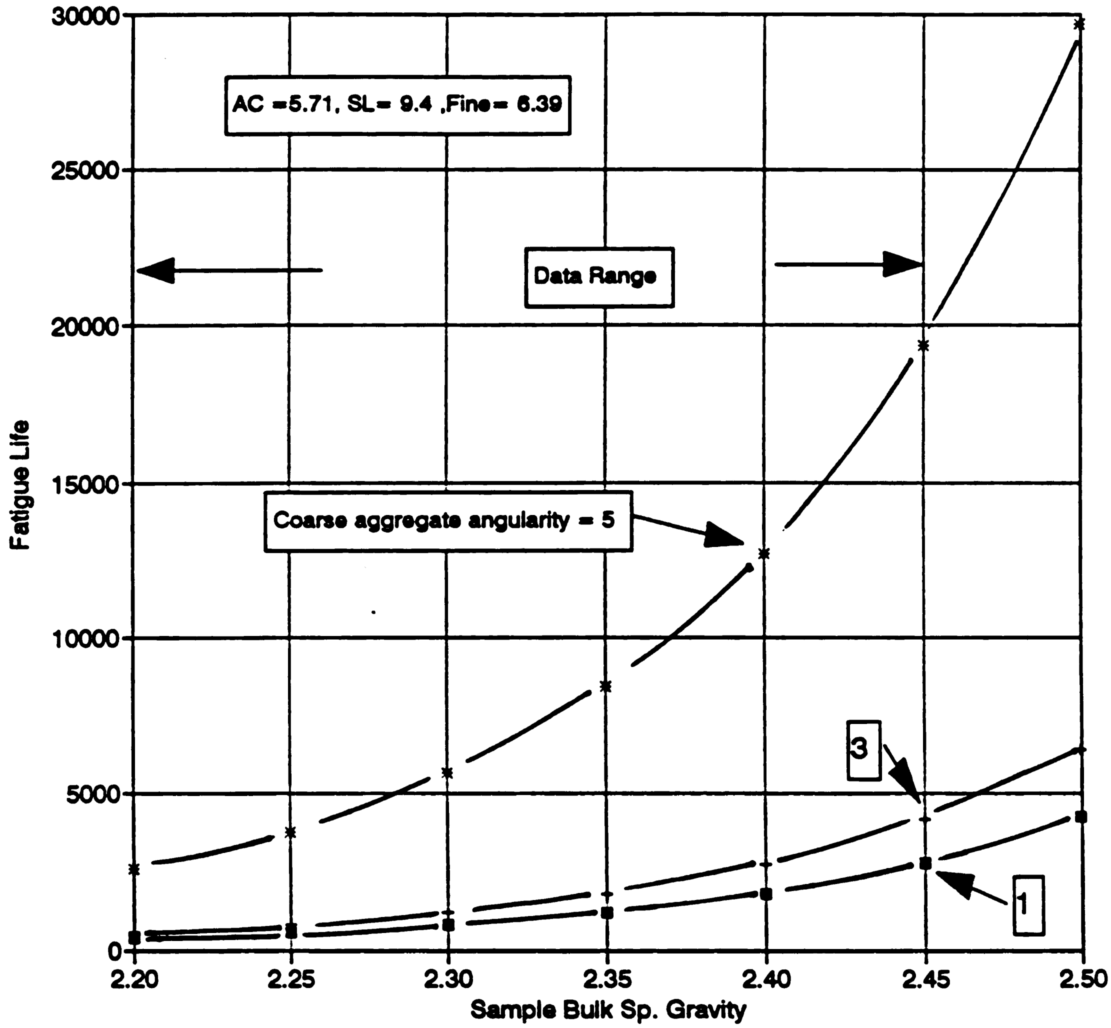

Figure 5.10 : **Laboratory fatigue life as a function of sample bulk specific gravity, for different levels of coarse aggregate angularity.**

that the incremental benefits of compaction increases as the compaction efforts (the number of roller paths) increases. However, the rate of increase in the bulk specific gravity with respect to increasing compaction efforts decreases at the higher values of specific gravity. Consequently, economic analysis regarding the benefits and costs should be conducted before a decision regarding the proper compaction effort can be reached.

Fine - Figure 5.11 depicts the fatigue life (predicted by using equation 5.4) as a function of the fine content for constant values of the asphalt content, service life and bulk specific gravity of the samples, and for three levels of aggregate angularity. It can be seen that fine content has a detrimental effect on the fatigue life. Higher fine contents cause lower fatigue life. Increasing the fine content from 4 to 10 percent (the data range) causes a decrease in the fatigue life by a factor of about 4.5. This observation should not be taken independent of that regarding the bulk specific gravity. Lower fine contents cause lower bulk specific gravity and lower asphalt content. Thus, either the combined effects of fine content, bulk specific gravity, and asphalt content should be addressed or the effects of each variable should be studied separately by stratifying the three variables. Due to the nature of the test samples in this study (core samples), the latter avenue was not possible. The former one can be analyzed through an example by using hypothetical data. Such an example is given at the end of the next paragraph.

Asphalt Content - Figure 5.12 displays the relationship between the predicted fatigue life and the asphalt content for constant values of the service life, bulk specific gravity of the sample, and fine content, and for three levels of aggregate angularity. It can be seen that higher asphalt contents cause lower fatigue life. As is the case for the fine content, the effects of the asphalt content should not be taken herein at face value. The asphalt content of an asphalt mix is affected

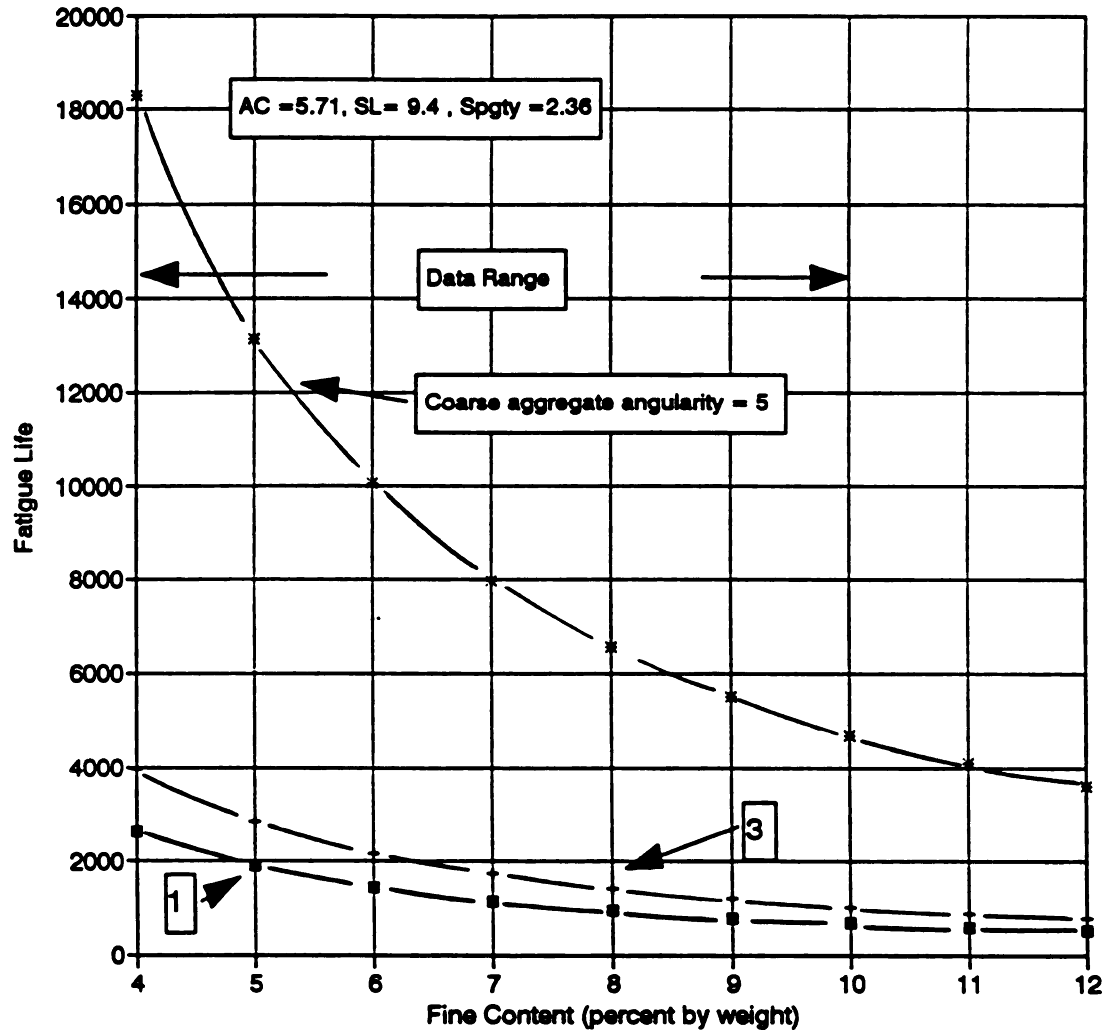

Figure 5.11 : **Laboratory fatigue life as a function of fines, for different levels of coarse aggregate angularity.**

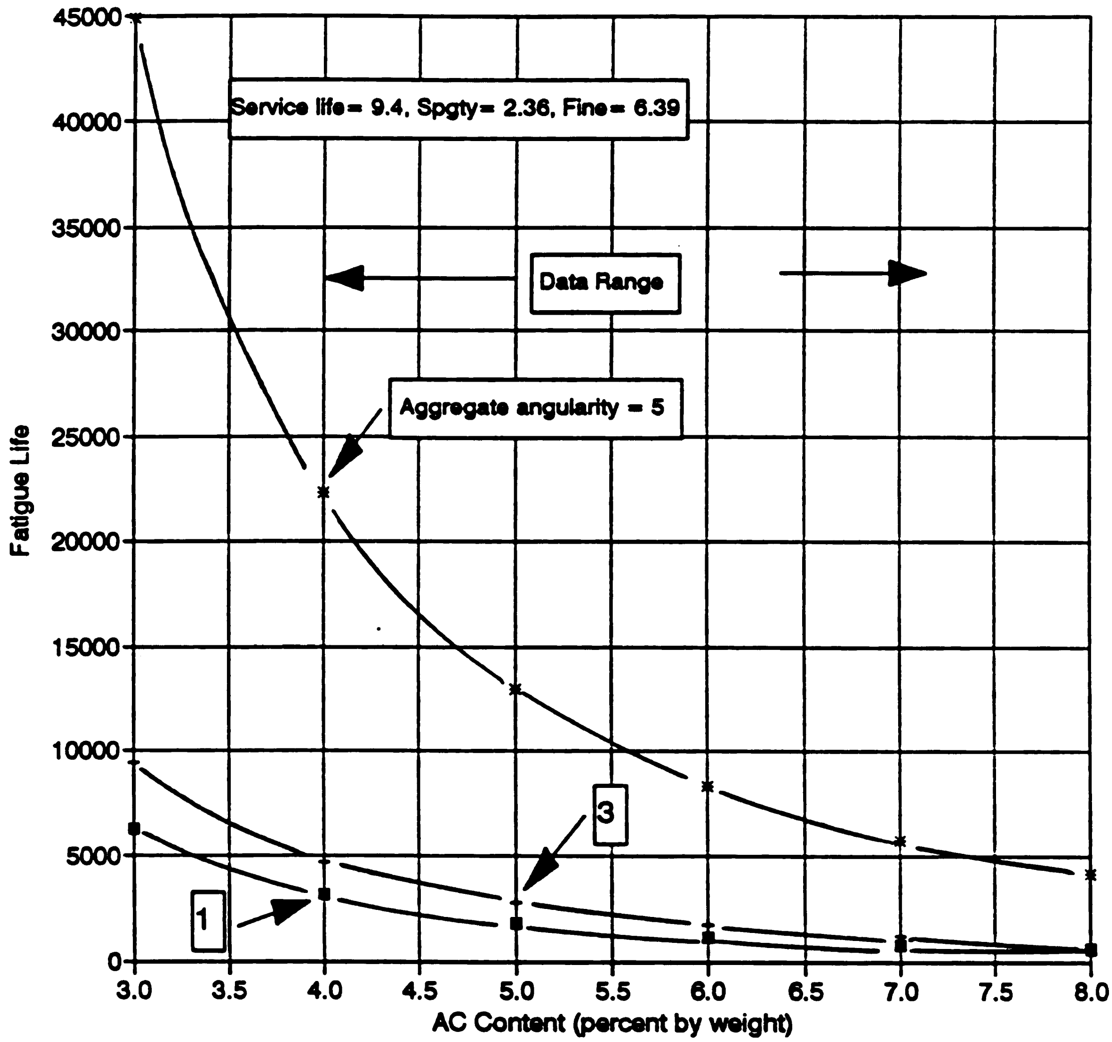

Figure 5.12 : **Laboratory fatigue life as a function of AC content, for different levels of coarse aggregate angularity.**

by the fine content and it influences the bulk specific gravity of the sample. Hence, the combined effects of the three variables (fine and asphalt contents and the bulk specific gravity is addressed by using an example in the next paragraph.

The Combined Effects of Bulk Specific Gravity and Asphalt and fine Contents - Consider an AC mix with a bulk specific gravity of 2.193, an AC content of 4.10 percent, a fine content of 3.10 percent, aggregate angularity of 2 and a service life of 15 years will yield a fatigue life of 2028 load repetitions using equation 5.4. Increasing the percent fine content of the mix to 7 percent will also increase the bulk specific gravity to 2.275. For new values of the percent fine content and the bulk specific gravity (rest of the variables same as before) equation 5.4 yields a fatigue life of 1142 load repetitions. The implication of the above observation is that although, increasing the fine content in the AC mix causes an increase in the bulk specific gravity of the mix, but the negative affect due to increase in the fine content on the fatigue life is overwhelming as compared to the positive affect of the bulk specific gravity. Similarly, if the AC content in the mix is increase from 4.10 to 4.5 , 5.0, and 5.5 percent, the respective increased values of the bulk specific gravity are 2.202, 2.213 and 2.224 and the predicted fatigue lives are 517, 436 and 376. Again the increase in the AC content has an overwhelming negative affect on the fatigue life as compared to the positive affect of the bulk specific gravity.

5.5 RUT ANALYSIS

Rut or plastic deformation of a pavement structure is a function of the construction practices, the properties and thicknesses of the AC, base, and subbase layers, the properties of the roadbed soil, environmental factors and traffic load and volume (1). Unfortunately, the properties of the base, subbase, and roadbed materials are not available to this study. Hence, the following assumptions were made at the onset of this analysis.

1. Rutting in flexible and composite pavements can be analyzed as a function of the AC layer and its material properties.
2. The material properties, layer thicknesses, construction specifications/practices and the construction quality remain the same within one job number.

The two assumptions are reasonable because of the following reasons:

1. In the absence of material properties for base, subbase and roadbed soil, their effects on the rutting of flexible pavements cannot be assessed. Whereas, in the case of composite pavements the entire rutting can be attributed to the AC layer due to the presence of a stiff concrete layer.
2. In this study the selected test sites within one pavement control section number (a number, used by MDOT to identify a pavement section) have had the same job number (a number, used by MDOT to identify a construction/rehabilitation project). It is the MDOT practice to divide longer pavement control sections into several smaller job sections for construction and/or rehabilitation purposes. The pavement thickness design, the material properties, and the specifications are then kept the same within the same job section (number) depending on the existing pavement, roadbed soil, and the traffic conditions. Thus, any pavement section within the same job number will have similar layers thicknesses and material properties.

Due to the first assumption, one should expect some bias in the developed rut model. That is, given the lack of information regarding the properties of the base, subbase and roadbed soils, their effects cannot be incorporated. Further, the assumption of constant material properties may not hold. Even though, in the presence of the same specifications and design, variations due to construction practices are always present in the form of the AC mix manufacturing, placement, and compaction. Nevertheless, the thickness of each AC layer in the pavement was obtained from the cores and the overall global AC mix properties for each core was determined as presented in the next section.

5.5.1 Determination of Material Properties for a Core Location

Based on the second assumption and due to economic and time constrains, it was decided to perform one extraction test per asphalt course for all 13 cored pavement sections to obtain the material properties of each AC course. For example, section 43F has four AC courses (see Table 4.5) therefore, one extraction test per AC course was performed to obtain its properties. Thus, four extraction tests were performed for section 43F. The global properties of each core were determined as the weighted average properties of the various AC courses of that core.

As stated in the fatigue analysis, the same AC courses of two or more cores obtained from one pavement site were combined to yield enough material for a single extraction test. For the combined cores the average material properties along with the average measured rut depth were assigned to the locations of those cores. This resulted in a total of 45 layer extraction tests for the 19 core locations of the 13 cored sections. Table 5.12 summarizes the global material properties for the 19 cored locations. These include the core designation number, AC thickness, Coarse aggregate angularity, air void, percent contents by weight of the AC, sand, fine and coarse aggregate in the asphalt mix, the service life of the pavement section, the cumulative 18-kip ESAL experienced by the pavement section in question during its service life, and the average rut depth of the core location. Table 5.13 summarizes the minimum, maximum,average, and standard deviation of each data entry of Table 5.12.

Two types of analysis were conducted in this study. One analysis is based on the properties of the paving materials, the other, on the measured deflection basins. The two types are presented below.

Table 5.12 : Material properties for the 19 core locations.

Line No.	Core Designation Number	AC Thick. (inch)	Angularity	Air Void	Recovered Penetration	Percent by weight AC	Sand	Fine	Agg.	Service Life (years)	Cum. ESAL (mill)	Rut depth (inch)
1	7131211	6.24	2.24	8.9	44	4.4	62	4	34	7	1.25	0.31
2	13117121	4.77	4.88	3.2	47	5.6	43	5	52	30	1.51	0.13
3	29117721	14.56	1.98	7.6	43	4.7	65	4	31	11	0.76	0.13
4	19150911	6.10	3.48	5.9	44	5.3	55	6	39	11	1.58	0.20
5	19131111	6.20	3.48	6.0	44	5.3	54	6	40	11	1.58	0.20
6	11257021	2.48	3.23	6.2	62	5.9	61	7	32	6	0.12	0.06
7	11265911	2.32	3.23	6.2	62	5.9	61	7	32	6	0.12	0.06
8	4226311	2.29	2.97	1.0	68	5.9	58	6	36	3	0.33	0.06
9	4212911	2.68	2.97	1.0	68	5.9	58	6	36	3	0.33	0.06
10	43141611	10.01	3.82	6.5	45	5.5	49	8	44	1	0.76	0.38
11	43131911	10.84	3.83	6.6	44	5.5	49	8	44	1	0.76	0.38
12	43152311	9.60	3.78	6.5	45	5.5	49	8	43	1	0.76	0.38
13	35118931	6.04	4.73	7.9	24	5.6	51	6	43	14	1.37	0.18
14	10131011	5.45	3.72	8.5	32	5.3	62	9	30	7	0.22	0.13
15	8221011	3.61	4.89	3.3	27	5.6	40	6	54	16	1.74	0.13
16	8231511	3.96	4.89	3.2	27	5.6	40	6	54	16	1.74	0.13
17	5258321	2.68	3.99	4.6	66	5.9	59	9	31	6	0.31	0.2
18	1261611	4.80	3.66	6.1	35	5.1	52	7	42	2	3.36	0.44
19	14121713	2.54	3.14	9.2	96	5.9	52	7	41	13	0.18	0.18

Table 5.13 : Descriptive statistics of the properties of the 19 pavement cores.

	AC Thick. (inch)	Angularity	Air Void	Recovered Penetration	Percent by weight				Service Life (years)	Cum. ESAL (mill)	Rut depth (inch)
					AC	Sand	Fine	Agg.			
Min.	2.29	1.98	1.0	24	4.4	40	4	31	1	0.12	0.06
Max.	14.56	4.89	9.2	96	5.9	59	9	52	30	3.36	0.44
Avg	5.64	3.63	5.7	49	5.5	54	7	40	9	0.99	0.20
Std.Dev.	3.33	0.80	2.4	18	0.4	7	1	7	7	0.80	0.12

5.5.2 Analysis of Rut as a Function of Material Properties

The objectives of this analysis are to :

1. Determine the influential factors affecting pavement rutting.
2. Recommend changes to the existing asphalt mix design and pavement construction practices to decrease the rut potential.

Statistical analysis were conducted to relate the measured pavement rut depth to the AC mix variables and the traffic volume. During the analysis, several collinearity problems were encountered. For example, as noted earlier, by the MDOT practices, higher angular aggregate contents, better construction practices, and stricter quality control are commonly used for most pavements designed for higher traffic volumes. By the nature of this practice, collinearity between the independent variables (the material properties, layer thicknesses, and traffic volume) exists as shown by the simple correlation matrix in Table 5.14. For example, the term ESAL (the cumulative 18-kip equivalent single axle load applications) has positive collinearities with the AC thickness, the percent aggregate and the aggregate angularity; and negative collinearities with the percent sand and fine contents, the recovered penetration, the amount of asphalt in the AC mix and with the air voids. The reason for this is that, in most pavement design methods (see Chapter 2), the traffic volume has the most influence on the thickness of the individual layers in a pavement structure. Thus, for higher traffic volumes, higher thicknesses, and higher quality materials are used to safeguard against excessive rutting and fatigue cracking. In the correlation matrix of Table 5.14, the positive correlation of ESAL to the coarse aggregate angularity and the percent coarse aggregate content and negative correlation with the percent sand and the fine contents, substantiate the fact that the MDOT pavement design practice is balanced and that better materials are being used for higher volume roads. It has already been proven (16,19,21,22) that the performance of AC mixes depends on providing adequate aggregate interlock and distributing the

Table 5.14 : Correlation matrix for the 19 extracted core locations.

	RUT	ESAL	ACTH	PEN	Percent by weight				ANG	AV
					AC	AGG	SAND	FINE		
RUT	1.000									
ESAL	.453	1.000								
AC TH	.513	.099	1.000							
PEN	-.264	-.617	-.393	1.000						
AC	-.445	-.428	-.613	.493	1.000					
AGG	.205	.541	-.001	-.387	.131	1.000				
SAND	-.251	-.488	.027	.355	-.227	-.983	1.000			
FINE	.214	-.360	-.136	.224	.490	-.237	.054	1.000		
ANG	.037	.357	-.224	-.462	.400	.755	-.814	.200	1.000	
AV	.392	-.056	.408	-.074	-.486	-.318	.307	.107	-.280	1.000

Rut = rut depth (inch);
ESAL = 18-kip cumulative ESAL during the service life;
AC TH= thickness of AC layer (inch);
PEN = recovered asphalt penetration;
AC = asphalt content (percent by weight);
AGG = aggregate (plus #4) in AC mix (percent by weight);
SAND = sand in AC mix (percent by weight);
FINE = fine in AC mix (percent by weight);
ANG = angularity of coarse aggregate (plus #4) in AC mix; and
AV = air voids in AC mix.

wheel load. Increases in the percent aggregate, reduce the amount of the sand and the fine in the AC mix. This leads to a better aggregate face to face contact and reduces the ball bearing effect due to the presence of excessive sand and fine in the AC mix.

The above scenario implies that the statistical analysis between the dependent and independent variables must be conducted on the basis of engineering knowledge rather than on the basis of statistic alone. This point can be illustrated by examination of the values of the correlation coefficients between the dependent variables (rut depth) and the independent variables (material properties, traffic volume, and service life). Such an examination leads to the following observations:

1. The rut depth increases with increasing the number of cumulative ESAL. This observation was expected and it is consistent with that reported in the literature. The reason for this is that pavement rutting is mainly caused by wheel loads and is accelerated by material and environmental factors.
2. The rut depth increases with increasing the thickness of the AC layer. This observation was not expected. Thicker AC thicknesses cause a decrease in the compressive stress and strain delivered to the base and subbase layers and to the roadbed soil. Further, such an observation should not lead to the conclusion that the rut depth potential can be decreased by decreasing the AC thickness. This observation is mainly a statistical one and it is caused by the collinearity between the traffic volume and the AC thickness. Once again, by the nature of the design and construction practices of most State Highway Agencies (SHA) including MDOT, pavements that are expected to carry higher traffic volumes are designed with thicker AC layers. Thus, the observation that a thicker AC layer leads to a higher rut depth may as well be interpreted as higher traffic volumes cause higher rut depths. The important point here is that the true effects of the thickness of the AC layer on rut depth cannot be understood unless the collinearity between the AC thickness and the traffic volume is resolved.

3. The rut depth increases with the decrease in the recovered asphalt penetration. This observation is not reasonable and it is not consistent with the literature. Softer asphalts produce softer asphalt mixes with lower resistance to rutting. Once again, the collinearity between the recovered asphalt penetration and the pavement service life presents a problem in interpreting the data. Longer service life of a pavement structure leads to more oxidation and hardening of the asphalt cement which should result in a lower future rut depth. However, a longer service life implies higher cumulative traffic volume and hence, higher rut depths. This supports the discussion made in item 2 above. The true effects of the recovered asphalt penetration cannot be found unless the collinearity problem between this variable and service life is resolved.

4. The rut depth decreases with an increase in the asphalt content in the mix. Two points can be made relative to this observation. These are:

    a) Higher traffic volume roads are typically built with thicker AC thicknesses. In general, the AC layer consists of several AC courses, with larger AC layer thicknesses requiring a larger number of courses. For example, a 7.5-inch AC layer may consists of a 1.5-inch surface course, a 3-inch leveling course, and a 3-inch base course. On the other hand, a 3-inch thick AC layer may consists of 1.5-inch surface course and a 1.5-inch base course. Hence, commonly, no leveling course is used in thin pavements. Since, in the State of Michigan, the AC content of the leveling course is a half-percent lower than that of the surface course, and the AC content of the base course is about 4.5 percent, higher traffic volume roads have lower asphalt contents. This can also be seen through the examination of the degree of collinearity between the AC content and the cumulative ESAL (see Table 5.14). A negative collinearity implies that higher ESAL volumes lead to lower AC contents. Again, this collinearity problem needs to be resolved prior to making any engineering decision.

b) The range of the AC content data is rather narrow, hence, the trend of the data may be affected by its variability.

5. The rut depth increases with increasing percent of coarse aggregate and with decreasing percent sand contents in the mix. Once again, both observations are not reasonable and they are the direct results of the pavement design practices. Higher percent coarse aggregate and lower percent sand contents are typically used in the construction of higher volume roads. Hence, the increase or decrease in the rut depth is mainly affected by the traffic volume.

6. The rut depth increases with increasing percent fine (passing sieve number 200) content. This observation is reasonable and consistent with that reported in the literature. Although, a certain degree of collinearity between the percent fine content and the cumulative ESAL exists, it appears that its effects is not significant to cause a reversal in the effects of the fine on the rut depth.

7. The rut depth increases with increasing aggregate angularity. For the same reasons stated above this observation is not reasonable and inconsistent with that reported in the literature.

8. Finally, the rut depth increases with increasing percent air voids. This observation is reasonable and consistent with that reported in the literature. One point should be noted is that no significant degree of collinearity can be found between the percent air voids and the cumulative ESAL. However, certain degrees of collinearity exist with other variables such as the percent coarse aggregate and sand contents.

The above observations indicate that the degrees of collinearity between the cumulative number of ESAL and the other variables are problematic. Stratification of the data to resolve the collinearity problem is not possible because of the nature of the field experiment. Hence, another solution must be found before balanced statistical and engineering analyses can be conducted.

In order to alleviate the problem and to analyze the rut depth as a function of the material variables without a significant interference by the traffic volume, a new term is introduced herein "Rate of Rutting (RRUT)". The rate of rutting or rut rate is defined as the amount of rut per million ESAL. Hence, a new dependent variable "RRUT" can be used and the independent variable "cumulative ESAL" can be eliminated from the pool of independent variables thereby eliminating significant degrees of collinearity. This solution however, does not necessarily eliminate other collinearity problems as discussed below.

Table 5.15 provides a list of the values of the correlation coefficients between the dependent variable (RRUT) and the independent variables "material properties". Examination of these values indicates that some degrees of collinearity between the independent variables still exist. These are:

1. The collinearity between the sand and aggregate contents. This can be eliminated by expressing the percent coarse aggregate contents in terms of the fine and sand contents as follows:

   $$AGG = 100 - (Fine + Sand)$$

   where AGG, Fine, and Sand are the percent aggregate, fine, and sand contents, respectively.
2. The collinearity between the thickness of the AC layer (AC TH) and the percent AC content (AC). The reason for this degree of collinearity was explained earlier. Unfortunately, because of the nature of this dependency, this collinearity problem cannot be resolved by expressing one variable in terms of the other.
3. The collinearity between the percent fine and the percent AC contents. This collinearity cannot be resolved prior to the statistical analysis. However, the combined effects of both variables can be assessed by using the resulting

Table 5.15 : Correlation matrix for rate of rutting (RRUT).

	RRUT	AC TH	PEN	Percent by weight				ANG	AV
				AC	AGG	SAND	FINE		
RRUT	1.000								
AC TH	-.088	1.000							
PEN	.638	-.393	1.000						
AC	.325	-.613	.493	1.000					
AGG	-.368	-.001	-.387	.131	1.000				
SAND	.251	.027	.355	-.227	-.983	1.000			
FINE	.670	-.136	.224	.490	-.237	.054	1.000		
ANG	-.205	-.224	-.462	.400	.755	-.814	.200	1.000	
AV	.472	.408	-.074	-.486	-.318	.307	.107	-.280	1.000

RRUT = rut/18-kips cumulative ESAL; and rest of the variables are same as Table 5.13.

statistical models along with some assumptions to express one variable in terms of the other.

4. The degrees of collinearity between the recovered asphalt penetration (PEN) and the percent AC content, the aggregate angularity, and the percent sand and aggregate contents. Once again, these collinarities cannot be resolved prior to the statistical analysis. Consequently, several statistical analysis were conducted whereby various transformations were used to express each independent variable. It was found that the elimination of the recovered asphalt penetration (PEN) variable from the pool of variables did not causes any significant bias in the resulting model. Therefore, the variable PEN was not included in the final analysis.

Based on the results of the statistical analyses presented in Tables 5.14 and 5.15, the discussion presented above, and the elimination of the variable PEN from the pool of variables, a third statistical analysis was conducted to obtain a regression equation relating the dependent and independent variables. This analysis is presented in the next section.

5.5.2.1 Regression Analysis

Prior to the commencement of the statistical analysis, the dependent variable (RRUT) was plotted against each of the independent variables. From the plots, the trend between the dependent and each of the independent variables was observed. For each independent variable, the observed trend was then modeled by using several transformations (e.g.,logarithmic, cubical, polynomial). The form that yielded the lowest FIN value, highest coefficient of correlation, highest significance level and lowest standard error in the presence of the other independent variables was selected for inclusion in the model.

Table 5.16 provides a list of the values of the correlation coefficients for all variables that satisfied the variable inclusion criteria (FIN) in the final model. It can be seen that only six variables are included. In their order of significance, these variables are:

1. the percent fine and sand content (F+S);
2. the percent air voids (AV) of the AC mix which is included in a polynomial form as AV1, AV2, and AV3;
3. the percent AC content (AC); and
4. the angularity of the coarse aggregate (ANG);

where;

RRUT	=	Rut/cumulative 18-kips ESAL over the service life (inch/million ESAL);
F+S	=	$Fine^3$ + Sand;
Fine	=	percent fine content;
Sand	=	percent sand content;
AV1	=	e^{AV} ;
AV2	=	AV^2 ;
AV3	=	AV^3 ;
ANG1	=	log (ANG);
AV	=	percent air voids; and
log	=	base 10 logarithm.

The degree of collinearity between the independent variables listed in Table 5.16 were examined. Table 5.17 provides, for each independent variable, a list of the seven eigenvalues and condition indices and the percent of variance attributed to each eigenvalue. The results indicate that the different terms of air void (AV1, AV2, and AV3) have high variance proportion values for the 7th eigenvalue thus indicating significant multicollinearity. A similar conclusion was

Table 5.16 : Correlation matrix for the final variables.

	RRUT	F+S	AV1	AC3	ANG1	AV2	AV3
RRUT	1.000						
F+S	.697	1.000					
AV1	.529	-.001	1.000				
AC3	.346	.344	-.235	1.000			
ANG1	-.127	.214	-.359	.411	1.000		
AV2	.496	.119	.826	-.459	-.375	1.000	
AV3	.498	.073	.905	-.422	-.404	.984	1.000

RRUT=rate of rutting per million ESAL;
F+S =(percent fine)^3 +percent sand;
AV1 =exp(air void);
AC3 =(percent AC content)^3;
ANG1=log(angularity);
AV2 =(air void)^2;and
AV3 =(air void)^3.

Table 5.17 : Collinearity diagnostics (eigenvalue, condition indices and the proportion of the variance attributable to the eigenvalue).

		Cond	Percent of variance attributed to the eigenvalue						
Number	Eigenval	Index	Constant	F+S	AV1	AC3	ANG1	AV2	AV3
1	5.69448	1.000	.00036	.00336	.00049	.00053	.00063	.00006	.00004
2	1.03648	2.344	.00073	.00939	.01288	.00201	.00240	.00015	.00027
3	.14162	6.341	.00891	.66514	.00393	.00932	.01551	.00016	.00006
4	.09968	7.558	.00155	.07967	.12915	.01753	.00002	.00660	.00224
5	.01854	17.528	.02739	.02672	.02542	.35733	.76259	.00041	.00068
6	.00825	26.272	.96070	.19463	.05262	.61323	.14558	.00739	.00286
7	.00096	77.146	.00036	.02109	.77550	.00005	.07327	.98523	.99384

also made based on the tolerance and VIF values listed in Table 5.18. These diagnostics indicate that a significant degree of collinearity exist only among the various polynomial terms of the same independent variable (the percent air void AV). Note that the presence of such a collinearity does not affect the estimated parameter of the other independent variables.

The results of the regression analysis are listed in Table 5.19. All the variables that are included in the resulting equation satisfy the specified criterion for the variable inclusion. It can be seen from the Table that all the variables have a "T" significance value of less than 0.05. Hence, they are statistically significant variables. The results of the regression analysis listed in Table 5.19 indicate that the standard error (S.E.) of the resulting model is 0.0797, the value of the coefficient of determination (R^2) is 0.93 and the adjusted R^2 is 0.90. The numbers listed under the column designated "B" in Table 5.19 are the regression constants for the indicated variables. Table 5.20 provides a list of the regression constants and the values of the R^2 and the standard error obtained from each step of the stepwise method of the SPSS computer program. It can be seen that the term percent fine and sand content (F+S) is the most significant variable and it alone explains 48 percent of the variation of the pavements rate of rutting (the dependent variable). This percentage increases, as it should be expected, with the inclusion of more variables in the model. The final model can be expressed as follows:

$$\mathbf{RRUT} = -.3656 + .00068\,((\mathrm{FINE})^3 + \mathrm{SAND}) + .00012\,(\mathrm{EXP(AV)}) + .0289\,(\mathrm{AV}^2) - .0037\,(\mathrm{AV}^3) + .00314\,(\mathrm{AC}^3) - .6614\,(\mathrm{LOG(ANG)}) \qquad (5.5)$$

$R^2 = 0.93$, SE = .079, F = 27.94, $F_{(sig)} = .000$

where

all the variables are the same as before.

Table 5.18 : Collinearity diagnostics TOL and VIF.

Variable	Tolerance	VIF
F+S	.666348	1.501
AV1	.042814	23.357
AC3	.490252	2.040
ANG1	.694469	1.440
AV2	.007450	134.234
AV3	.004235	236.112

Table 5.19 : Results of regression analysis.

Multiple R	.96603
R Square	.93321
Adjusted R Square	.89982
Standard Error	.07965

Analysis of Variance

	DF	Sum of Squares	Mean Square
Regression	6	1.06385	.17731
Residual	12	.07614	.00634

F = 27.94516 Signif F = .0000

* * * * M U L T I P L E R E G R E S S I O N * * * *

Equation Number 1 Dependent Variable.. RRUT

------------------ Variables in the Equation ------------------

Variable	B	SE B	Beta	T	Sig T
F+S	6.840148E-04	1.20564E-04	.518512	5.673	.0001
AV1	1.186727E-04	3.26269E-05	1.311425	3.637	.0034
AC3	.003135	7.58457E-04	.440393	4.133	.0014
ANG1	-.661445	.212961	-.278054	-3.106	.0091
AV2	.028855	.008632	2.889327	3.343	.0059
AV3	-.003734	.001224	-3.496769	-3.050	.0101
(Constant)	-.365607	.162551		-2.249	.0441

Table 5.20: Regression matrix for rate of rutting.

RRUT	Intercept	Regression coefficient of independent variable							
		F+S	AV1	AC3	ANG1	AV2	AV3	R.Sq.	S.E.
	-.0159	.0009						.480	.1857
	-.0952	.0009	.00005					.767	.1289
	-.3905	.0008	.00005	.0020				.831	.1134
	-.1958	.0008	.00005	.0024	-.4992			.864	.1053
	-.3797	.0007	.00003	.0032	-.4887	.0031		.881	.1020
	-.3656	.0007	.00012	.0031	-.6615	.0289	-.0037	.933	.0797

Based on the statistics of the model (equation 5.5), the following observations were noted.

1. The null hypothesis of no linear relationship between the independent variables and RRUT was rejected and it was concluded that at a probability $F_{(sig)}$ of zero, 93 percent of the variation of the dependent variable (RRUT) is explained by the independent variables included in the equation.
2. The largest value of "T" significance is .04. This implies that all the variables in the model are statistically significant.

In addition, the following statistics were calculated to study the values of the residuals and the predicted RRUT values and are listed in Table 5.21.

1. PRED = the unstandardized predicted values;
2. RESID = the unstandardized residual values;
3. ZPRED = the standardized predicted values;
4. ZRESID = the standardized residual values; and
5. D.W.S. = the Durbin Watson statistics.

The Durbin-Watson statistics of equation 5.5 listed in Table 5.21 signifies a satisfactory non autocorrelation between the residuals. Further, the maximum, minimum, mean and standard deviation of the unstandardized and standardized predicted values and the residuals are also listed in the Table. Based on the values of the residuals and the standardized residuals, the ten worst residual cases are listed in Table 5.22. It should be noted that the ten worst residual cases are based on the absolute difference and not on the percent error between the predicted and measured RRUT values.

Table 5.21 : Residual statistics of equation 5.5.

	Min	Max	Mean	Std Dev	N
*PRED	.0128	.9715	.3258	.2431	19
*RESID	-.1030	.1042	.0000	.0650	19
*ZPRED	-1.2872	2.6560	.0000	1.0000	19
*ZRESID	-1.2935	1.3087	.0000	.8165	19
Durbin-Watson Test = 1.48605					

Table 5.22 : Ten worst Residuals.

Case #	*Resid	*ZRESID
10	.1042	1.30870
13	-.1030	-1.29352
11	.1017	1.27703
12	.0883	1.10899
19	-.0855	-1.07324
4	-.0825	-1.03583
2	.0820	1.02939
17	-.0819	-1.02829
5	-.0794	-.99707
3	.0383	.48024

5.5.2.2 Sensitivity Analysis and Engineering Interpretation

The statistical model presented by equation 5.5 was used to predict the rate of rutting at the 19 core locations. Figure 5.13 depicts the values of the predicted rate of rutting versus the observed one. The straight line in the Figure represents the locus of those points where the observed and predicted rut depth are equal. It can be seen that all of the predicted values are close to the observed ones. Figure 5.14 depicts the percent errors between the predicted and the observed rate of rutting. Examination of the Figure indicates that most predicted rates of rutting are within 50 percent of the observed values. This indicates that the statistical model is relatively accurate.

One additional point should be made herein is that, the rut depth of a pavement structure is a function of several variables including the stiffnesses and thicknesses of the various pavement layers, the properties of the materials in the AC mix, the traffic volume, load, and environmental factors. In this study, only the asphalt mix properties and the traffic load and volume data are used. Consequently, one should not expect the statistical model presented in equation 5.5 to fully explain the variations in the rate of rutting.

The statistical model of equation 5.5 expresses the dependent variables as the ratio of rut depth to the cumulative number of ESAL. Hence, the model can be rewritten as follows:

$$\mathrm{RUT} = \mathrm{ESAL}\,(-.3656 + .00068\,((\mathrm{FINE})^3 + \mathrm{SAND}) + .00012\,(\mathrm{EXP(AV)}) + .0289\,(\mathrm{AV}^2) - .0037\,(\mathrm{AV}^3) + .00314\,(\mathrm{AC}^3) - .6614\,(\mathrm{LOG(ANG)})) \qquad (5.6)$$

where

all the variables are the same as before.

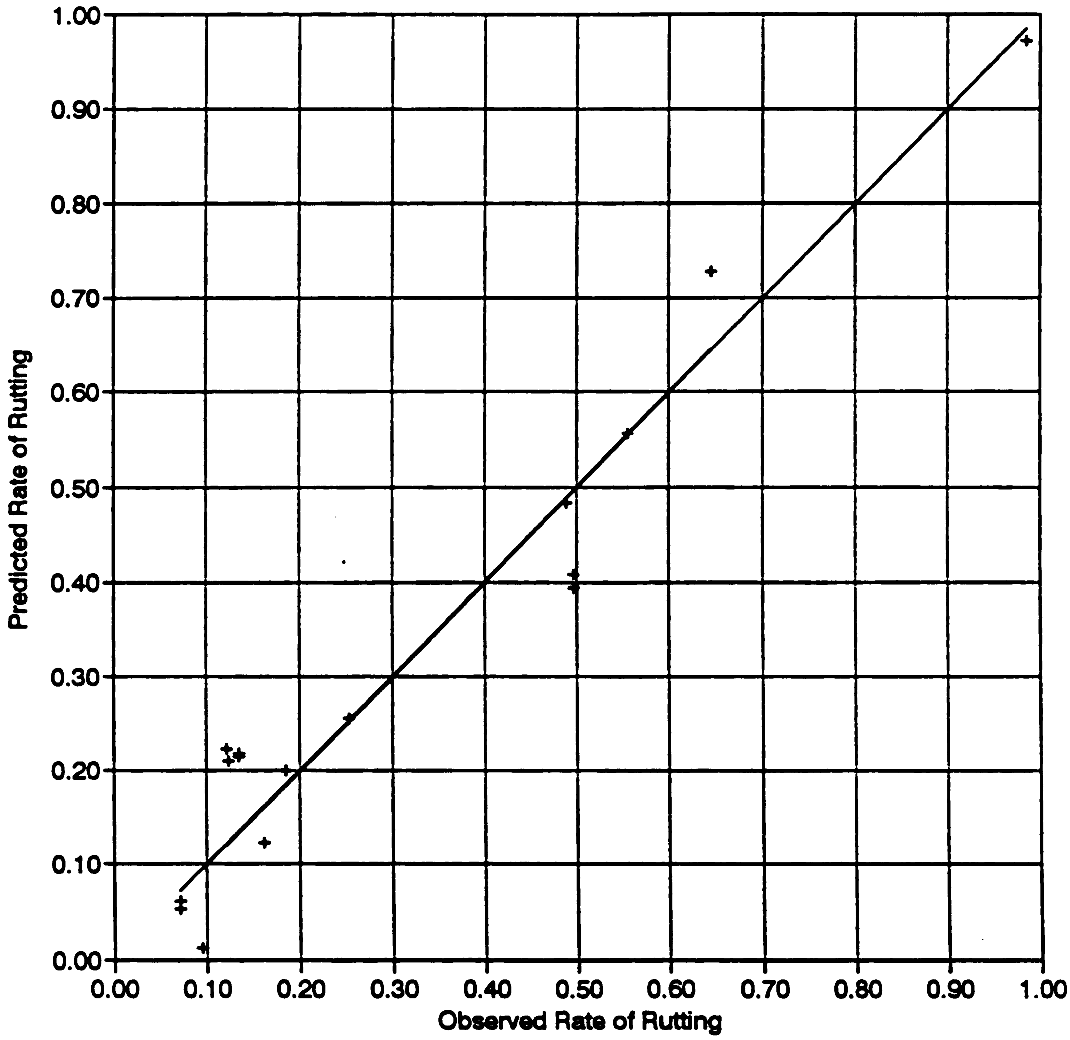

Figure 5.13 : **Observed versus the predicted rate of rutting at the 19 core locations.**

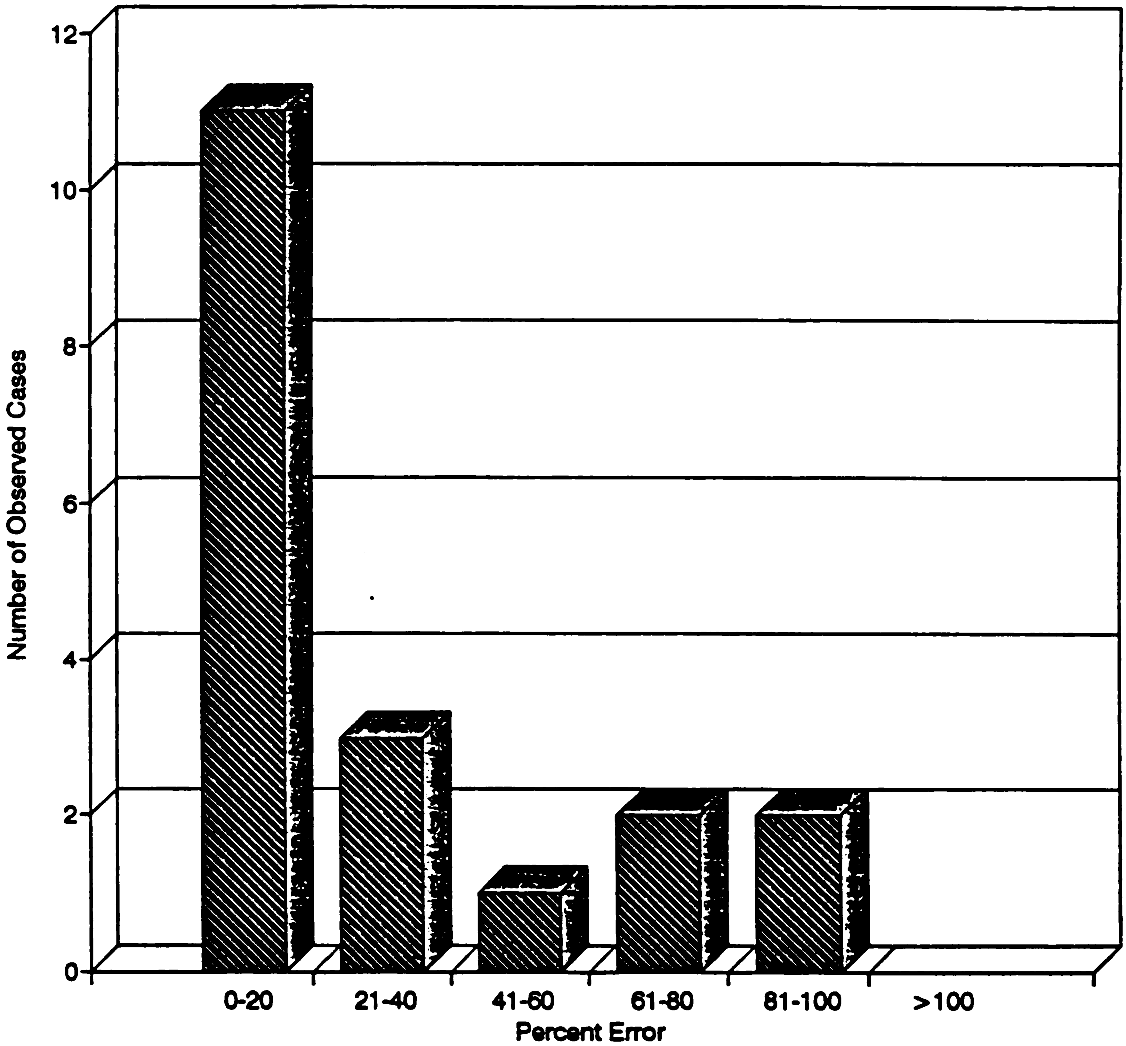

Figure 5.14 : **Percent differences between the observed and the predicted rate of rutting for the 19 core locations.**

The sensitivity of equation 5.6 to variations in each independent variable and the engineering interpretations of the model are presented below.

A sensitivity analysis of equation 5.6 was performed to determine the effect of each variable in the equation on the predicted rut depth at the 19 core locations. The sensitivity of the model to each variable was analyzed such that:

1. The values of four variables in the equation were held constant.
2. The value of a fifth, variable (the coarse aggregate angularity) was changed from a low, to a medium, to a high value within the range of values of that variable.
3. The value of the variable in question was varied from one end of its range to the other.

Results of the sensitivity analysis are presented and discussed below.

Fine - Figure 5.15 shows the relationship between the predicted rut depth and the percent fine content in the AC mix for constant values of the sand content, the percent air voids, the AC content, ESAL and for three levels of coarse aggregate angularity (1, 3, and 5). It can be seen that:

1. Increasing the percent fine content from 0 to 10 causes increases in the rut depth by factors of about 2, 5 and 33 for the respective aggregate angularity of 1, 3, and 5.
2. There is no appreciable increase in rut depth as the percent fine content increases from 0 to about 5 percent. Further increase in the percent fine content causes substantial increase in pavement rutting. The implication of these two observations is that fine contents in the order of 0 to 5 percent will have a minimum impact on pavement rutting.

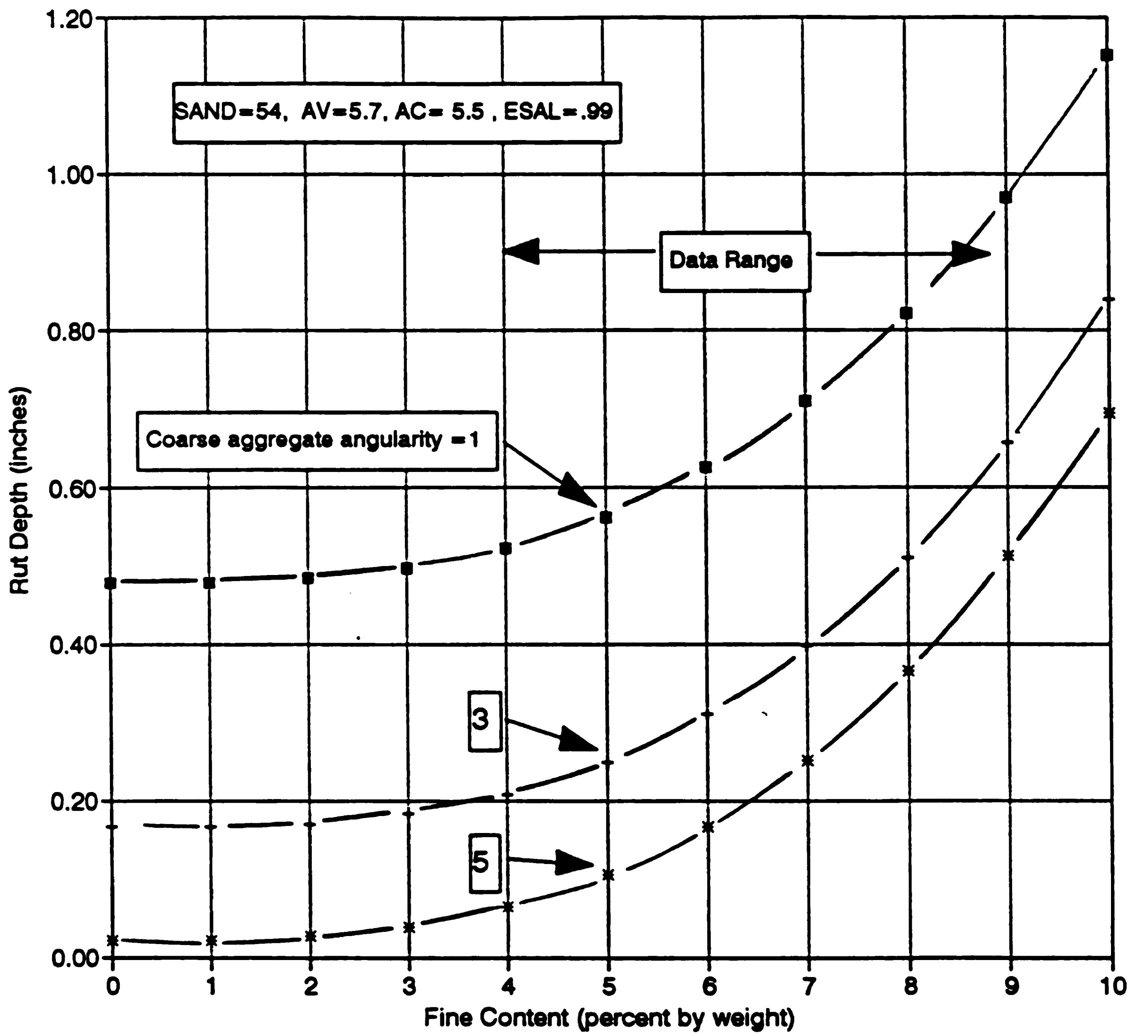

Figure 5.15 : **Rut depth as a function of the percent fine content, for three levels of coarse aggregate angularity.**

Air Voids -Figure 5.16 depicts the sensitivity of the predicted rut depth to the percent air voids for constant values of the fine, sand and asphalt contents, and the 18-kip ESAL, and for three levels of coarse aggregate angularity (1, 3, and 5). Examination of the Figure indicates that:

1. Increasing the percent air voids from 3 to 10 percent causes increases in the rut depth by factors of about 4, 10 and 42 for the respective aggregate angularity of 1, 3, and 5 .
2. Increasing the percent air voids from 1 to 6 percent causes an insignificant increase in the rut depth. Increasing the percent air voids above the 6 percent level causes a substantial increase in rut. The implication of the above observation is that the effects of the air void content on pavement rutting can be minimized by specifying a maximum of 3 to 6 percent air voids in the AC mix. It should be noted that percent air void contents between 0 and 2 percent cause high shear deformation and consequently rutting and bleeding.

Asphalt Content - Figure 5.17 represents the relationship between the predicted rut depth and the asphalt content for constant values of the percent fine, sand, and air voids contents, and ESAL and for three levels of coarse aggregate angularity (1, 3, 5). It can be seen that increasing asphalt content from 4 to 8 percent causes an increase in the rut depth by factors of 3, 7 and 33 for the respective aggregate angularity of 1, 3, and 5. Recall that MDOT uses 4.5 percent AC content for most asphalt base courses. The above observation supports the MDOT practice. It should be noted that AC contents much lower than the 4.5 percent may cause stripping and low adhesion of the AC.

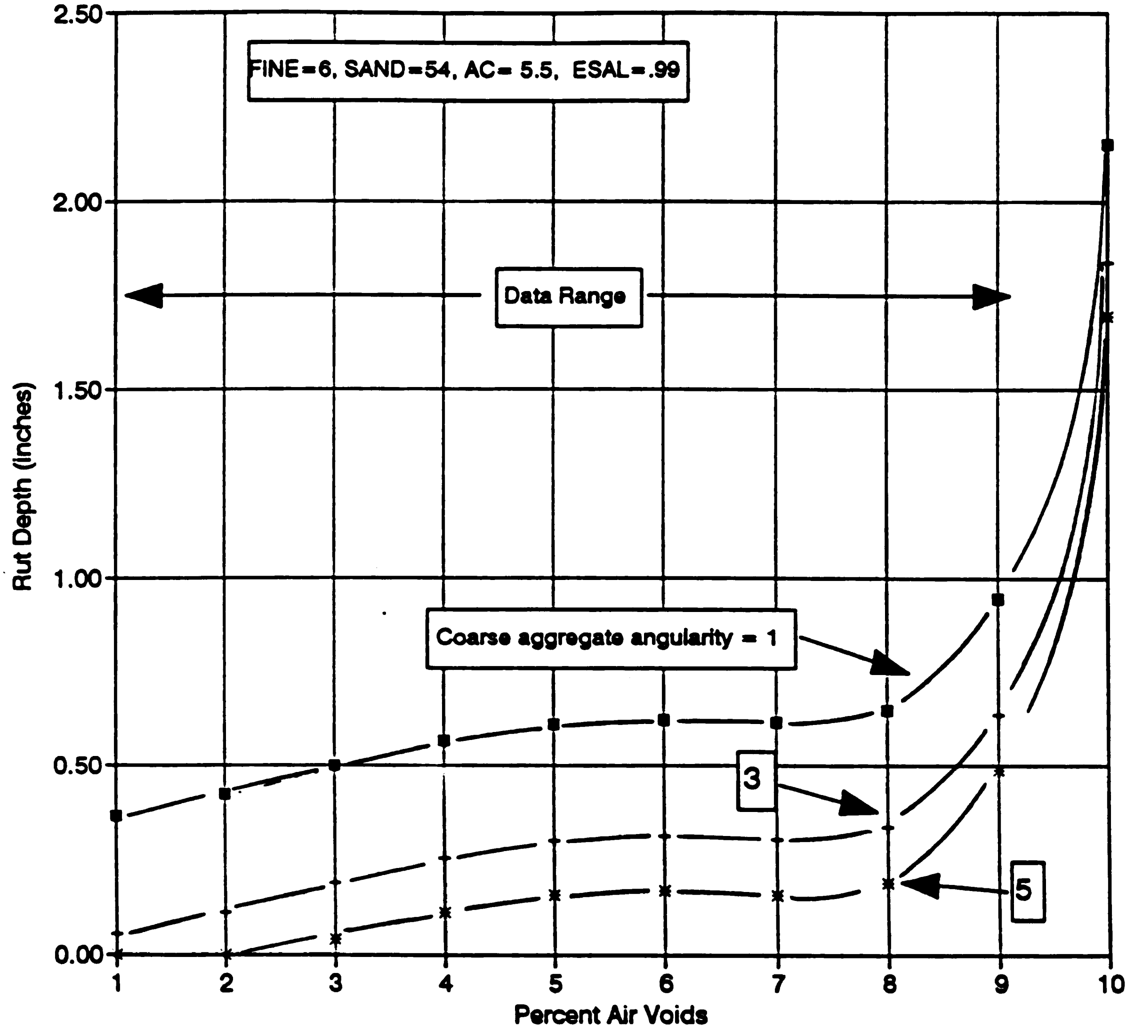

Figure 5.16 : **Rut depth as a function of the percent air voids for three levels of coarse aggregate angularity.**

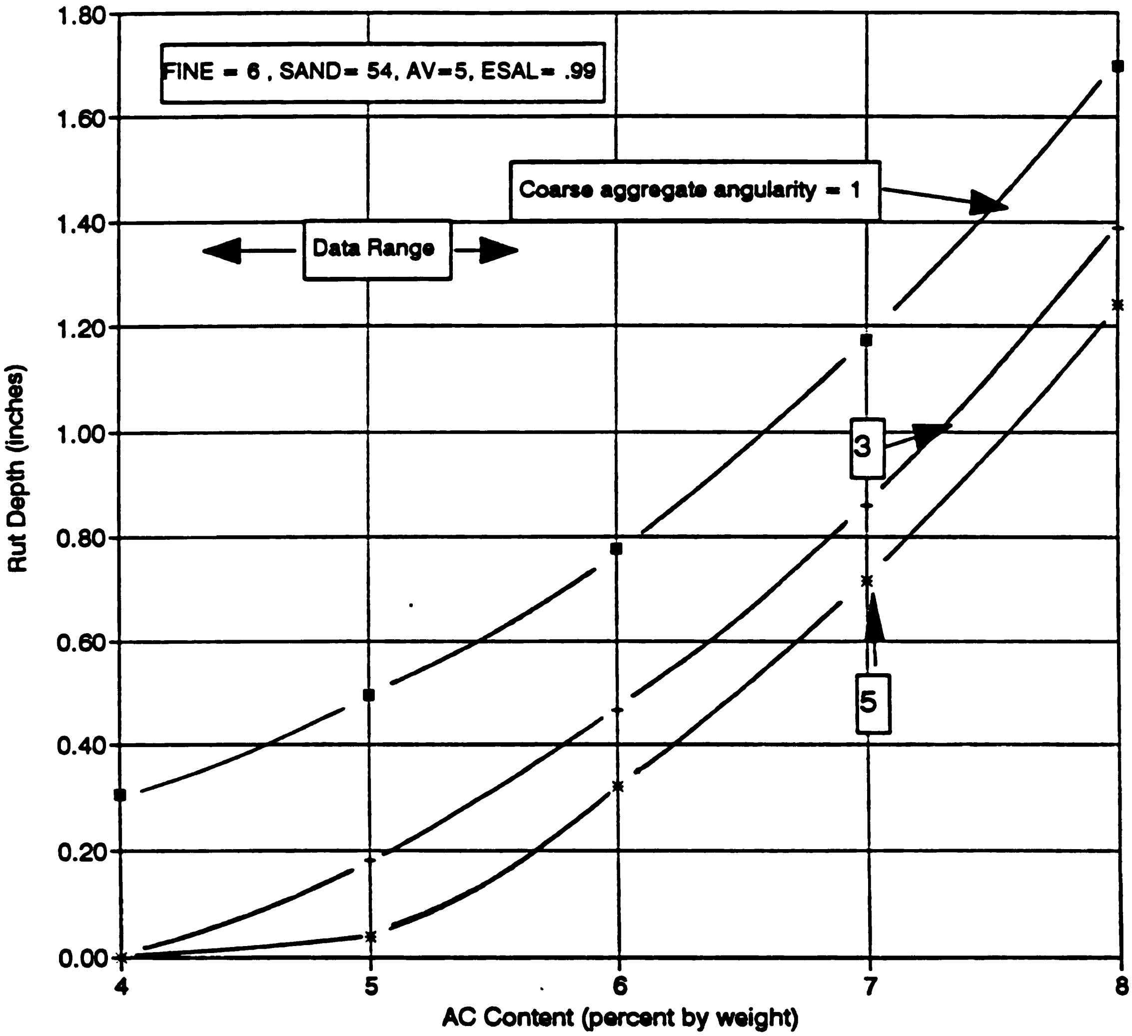

Figure 5.17 : **Rut depth as a function of percent AC content, for three levels of aggregate angularity.**

Aggregate Angularity - Figure 5.18 depicts the sensitivity of the predicted rut depth to the aggregate angularity for constant values of the percent sand , air voids and AC contents, and ESAL and for three levels of the percent fine content (4, 7, and 9). Examination of the Figure indicates that:

1. The relationship is almost linear.
2. Increasing aggregate angularity from 1 (rounded aggregate such as river gravel) to 5 (aggregate crushed on all sides) causes a decrease in the rut depth by factors of about 8, 3 and 2 for the respective fine contents of 4, 7, and 9 percent. The implication of these observations is that the use of angular aggregates in the AC mix of a pavement structure decreases its rut potential. However, the benefit of using such aggregates diminishes as the percent fine and the percent sand contents increase. These findings were expected because as the percent fine and/or the percent sand contents increase, the ball bearing effects increase causing a decrease in the face to face contact between the aggregate particles. Further increases in the percent fine and sand contents cause, the coarse aggregates to float in the fine and sand matrix. One important point should be noted here is that the benefits of using angular aggregates in terms of decreased rut depth potential should be evaluated against the expected service life and the costs of the pavement structure in question. For example, the use of angular aggregates (higher cost) in a pavement structure cannot be justified if that pavement is designed for a shorter service life period than the period during which the rut depth of the pavement will exceed the maximum acceptable rut. That is, if the pavement design process assumes that the pavement will be rehabilitated (for

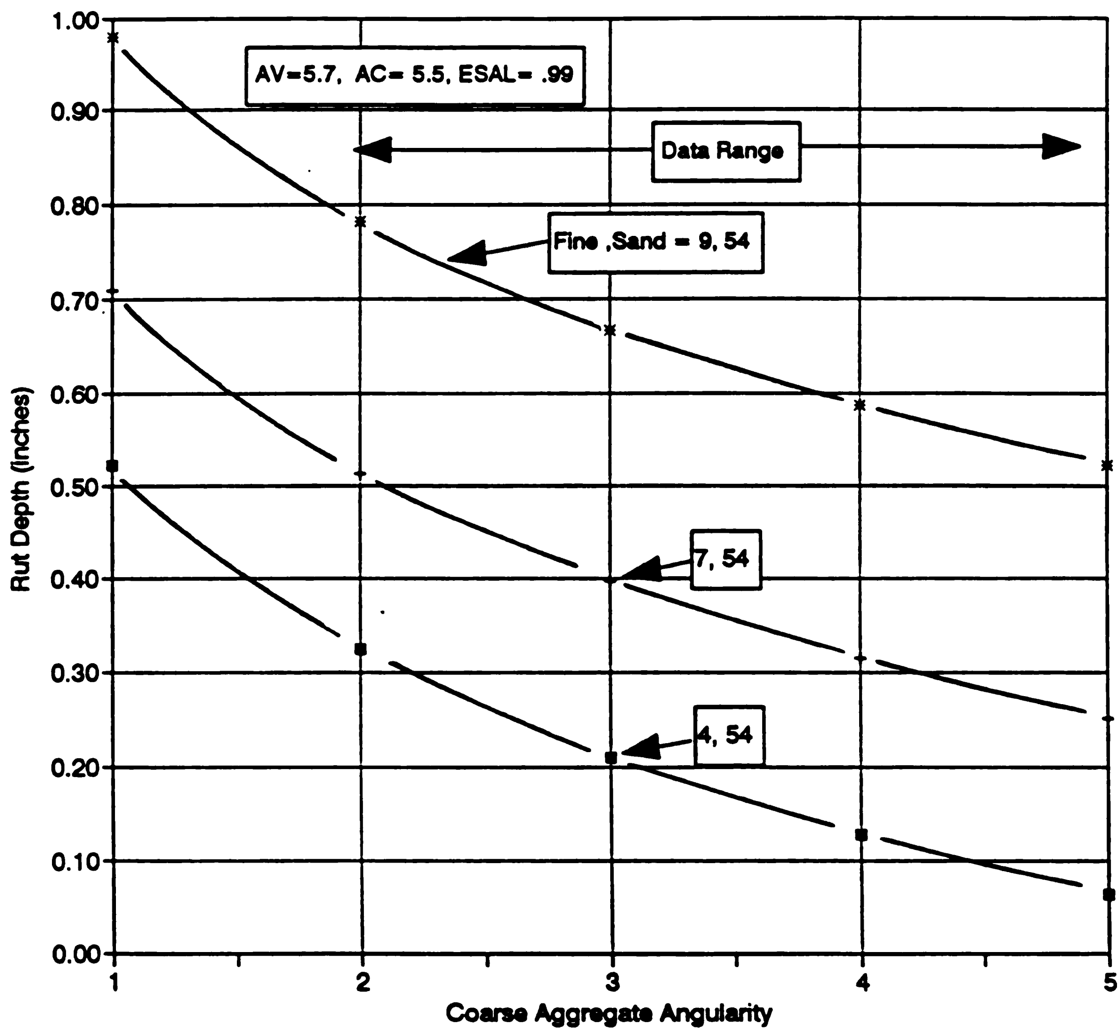

Figure 5.18 : **Rut depth as a function of coarse aggregate angularity, for three levels of the percent fine content.**

roughness, temperature cracking, or other expected types of distress) within a ten-year period after construction and that the expected rut depth of that pavement during the same period is less than the maximum acceptable standard, then it would not be wise to use expensive crushed aggregates in the AC mix to extend the pavement service life relative to rutting to 20-years. Stated differently, the benefits of using crushed aggregates in the AC mix should be assessed during a systematic and comprehensive design processes whereby the expected pavement service lives relative to each of the expected distress types are evaluated.

ESAL - Figure 5.19 depicts the relationship between the rut depth and the cumulative 18-kip ESAL for the constant values of fine, sand, air voids, and asphalt contents shown in the Figure, and for three levels of coarse aggregate angularity of 1, 3, and 5. It can be seen that the rut depth increases linearly with increasing number of 18-kip ESAL (e.g., increasing the number of ESAL by a factor of 10 causes an increase in the rut depth by the same factor). This observation was not expected and it cannot be supported by either field or laboratory data. In general, the rate of pavement rutting decreases as the number of 18-kip ESAL increases. One of the reasons for this discrepancy between the model and the observed data could be the collinearity of the variable ESAL with the other independent variables such as the percent aggregate, sand, fine, and asphalt contents that was discussed earlier. Another reason is the MDOT practice regarding the collection of traffic data and the computation of ESAL (the average daily traffic (ADT) data is multiplied by an estimated percent commercial and by an estimated average ESAL per vehicle). This practice can be enhanced by collecting weigh in motion (WIM) data which

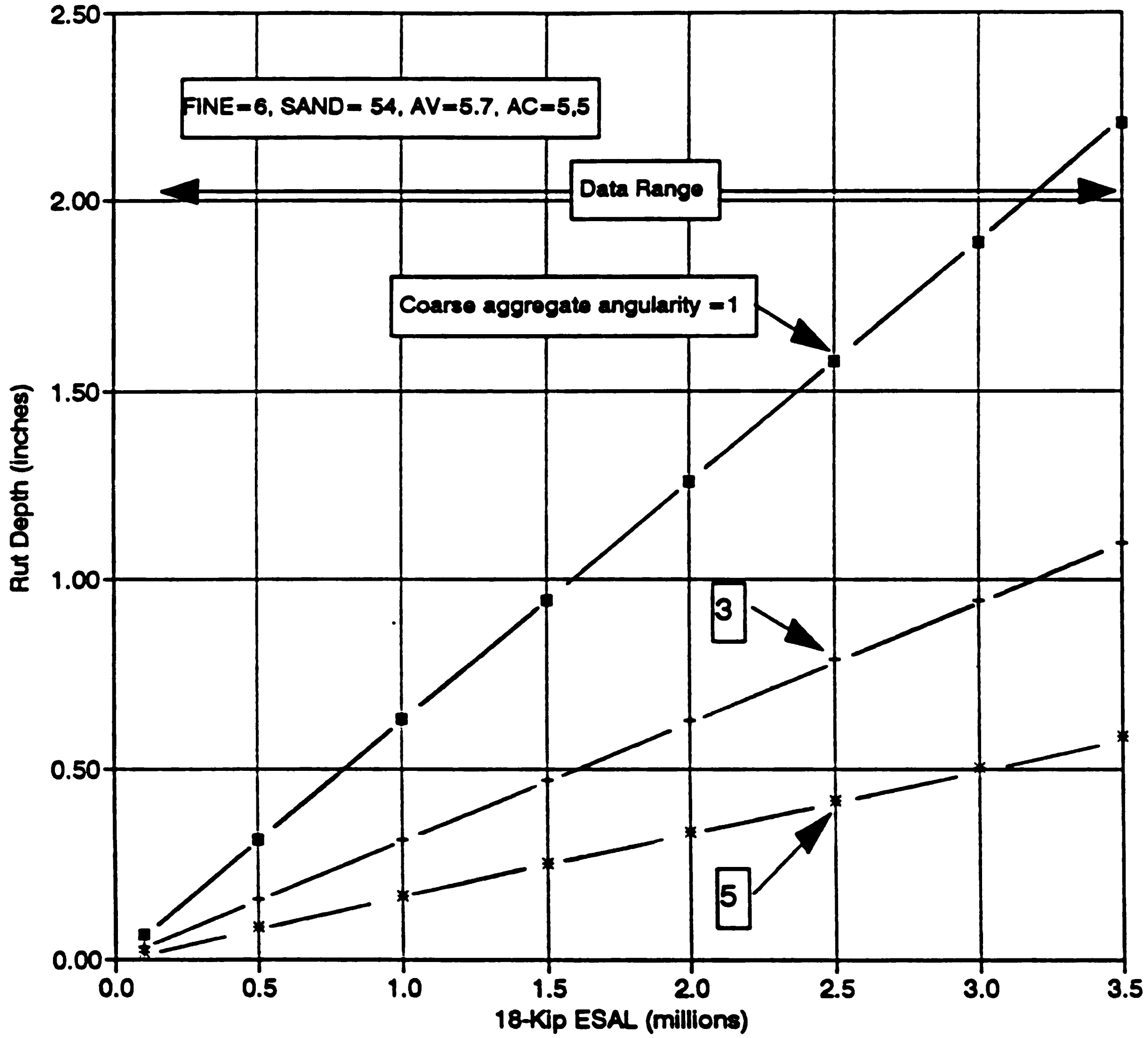

Figure 5.19 : **Rut depth as a function of 18-kip ESAL, for three levels of aggregate angularity.**

can be used to directly calculate, not assume, the ESAL per vehicle and the total number of 18-kip ESAL.

5.5.2.3 Rut Prediction Based on Assigned Material Properties

Recall that the statistical rut depth model presented by equation 5.6 was developed by using the material data for the 19 extracted core locations. In this study, the pavement rut depths at 88 other cored locations were also measured. However, no material data are available at these locations. In order to apply the model to the other locations, the following assumptions were made:

1. The material properties determined from each extracted AC course represent the properties and the thickness of similar AC course encountered at other cored locations.
2. The global properties of each core were determined as the weighted average properties of the various AC courses of that core.

In regard to the above assumptions, several points should be made. These are:

1. Because of economical and other constraints, it is not practical nor is possible to conduct extraction tests to obtain the properties for each core location. The reason is that several cores must be combined in order to obtain enough materials to conduct extraction tests. Hence, only the average material properties obtained from several cores can be determined.
2. The cross-sectional data obtained from MDOT regarding the layer thicknesses represent the as-designed thicknesses not the as-constructed ones. Variations between the MDOT cross-sectional data and the layer thicknesses obtained from the cores were observed. Figure 5.20 represents the percent difference between the AC layer thicknesses

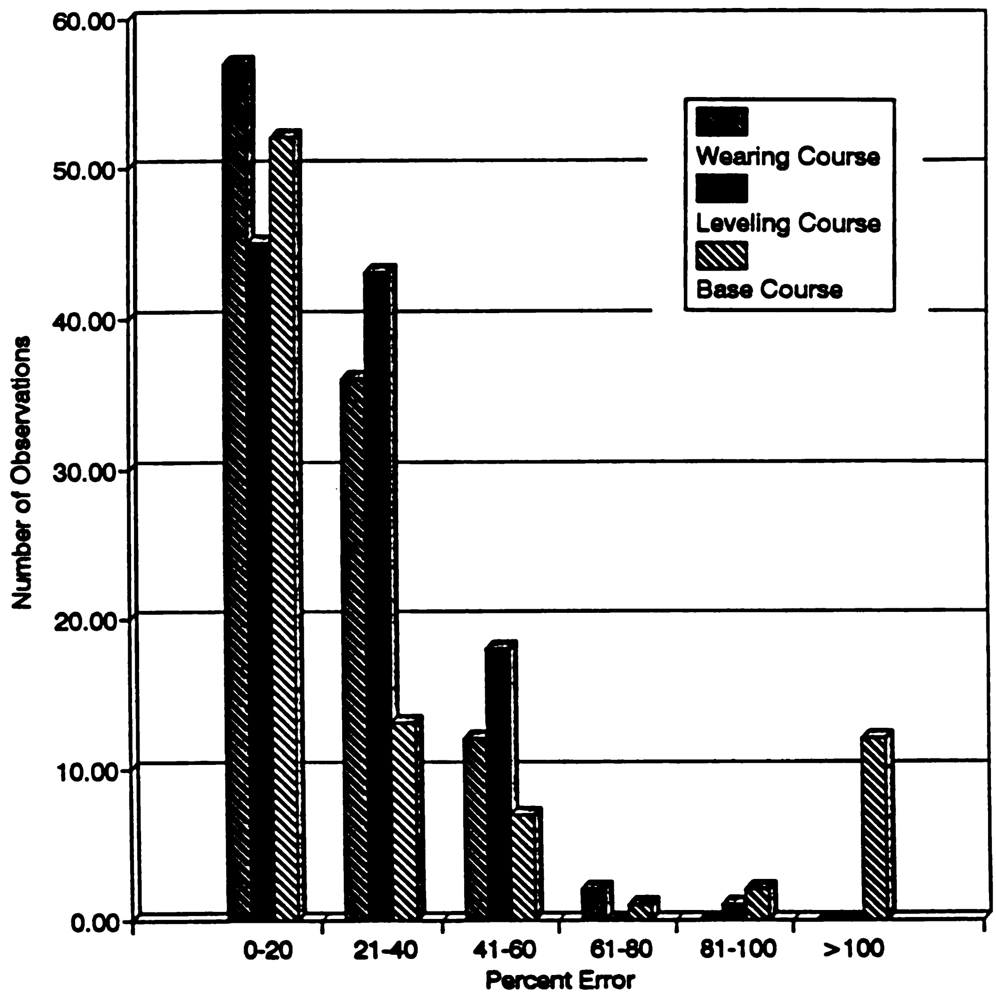

Figure 5.20 : **Percent difference between the proposed and as-constructed AC courses thicknesses.**

obtained from the MDOT cross-section data file and the AC thickness determined from the cores of the 107 core locations. It can be seen that variations by as much as 100 percent was observed for the base course whereas, variation upto 40 to 60 percent was common for wearing and leveling courses.

Nevertheless, material properties for the other 88 core locations were assigned based on the above two assumptions. Table 5.23 summarizes the core designation number, the coarse aggregate angularity, the percent air voids, the percent AC, fine, sand, and aggregate contents, the pavement service life, the estimated cumulative 18-kip ESAL, the measured rut depths, the rut depths predicted by using equation 5.6, and the percent difference between the predicted and the measured values. Figure 5.21 shows the predicted and the measured rut depths of 107 pavement locations (open squares in the Figure indicate the 19 core locations for which equation 5.6 was developed). Once again, the locus of the straight line in the Figure represents those points where the predicted rut depth values are equal to the measured ones.

The variations between the predicted and measured rut depths shown in Figure 5.22 are expected. As stated earlier, the reasons for these variations are:

1. Because of construction practices and variations, the as-constructed layer thicknesses and material properties vary from one point to another. For example, Figure 5.20 depicts the percent difference between the as-designed layer thicknesses (obtained from the MDOT files) and the actual thickness determined for the 107 core locations.
2. Figure 5.23 shows the variations in the average peak pavement deflection along pavement control section number 43F. This section was designed and it was supposedly constructed by using the same material properties and layer thicknesses. However, the peak pavement deflection which

Table 5.23 : Material properties for the 107 core locations.

Line No.	Core Designation Number	Extracted Cores	Agg Angularity	Air Void	Percent by weight AC	Sand	Fine	Agg	Service Life (years)	Cum. ESAL (mill)	Rut (inch)	Predicted Rut (inch)	Percent Difference (actual)
1	7112011	No	2.21	9.2	4.3	63	4	33	7	1.25	0.19	0.63	230.9
2	7122411	No	2.18	9.2	4.4	61	4	35	7	1.25	0.19	0.64	237.0
3	7137022	No	2.27	8.6	4.4	61	4	35	7	1.25	0.44	0.23	-48.6
4	7127721	No	2.24	8.9	4.4	61	4	35	7	1.25	0.19	0.37	92.6
5	7128332	No	2.23	8.9	4.4	61	4	35	7	1.25	0.25	0.38	51.6
6	7131211	Yes	2.24	8.9	4.4	62	4	34	7	1.25	0.31	0.37	18.2
7	7141211	No	2.34	8.0	4.5	60	4	36	7	1.25	0.50	0.10	-80.5
	Avg.		2.25	8.8	4.4	61	4	35	7	1.25	0.30	0.39	71.59
	Std.Dev.		0.05	0.4	0.0	1	0	1	0	0.00	0.12	0.18	115.88
8	13156621	No	4.89	2.9	5.6	42	4	53	30	1.51	0.19	-0.04	-121.5
9	13142311	No	4.89	2.8	5.6	42	5	53	30	1.51	0.13	-0.05	-140.9
10	13132911	No	4.88	2.9	5.6	43	5	53	30	1.51	0.31	-0.03	-109.0
11	13117121	Yes	4.88	3.2	5.6	43	5	52	30	1.51	0.13	0.02	-82.8
12	13126311	No	4.90	2.9	5.6	42	4	53	30	1.51	0.25	-0.03	-111.7
13	13142922	No	4.87	2.9	5.6	43	5	52	30	1.51	0.13	-0.02	-115.8
14	13151511	No	4.89	3.0	5.6	43	5	53	30	1.51	0.19	-0.02	-110.8
15	13164311	No	4.90	2.9	5.6	42	4	53	30	1.51	0.19	-0.04	-118.8
	Avg.		4.89	2.9	5.6	43	5	53	30	1.51	0.19	-0.03	-113.93
	Std.Dev.		0.01	0.1	0.0	0	0	0	0	0.00	0.06	0.02	15.07
16	29172711	No	1.89	7.5	4.7	65	4	30	11	0.76	0.13	0.12	-4.9
17	29117721	Yes	1.98	7.6	4.7	65	4	31	11	0.76	0.13	0.11	-15.7
18	29186711	No	1.95	7.6	4.7	65	4	31	11	0.76	0.13	0.11	-12.8
19	29111711	No	1.95	7.6	4.7	65	4	31	11	0.76	0.13	0.11	-14.6
20	29134511	No	1.86	7.6	4.7	65	4	30	11	0.76	0.06	0.12	100.5
21	29146911	No	1.92	7.6	4.7	65	4	31	11	0.76	0.00	0.12	
22	29176321	No	1.89	7.6	4.7	65	4	30	11	0.76	0.13	0.12	-8.9
23	29183321	No	1.87	7.5	4.7	66	4	30	11	0.76	0.13	0.12	-6.6
	Avg.		1.91	7.6	4.7	65	4	31	11	0.76	0.10	0.12	5.28
	Std.Dev.		0.04	0.0	0.0	0	0	0	0	0.00	0.05	0.00	39.05

Table 5.23 : Material properties for the 107 core locations (continued).

Line No.	Core Designation Number	Extracted Cores	Agg Angularity	Air Void	Percent by weight AC	Sand	Fine	Agg	Service Life (years)	Cum. ESAL (mill)	Rut (inch)	Predicted Rut (inch)	Percent Difference (actual)
24	19118331	No	3.44	5.7	5.3	55	6	39	11	1.58	0.23	0.38	66.3
25	19141811	No	3.47	5.8	5.3	55	6	39	11	1.58	0.25	0.36	45.3
26	19132322	No	3.45	5.8	5.3	55	6	39	11	1.58	0.23	0.37	62.8
27	19150911	Yes	3.48	5.9	5.3	55	6	39	11	1.58	0.20	0.36	78.3
28	19131111	Yes	3.48	5.9	5.3	54	6	40	11	1.58	0.20	0.35	77.1
29	19113011	No	3.53	6.2	5.4	53	6	42	11	1.58	0.20	0.31	56.3
30	19121611	No	3.51	6.0	5.3	54	6	40	11	1.58	0.20	0.33	66.1
31	19128221	No	3.49	5.9	5.3	54	6	40	11	1.58	0.25	0.34	37.3
32	19137431	No	3.49	5.9	5.3	54	6	39	11	1.58	0.20	0.35	73.2
33	19148131	No	3.50	6.0	5.3	54	6	40	11	1.58	0.20	0.33	67.4
34	19161211	No	3.42	5.7	5.3	55	6	39	11	1.58	0.28	0.39	39.9
35	19169131	No	3.47	5.8	5.2	55	6	39	11	1.58	0.20	0.36	81.8
	Avg.		3.48	5.9	5.3	54	6	39	11	1.58	0.22	0.35	62.65
	Std.Dev.		0.03	0.1	0.0	1	0	1	0	0.00	0.03	0.02	14.38
36	11257021	Yes	3.23	6.2	5.9	61	7	32	6	0.12	0.06	0.06	0.9
37	11245021	No	3.22	6.2	5.9	61	7	32	6	0.12	0.06	0.06	1.3
38	11265911	Yes	3.23	6.2	5.9	61	7	32	6	0.12	0.06	0.06	0.8
39	11227022	No	3.23	6.1	5.9	61	7	32	6	0.12	0.19	0.06	-68.3
40	11241012	No	3.22	6.2	5.9	61	7	32	6	0.12	0.06	0.06	1.2
41	11222311	No	3.21	6.3	5.9	61	7	32	6	0.12	0.19	0.06	-67.8
	Avg.		3.22	6.2	5.9	61	7	32	6	0.12	0.10	0.06	-21.98
	Std.Dev.		0.01	0.1	0.0	0	0	0	0	0.00	0.06	0.00	32.55
42	4226311	Yes	2.97	1.0	5.9	58	6	36	3	0.33	0.06	0.07	10.8
43	4233011	No	2.97	1.3	5.9	58	6	36	3	0.33	0.00	0.07	
44	4227622	No	2.98	0.2	5.9	56	6	38	3	0.33	0.00	0.05	
45	4215921	No	2.97	1.1	5.9	58	6	36	3	0.33	0.00	0.07	
46	4212911	Yes	2.97	1.0	5.9	58	6	36	3	0.33	0.06	0.07	11.1
	Avg.		2.97	0.9	5.9	57	6	36	3	0.33	0.02	0.06	10.98
	Std.Dev.		0.00	0.4	0.0	1	0	1	0	0.00	0.03	0.01	0.17

Table 5.23 : Material properties for the 107 core locations (continued).

Line No.	Core Designation Number	Extracted Cores	Agg Angularity	Air Void	Percent by weight AC	Sand	Fine	Agg	Service Life (years)	Cum. ESAL (mill)	Rut (inch)	Predicted Rut (inch)	Percent Difference (actual)
47	43148341	No	3.83	6.5	5.4	49	8	43	1	0.76	0.38	0.30	-20.9
48	43141611	Yes	3.82	6.5	5.5	49	8	44	1	0.76	0.38	0.31	-19.4
49	43131911	Yes	3.83	6.6	5.5	49	8	44	1	0.76	0.38	0.31	-18.8
50	43178112	No	3.82	6.4	5.4	49	8	43	1	0.76	0.06	0.30	403.3
51	43152311	Yes	3.78	6.5	5.5	49	8	43	1	0.76	0.38	0.32	-16.2
52	43111711	No	3.88	6.7	5.4	48	8	44	1	0.76	0.19	0.30	57.5
53	43121811	No	3.82	6.6	5.5	49	8	43	1	0.76	0.25	0.31	24.2
54	43148333	No	3.89	6.6	5.4	48	8	44	1	0.76	0.38	0.29	-24.1
55	43161411	No	3.83	6.5	5.5	49	8	44	1	0.76	0.38	0.31	-19.5
56	43178521	No	3.83	6.5	5.5	49	8	43	1	0.76	0.06	0.30	406.7
57	43188121	No	3.83	6.5	5.5	49	8	43	1	0.76	0.06	0.30	404.3
58	43191411	No	3.85	6.6	5.4	49	8	44	1	0.76	0.13	0.30	129.7
	Avg.		3.83	6.5	5.4	49	8	44	1	0.76	0.25	0.30	108.91
	Std.Dev.		0.03	0.1	0.0	0	0	0	0	0.00	0.14	0.01	176.14
59	35136221	No	4.73	7.9	5.6	51	6	43	14	1.37	0.30	0.28	-5.6
60	35118931	Yes	4.73	7.9	5.6	51	6	43	14	1.37	0.18	0.34	87.5
61	35114222	No	4.75	7.7	5.8	53	6	40	14	1.37	0.15	0.37	146.5
62	35123311	No	4.72	8.0	5.6	51	6	43	14	1.37	0.13	0.34	159.4
63	35128321	No	4.73	7.8	5.6	51	6	43	14	1.37	0.13	0.29	123.4
64	35132611	No	4.74	7.8	5.6	52	6	43	14	1.37	0.18	0.29	60.9
65	35112211	No	4.73	7.9	5.6	51	6	42	14	1.37	0.15	0.34	124.3
66	35143911	No	4.72	8.0	5.5	50	6	44	14	1.37	0.15	0.28	87.3
67	35152311	No	4.73	7.8	5.6	51	6	43	14	1.37	0.23	0.29	27.2
68	35159121	No	4.72	7.9	5.6	51	6	43	14	1.37	0.20	0.32	62.3
69	35161411	No	4.73	7.9	5.6	51	6	43	14	1.37	0.13	0.30	128.1
70	35167331	No	4.73	7.8	5.6	51	6	43	14	1.37	0.18	0.29	60.5
	Avg.		4.73	7.9	5.6	51	6	43	14	1.37	0.18	0.31	88.49
	Std.Dev.		0.01	0.1	0.1	1	0	1	0	0.00	0.05	0.03	47.70

Table 5.23 : Material properties for the 107 core locations (continued).

Line No.	Core Designation Number	Extracted Cores	Agg Angularity	Air Void	Percent by weight AC	Sand	Fine	Agg	Service Life (years)	Cum. ESAL (mill)	Rut (inch)	Predicted Rut (inch)	Percent Difference (actual)
71	10131011	Yes	3.72	8.5	5.3	62	9	30	7	0.22	0.13	0.13	-2.8
72	10128121	No	3.72	7.7	5.6	61	8	30	7	0.22	0.18	0.11	-37.0
73	10136641	No	3.71	7.3	5.7	61	8	30	7	0.22	0.05	0.12	132.4
74	10118731	No	3.59	3.8	7.3	61	6	33	7	0.22	0.43	0.20	-53.8
75	10117322	No	3.66	3.8	7.1	61	7	32	7	0.22	0.40	0.19	-52.5
76	10111711	No	3.63	3.8	7.2	61	7	32	7	0.22	0.35	0.19	-44.7
77	10131821	No	3.68	6.8	6.0	61	8	31	7	0.22	0.13	0.13	-3.7
	Avg.		3.67	6.0	6.3	61	8	31	7	0.22	0.24	0.15	-8.87
	Std.Dev.		0.04	1.9	0.8	0	1	1	0	0.00	0.14	0.04	60.98
78	8213022	No	4.88	3.2	5.6	41	6	53	16	1.74	0.25	0.12	-52.9
79	8260911	No	4.85	3.0	5.7	43	6	51	16	1.74	0.06	0.15	156.7
80	8261622	No	4.86	3.2	5.7	43	6	51	16	1.74	0.06	0.18	198.2
81	8221011	Yes	4.89	3.3	5.6	40	6	54	16	1.74	0.13	0.11	-15.1
82	8231511	Yes	4.89	3.2	5.6	40	6	54	16	1.74	0.13	0.10	-26.1
83	8251811	No	4.88	3.2	5.6	41	6	53	16	1.74	0.06	0.10	60.0
84	8211211	No	4.87	3.1	5.6	42	6	52	16	1.74	0.25	0.12	-51.0
85	8241011	No	4.89	3.2	5.6	40	6	54	16	1.74	0.06	0.09	44.2
	Avg.		4.88	3.2	5.6	41	6	53	16	1.74	0.13	0.12	39.26
	Std.Dev.		0.02	0.1	0.0	1	0	1	0	0.00	0.08	0.03	89.01
86	5258321	Yes	3.99	4.6	5.9	59	9	31	6	0.31	0.20	0.23	13.1
87	5229221	No	3.98	5.8	6.0	58	9	33	6	0.31	0.45	0.23	-49.7
88	5241411	No	3.93	4.4	5.9	59	9	31	6	0.31	0.15	0.24	59.0
89	5261712	No	4.03	4.7	5.9	60	9	31	6	0.31	0.20	0.22	8.7
90	5218631	No	3.99	5.2	6.0	58	9	33	6	0.31	0.55	0.22	-59.5
	Avg.	No	3.98	4.9	5.9	59	9	32	6	0.31	0.31	0.23	-5.70
	Std.Dev.	No	0.03	0.5	0.0	1	0	1	0	0.00	0.16	0.01	43.76

Table 5.23 : Material properties for the 107 core locations (continued).

Line No.	Core Designation Number	Extracted Cores	Agg Angularity	Air Void	Percent by weight				Service Life (years)	Cum. ESAL (mill)	Rut (inch)	Predicted Rut (inch)	Percent Difference (actual)
					AC	Sand	Fine	Agg					
91	1251611	No	4.06	5.9	5.1	48	6	46	2	3.36	0.63	0.48	-24.1
92	1261611	Yes	3.66	6.1	5.1	52	7	42	2	3.36	0.44	0.79	80.3
93	1284611	No	4.17	5.8	5.0	46	6	48	2	3.36	0.31	0.31	1.0
94	1272411	No	3.85	5.4	5.0	47	6	47	2	3.36	0.31	0.31	1.3
95	1248931	No	4.12	6.4	5.1	48	6	46	2	3.36	0.56	0.41	-26.1
96	1232611	No	4.05	6.2	5.0	47	6	46	2	3.36	0.19	0.41	117.5
97	1221711	No	3.73	5.6	4.9	47	6	47	2	3.36	0.38	0.39	3.5
98	1214111	No	3.95	5.8	5.0	47	6	47	2	3.36	0.31	0.40	29.2
	Avg.		3.95	5.9	5.0	48	6	46	2	3.36	0.39	0.44	22.81
	Std.Dev.		0.17	0.3	0.1	2	0	2	0	0.00	0.14	0.14	47.71
99	14151513	No	3.20	12.3	6.2	52	7	42	13	0.18	0.40	4.32	979.2
100	14161813	No	3.19	11.0	6.1	51	7	42	13	0.18	0.18	1.06	490.0
101	14155123	No	3.16	9.0	6.0	52	7	41	13	0.18	0.40	0.15	-62.6
102	14121713	Yes	3.14	9.2	5.9	52	7	41	13	0.18	0.18	0.18	1.1
103	14113023	No	3.16	9.7	6.0	51	7	41	13	0.18	0.50	0.29	-42.7
104	14148233	No	3.19	10.7	6.1	52	7	42	13	0.18	0.00	0.82	
105	14124223	No	3.16	10.0	6.0	51	7	42	13	0.18	0.40	0.37	-7.9
106	14137831	No	3.18	10.7	6.1	51	7	42	13	0.18	0.10	0.82	720.4
107	14143711	No	3.17	10.2	6.0	51	7	42	13	0.18	0.10	0.48	382.0
	Avg.		3.17	10.3	6.0	51	7	42	13	0.18	0.25	0.94	307.45
	Std.Dev.		0.02	1.0	0.1	0	0	0	0	0.00	0.17	1.23	373.09

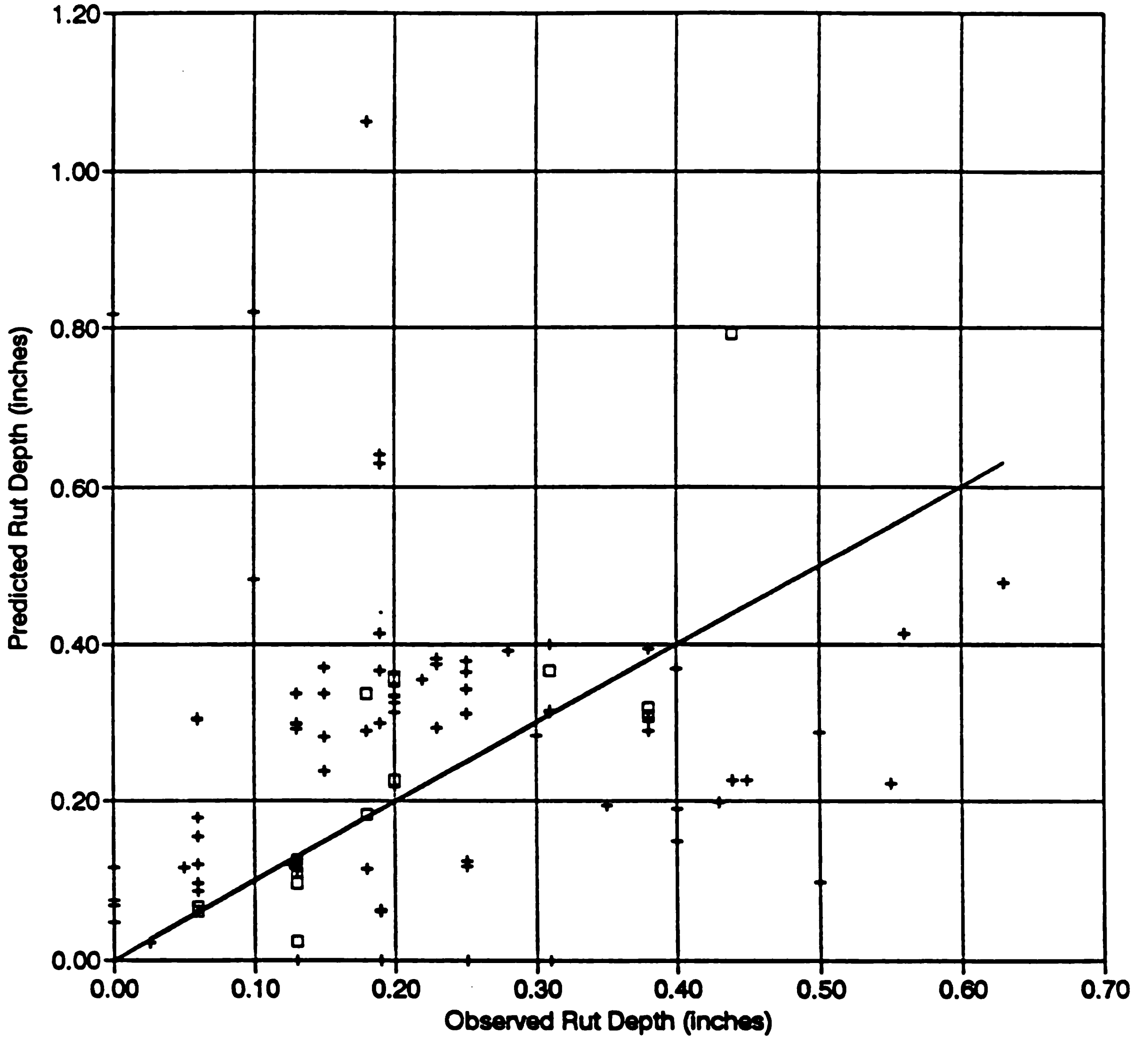

Figure 5.21 : **Observed versus the predicted rut depths at 107 core locations.**

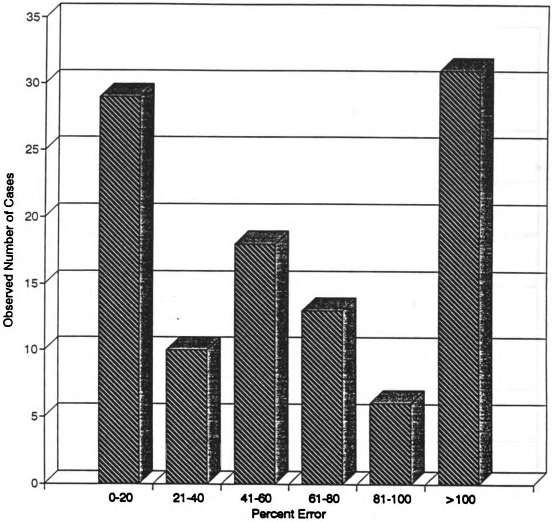

Figure 5.22 : **Percent differences between the observed and the predicted rut depths for the 107 core locations.**

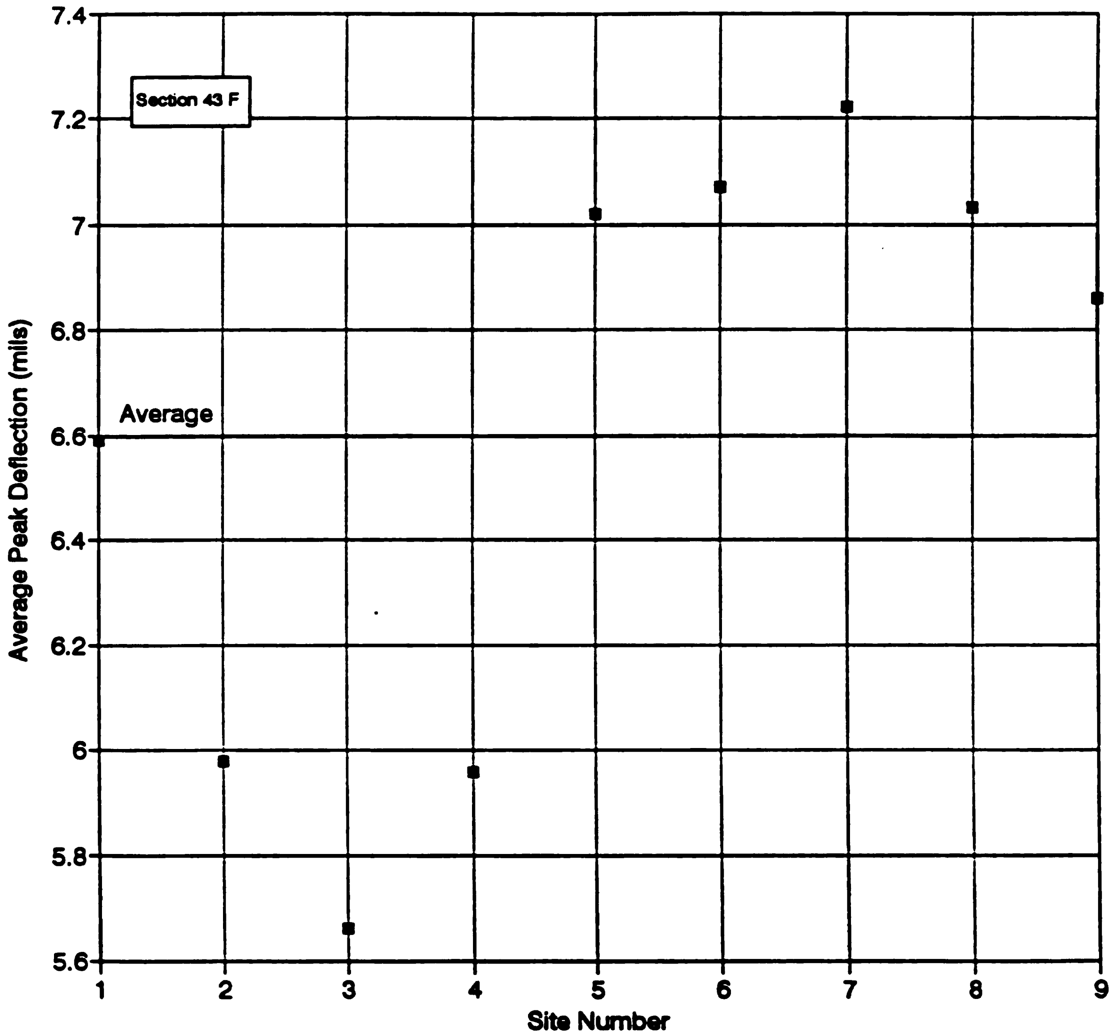

Figure 5.23 : **Average peak deflection variation along section 43F.**

represents the pavement response to a 9000 pounds load vary from one location to another. Variations in the pavement deflection is the direct consequence of variations in the material properties and layer thicknesses between one point and another.

3. Measured rut depth is also a function of the other layers in the pavement structure besides the AC course. Since, most of the extreme cases are of the over prediction, the contribution of rut due to other pavement layers such as base, subbase and roadbed soil can easily be ruled out. Thus, it can be concluded that the assumption of similar material properties within a section can be questionable if proper quality controls are not exercised.

5.5.3 Analysis of Rut as a Function of the Pavement Deflection

5.5.3.1 Introduction

Nondestructive deflection tests (NDT) have evolved over time from the Benkelman beam (introduced by A.C. Benkelman in connection with the Western Association of State Highway Officials (WASHO)) to the falling weight deflectometer (FWD) introduced during the 1980,s. The NDT tests are currently very popular and are used by most State Highway Agencies. The tests are easy to perform and they do not require the closing of the highway pavement to traffic for a prolonged period of time. Using the FWD, the NDT test consists of raising a calibrated weight to a certain height, dropping the weight on a steel plate, and measuring the resulting dynamic load and the pavement response (deflections). It should be noted that pavement deflection represents the pavement system (surface, base, and subbase layers and the roadbed soil) response to load. It is a direct consequence of the mechanics by which the energy induced into the pavement structure attenuate with distance and depth from the point of load application. Deflection data is generally affected by the following factors:

1. The structural integrity and capacity of the pavement, which include the stiffnesses and thicknesses of all pavement layers, the stiffness of the roadbed soil, and the depth to a stiff layer such as the bedrock.
2. The environmental conditions including moisture and temperature.
3. The pavement conditions such as the type, extent, and severity of the distress (e.g., rut, fatigue cracks, and other types of cracks).
4. The applied load magnitude, frequency, and duration.
5. The test location relative to the pavement edge, joint, or crack.
6. The service life of the pavement and the traffic history.

Interpretation of the NDT data has always been a complex and difficult task. The data has traditionally been used as a tool to evaluate the structural capacity and integrity of the pavements. One of the earliest uses of pavement deflection (using the Benkelman beam) was that made in California in 1938 and reported by Haveem (82). He stated that flexible pavements would have satisfactory performance if the peak deflection under a 15000-pound single axle load is less than 0.02-inch. Similarly, results of the WASHO Road Test (conducted in Huba Valley on flexible pavements) indicated that a satisfactory pavement performance can be achieved if the peak pavement deflection is less than 0.030-inch for pavement located in cold regions and less than 0.040-inch for those located in warm regions (83, 84). Recently, NDTs are conducted and the measured deflection data are being used for the purposes of pavement evaluation and management and for determining the required thicknesses of the asphalt overlays. In this regard, various State Highway Agencies (SHAs) and other organizations such as Utah DOT (85), California DOT (86), Oklahoma DOT (87), Louisiana DOT (88), Texas DOT (89), and the Asphalt Institute (90) have developed various procedures and protocols for the interpretation and use of the

NDT data.

Analysis of the measured pavement deflection data provides a quantitative basis for evaluation of the pavement structural condition at any time during its service life. Other important information relative to pavement rehabilitation and maintenance requirements can also be inferred from the deflection profile (deflection basin). Because the NDTs are nondestructive in nature and because they are easily and quickly performed, the tests cause a minimum hindrance to normal traffic flow and they are less hazardous and more economical to undertake. In addition, the measured pavement deflections represent the direct pavement response to the applied load.

To this end, a complementary component of this study involves the development of a computer program (called MICHBACK) for the backcalculation of the pavement layer moduli using NDT data (91). The pavement sections selected for the NDT part of the study are the same as those selected in this part. As noted in Chapter 4, 49 flexible and 15 composite pavement sections were selected and each section was divided into several 100-feet long test sites. At each test site, at least five NDT tests (spaced at 20-feet intervals) were performed using the MDOT FWD KUAB model. Additional NDT tests were also conducted at each core location within the pavement sites. Several observations regarding the NDT tests should be noted. These are:

1. The seven deflection sensors of the MDOT FWD were spaced as follows 0, 8, 12, 18, 24, 36, and 60 inch from the center of the load plate of the FWD.
2. Each test consisted of three drops. For each drop, the weight and the height of the drop was set such that the load delivered to the pavement is about 9000-pounds. The actual measured load, however, varied slightly from the target value of 9000-pounds.

3. All measured deflection data were normalized to the 9000-pound level and for each deflection sensor, the average of the deflections obtained from the three drops was calculated.
4. During each test, both the pavement and the air temperatures were recorded directly on the deflection file.
5. Each pavement section was tested once during each of the following seasons fall of 1991, spring of 1992, summer of 1992, and spring of 1993.

In this study, the pavement deflection data measured during the summer of 1991, the pavement cross-section data, and the traffic volume in terms of the number of 18-kip ESAL for the 13 cored sections (104 cored locations) were used to develop a second statistical rut-depth prediction model. This model is presented and discussed in the next subsection.

5.5.3.2 Statistical Analysis

As noted above, in this study, a total of 49 flexible and 15 composite pavement sections were selected and each section was divided into several 100-feet long test sites. During the summer of 1991, at least five NDT tests (each test consisted of three drops) were conducted along each pavement site (the test locations were spaced at 20-feet intervals) and one test at each core location within the site. For each test location and for each drop, the measured deflection data were first normalized to the 9000-pound level and then the average deflection of the three drops was calculated.

Table 5.24 provides the minimum, maximum, average, and standard deviation of the pavement service life, cumulative 18-kips ESAL, layer thicknesses, and the deflection of each of the seven sensors for the 563 NDT

Table 5.24 : Descriptive statistics of the data.

	Thickness (inch)			Cum. ESAL (millions)	Ser. Life (years)	Sensor Deflection (mils)						
	AC	Base	Sub Base			D1	D2	D3	D4	D5	D6	D7
Min.	2.20	4.00	0.00	0.12	1.00	2.72	2.54	2.32	2.12	1.73	1.05	0.72
Max.	14.00	18.00	29.00	8.48	30.00	25.31	18.11	13.45	12.36	11.11	9.10	5.70
Avg.	5.59	6.90	16.50	1.73	14.00	9.09	6.86	5.73	4.49	3.56	2.44	1.40
Std.Dev.	2.48	3.36	8.50	1.91	8.20	5.35	2.42	1.95	1.56	1.31	1.03	0.64

locations. The detailed data can be found in appendix "B". Two very important points should be noted herein are:

1. Pavement cores were obtained from only 104 of the 563 NDT locations. Hence, for these 104 locations, the AC thicknesses presented in appendix "B" represent the actual thicknesses measured from the cores. The AC thicknesses for the remaining 459 test locations are those obtained from the MDOT records (the as designed thicknesses). Hence, for each non-cored test location, the actual AC thickness varies from that listed in appendix "B".

2. For each NDT location, whether the pavement was cored or not, the thicknesses of the base and subbase layers were not easily identifiable. The main reason is that the typical base and subbase materials used in the State of Michigan are very similar. Consequently, it was almost impossible to separate the two materials during coring. Therefore, the thicknesses of the base and subbase layers listed in appendix "B" were obtained from the MDOT file. For the cored section, the total thicknesses of the base and subbase layers found in the MDOT files were verified during pavement coring.

Nevertheless, prior to the commencement of the statistical analysis, several engineering issues that are significant to the statistical analysis should be noted. These are:

1. In general, the magnitude of the pavement deflection varies from time to time and it depends on the existing pavement conditions, environmental factors, and traffic load, volume, and speed. If one is to assume that the traffic load and speed and the environmental conditions are constant with time, then the magnitude of the present deflection of a pavement structure is a function of the cumulative traffic volume since construction. Figure 5.24 shows a generalized peak pavement deflection as a function of time.It

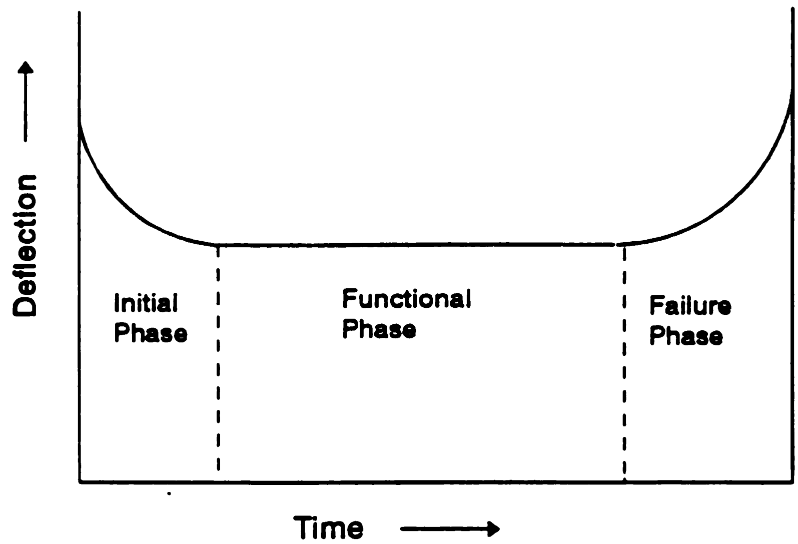

Figure 5.24 : Pavement deflection as a function of time.

can be seen that the magnitude of the pavement deflection immediately after construction is high, it decreases with increasing traffic volume due to pavement consolidation and seating under traffic loading, and it increases as the pavement deteriorates and loses its structural capacity and integrity with time. Pavement rutting is the direct consequences of pavement consolidation and/or seating.

2. For any pavement structure, its rut depth measured at time "t" is a function of the as-constructed pavement conditions (at time t_o) in terms of structural capacity and integrity that corresponds to time "t_o", the number of 18-kip ESAL trafficked that pavement during the time period "$t - t_o$", and the environmental conditions during that time period. The as-constructed pavement structural capacity, on the other hand, can be represented by the as-constructed deflection basin. That is, if the deflection basin of a pavement structure is measured directly after construction and prior to opening the pavement to traffic, then that deflection basin expresses the structural capacity and integrity of that pavement including the quality of construction and compaction. This scenario implies that the pavement rut depth at time "t" is a function of the as-constructed deflection basin. Unfortunately, the as-constructed deflection basins of the pavement sections of this study were not measured and they are not available.

3. The deflection basin of a pavement structure measured at time "t" is a function of the existing rut depth of the pavement, the load magnitude, the environmental factors such as moisture and temperature, and the other pavement physical conditions such as the state of cracking and shoving.

The three issues presented above imply that the as-constructed pavement deflection should be used to model the pavement rutting potential. Because of the lack of such data at the present time, and in order to introduce an empirical model relating the deflection basins and rut, the statistical analyses below are presented as an attempt to explain the variation in the measured rut depths as a function of the present pavement deflections and the pavement cross-sections.

To this end, the scenario presented below, although it applies to the other statistical analyses presented in this thesis, is very crucial to the development of the rut distress model. The reason is that, none of the so called independent variables can be truly identified as such. For example, a deflection basin consists of seven deflection readings made at various lateral distances from the point of load application. The value of each deflection reading is a function of the other deflection readings, the pavement cross-section, the material properties (which are not known), the magnitude of the applied load, the state of the pavement distress, the moisture levels in the base subbase and roadbed soil, and the pavement temperature. In addition, the pavement layer thicknesses are a function of the traffic (thicker layers are used in pavements that are expected to carry higher traffic load and volumes). Hence, the statistical analysis must be conducted carefully and in steps.

For any statistical analysis, the first essential step is the identification of potential explanatory variables to be used in the development of the predictive/correlation equation. In a statistical sense, these explanatory variables are referred to as independent variables. In reality, various levels of dependency exist between these variables and the pavement rut (the dependent variable) and among the variables themselves. In some instances, the problem of collinearity between the dependent variables can be minimized by combining them into clusters based upon analytical and engineering backgrounds. In other situations (such as large sample population), the variables may be stratified. Still in others, the variables can be included as polynomial terms of the same variables. For example, the deflection measured at lateral distances of 8 and 12-inch from the center of the loaded area can be thought of as two terms of a polynomial function that is dependent on the deflection measured under the load and the pavement cross-section. It is in this context (polynomial terms, and variable clusters), the statistical analysis of the measured deflection and rut data was conducted. To illustrate, consider the coefficient of correlations between the rut depth and the measured deflections at the seven sensor locations (D1 through D7) listed in Table 5.25. It can be seen that:

1. As it was expected, the seven deflection values are highly collinear. The deflection measured at any sensor location is strongly related to the other deflection values.
2. The rut depth increases with an increase in the peak deflection. This observation is reasonable. Weaker pavements deflect more under traffic loading and are prone to higher rutting.
3. The outer sensor deflections (D2 through D7) are negatively correlated to the rut depth. That is increasing deflections cause decreasing rut. This observation was also expected because stiffer AC pavements distribute the load over larger areas as compared to softer AC pavements. Hence, stiffer AC courses cause a lower rut potential.
4. The highest value of the coefficient of correlation in the Table is "-0.260". This should not be interpreted as an absence of significant correlation between the various deflections and the pavement rut. The seven values of the measured deflections represent only a few terms of the deflection basin that affect rut. For example, the slope and the area of the deflection basin (which affect the pavement rutting) can be calculated by clustering various deflection terms which can be related to the rut depth.

Table 5.25 : Correlation matrix for rut and sensors deflection.

	Rut	Sensor Deflection						
		D1	D2	D3	D4	D5	D6	D7
Rut	1.000							
D1	.047	1.000						
D2	-.005	.975	1.000					
D3	-.051	.919	.977	1.000				
D4	-.137	.749	.860	.945	1.000			
D5	-.206	.536	.681	.809	.954	1.000		
D6	-.260	.183	.346	.507	.745	.907	1.000	
D7	-.213	.048	.194	.337	.576	.768	.950	1.000

D = Sensor deflection (1 to 7).

The second step in the statistical analysis is to observe the trends between the dependent variable (rut depth) and the independent variables (polynomial terms and variable clusters) to infer the proper variable transformation forms. To this end, the polynomial terms and the variable clusters were plotted against the rut depth. From the plots, the trend between the dependent and each of the independent variable was observed. Based on the observations, several applicable transformation forms were studied and the one that led to the lowest standard error were selected. Analysis based on these variable strings and clusters are presented in the next sections.

5.5.3.3 Regression Analysis

As noted above, the measured deflections at the seven sensor locations (0, 8, 12, 18, 24, 36, and 60-inch from the center of the loaded area) are given the following symbols (D1, D2, D3, D4, D5, D6, and D7), respectively. The deflections were used in a polynomial strings and they were clustered as to calculate the various parameters of the deflection basins. These strings of variables are presented below.

ESL = The cumulative 18-kip single axle load (ESAL) and the pavement service life terms were clustered into one term by using the following equation:

$$ESL = (LOG(1+CUM.ESAL^{1.5})/(1+Service\ Life))$$

The above cluster approximates the average yearly 18-kip ESAL traveled the pavement section. This cluster combined two collinear terms, the service life and the cumulative ESAL.

$D1_{AC}$ = The deflection measured under the center of the load (D1) was normalized relative to the thickness of the AC layer (T_1.) using the following equation:

$$D1_{AC} = (lOG(D1)/T_1^{1.2})$$

The term $D1_{AC}$ approximates the rate of deflection per inch of the AC thickness. Higher AC thicknesses yield lower D1.

R61 = Expresses the ratio of the deflection (D6) measured at a lateral distance of 36-inch from the center of the load normalized with respect to the term $D1_{AC}$ as follows:

$$R61 = LOG(ABS(D6/D1_{AC}))$$

R21 = The term is similar to the previous one (R61) except it normalizes the deflection (D2) measured at a lateral distance of 8-inch from the center of the loaded area as follows:

$$R21 = LOG(ABS(D2/D1_{AC}))$$

R12 = The term is similar to the previous two terms (R61 and R21) except it normalizes the deflection (D1) measured at the center of the loaded area as follows:

$$R12 = (D1/(D1+D2))^{.25}$$

R71 = The term is also similar to the previous terms except it normalizes the deflection (D7) measured at a lateral distance of 60-inch from the center of the loaded area as follows:

$$R71 = LOG(ABS(D7/D1_{AC})$$

S = For each deflection basin, the slopes between adjacent deflection sensor locations were calculated. These include the following terms and their definitions:

$$S56 = (ABS(D5-D6)/12)^{0.25}$$

$$S34 = (ABS(D3-D4)/6)^{.75}$$

$$S67 = (ABS(D6-D7)/24)$$

$$S23 = LOG(ABS(D2-D3)/4)$$

$S45 = (ABS(D4-D5)/6)^{-1}$.

T_{BS} = This term represents the thicknesses of the base (T_1) and subbase (T_2) as follows:

$$T_{BS} = (T_2 + T_3^2)$$

A = For each deflection basin, the area between adjacent deflection sensor locations were calculated. These include the following terms and their definitions:

A12 = (4*(D1+D2))

A23 = LOG(2*(ABS(D2)+ABS(D3)))

A45 = (3*(ABS(D4)+ABS(D5)))

A56 = (6*(ABS(D5)+ABS(D6)))

AA = $((D1+D2+D3+D4+D5+D6+D7)^{-3})$.

Based on the above definitions, variable strings and variable clusters were formed and two statistical analysis were conducted and are presented in the next two subsections.

5.5.3.3.1 Statistical Analysis Based on Strings of Variables

The results of the regression analysis based on strings of variables are listed in Table 5.26. It can be seen from the Table that all the variables in the equation have a "T" significance values of less than 0.060. Hence, they are significant variables. The results of the regression analysis listed in Table 5.26 indicate that the standard error (S.E.) of the resulting model is 0.093. The value of the coefficient of determination (R^2) is 0.591 and the adjusted R^2 is 0.527. The numbers listed under the column designated "B" are the regression constants for the indicated variables. Table 5.27 provides a list of the regression constants and the values of the R^2 and the standard error obtained from each step of the

Table 5.26 : Results of regression analysis.

Multiple R	.76881
R Square	.59107
Adjusted R Square	.52674
Standard Error	.09325

Analysis of Variance

	DF	Sum of Squares	Mean Square
Regression	14	1.11850	.07989
Residual	89	.77384	.00869

F = 9.18852 Signif F = .0000

* * * * M U L T I P L E R E G R E S S I O N * * * *

Equation Number 1 Dependent Variable.. P RUT

------------------ Variables in the Equation ------------------

Variable	B	SE B	Beta	T	Sig T
ESL	.743214	.205337	.389246	3.619	.0005
R61	-3.016448	.684141	-6.653747	-4.409	.0000
TBS	4.975570E-04	9.60488E-05	.586535	5.180	.0000
$D1_{AC}$	1.109569	.410918	.950740	2.700	.0083
A23	-24.076327	4.347756	-28.813294	-5.538	.0000
S56	5.741293	1.129381	2.808077	5.084	.0000
AA	16.586406	3.125505	34.256700	5.307	.0000
R12	-21.068777	4.240290	-1.815557	-4.969	.0000
A45	-.129160	.027572	-7.343351	-4.684	.0000
R21	3.255857	.721157	5.853058	4.515	.0000
A12	-.037492	.009048	-7.368830	-4.144	.0001
S34	1.996104	.717777	2.304049	2.781	.0066
S67	8.008854	3.789590	.948452	2.113	.0374
S23	.155544	.082450	.563991	1.887	.0625
(Constant)	3.995250	1.887115		2.117	.0370

ESL = (LOG(1+CUM.ESAL$^{1.5}$)/(1+Service Life));
$D1_{AC}$ = (lOG(D1)/ACTH$^{1.2}$);
R61 = LOG(ABS(D6/$D1_{AC}$));
TBS = (Base+Subbase^{2});
A23 = LOG(2*(ABS(D2)+ABS(D3)));
S56 = (abs(D5-D6)/12)$^{.26}$;
A56 = (6*(ABS(D5)+ABS(D6)));
AA = ((D1+D2+D3+D4+D5+D6+D7)$^{.3}$);
R12 = (D1/(D1+D2))$^{.26}$;
A45 = (3*(ABS(D4)+ABS(D5)));
R21 = LOG(ABS(D2/$D1_{AC}$));
A12 = (4*(D1+D2));
S34 = (abs(D3-D4)/6)$^{.75}$;
S67 = (ABS(D6-D7)/24); and
S23 = LOG(ABS(D2-D3)/4).

Table 5.27 : Regression matrix for rutting.

Intercept	Regression coefficient of independent variables																R.Sq	S.E.
	ESL	R61	TBS	S67	$D1_{AC}$	A23	A12	S56	AA	R12	A45	R21	A12	S34	S67	S23		
.17417	.7674																.162	.1447
.3688	1.1781	-.1646															.250	.1189
.3333	1.1502	-.1628	.000194														.299	.1152
.3685	1.0726	-.1532	.000181	-.9684													.311	.1148
-.1008	.7731	.2168	.000299	-5.4098	1.1236												.395	.108
-.0042	.7253	.2291	.000333	-5.2189	1.2412	-.1057											.399	.1082
.7717	.6202	.1756	.00039	-2.2955	.8934	-.8952	.0047										.441	.1049
.6204	.6810	.2002	.00035	-3.1373	1.0762	-1.0401	.0038	.7138									.451	.1045
-.3868	.6970	.1020	.00031	-6.0870	.8063	-2.6553	.0011	1.9524	1.0670								.470	.1032
.4394	.7428	.0755	.00029	-6.5434	.7222	-2.7807	.0013	2.0995	1.1281	-.9809							.473	.1035
.3933	.7508	.0711	.00033	-3.2338	.7630	-4.9214	-.00031	3.0240	3.0391	-3.4339	-.0356						.489	.103
.4752	.7461	.0724	.00033	-3.1072	.7562	-4.8230	D	2.9364	2.9466	-3.3843	-.0347						.489	.102
1.2832	.6941	-.2849	.00039	-1.0619	.7838	-5.8526	D	2.5117	3.4593	-4.4518	-.03578	.4006					.499	.102
1.3648	.6918	-.3283	.00040	D	.7764	-.6153	D	2.4888	3.6989	-4.7873	-.0404	.4441					.498	.101
.5642	.7123	-1.5565	.00044	D	1.1730	-13.42	D	4.7661	9.0157	-10.0583	-.0776	1.7672	-.0134				.537	.098
.8280	.7456	-2.1431	.00041	D	1.2524	-17.4994	D	5.2720	11.8166	-13.0995	-.0819	2.4031	-.0279	1.4641			.562	.095
1.2853	.7489	-2.7834	.000484	D	1.2952	-21.7749	D	5.6465	14.9831	-16.8931	-.1146	3.0763	-.0355	2.0547	5.9369		.575	.095
3.995	.7432	-3.0164	.00049	D	1.1095	-24.0763	D	5.7413	16.5864	-21.0687	-.1292	3.2558	-.0375	1.9961	8.0089	.1555	.591	.093

stepwise method of the SPSS computer program. As it can be seen that the variable ESL is the most important variable and it alone explains about 16 percent of the variation of the measured rut depth. This percentage increases, with the inclusion of more variables in the model. The final form of the equation modelling pavement rut as a function of the various sensor deflection, the pavement cross-section, and the 18-kip ESAL is presented below:

$$\begin{aligned}\mathrm{RUT} = {} & 3.9952 + 0.7432\,(\mathrm{ESL}) - 3.0164\,(\mathrm{R61}) + 0.000498\,(\mathrm{TBS}) + 1.1096\,(\mathrm{D1}_{AC}) - 24.0763 \\ & (\mathrm{A23}) + 5.7413\,(\mathrm{S56}) + 16.5864\,(\mathrm{AA}) - 21.0688\,(\mathrm{R12}) - 0.1292\,(\mathrm{A45}) + 3.2559\,(\mathrm{R21}) \\ & - 0.0375\,(\mathrm{A12}) + 1.9961\,(\mathrm{S34}) + 8.0089\,(\mathrm{S67}) + 0.1555\,(\mathrm{S23}) \qquad (5.6)\end{aligned}$$

$R^2 = 0.591$, $SE = 0.093$, $F = 9.188$, $F_{(Sig)} = 0.000$

Where the terms are the same as before.

Based on the statistics of the model, the following observations were made.

1. The null hypothesis of no linear relationship between the independent variables and RUT was rejected and it was concluded that at a probability of $F_{(sig)}$ zero, 59 percent of the variation of the dependent variable is explained by the above strings of variables.
2. The largest value of "T" significance is .06. This implies that all the variables in the model are statistically significant.

The Durbin-Watson statistics of equation 5.6 which is listed in Table 5.28 signifies a satisfactory non autocorrelation between the residuals. Further, the maximum, minimum, mean and standard deviation of the unstandardized and standardized predicted values and the residuals are also listed in the Table. Based on the values of the residuals and the standardized residuals, the ten worst residuals cases are presented in Table 5.29.

Figure 5.25 depicts the calculated and the observed rut depth values. As it can be seen, most of the data points are located close to the line of equality.

Table 5.28 : Residual statistics of equation 5.6

	Min	Max	Mean	Std Dev	N
*PRED	.0221	.4945	.2132	.1042	104
*RESID	-.2859	.2295	.0000	.0867	104
*ZPRED	-1.8339	2.6989	.0000	1.0000	104
*ZRESID	-3.0658	2.4612	.0000	.9296	104
Durbin-Watson Test = 2.06219					

Table 5.29 : Ten worst residuals.

Case #	*RESID	*ZRESID
93	-.2859	-3.0658
87	.2295	2.46119
88	.2208	2.36745
70	-.1692	-1.81459
101	-.1644	-1.76338
74	-.1596	-1.71208
56	.1557	1.66968
45	.1473	1.57921
54	-.1471	-1.57766
77	-.1325	-1.42076

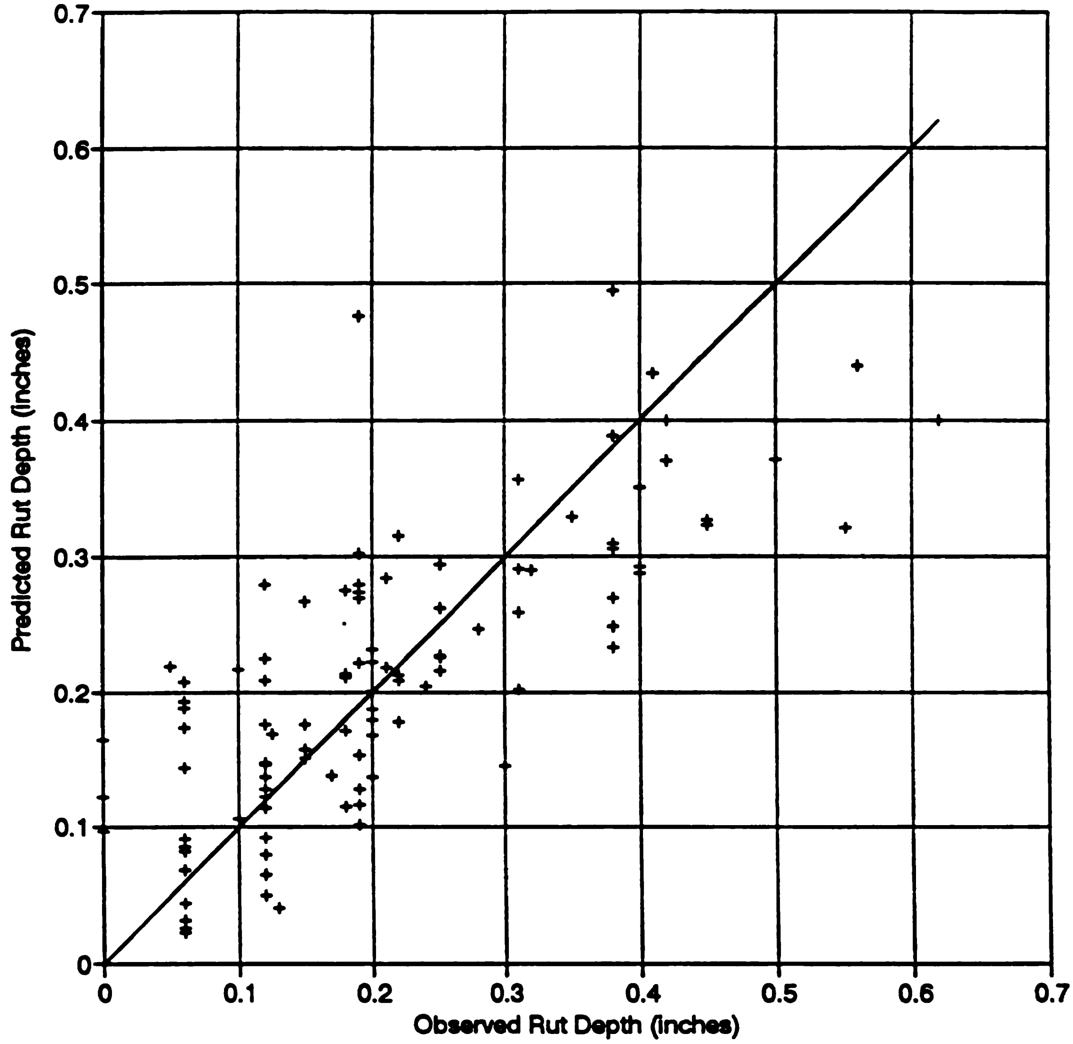

Figure 5.25 : Observed versus predicted rut depths.

The percent error between the calculated and the observed values are depicted in Figure 5.26. Examination of the Figure indicates that most of the calculated rut values are within 60 percent of the observed values. This indicates that the statistical model is relatively accurate.

Equation 5.6 was extended to estimate the rut depth at other pavement locations where the deflection data was available. Figure 5.27 shows the predicted and the measured rut depths of 563 pavement locations (plus sign in the Figure indicates the 104 core locations from which the equation was developed). The variation between the predicted and the measured rut depths shown in Figure 5.27 are expected. The main reason for this variation is that (as it was mentioned earlier) for the non-cored pavement sections the pavement cross-section data were obtained from the MDOT files. Thus, the AC course, the base and the subbase thicknesses were assumed to be constant for each non-cored section. However, it was shown earlier (see Figure 5.20) that variation in the AC layer thickness of upto 40 percent were very common for the wearing and leveling courses. Further, comments regarding the poor prediction are presented at the end of next section.

5.5.3.3.2 Regression Analysis Based on Cluster of Variables

A second statistical analysis was conducted by using variable clusters. The previously defined variable strings are clustered together and the resulting terms are used as super single variables in this analysis. The variable clusters and their definitions are listed below.

ESL = Traffic factor which is defined in the previous section.

$D1_{AC}$ = Normalized peak deflection which is also defined in the previous section.

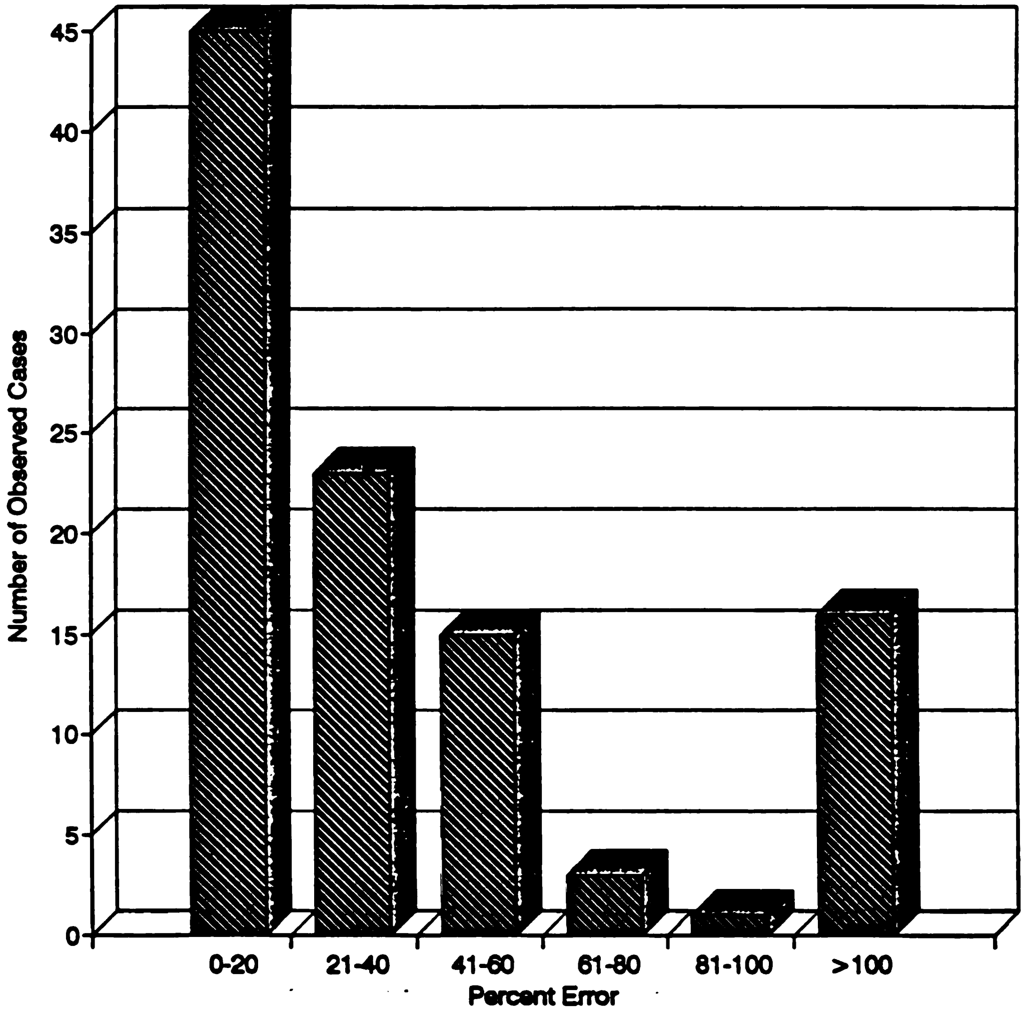

Figure 5.26 : Percent error between the observed and the predicted rut depth values.

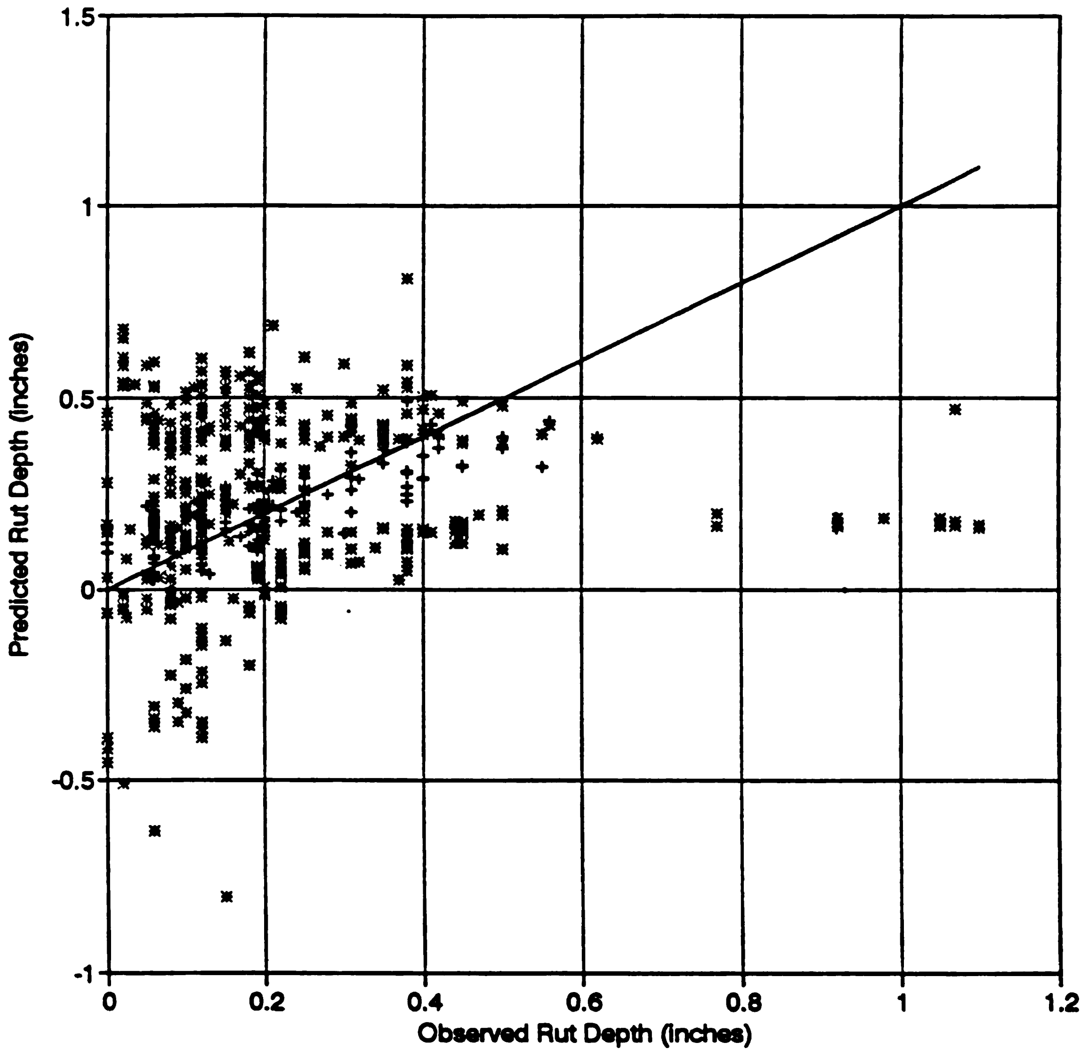

Figure 5.27 : Observed versus predicted rut depths for the 563 pavement locations.

SF = Slope factor defined by the sum of the slopes between all adjacent pairs of deflection sensors. The slope factor is calculated as follows:

$$SF = (1/ABS(S23+S34+S45+S56+S67^2))^{1.25}$$

where all terms are as previously defined.

DF = Deflection factor defined as the sum of the deflection ratios of all adjacent sensor deflections. The deflection factor is calculated as follows:

$$DF = D1_{AC}/(D1_{AC}+R21+R61+R71)^2$$

where all terms are as previously defined.

G1 = Thickness factor defined as the sum of the thickness of the base (T_2) and subbase (T_3) layers as follows:

$$T_{BS1} = (T_2^{2.5}+T_3^{2.5})$$

The results of the regression analysis are listed in Table 5.30. It can be seen that all clusters in the Table have a "T" significance values of less than 0.050. Hence, they are significant variables. The results of the regression analysis listed in Table 5.30 indicate that the standard error of the resulting model is 0.089. The value of coefficient of determination (R^2) is 0.560 and the adjusted R^2 is 0.537. Table 5.31 provides a list of the regression constants and the values of the R^2 and the standard error obtained from each step of the stepwise method of the SPSS computer program. It can be noted that the traffic factor (ESL) is the most important variable and it alone explains about 20 percent of the variation of the pavement rut (the dependent variable). This percentage increases, with the inclusion of more variable clusters in the model. The final form of the equation expressing pavement rut as a function of the various variable clusters is presented below.

Table 5.30 : Results of regression analysis.

```
Multiple R           .74829
R Square             .55994
Adjusted R Square    .53702
Standard Error       .08879

Analysis of Variance
                     DF      Sum of Squares      Mean Square
Regression            5              .96289           .19258
Residual             96              .75675           .00788

F =      24.43015       Signif F =  .0000

     * * * *   M U L T I P L E   R E G R E S S I O N   * * *

Equation Number 1    Dependent Variable..   P   RUT

----------------- Variables in the Equation -----------------

Variable                 B          SE B        Beta         T  Sig T

ESL                .870205       .172627     .476513     5.041  .0000
G1          8.194847E-05 1.35422E-05     .428528     6.051  .0000
DF               24.974873      4.817170    2.052168     5.185  .0000
Q1               -2.006910       .453242   -1.796698    -4.428  .0000
SF                 .002031  7.08989E-04     .243000     2.865  .0051
(Constant)         .100403       .030668                 3.274  .0015
```

Table 5.31 : Regression matrix for rutting.

Intercept						R.Sq.	S.E.
	ESL	G1	DF	Q1	SF		
.16526	.8190					.201	.117
.07741	.9479	7.6715E-05				.357	.105
.01373	1.2563	7.7938E-05	4.3276			.455	.097
.08936	1.1357	7.3396E-05	21.9264	-1.6747		.522	.092
.10040	.8702	8.1948E-05	24.9748	-2.0069	.0020	.560	.089

$$RUT = 0.1004 + 0.8702\ (ESL) + 8.1948E\text{-}05\ (G1) + 24.9749\ (DF) - 2.0069\ (D1_{AC})\ 0.0020\ (SF) \quad (5.7)$$

$R^2 = 0.56$, $SE = 0.088$, $F = 24.43$, $F_{(sig)} = 0.000$

where all variable are previously defined.

Based on the various statistics of the model and the statistics of the residuals presented in Tables 5.32 and 5.33, the following observations are made.

1. The null hypothesis of no linear relationship between the independent variables and RUT was rejected and it was concluded that at a probability of $F_{(sig)}$ zero, 56 percent of the variation of the dependent variable is explained by the variable clusters included in equation 5.7.
2. The largest value of "T" significance is .005. This implies that all the variables in the model are significant.

Figure 5.28 displays a plot of the rut depth calculated by using equation 5.7 and the measured rut depth values. As it can be seen, most of the calculated rut values are located close to the 45 degree line (line of equality between calculated and measured values). The percent error between the measured and the calculated values are depicted in Figure 5.29. Examination of the Figure indicates that about 75 percent of the predicted rut values are within 60 percent of the observed values.

Equation 5.7 was also extended to calculate the rut values at other pavement locations where the pavement deflection data are available but the exact pavement cross-sections are not available. Figure 5.30 shows the calculated and the measured rut depths of 563 pavement core locations. As it can be seen, given the lack of accurate information regarding the pavement cross-section data, the statistical model (equation 5.7) seems to be reasonable. Several observations regarding both statistical analyses presented above are discussed in the next

Table 5.32 : Residual statistics of equation 5.7.

	Min	Max	Mean	Std Dev	N
*PRED	.0487	.5027	.2076	.0976	104
*RESID	-.2035	.2020	.0000	.0866	104
*ZPRED	-1.6277	3.0222	.0000	1.0000	104
*ZRESID	-2.2922	2.2748	.0000	.9749	104
Durbin-Watson Test = 2.40685					

Table 5.33 : Ten worst residuals.

Case #	*RESID	*ZRESID
99	-.2035	-2.29224
7	.2020	2.27483
54	-.1864	-2.09907
98	.1835	2.06709
47	-.1736	-1.95490
53	-.1706	-1.92135
94	.1605	1.80828
97	-.1584	-1.78461
81	.1575	1.77415
3	.1528	1.72052

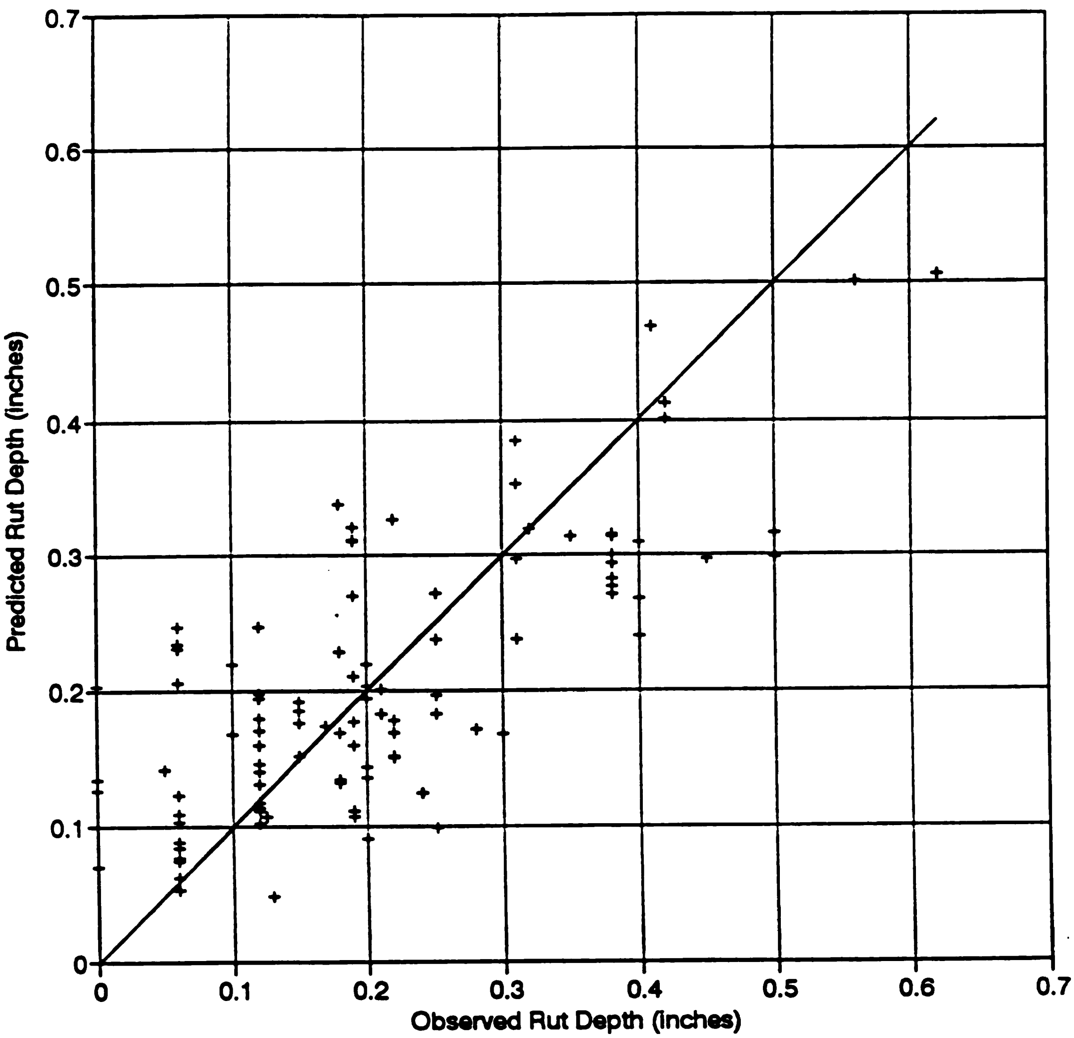

Figure 5.28 : Observed versus predicted rut depths.

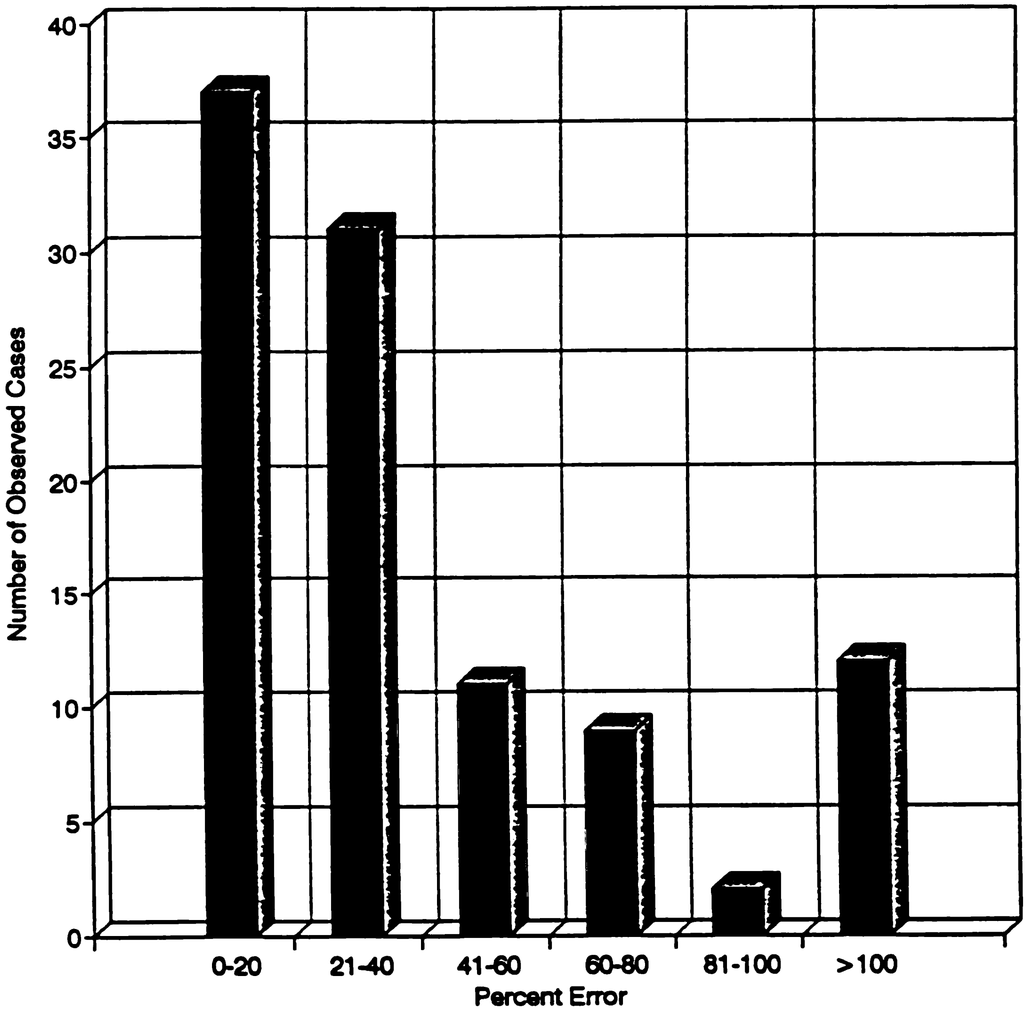

Figure 5.29 : **Percent error between the observed and the predicted rut depth values.**

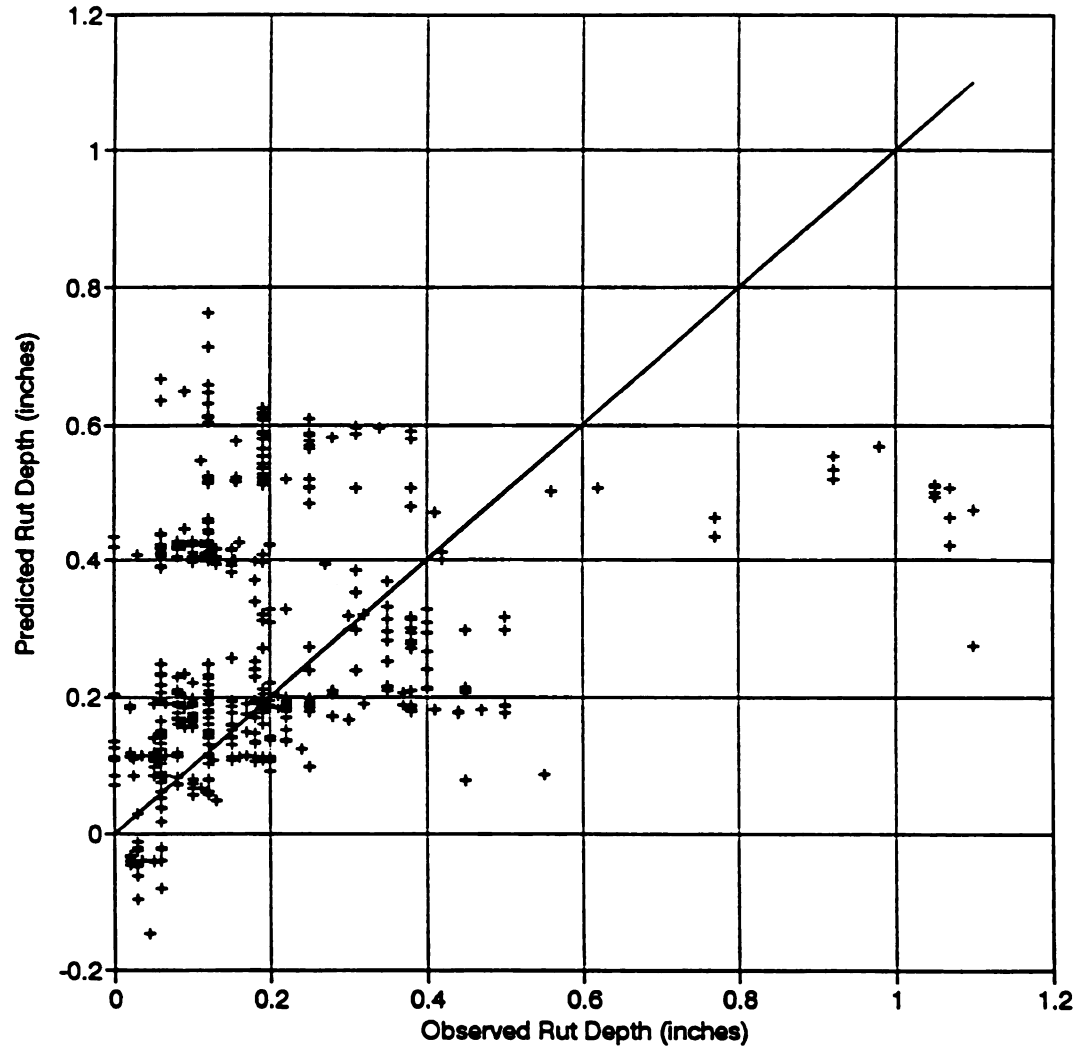

Figure 5.30 : **Observed versus predicted rut depths for the 563 pavement locations.**

section.

5.5.3.4 Observations and Discussion

The above presented statistical analyses present an attempt to model pavement rut using nondestructive deflection testing data. Most available rut prediction models are based on pavement layer properties and hence, destructive tests need to be conducted to assess such properties. Several attempts to predict pavement rut depths using NDT data were also made in the past. The results can be considered as poor at best. The issues in predicting rut depths by using NDT data can be divided into two categories, statistical and physical.

The statistical issues are mainly related to the nature of the measured deflection data. Since the pavement deflection measured at any lateral distance from the applied load is a function of the pavement layer properties and geometry, the magnitude of the applied load, the stress history (the number of 18-kip ESAL traveled the pavement section), the environmental factors (moisture, temperature, and time), and the state of the pavement distress, the various deflection values are not truly independent. Further, various aspects of the deflection basin are related to the material properties. For example, the slope of the deflection basin between any pair of adjacent deflection sensor is mainly related to the moduli ratio and thicknesses of the pavement layers. Hence, the elimination of the slopes of the deflection basin from the string of variables to be included in the statistical analysis is a problem related to the elimination of valuable information. Likewise, the area of the deflection basin defined by any two adjacent deflection sensor is a function of the amount of energy delivered to one or more of the pavement layers due to the application of the load. The above scenario implies that the elimination of one or more slopes, one or more areas, and/or one or more deflection values will induce bias in the resulting model.

The physical issues are related to the available information regarding the pavement geometry (layer thicknesses). During this study, it was noticed that the actual layer thickness mat vary by as much as 60 percent from the as-designed values (A typical SHA record contains only the as-designed layer thicknesses). Since, layer thicknesses have a major impact on pavement rut and deflection, extending a statistical model to locations where such information are not accurately available is problematic in nature. Indeed, even rut prediction models developed on the basis of material properties cannot successfully be used to predict pavement rut if accurate information regarding the material properties and layer thicknesses at the desirable points are not available.

The above issues indicate that the development of statistical models relating a dependent variable to various independent but collinear variables is, from the statistical view point, problematic. In addition, if a variable includes more than one set of independent information that cannot be obtained by any means other than using the variable in two or more terms in the statistical model, then such use should not be considered invalid. For example, if a real mechanistic model expresses the value of "Y" in terms of the values of "x" as "$Y = X + X^{1.25} + X^{2.25} + X^{4}$", and if the values of "Y" and "X" are known, then the most correct model to predict "Y" from "X" must have the term "X" as three independent but collinear terms in the model.

Similarly, the method of variable clusters is very powerful in some statistical analysis. To illustrate, consider a traffic congestion model for road number 101, the number of vehicles to be used in the model is the cluster of several independent but collinear variables that include the number of passenger cars, trucks, and other vehicles traveling the pavement during the peak hours.

The reason that the various terms are collinear is that the number of each vehicle class is a function of the same variables (road geometry, location, origination and destination points, the number of traffic lights, availability of other routes, and so forth). Now, for the same road 101, a rut or fatigue prediction model would have the traffic data clustered in a different fashion. For these models, it is the load placed and distributed by each vehicle axle is important. Hence, the traffic data is assigned different weights (load equivalency factor) prior to clustering the data. Another important point regarding the accuracy of the statistical analyses relative to the various errors of the measured data is presented in the next section.

5.6 ERRORS

Several errors are typically associated with the measurements of any field and laboratory types of data. These include systematic and random errors. Systematic errors are defined as the error due to the inaccuracy of the measuring system whereas random errors are variations due to the working of a number of uncontrolled variables, each of which affects the outcome in a small quantity (92). The following systematic and random errors can be identified in this study.

1. The rut data was obtained by using a straight edge and two MDOT's prefabricated graduated gauges with accuracies of 0.0625 and 0.025 of an inch. The rut depth measurement method consists of setting the straight edge on the pavement across the rut channel and inserting the graduated rut gauge in the gap between the pavement and the straight edge. The gauge was then moved in a lateral direction until the maximum number of graduates are inserted. The total rut depth was then recorded as the total number of graduate times the graduate thickness (0.0625 or 0.025-inch depending on the type of graduate being used). This implies that the systematic error in the measured rut depths could be as high

as the thickness of one graduate. Although, the magnitude of this systematic error is random in nature and is the same for all measurements, the percent error is very high for the lower rut depths. For example, a measured rut depth of "0.0625-inch" could in reality be any where from 0,0625 to 0.12-inch (about 100 percent error). On the other hand, a measured rut depth of 1-inch could be any where from 1 to 1.0624-inch (a 6.24 percent error). Hence, the percent error has more bias toward the lower rut measurements than toward the higher ones.

2. The random error associated with the rut measurements is related to the pavement texture and to the presence or absence of loose particles on the pavement surface. Higher textured (rough as in open-graded asphalt mix) pavement surface would yield higher error because the rut gauge could be setting on either the higher or the lower ends of the aggregates. The presence of small soil particles on the pavement surface also produce a random errors in the rut measurements. Both of these random errors are very significant for shallow rut depth and are insignificant for higher rut values.

3. Systematic error associated with the deflection measurements. The deflection resolution of the MDOT Kuab 2-M FWd model is 0.04 mils and the relative accuracy of the deflection measurements is 0.08 mils $\pm$ 2 percent (93). Which implies that the outer deflection sensors can be off by as much as 100 percent. One point should be noted here is that this is the accuracy of the entire KUAB system whereas more accurate gauges are used for the outer sensors to minimize this error. In addition, the pavement surface texture and the presence of fine particles on the pavement surface cause random errors in the measured deflections.

4. A systematic error in the laboratory measurements of the thicknesses of the AC layers for the cored pavement sections. The AC layer thicknesses were measured by using a hand held scale with an accuracy of 0.0625-inch. The systematic error

is related to this measurement error as well as to the degree of the intrusion of the base material into the AC layer. Both errors can be considered as random. The error of the AC thicknesses of the non-cored pavement sections is related to construction practices and the enforced quality control policy at the time of construction. For any one pavement section constructed at the same time, this error is random in nature. However, the magnitude and the percent of the error varies from one section to another.

5. As noted earlier, pavement deflections represent the pavement system response to load. Further, pavement deflection data and the various deflection basin parameters provides a quantitative basis for the evaluation of the pavement structural condition at any time during its service life. One of the objectives of the above presented statistical analyses is to explore the potential of using the NDT and other data to predict the pavement rutting. For these reasons, all possible deflection basin parameter (deflections, slopes, and areas) were included in the development of the regression models. Although the legitimacy of the high number of variables included in the predictive equations can be argued, there are no formal rules regarding the minimum or maximum number of variables to be included in an equation. However, it is known that various problems associated with use of large number of collinear variables exist. The most important one of these problems is that each variable in the final regression model has some input error associated with it that causes an error in the estimates. The total error in the estimates (due to various variables) can be additive in nature as it is expressed in the following formula (94):

If $Z = f(x_1, \ldots. x_n)$,

$$e_z^2 = \sum_i f_{xi}^2 e_{xi}^2 + \sum_i \sum_j f_{xi} f_{xj} e_{xi} e_{xj} r_{ij} \tag{5.8}$$

where e_z = the error of z;

f_{xi} = the partial derivative of f with respect to x_i;

e_{xi} = the measurement error in the x_i; and

r_{ij} = the correlation between x_i and x_j.

The second term on the right-hand side of equation 5.8 indicates that the error in the estimates can increase very rapidly when collinear variables are used to calculate the estimates. Moreover, as the number of independent variables increases so does the error of the estimates.

Given the above scenario, the two regression equations relating pavement rut to the deflection basin are exploratory in nature. The equations should not be used and/or extended to predict rut depth of any pavement section without further study and verification.

5.7 VERIFICATION OF THE SHIFT FACTORS OF THE FATIGUE LIFE

The sensitivity of the shifts factors of the fatigue life (presented in section 5.4.5) to the variations in the values of the variables of the fatigue model (equation 5.4) was analyzed and is presented in this section. The purpose of the analysis is to determine whether the values of the shifts factors are random in nature or they are pavement site specific. The analysis was accomplished in three steps as follows:

1. For each pavement section, the average, maximum, and minimum values of the measured material properties (angularity, percent AC and fine contents, and specific gravity) were obtained. These values are listed in Table 5.34 such that, for each pavement section, the first two lines in the table include the maximum and minimum aggregate angularity and the average values of the other three material properties (percent AC and fine contents and specific gravity). The second set of two lines include the maximum and minimum of the percent AC content and the average values of the other three properties. The third and fourth sets of two lines include the maximum and minimum percent fine contents and

Table 5.34 : The maximum, minimum, and the average values of the shift factors for the indicated pavement section.

Section Number	Angularity	Percent AC	Percent Fine	Sp.Gty.	Service Life (years)	ESAL	Fatigue Life	Fatigue Life,SL=0	Shift Factor
7F	1.97	4.4	4.0	2.326	7	1.25	4610	6194	
	2.61	4.4	4.0	2.326	7	1.25	5414	7274	
	2.3	4.10	4.0	2.326	7	1.25	5817	7816	
	2.3	4.70	4.0	2.326	7	1.25	4176	5611	
	2.3	4.4	3.10	2.326	7	1.25	7248	9737	
	2.3	4.4	4.98	2.326	7	1.25	3587	4819	
	2.3	4.4	4.0	2.193	7	1.25	1741	2339	2091
	2.3	4.4	4.0	2.441	7	1.25	12735	17109	286
Avg.	2.3	4.4	4.0	2.326	7	1.25	4962	6667	733
29F	1.48	4.8	4.4	2.318	11	0.76	2390	3801	539
	4.33	4.8	4.4	2.318	11	0.76	8230	13089	156
	2.9	4.60	4.4	2.318	11	0.76	3677	5848	
	2.9	5.08	4.4	2.318	11	0.76	2890	4596	
	2.9	4.8	4.26	2.318	11	0.76	3491	5552	
	2.9	4.8	4.63	2.318	11	0.76	3085	4907	
	2.9	4.8	4.4	2.277	11	0.76	2420	3849	
	2.9	4.8	4.4	2.362	11	0.76	4791	7620	
Avg.	2.9	4.8	4.4	2.318	11	0.76	3354	5334	384
19F	3.04	5.5	6.6	2.365	11	1.58	1886	2999	
	3.29	5.5	6.6	2.365	11	1.58	2125	3379	
	3.2	5.41	6.6	2.365	11	1.58	2132	3390	
	3.2	5.71	6.6	2.365	11	1.58	1870	2974	
	3.2	5.5	6.53	2.365	11	1.58	2030	3229	
	3.2	5.5	6.57	2.365	11	1.58	2012	3200	
	3.2	5.5	6.6	2.322	11	1.58	1547	2461	1730
	3.2	5.5	6.6	2.419	11	1.58	3431	5456	780
Avg.	3.2	5.5	6.6	2.365	11	1.58	2035	3236	1315
43F	2.79	6.3	7.1	2.372	1	0.76	1933	2016	
	4.16	6.3	7.1	2.372	1	0.76	4291	4476	4111
	3.0	5.10	7.1	2.372	1	0.76	3522	3673	
	3.0	6.54	7.1	2.372	1	0.76	1926	2009	
	3.0	6.3	6.81	2.372	1	0.76	2206	2303	
	3.0	6.3	8.30	2.372	1	0.76	1646	1717	
	3.0	6.3	7.1	2.337	1	0.76	1573	1641	11214
	3.0	6.3	7.1	2.402	1	0.76	2682	2797	
Avg.	3	6.3	7.1	2.372	1	0.76	2100	2191	8399

Table 5.34 : The maximum, minimum, and the average values of the shift factors for the indicated pavement section (continued).

Section Number	Angularity	Percent		Sp.Gty.	Service Life (years)	ESAL	Fatigue Life	Fatigue Life,SL=0	Shift Factor
		AC	Fine						
35F	4.79	5.9	5.7	2.303	14	1.37	4122	7441	
	4.82	5.9	5.7	2.303	14	1.37	4260	7690	
	4.8	5.88	5.7	2.303	14	1.37	4272	7710	
	4.8	6.06	5.7	2.303	14	1.37	3970	7166	
	4.8	5.9	5.67	2.303	14	1.37	4211	7601	
	4.8	5.9	5.97	2.303	14	1.37	3901	7041	
	4.8	5.9	5.7	2.256	14	1.37	2876	5191	592
	4.8	5.9	5.7	2.361	14	1.37	6658	12017	256
Avg.	4.8	5.9	5.7	2.303	14	1.37	4246	7667	401
10F	3.59	7.2	6.6	2.387	7	0.22	1996	2682	
	3.63	7.2	6.6	2.387	7	0.22	2047	2750	
	3.6	7.19	6.6	2.387	7	0.22	2056	2762	
	3.6	7.29	6.6	2.387	7	0.22	1988	2671	
	3.6	7.2	6.44	2.387	7	0.22	2092	2810	
	3.6	7.2	6.72	2.387	7	0.22	1964	2638	
	3.6	7.2	6.6	2.373	7	0.22	1801	2420	356
	3.6	7.2	6.6	2.396	7	0.22	2178	2926	294
Avg.	3.6	7.2	6.6	2.387	7	0.22	2031	2729	315
14F	3.12	5.9	7.3	2.374	13	0.18	1556	2693	
	3.15	5.9	7.3	2.374	13	0.18	1578	2731	
	3.1	5.80	7.3	2.374	13	0.18	1617	2798	152
	3.1	5.94	7.3	2.374	13	0.18	1526	2641	161
	3.1	5.9	7.15	2.374	13	0.18	1610	2786	
	3.1	5.9	7.40	2.374	13	0.18	1530	2647	
	3.1	5.9	7.3	2.372	13	0.18	1545	2674	
	3.1	5.9	7.3	2.375	13	0.18	1584	2740	
Avg.	3.14	5.9	7.3	2.374	13	0.18	1542	2668	160
13F	4.78	5.7	6.9	2.406	30	1.51	4006	14199	
	4.86	5.7	6.9	2.406	30	1.51	4376	15512	
	4.8	5.63	6.9	2.406	30	1.51	4306	15261	
	4.8	5.74	6.9	2.405	30	1.51	4108	14561	
	4.8	5.7	6.50	2.405	30	1.51	4654	16497	
	4.8	5.7	8.14	2.405	30	1.51	3333	11814	
	4.8	5.7	6.9	2.450	30	1.51	6178	21899	96
	4.8	5.7	6.9	2.348	30	1.51	2647	9384	224
Avg.	4.8	5.7	6.9	2.406	30	1.51	4042	14326	147

the maximum and minimum specific gravities, respectively. Finally, the data in the last line includes the average material properties.

2. For each data line of Table 5.34, the fatigue model (equation 5.4) was then used to predict two values of the fatigue life; one using the actual pavement service life and the other for a zero service life.

3. The shift factor for each data line of each pavement section was then calculated by dividing the cumulative 18-kip ESAL by the difference in the two values of the fatigue life (the one calculated for the actual pavement service life and the one for zero service life). For each pavement section, the last column of Table 5.34 provides a list of the maximum, minimum, and the average values of the shift factor. It should be noted that, for the eight pavement section, the average value of the shift factor corresponds to the average material properties.

Figure 5.31 depicts the maximum, minimum, and average values of the shift factors of the eight pavement sections. Examination of figure 5.31 and the maximum, minimum, and the average values of the shift factors listed in table 5.34 indicates that:

1. For five pavement sections (7F, 19F, 35F, 10F, and 13F), the maximum and minimum values of the shift factor correspond to variations in the values of the specific gravity of the asphalt mix of those sections. Higher values of the specific gravity of the AC mix cause lower shift factors (low ratio of the field to the laboratory fatigue lives).

2. For pavement section 29F, the maximum and minimum values of the shift factor correspond to variations in the values of the aggregate angularity. Higher values of aggregate angularity cause lower shift factors.

'3. For pavement section 14F, the maximum and minimum values of the shift factor correspond to variations in the values of the asphalt content of the AC mix. Higher values of asphalt contents cause lower shift factors.

4. For pavement section 43F, the maximum and minimum values of the shift factor

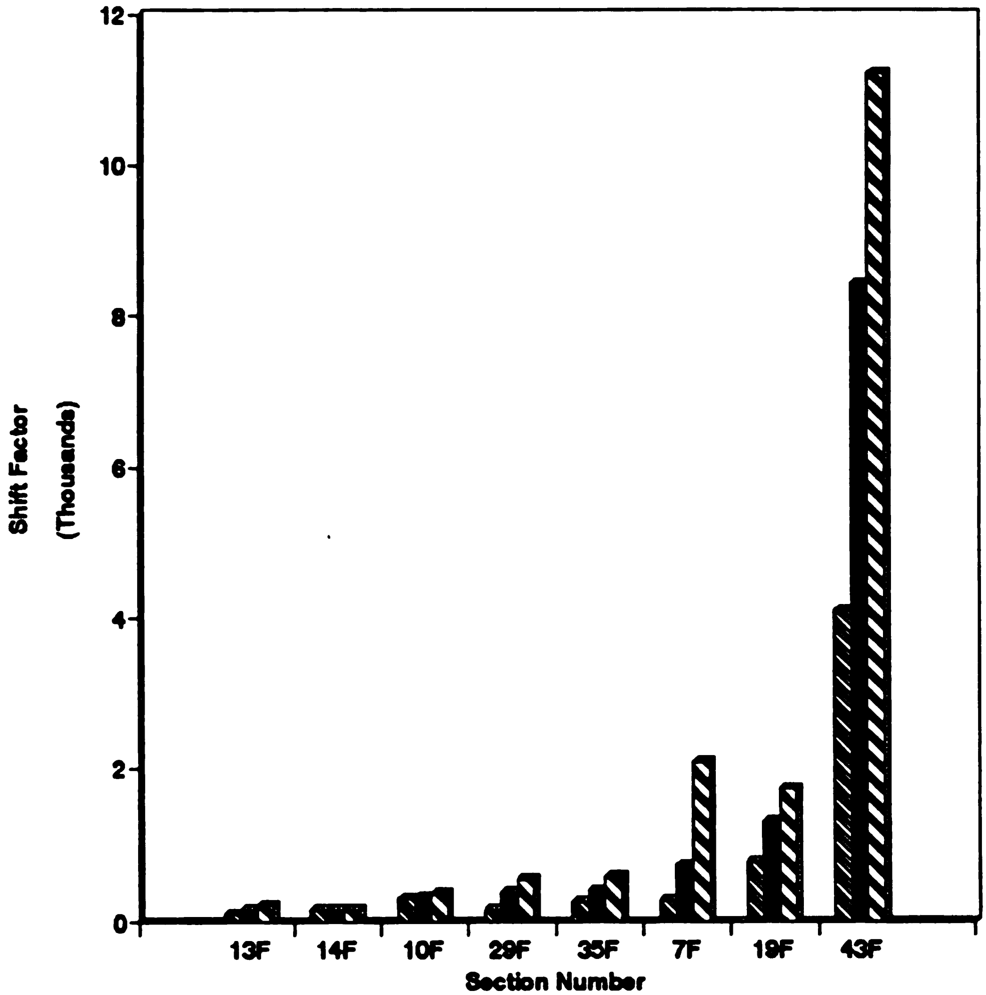

Figure 5.31 : The maximum, minimum, and average values of the shift factors of the fatigue life versus the indicated pavement section number.

correspond to the lowest values of the specific gravity of the AC mix and to the highest aggregate angularity, respectively.

The above observations indicate that the variation and the values of the shift factors are a function of the variations of the various properties of the AC mix. Since the design of the AC mix is site specific (different mix is typically used for different pavements), and since the construction and quality control practices differ from one job to another, one can conclude that the values of the shift factor relating the field and laboratory fatigue lives are also pavement site specific.

One important point should be noted is that the fatigue model (equation 5.4) predicts the number of load repetition to crack initiation. In the field, alligator cracks may exist (at the bottom-side of the AC layer) in a pavement section for a long time before they can be observed on the surface of the pavement. The time lapse between crack initiation and crack observation on the pavement surface is a function of the pavement layer thicknesses, the traffic volume and load, and the environmental conditions. Given the above scenario, analysis of the relative accuracy of the shift factor was conducted. First, the two pavement sections (13F and 7F) with existing fatigue cracks were chosen and from each section, a pavement core was obtained from the pavement area between the wheelpaths. Each core was then tested in the laboratory, and the fatigue lives of the cores were determined and are listed in Table 5.35 along with the corresponding average values of the shift factor. For each pavement section, the predicted field fatigue life was then calculated by multiplying the laboratory fatigue life by the corresponding shift factor. The results are listed in Table 5.35 along with the cumulative 18-kip ESAL experienced by the two pavement sections. Examination of the values of the predicted field fatigue life and the cumulative 18-kip ESAL indicates that, for both pavement section, the predicted fatigue life is shorter that the observed 18-kip ESAL. For example, for pavement section 13F, the predicted fatigue life is 840,000 18-kip ESAL and the observed cumulative 18-kip ESAL is 1,510,000. The reason that the

Table 5.35 : Predicted and observed fatigue lives of two pavement sections with fatigue cracks.

Section No.	Designation No.	Laboratory Fatigue Life	Shift Factor	Predicted field Fatigue Life (ESAL)	Observed ESAL 1991	Severity of the observed Fatigue cracking (percent of the section)
13F	13142922-1	6000	140	0.84	1.51	Low severity (100%)
7F	7137022-1	1400	739	1.035	1.25	Low severity (50%)

observed number of ESAL is about twice as much as the predicted one is that the 1,510,000 ESAL is the cumulative ESAL from construction to the time where low severity alligator cracks were observed along the entire pavement section. Hence the number of ESAL to crack initiation is much smaller than the 1,510,000. Likewise, the ratio between the observed (1,250,000) and the predicted (1,035,000) ESAL is about 1.2. The section has low severity alligator cracks along 50 percent of its length. This implies that the number of ESAL to crack initiation is lower than the observed one. In addition, the data from the two pavement sections indicate that the ratio of the observed to the predicted ESAL increases as the extent of the alligator cracking increases. This is reasonable and consistent with the mechanism of the crack propagation.

CHAPTER 6

SUMMARY, ACCOMPLISHMENTS, CONCLUSIONS AND RECOMMENDATIONS

6.1 SUMMARY

The effects of the asphalt mix variables on the laboratory fatigue life and field rutting were investigated in this study. Full depth AC cores were obtained from selected pavement sections. The properties of the AC mixes were determined as described in chapter 4. Indirect cyclic load tensile tests were conducted to determine the resilient and plastic deformations and the fatigue lives of the core samples.

Prediction models of the laboratory fatigue life and field rutting were developed. The laboratory fatigue life model is based on the AC mix properties and the pavement service life. The field rutting model is based on the AC mix properties and the cumulative 18-kip ESAL. Sensitivity analysis of the models were conducted to determine the influence of each variable on pavement rutting and fatigue life. It is shown that the aggregate angularity is the most significant variable affecting the fatigue life and that the percent fine and sand contents in the AC mix are the most significant variables affecting pavement rutting. Shift factors relating the laboratory and field fatigue lives were developed and their variabilities were assessed. An exploratory statistical rut model based on nondestructive deflection testing was also developed. It is shown that the NDT data can be used to predict the pavement rut potential.

6.2 ACCOMPLISHMENTS

The following accomplishments have been made in this study.

1. The factors affecting the rut and fatigue cracking potential of the AC mixes presently being used in the State of Michigan were identified.

2. A test procedure to characterize aggregate angularity in terms of the number of crushed faces, was developed.
3. The effect of coarse aggregate angularity (in terms of the weighted average number of crushed faces) on rut and fatigue cracking potential of the AC mixes were determined.
4. A field rut prediction model based on the 18-kip ESAL and the AC mix properties was developed.
5. A laboratory fatigue life prediction model based on the AC mix properties and the pavement service life was developed.
6. Sift factors relating the laboratory and field fatigue lives were developed and verified.
7. An exploratory model relating pavement rut and NDT data was developed.
8. Several problems related to the asphalt mix design procedure and construction practices were identified.

6.3 CONCLUSIONS

Based on the field and test data and on the analysis, the following conclusions were drawn.

1. Coarse aggregate angularity is the most influential factor affecting the fatigue life. Angular aggregate provides a better rut and fatigue cracking resistance.
2. The most beneficial aggregate angularity is that of aggregates crushed on all sides (no flat particles).
3. Rut and fatigue cracking resistance of the AC mixes can be maximized by specifying a maximum of 3 to 6 percent air voids.
4. The percent fine and sand contents in the AC mix are the most significant factors affecting rut. A fine content of less than 5 percent and a sand content of less than

20 percent provide a better rut and fatigue cracking resistance.

5. For an AC pavement, the laboratory fatigue life of core samples tested in the indirect cyclic load tensile test mode is related to the pavement fatigue life through a shift factor.
6. Significant variation in the thicknesses of the various AC courses were observed within one pavement section.
7. Significant variation in the AC mix properties were observed for the same AC courses within one pavement section.
8. NDT data can be used to assess the strength of the pavement structure. A preliminary model suggests that the data can be used to estimate the pavement rut potential.
9. The model interaction between the various variables affecting pavement performance can be minimized by using Proper normalization techniques.

6.4 RECOMMENDATIONS

Based on the findings and conclusions of this study the following recommendations are made.

1. For high traffic, when economically feasible, a high percentage of coarse angular aggregates (crushed on all sides) should be used to maximize rut and fatigue resistance of the AC mix.
2. To improve rut and fatigue resistance of the AC mix, air voids between 3 to 6 percent should be specified.
3. Quality assurance /Quality control (QA/QC) practices regarding pavement construction and AC mix manufacturing operations should be modified and/or enforced.
4. The rut and fatigue cracking models presented in this thesis should be extended

to include the effects of the base, subbase layers and the roadbed soil properties on rut and fatigue potentials.

5. The results of this investigation have indicated that the as-constructed NDT data should be collected and used:

    a) To asses the uniformity or variability of the pavement along any given project.

    b) As a tool of quality control.

    c) As a tool to determine the structural capacity of the pavement.

    d) As a predictor of pavement rutting.

    e) As a part of the pavement management database.

    f) To backcalculate the as-constructed material properties.

List of References

1. Yoder E. J. and M. W. Witczak, "Principles of pavement design". A Wiley-Interscience Publication, John Wiley and Sons, Inc., 1975.

2. Santucci L. E., and R. J. Schmidt, "The effect of asphalt properties on the fatigue resistance of asphalt paving mixtures,". Asphalt Paving Technology (APT) Vol. 38, 1969.

3. Baladi G. Y., "Integrated material and structural design method for flexible pavements," Vol. 1: Technical Report, FHWA, 1988.

4. Report 5, Highway Research Board Special Report 61E, "The AASHO Road Test," 1962.

5. Morris J., "The predication of permanent deformation in asphalt concrete pavement," Department of Civil Engineering, University of Waterloo, Waterloo Ontario Canada, 1973.

6. Morris J., Ralph C. G. Hass, Park Reilly, and Edward T. Hignell, "Permanent deformation in asphalt pavement can be predicted," APT Vol. 43, 1974.

7. Hughes C. S. and G. W. Maupin, Jr., "Experimental bituminous mixes to minimize pavement rutting," APT Vol. 56, 1987.

8. Bonquist, R., R.,"Effects of tire pressure on flexible pavement response and performance," Draft Report, Federal Highway Administration, Washington, D.C., 1989.

9. Harry A. Smith, "Truck tire characteristics and asphalt concrete pavement rutting," Paper No. 910035, Transportation Research Board (TRB) 70th Annual Meeting, 1991.

10. Hsien H. Chen, Kurt M. Marshek, and Chhotel L, Saraf, "Effect of truck tire contact pressure distribution on the design of flexible pavement: A three dimensional finite element approach," Transportation Research Record (TRR), ,Transportation Research Board (TRB), 1095, 1986.

11. Richard. D. Barksdale, "Practical application of fatigue and rutting tests on bituminous based mixes," APT Vol. 47, 1978.

12. Robert N. Linden, Joe P. Mahoney, and Newton C. Jackson, "Effect of compaction on asphalt concrete performance," TRR. 1217, 1989.

13. Finn F. N. and J. A. Epps, "Compaction of hot mix asphalt concrete," Research report 214-21, Texas Transportation Institute, Texas A and M University, College Station, 1980.

14. "Fatigue of asphalt concrete mixtures-Summary of existing information," Special technical publication 508. ASTM, Philadelphia, Pa, 1971.

15. Puangchit P., R. G. Hicks, J. E. Wilson, and C. A. Bell, "Impact of variation in material properties on asphalt pavements life," Report FHWA-OR-82-3. Oregon Department of Transportation, 1982.

16. Miller C. Ford, Jr., "Pavement densification related to asphalt mix characteristics," TRR. 1178, 1988.

17. Jon A. Epps, and Carl L. Monismith, "Influence of mixture variables on the flexural fatigue properties of asphalt concrete," APT Vol. 38, 1969 .

18. Brown E. R., "Mix design and construction of asphalt concrete to support high tire pressure," Presented at AASHTO/FHWA Symposium on high pressure truck tires, Austin, Texas, 1987.

19. Huber G. A. and G. H. Heiman, "Effect of asphalt concrete parameter on rutting performance. A field investigation," APT Vol. 56, 1987.

20. Hani A. Lotfi, Charles W. Schwartz, and Matthew W. Witczak, "Compaction specification for the control of pavement subgrade rutting," TRR. 1196, 1988.

21. "Essential physical properties of sand, gravel, slag and broken stone for use in bituminous pavements," Better roads and streets. Vol 6, No 3.

22. "Mix design methods for asphalt concrete," Asphalt Institute Manual Series NO. 2(MS-2).

23. Hicks, R. G., and David C. Esch, " State of the art on rutting in asphalt concrete," Alaska DOT and PF Fairbanks, AK 99701, 1990.

24. Brown E. R., and Charles E. Bassett, "Effects of maximum aggregate size on rutting potential and other properties of asphalt aggregates mixtures," TRR. 1259, 1990.

25. Kamyar Mahboub, and David L. Allen, "Characterization of rutting potential of large-stone asphalt mixes in Kentucky," TRR. 1259, 1990.

26. Moreland Herrin, and W. H. Goetz, "Effect of Aggregate Shape on Stability of Bituminous Mixes," Joint highway Research Project, Purdue University. HRB. Proceedings 33th Anual Meeting 1954.

27. Mohammed Osman Khalifa, and Moreland Herrin, "The behavior of asphaltic concrete constructed with large-sized Aggregates," APT Vol. 39, 1970.

28. Joe W. Button, Dario Perdomo, and Robert L. Lytton, "Influence of aggregate on rutting in asphalt concrete pavements," TRR. 1259, 1990.

29. Mendenhall W. S., Jr., Chairman, " Ad hoc task force on asphalt pavement rutting and stripping," August 14, 1987.

30. Young M. A. and G. Y. Baladi, "Repeated load triaxial testing, state of the art," Michigan State University. Department of Civil Engineering, 1977.

31. Neil C. Kruts, Raj Siddharthan and Mary Stroup-Gradiner, "Investigation of rutting potential using static creep testing on polymer modified AC mixture," Paper # 910705, 70th meeting TRB, 1991.

32. Brown E. R., and Stephen A. Cross, "A study of in-place rutting of asphalt pavements," APT Vol. 58, 1989.

33. Hensley M. J., and Rita B. Leahy, "Asphalt concrete mixtures as related to pavement rutting: Case study," TRR. 1217, 1989.

34. Dale S. Decker and Joseph L. Goodrich, "Asphalt cement properties related to pavement performance," APT Vol. 58, 1989.

35. Kim Y. R., N. P. Khosla, and N. Kim, "Effect of temperature and mixture variables on fatigue life predicted by diametral fatigue testing," TRR 1317, 1991.

36. Vallerga B. A., F. N. Finn and R. G. Hicks, " Effect of asphalt aging on the fatigue properties of asphalt concrete," Proc. Second Int. Conf. on the Structural Design of Asphalt Pavements, 1967.

37. William D. O. Paterson, "Models for planning and management," Road deterioration and maintenance effects. A World Bank Publication, 1990.

38. Harold Von Quintus, and Thomas W. Kennedy, "AAMAS mixture properties related to pavement performance," APT Vol. 58, 1989.

39. James A. Scherocman, and Mike Acott, " Hot mix asphalt production, placement, and compaction related to pavement performance," APT Vol. 58, 1989.

40. Barksdale R. D., "Compressive Stress Pulse Time in Flexible Pavements for use in Dynamic Testing, " Highway Research Board (HRB). Highway Research Record (HRR), No. 345, 1971.

41. Barksdale R. D., "Laboratory Evaluation of Rutting in Base course Materials," Pro. Third Int. Conf. on the Structural Design of Asphalt Pavements, London 1972.

42. Heukelom W., and A. J. G. Klomp, "Consideration of Calculated Strain at Various Depths in Connection with the Stability of Asphalt Pavements," Pro. Second Int. Conf. on the Structural Design of Asphalt Pavements, Ann Arbor 1967.

43. Romain J. E., "Rut Depth Prediction in Asphalt Pavement," Pro. Third Int. Conf. on the Structural Design of Asphalt Pavements, London 1972.

44. Barksdale R. D., and Gerald A. Lenards, "Predicting performance of bituminous surfaced pavements," Pro. 2nd Int. Conf. on the Structural Design of Asphalt Pavements, Ann Arbor 1967.

45. Soussou, J. E., and Moavenzadeh, F., "Statistical characteristics of fatigue damage accumulation in flexible pavements," American Society for Testing and Material. Special Technical Paper No. 561, 1973.

46. Rita B. Leahy, and Matthew W. Witczak, "The influence of test conditions and asphalt concrete mix parameters on permanent deformation coefficients Alpha and MU, " APT Vol. 60, 1991.

47. Baladi G. Y., "Fatigue life and permanent deformation characteristics of asphalt concrete mixes," TRR, TRB, 1227, 1989.

48. "Fatigue and dynamic testing of bituminous mixtures," American Society for Testing and Material (ASTM). STP 561, 1973.

49. Pell, P. S., and Cooper, K. E., "The effect of testing and mix variables on the fatigue performance of bituminous materials," APT Vol. 44, 1975.

50. Prithvi S. Kandhal, "Design of large-stone asphalt mixes to minimize rutting," TRR. 1259, 1990.

51. "Technical information," Michigan U.S.A, demonstration August 6 and 7, 1991. Michigan Department of Transportation.

52. Robert A. Romine, Maghsoud Tahmaressi, R. David Rowlett, and D. Fred Martinez, " Survey of state highway authorities and asphalt modifier manufacturers on the performance of asphalt modifiers," Paper No 910242. TRB. Meeting Washington, D.C., 1991.

53. Collins J. H., M. G. Boulddin, R. Gelles, and A.Berker, "Improved performance of paving asphalt by polymer modification," APT Vol. 60, 1991.

54. Carpenter S. H., and Tom Vandam, "Laboratory performance comparisons of polymer-modified and unmodified asphalt concrete mixtures," TRR. 1115, 1987.

55. William A. Higgins, "Chemical modifiers to improve the strength and durability of asphalt concrete," TRR. 1115, 1987.

56. Brown S. F., and M. S. Snaith, "The pavement deformation characteristics of a dense bitumen macadam subjected to repeated loading," APT Vol 43, 1974.

57. Monismith C. L., and A. A. Tayebali, "Permanent deformation (rutting) consideration in asphalt concrete pavement sections," APT Vol. 57, 1988.

58. Wijeratne A. and M. Sargious, "Prediction of rutting in virgin and recycled asphalt mixtures for pavement using triaxial tests," APT Vol. 56, 1987.

59. Dramawardene, M. W. W., "Permanent deformation characteristics of granular base course materials subjected to highway loading," Masters Thesis, University of Waterloo, Canada, 1972.

60. Hass, R., and Meyer, F., "Cyclic creep of bituminous materials under transient, high volume loads," TRR. No 549, 1975.

61. Vallejo, J., Kennedy, T. W., and Hass, R., "Permanent deformation characteristics of asphalt mixtures by repeated load indirect tensile test," Report No CFHR 3-9-72-183-7, Transportation planning division , Texas state department of highway and public transportation, Austin, Texas, 1976.

62. Reynaldo Roque, and William G. Buttlar, "The development of a measurement and analysis system to accurately determine asphalt concrete properties using the indirect tensile mode," Draft submitted to APT for the 1992 annual meeting.

63. Baladi G. Y. and Ronald S. Harichandran, "Asphalt mix design and the indirect test. A new horizon. Asphalt Concrete Mix Design: Development of more rational approaches," ASTM SPT 1041, W. Gartner, Jr., Ed. American society for testing and materials (ASTM), Philadelphia, 1989.

64. Barksdale, R. D., "Compressive stress pulse times in flexible pavements for use

in dynamic testing," HRB. 345, 1971.

65. Allen, J. J., and Thompson, M. R., "Resilient response of granular materials subjected to time-dependent lateral stresses," TRB. 510, 1974.

66. Bonnaure, F. P., Huibers, A. H. J. J., and Uge, P., "A laboratory investigation of the influence of rest periods on the fatigue characteristics of bituminous mixes," APT Vol. 51, 1982.

67. Roque R., and B. E. Ruth, "Material characterization and response of flexible pavements at low temperatures," APT Vol. 56, 1987.

68. Terrel, R. L., Awad, I. S., and Foss, L. R.,"Techniques for characterizing bituminous material using a versatile triaxial testing system," Fatigue and dynamic testing of bituminous mixtures, ASTM STP 561, American society for testing and materials 1974.

69. Monismith, C. L., Secor, K. E., and Blackmer, E. W., "Asphalt mixture behavior in repeated flexure," APT Vol. 30, 1961.

70. Baladi G. Y., Ronald S. H., and Richard W. Lyles, "New relationships between structural properties and asphalt mix parameters," TRR,1171 1988.

71. Baladi G. Y., Richard W. L., and Ronald S. H., "Asphalt mix design: An innovative approach" TRR, 1171, 1988.

72. Lentz R.W., "Permanent deformation of cohesionless subgrade material under cyclic loading," Ph.D. Thesis Michigan State University, 1979.

73. Tresca, H. "Memoire Sur L'ecoulement Des Corps Solides," Mem. Pres. par div. savants 18, 1868.

74. Venant, B. de Saint, "Memoire sur L'establishment des Equations Differentielles des Mouvements Interieurs operes Dans les Corps Solids Ductiles au Dela des Limites au L'elasticite Pourrait les Ramener a Leur Premier Etat," C.R. Acad. Sci. (Paris), 70, 1870.

75. Levy, M., "Memoires sue L'equations Generales des Mouvements interieurs des Corps Solides Ductiles au Dela des Limits ou L'elasticite Pourrait les Ramener a Leur Premier Etat," C.R. Acad. Sci. (Paris), 70, 1870.

76. Prager, W., "An Introduction to Plasticity," Addison-Wesley Publishing Company, Inc., London, England, 1959.

77. ERES Consultants, Inc., "Pavement design principles and practices," Champaign

Illinois, National Highway Institute, Washington, D.C., 1987.

78. Majidzadeh, U. and G. Ilves, " Flexible pavement overlay design procedures, volume I, Evaluation and modification of the design methods," Final report FHWA-RD-82a32. 1981.

79. John O. Rawlings, "Applied regression analysis, a research tool," Wadsworthand Brooks/Cole, Statistics/Probability Series,1988.

80. David A. Belsley, Edwin Kuh, Roy E. Welsch, "Regression diagnostics, identifying influential data and sources of collinearity," Wiley series in probability and mathematical statistics, 1980.

81. Marija J. Norusis/SPSS Inc, "SPSS statistical data analysis ", 1990.

82. Haveem F. N., "Pavement deflections and fatigue failures," Bulletin 114, Highway Research Board, Washington, D. C.

83. Davies, G., T., and Mamlouk, S., M., "Theoretical response of multilayer pavement system to dynamic nondestructive testing," TRR No. 1022. 1985.

84. Kausek, E., and Peek, R., "Dynamic loads in the interior of a layered stratum: An explicit solution," Bulletin of the Seismological Society of America, Vol. 72, No. 5, October, 1982.

85. Molenaar, A. A. A., and Van Gurp, C. A. P. M., "Structural performance model and overlay design for asphalt concrete pavements," TRR No. 888, Highway Research Board, National Research Council, Washington, D. C., 1982.

86. California Division of Highways, "Methods of test to determine overlay requirements by pavement deflection measurements," Test Method California 356, D, dated October 1973.

87. "AASHO," American Association of State Highway Officials, "AASHO interim guide for design of pavement, structures," Washington, D. C., 1972.

88. Kinchen, R. W., and Temple, W. H., "Asphalt concrete overlays of rigid and flexible pavements," Report No. FHWA-LA-109, Federal Highway Administration, Washington, D. C., September 1977.

89. Brown, J. L., and Orellara, H. E., " Utilizing deflection measurements to upgrade pavement structures," Report No. 191-IF, Texas State Department of Highways and Public Transportation, Austin, December, 1970.

90. " Pavement Rehabilitation: Proceedings of a Workshop," Report No. FHWA-RD-

74-60, Transportation Research Board, Federal Highway Administration, Washington, D. C., June 1974.

91. Ronald, S. Harichandran, Tariq Mahmood, A. Robert Raab, and Gilbert Y. Baladi., "Modified Newton Algorithm for Backcalculation of Pavement Layer Properties," TRB, TRR 1384, 1993.

92. Bright, E. Wilson, Jr., "An Introduction to Scientific Research," McGraw-Hill, 1975.

93. Crovetti, J. A., Shahin M. Y., and Touma B. B., "Comparison of Two Falling weight Deflectometer Devices, Dynatest 8000 and Kuab 2-M FWD," ASTM STP 1026, A. J. Bush III, and G. Y. Baladi, Eds., American Society for testing and Materials, 1989.

94. Alonso, William, "Predicting Best With Imperfect Data," Journal of the American Institute of Planners 34, No. 4, 1968.

APPENDIX A

APPENDIX A

The data acquisition and reduction software for indirect cyclic load tensile test (six inch diameter sample) is presented. The software was originally developed by the Michigan Department of Transportation (MDOT) and was modified for the requirements of this study.

```
REM program revised March 6,1992, by Hamid
REM program to calibrate sensors and
REM perform a constant cyclic load test
REM Program is Menu Driven
DIM DIO%(15)
DIM A%(5000)
DIM DATA1%(12000)
COMMON SHARED DIO%(), DATA1%()
DECLARE SUB QBHRES (MD%, BYVAL DUMMY%, FLAG%)
IOADR% = &H300          'I/O QBHRES base address
DIM C(18), V(18), PNT(100), XAXIS(100), DEV(18)
DIM MEMBUF%(18), SKIPC&(19), SKIP&(18), EFV(18), FGV(18), TDEFV(18), TDEFV1(18), DEH(18)
DIM VMIN1(4, 18), VMIN2(4, 18), VMAX(4, 18), EFH(18), FGH(18), TDEFH(18)
DIM VSAMP%(4, 18), PMAX(4, 18), PMIN(4, 18), AVGLOAD(18), dd(18), HH(18)
DIM BCNT%(4, 18), LDPOS%(4, 18), RDELTA%(4, 18), VV(18), VV1(18), AA(18), TDD(18)
DIM HMAX(4, 18), HMIN(4, 18), HDELTA%(4, 18), HHH(18), VVV(18), AAA(18)
DIM HB(4, 18), HC(4, 18), RMAX(4, 18), RMIN(4, 18), DER(18), EFR(18)
DIM RB(4, 18), RC(4, 18), VMIN(4, 18), VDELTA%(4, 18), FGR(18), TDEFR(18)
DIM VB(4, 18), VC(4, 18), PMAXS(18), PMINS(18), VMAXS(18), MR(18), MR1(18), EE(18), EE1(18)
DIM VMINS(18), VDELTS%(18), VBS(18), VCS(18), HBS(18), UU(18), TUU(18), EEH(18)
DIM HMAXS(18), HMINS(18), HDELTS%(18), HCS(18), CCC(18), HFG1(18), HFG2(18)
DIM RMAXS(18), RMINS(18), RDELTS%(18), RBS(18), RCS(18), DIV(18)
DIM HCSW(18), VAB(4, 18), H1AB(4, 18), H2AB(4, 18), R1AB(4, 18), R2AB(4, 18)
DIM VABS(18), H1ABS(18), H2ABS(18), R1ABS(18), R2ABS(18), RFG1(18), RFG2(18)
DIM dz%(200)
DIM SLOPE%(3)
8 MEMBUF%(1) = &H4F00  'Memory Buffer address QBHRES - 128k
MEMBUF%(2) = &H5000
MEMBUF%(3) = &H5F00
MEMBUF%(4) = &H6000
MEMBUF%(5) = &H6F00
MEMBUF%(6) = &HA000
MEMBUF%(7) = &HB000
MEMBUF%(8) = &HC000
MEMBUF%(9) = &HD000
MEMBUF%(10) = &HE000
REM THIS IS A 3rd ORDER LOW PAS BUTTERWORTH CASCADE FILTER
 WC = .05
 C = 1! / TAN(3.1415926# * WC)
 Q = 1! / (1! + C) * 1! / (1! + C + C ^ 2)
 A1 = 2!: AA1 = 1!
 B1 = (2! - 2! * C ^ 2) / (1! + C + C ^ 2)
 B2 = (1! - C + C ^ 2) / (1! + C + C ^ 2)
 BB1 = (1 - C) / (1! + C)
 SCREEN 0, 0, 0: WIDTH 80
50 TYPE TRANSDUCER
     CH AS INTEGER
     UNIT AS STRING * 10
     C AS SINGLE
     DATE1 AS STRING * 10
     MFG AS STRING * 14
     SN AS STRING * 10
     LOCATION AS STRING * 14
 END TYPE
 DIM DUCERITEM AS TRANSDUCER
99 REM CLS
  PRINT : PRINT : PRINT : PRINT : PRINT
100 PRINT "Constant Cyclic Load Program"
110 PRINT
120 PRINT "Select Task"
130 PRINT "1. Calibrate all Transducers"
140 PRINT "2. View Transducer Calibrations"
150 PRINT "3. Change Calibration"
160 PRINT "4. Run Test"
  PRINT "5. View Raw Data"
170 PRINT "6. Process Data on Disk"
180 PRINT "7. Exit Program"
200 PRINT
210 PRINT "Select Task"
215 INPUT T$
  TASK = VAL(T$)
```

```
    IF TASK <= 0 THEN 215
    IF TASK > 8 THEN 215
    ON TASK GOSUB 1000, 2000, 3000, 4000, 4675, 15000, 9000
    GOTO 99
1000 REM SUBROUTINE TO CALIBRATE TRANSDUCERS
1005 GOSUB 7010  'INIT A/D
1010 CLS
1020 PRINT "Sensor Calibration"
1030 PRINT
1040 PRINT "Input Sensor Unit of Measurement - Load:Lbs, Displacement:Inches"
1050 INPUT UNITS$
1060 PRINT "Input Sensor Manufacturer"
1070 INPUT MFG$
1080 PRINT "Input Sensor Serial Number?"
1090 INPUT SN$
1100 PRINT "Input Sensor Location?"
1110 INPUT LOCATION$
1120 PRINT "What channel will this sensor be connected to?"
1130 INPUT CH%: IF CH% >= 7 THEN 1120: IF CH% < 0 THEN 1120
1140 PRINT "Zero transducer and type any key"
1150 DUM$ = INPUT$(1)
1160 GOSUB 1600 ' READ DATA ON CHANNEL (DAT1)
1165 DAT1 = val1%
1170 PRINT "Now apply load or move known distance"
1180 PRINT "Type any key when ready"
1190 DUM$ = INPUT$(1)
1200 GOSUB 1600 ' READ CAL SIGNAL ON CHANNEL (DAT2)
1205 DAT2 = val1%
1210 PRINT "Type in  "; UNITS$; "  Applied"
1220 INPUT Cal
1230 C(CH%) = ABS(DAT2 - DAT1) / Cal  'VOLTS/UNIT
1235 C(CH%) = C(CH%) / 3276
12040 PRINT "SENSOR CALIBRATION IS: "; C(CH%); " VOLTS/"; UNITS$
1250 PRINT
1260 PRINT "If satisfactory type Y otherwise N "
1270 DUM$ = UCASE$(INPUT$(1))
1280 IF DUM$ = "N" THEN 1140
1290 IF DUM$ = "Y" THEN 1350
1300 GOTO 1260
1310 REM STORE SENSOR DATA IN CAL FILE
1315 REM CALDAT IS PERMANENT FILE FOR DATA
1330 REM EACH SENSOR REQUIRES TWO LINES
1340 REM THEY ARE STORED IN NUMERICAL ORDER
1350 CLOSE 2: OPEN "CALDAT" FOR RANDOM AS 2 LEN = LEN(DUCERITEM)
1352 DUCERITEM.CH = CH%: DUCERITEM.UNIT = LEFT$(UNITS$, 10): DUCERITEM.C = C(CH%)
     DUCERITEM.DATE1 = DATE$: DUCERITEM.MFG = LEFT$(MFG$, 14): DUCERITEM.SN = LEFT$(SN$, 10)
     DUCERITEM.LOCATION = LOCATION$
1400 CH% = CH% + 1
1420 PUT #2, CH%, DUCERITEM
1440 CLOSE 2
1450 PRINT "Are there more sensors to calibrate? (Y-N)"
1460 DUM$ = UCASE$(INPUT$(1))
1470 IF DUM$ = "N" THEN 1500
1480 IF DUM$ = "Y" THEN 1520
1490 GOTO 1450
1500 PRINT "Done with sensor calibration"
1510 CLS : GOTO 100
1520 GOTO 1010
1599 REM READ A/D
1600 MD% = 1
1610 DIO%(0) = CH%: DIO%(1) = CH%
1620 CALL QBHRES(MD%, VARPTR(DIO%(0)), FLAG%)
1630 IF FLAG% > 0 THEN 7210
1640 val1 = 0
1650 MD% = 3
1660 FOR I = 1 TO 10
1670 CALL QBHRES(MD%, VARPTR(DIO%(0)), FLAG%)
1671 LPRINT DIO%(1), val1, DIO%(0)
1672 val2 = DIO%(0) / 1000
1680 val1 = val1 + val2
1690 NEXT I
```

```
1700 val1% = (val1 / 10) * 1000'AVERAGE
1701 LPRINT val1%
1710 RETURN
1990 REM VIEW CALIBRATION DATA
2000 CLOSE1: OPEN "CALDAT" FOR RANDOM AS 1 LEN = LEN(DUCERITEM)
     NumberOfRecords = LOF(1) \ LEN(DUCERITEM)
     CLS
     PRINT "CH  UNITS       CAL FACTOR     DATE      MFG              S/N      LOCATION"
     PRINT
     FM1$ = "##  \        \#####.#####   \         \ \              \ \       \ \            \"
     FOR J = 1 TO NumberOfRecords
        GET #1, J, DUCERITEM
        PRINT USING FM1$; DUCERITEM.CH; DUCERITEM.UNIT; DUCERITEM.C; DUCERITEM.DATE1; DUCERITEM.MFG;
DUCERITEM.SN; DUCERITEM.LOCATION
2090 NEXT J
2100 CLOSE 1
     PRINT "STRIKE ANY KEY TO CONTINUE": JUNK$ = INPUT$(1)
2110 RETURN
2990 REM MODIFY EXISTING CALIBRATION VALUES
3000 CLS
3010 PRINT "What channel do you want to modify?"
3020 CH% = VAL(INPUT$(1)): CH% = CH% + 1
3030 CLOSE 1: OPEN "CALDAT" FOR RANDOM AS 1 LEN = LEN(DUCERITEM)
     NumberOfRecords = LOF(1) / LEN(DUCERITEM)
     IF CH% > NumberOfRecords THEN 3070
3050 GOTO 3100
3070 PRINT "NO DATA AVAILABLE FOR CHANNEL "; CH% - 1: GOTO 3010
3100 GET #1, CH%, DUCERITEM
     PRINT DUCERITEM.CH; " "; DUCERITEM.UNIT; " "; DUCERITEM.C; " ";
     PRINT DUCERITEM.DATE1; " "; DUCERITEM.MFG; " "; DUCERITEM.SN; " "; DUCERITEM.LOCATION
3180 PRINT
3190 PRINT "TYPE IN NEW CALIBRATION VALUE "
3200 INPUT C(CH%): DUCERITEM.C = C(CH%)
3230 PUT #1, CH%, DUCERITEM
3350 CLOSE 1: RETURN
3990 REM RUN TEST
4000 CLOSE 1: OPEN "CALDAT" FOR RANDOM AS 1 LEN = LEN(DUCERITEM)
     NCH = LOF(1) \ LEN(DUCERITEM)
     FOR I = 1 TO NCH
     GET #1, I, DUCERITEM
     CH% = DUCERITEM.CH: UNITS$ = DUCERITEM.UNIT: C(I - 1) = DUCERITEM.C
     DATE1$ = DUCERITEM.DATE1: MFG$ = DUCERITEM.MFG: SN$ = DUCERITEM.SN
     LOCATION$ = DUCERITEM.LOCATION
     NEXT I
     GOSUB 16000
     CLS
4010 PRINT "CONSTANT CYCLIC LOAD TEST"
4020 PRINT
4025 DATE1$ = DATE$
4030 PRINT "INPUT SAMPLE NUMBER"
4040 INPUT SAPNO$
4050 PRINT "PROJECT # ?"
4060 INPUT PROJ$
4070 PRINT "MATERIAL DESCRIPTION ?"
4080 INPUT MATD$
     PRINT "INPUT SPECIMEN LENGTH (inches)"
     INPUT SPLNTH
     PRINT "INPUT SPECIMEN DIAMETER (inches)"
     INPUT SPDIA
     PRINT "INPUT CHAMBER TEMP..F ?"
     INPUT TEMPF
4110 CLS
     PRINT "HOW MANY CREEP TESTS FOR SAMPLE ?(MAX=10)"
     INPUT SAPER%
     PRINT "TYPE "; SAPER%; " VALUES FOR NUMBER OF LOAD CYCLES BETWEEN CREEP MEASUREMENTS"
     FOR I = 1 TO SAPER%: INPUT SKIP&(I): NEXT I
     REM ACCUMULATE COUNT FOR COUNTER
     SAPER% = SAPER% + 1'ADD 1 FOR INITIAL CONDITIONS
     SKIPC&(1) = 20'INITIAL DELAY BEFORE COLLECTING DATA
     SKIPC&(2) = SKIP&(1)
     FOR I = 3 TO SAPER%
```

```
     SKIPC&(I) = SKIPC&(I - 1) + SKIP&(I - 1)
     NEXT I
     test = 0' INITIALIZE NUMBER OF CREEP TESTS
4180 PRINT "HOW MANY CYCLES OF DATA IN EACH CREEP TEST ?"
4190 INPUT SP%
     IF SP% > 10 THEN 4195 ELSE 4200
4195 PRINT "MAXIMUN LOAD CYCLES IS 4": GOTO 4180
4200 PRINT "WHAT IS THE LOAD THRESHOLD FOR DATA COLLECTION ?"
4210 INPUT thres
4215 thrs = thres * C(0) * 3276
     thrs% = thrs
4220 CLS
4230 PRINT "INSURE THAT ALL SENSORS ARE OPERATIONAL"
4240 PRINT "INSURE THAT ALL SENSOR CALIBRATIONS ARE COMPLETE"
4250 PRINT "AND ON APPROPRIATE CHANNEL"
     PRINT
     PRINT "DO YOU WANT TO VIEW DATA(Y-N) ?"
     VIEW$ = UCASE$(INPUT$(1))
     IF VIEW$ = "Y" THEN 4260
     PRINT "PLACE A FORMATED DISK IN DRIVE B"
     PRINT "HIT ANY KEY TO CONTINUE": DUM$ = INPUT$(1)
4260 GOSUB 7010 'INITIALIZE A/D MODULE
     NXTCNT% = -1 'COUNT= 65536
     GOSUB 6500  'INITIALIZE COUNTER
     DIO%(0) = 1
     MD% = 12'READ COUNTER
     CALL QBHRES(MD%, VARPTR(DIO%(0)), FLAG%)
     IF FLAG% > 0 THEN 7210
     FSTCT% = DIO%(1)'COUNTER DOESN"T RESET UNTIL 1ST PULSE
     CLS : LOCATE 2, 30: COLOR 0, 7: PRINT "PROCEED WITH TEST": COLOR 7, 0
     LOCATE 5, 35: COLOR 0, 7: PRINT "START MTS": COLOR 7, 0
4300 MD% = 12
     DIO%(0) = 1        'READ COUNTER
     CALL QBHRES(MD%, VARPTR(DIO%(0)), FLAG%)'sit here until 1st pulse
4500 IF FLAG% > 0 THEN 7210
     IF DIO%(1) = FSTCT% THEN 4300
     FOR CP = 1 TO SAPER%'SEE LINE 5410 FOR NEXT
     CLS : LOCATE 2, 30: COLOR 0, 7: PRINT "PROCEED WITH TEST": COLOR 7, 0
     REM START TO COLLECT DATA
     LOCATE 5, 35: COLOR 0, 7: PRINT "START MTS": COLOR 7, 0
4501 DIO%(0) = 1
     MD% = 12
     CALL QBHRES(MD%, VARPTR(DIO%(0)), FLAG%)
     IF FLAG% > 0 THEN 7210
     IF CNTT < 65535 THEN
     IF DIO%(1) < 0 THEN
       COUNT = 65536 + DIO%(1)
     ELSE
       COUNT = DIO%(1)
     END IF
       COUNT = 65536 - COUNT
     END IF
     IF CNTT >= 65535 AND CNTT < 131071 THEN
     IF DIO%(1) <= 0 THEN
       COUNT = 65536 + DIO%(1)
     ELSE
       COUNT = DIO%(1)
     END IF
       COUNT = 131072 - COUNT
     IF DIO%(1) = 1 AND CNTT = 65535 THEN
     COUNT = 65535
     END IF
     END IF
     IF CNTT >= 131071 AND CNTT < 196607 THEN
     IF DIO%(1) <= 0 THEN
       COUNT = 65536 + DIO%(1)
     ELSE
       COUNT = DIO%(1)
     END IF
       COUNT = 196608 - COUNT
     IF DIO%(1) = 1 AND CNTT = 131071 THEN
```

```
COUNT = 131071
END IF
END IF
IF CNTT >= 196607 AND CNTT < 262143 THEN
IF DIO%(1) <= 0 THEN
   COUNT = 65536 + DIO%(1)
ELSE
    COUNT = DIO%(1)
END IF
    COUNT = 262144 - COUNT
IF DIO%(1) = 1 AND CNTT = 196607 THEN
COUNT = 196607
END IF
END IF
IF CNTT >= 262143 AND CNTT < 327679 THEN
IF DIO%(1) <= 0 THEN
   COUNT = 65536 + DIO%(1)
ELSE
    COUNT = DIO%(1)
END IF
    COUNT = 327680 - COUNT
IF DIO%(1) = 1 AND CNTT = 262143 THEN
COUNT = 262143
END IF
END IF
IF CNTT >= 327679 AND CNTT < 393215 THEN
IF DIO%(1) <= 0 THEN
    COUNT = 65536 + DIO%(1)
ELSE
    COUNT = DIO%(1)
END IF
    COUNT = 393216 - COUNT
IF DIO%(1) = 1 AND CNTT = 327679 THEN
COUNT = 327679
END IF
END IF
IF CNTT >= 393215 AND CNTT < 458751 THEN
IF DIO%(1) <= 0 THEN
    COUNT = 65536 + DIO%(1)
ELSE
    COUNT = DIO%(1)
END IF
    COUNT = 458752 - COUNT
IF DIO%(1) = 1 AND CNTT = 393215 THEN
COUNT = 393215
END IF
END IF
IF CNTT >= 458751 AND CNTT < 524287 THEN
IF DIO%(1) <= 0 THEN
    COUNT = 65536 + DIO%(1)
ELSE
    COUNT = DIO%(1)
END IF
    COUNT = 524288 - COUNT
IF DIO%(1) = 1 AND CNTT = 458751 THEN
COUNT = 458751
END IF
END IF
IF CNTT >= 524287 AND CNTT < 589823 THEN
IF DIO%(1) <= 0 THEN
    COUNT = 65536 + DIO%(1)
ELSE
    COUNT = DIO%(1)
END IF
     COUNT = 589824 - COUNT
IF DIO%(1) = 1 AND CNTT = 524287 THEN
COUNT = 524287
END IF
END IF
IF CNTT >= 589823 AND CNTT < 655359 THEN
IF DIO%(1) <= 0 THEN
```

```
     COUNT = 65536 + DIO%(1)
ELSE
     COUNT = DIO%(1)
END IF
     COUNT = 655360 - COUNT
IF DIO%(1) = 1 AND CNTT = 589823 THEN
COUNT = 589823
END IF
END IF
IF CNTT >= 655359 AND CNTT < 720895 THEN
IF DIO%(1) <= 0 THEN
   COUNT = 65536 + DIO%(1)
ELSE
   COUNT = DIO%(1)
END IF
   COUNT = 720896 - COUNT
IF DIO%(1) = 1 AND CNTT = 655359 THEN
COUNT = 655359
END IF
END IF
IF CNTT >= 720895 AND CNTT < 786431 THEN
IF DIO%(1) <= 0 THEN
    COUNT = 65536 + DIO%(1)
ELSE
    COUNT = DIO%(1)
END IF
    COUNT = 786432 - COUNT
IF DIO%(1) = 1 AND CNTT = 720895 THEN
COUNT = 720895
END IF
END IF
IF CNTT >= 786431 AND CNTT < 851967 THEN
IF DIO%(1) <= 0 THEN
    COUNT = 65536 + DIO%(1)
ELSE
    COUNT = DIO%(1)
END IF
    COUNT = 851968 - COUNT
IF DIO%(1) = 1 AND CNTT = 786431 THEN
COUNT = 786431
END IF
END IF
IF CNTT >= 851967 AND CNTT < 917503 THEN
IF DIO%(1) <= 0 THEN
    COUNT = 65536 + DIO%(1)
ELSE
    COUNT = DIO%(1)
END IF
    COUNT = 917504 - COUNT
IF DIO%(1) = 1 AND CNTT = 851967 THEN
COUNT = 851967
END IF
END IF
IF CNTT >= 917503 AND CNTT < 983039 THEN
IF DIO%(1) <= 0 THEN
    COUNT = 65536 + DIO%(1)
ELSE
    COUNT = DIO%(1)
END IF
    COUNT = 983040 - COUNT
IF DIO%(1) = 1 AND CNTT = 917503 THEN
COUNT = 917503
END IF
END IF
IF CNTT >= 983039 AND CNTT < 1048575 THEN
IF DIO%(1) <= 0 THEN
   COUNT = 65536 + DIO%(1)
ELSE
   COUNT = DIO%(1)
END IF
   COUNT = 1048576 - COUNT
```

```
     IF DIO%(1) = 1 AND CNTT = 983039 THEN
     COUNT = 983039
     END IF
     END IF
     CNTT = COUNT
     LOCATE 8, 30: PRINT "PULSES COUNTED = "; CNTT
     PRINT CP, CNTT, SKIPC&(CP)
     IF CNTT < SKIPC&(CP) THEN 4501      'DID NOT REACH SKIP
     REM DID REACH COUNT
     NXTCNT% = DIO%(1)'SAVE COUNT FOR NEXT CYCLE
     N% = SP% * 6 * 200                  'TOTAL NUMBER OF SAMPLES
     FOR I = 1 TO SP%
4502 MD% = 1: DIO%(0) = 0: DIO%(1) = 0
     CALL QBHRES(MD%, VARPTR(DIO%(0)), FLAGE%)
4503 MD% = 3
     CALL QBHRES(MD%, VARPTR(DIO%(0)), FLAGE%)
     BACK%(1) = DIO%(0)
     CALL QBHRES(MD%, VARPTR(DIO%(0)), FLAGE%)
     BACK%(2) = DIO%(0)
     CALL QBHRES(MD%, VARPTR(DIO%(0)), FLAGE%)
     BACK%(3) = DIO%(0)
     PRINT BACK%(1); BACK%(2); BACK%(3)
     IF BACK%(3) > BACK%(2) AND BACK%(2) > BACK%(1) AND BACK%(3) >= thrs% THEN
     GOTO 4504
     ELSE
     GOTO 4503
     END IF
4504 MD% = 1: DIO%(0) = 0: DIO%(1) = 5
     CALL QBHRES(MD%, VARPTR(DIO%(0)), FLAGE%)
4505 MD% = 6    'SET UP TO READ DATA"
     DIO%(0) = 1200
     DIO%(1) = MEMBUF%(I)   '128K
     DIO%(2) = 1
     DIO%(3) = 0
     DIO%(4) = 0'CHANNEL GAIN
     CALL QBHRES(MD%, VARPTR(DIO%(0)), FLAG%)
     IF FLAG% > 0 THEN 7210
4613 MD% = 8                                 'SEE IF DONE
     CALL QBHRES(MD%, VARPTR(DIO%(0)), FLAG%)
     IF FLAG% > 0 THEN 7210
     IF DIO%(1) = 0 THEN 4615 ELSE 4613
4615 NEXT I
     PRINT " now ready to transfer memory to array"
     GOSUB 7010 'INITIALIZE A/D FOR NEXT CYCLE
     REM  NXTCNT% =START COUNT
     GOSUB 6500 'INITIALIZE COUNTER FOR NEXT
4620 REM NOW PROCESS DATA
     FOR I = 1 TO SP%
     MD% = 9                                   'TRANSFER MEMORY TO ARRAY
     DIO%(0) = 1200: DIO%(1) = MEMBUF%(I): DIO%(2) = 0
     DIO%(3) = VARPTR(DATA1%(0)) + (I - 1) * 2 * 1200
     DIO%(4) = 0
     CALL QBHRES(MD%, VARPTR(DIO%(0)), FLAG%)
     IF FLAG > 0 THEN 7210
     NEXT I
     GOSUB 6000  'STORE DATA ON DISK
4672 IF VIEW$ = "N" THEN 4700
4673 PRINT " DO YOU WANT TO VIEW DATA ?(Y-N)"
     DUM$ = UCASE$(INPUT$(1))
     IF DUM$ = "N" THEN 4700
4675 PRINT "THERE ARE "; SP%; " LOAD CYCLES"
     PRINT "WHAT CYCLE DO YOU WANT TO DISPLAY ?"
     INPUT SCN%: J = 1200 * (SCN% - 1)
     LPRINT C(0); C(1); C(2); C(3); C(4); C(5)
     FOR W = 0 TO 1080 STEP 120
     CLS
     PRINT "     LOAD        LONGTL-1     LONGTL-2      HORIZ-1      HORIZ-2      VERT"
     PRINT "      #          INCHES       INCHES        INCHES       INCHES       INCHES "
     FOR L = 0 TO 114 STEP 6
     I = W + L + J
     D0 = DATA1%(I) / (C(0) * 3276): D1 = DATA1%(I + 1) / (C(1) * 3276)
```

```
    D2 = DATA1%(I + 2) / (C(2) * 3276): D3 = DATA1%(I + 3) / (C(3) * 3276)
    D4 = DATA1%(I + 4) / (C(4) * 3276): D5 = DATA1%(I + 5) / (C(5) * 3276)
    PRINT USING " ####.##    "; D0; : PRINT USING " ####.#######"; D1; D2; D3; D4;
    PRINT USING "####.######"; D5
    NEXT L
    DUM$ = INPUT$(1)
    NEXT W
4677 PRINT " DO YOU WANT TO VIEW MORE DATA ?(Y-N)"
    DUM$ = UCASE$(INPUT$(1))
    IF DUM$ = "N" THEN 4700
    IF DUM$ = "Y" THEN 4675
    GOTO 4677
4680 REM DETERMINE MIN-MAX LOAD FOR EACH LOAD CYCLE
4700 CLS
    DIPY% = CP
    PRINT "PROCESSING CREEP PERIOD "; DIPY%
4710 IF VIEW$ = "N" THEN 4725
    ' "..........LOAD APPLIED..........:"
    ' "RESULTS FOR SAMPLE # "; SAPNO$
    ' "RESULTS FOR CREEP MEASUREMENT # "; CP
    CCC = SKIPC&(test + 1)
    ' "CYCLE COUNT ="; CCC
    '
4725 J = 0: K = 0
    FOR H = 1 TO SP%
    GOSUB 14000
    PMAX = LMAX% / (C(0) * 3276)
    PMIN = LMIN% / (C(0) * 3276)
    IF CMAX% = 1 THEN 4750'ONLY ONE PEAK VALUE
    POSS% = POSS% + CMAX% / 2
4750 LDPOS% = POSS%    'SAMPLE # OF PEAK LOAD(RELATIVE TO 200)
4760 IF VIEW$ = "N" THEN 4782
    '
    ' "MINIMUM LOAD = "; PMIN; " FOR THE "; H; " CYCLE"
    ' "MAXIMUM LOAD = "; PMAX; " AT THE "; POSS%; " SAMPLE"
    ' "THERE ARE "; CMAX%; "MAX VALUES"
    RLAX% = BCNT% / 6 + 1
    ' "THE RELAXATION TIME OCCURED AT THE "; RLAX%; "SAMPLE"
4782 RLAX% = BCNT% / 6 + 1
    REM STORE DATA FOR CREEP ANALYSIS
    PMAX(H, CP) = PMAX
    PMIN(H, CP) = PMIN
    BCNT%(H, CP) = BCNT% '(RELAX ADDRESS)
    LDPOS%(H, CP) = LDPOS%
    J = J + 1200
    NEXT H
    IF VIEW$ = "N" THEN 4830
    PRINT
4830 REM CALC VERTICAL DEFLECTION CH #5
    PRINT " PROCESSING VERTICAL DEFLECTION"
4832 IF VIEW$ = "N" THEN 4833
    GOTO 4833
    LPRINT : LPRINT : LPRINT
    LPRINT "..........VERTICAL DEFLECTION.........."
    LPRINT "RESULTS FOR SAMPLE # "; SAPNO$
    LPRINT "RESULTS FOR CREEP MEASUREMENT # "; CP
    CCC = SKIPC&(test + 1)
    LPRINT "CYCLE COUNT = "; CCC
4833 J = 0: K = 5
    FOR H = 1 TO SP%
    GOSUB 14000
    MIN1 = LMIN1% / (C(5) * 3276)        'PRE-LOAD MIN
    VMIN2 = LMIN2% / (C(5) * 3276)    'POST-LOAD MIN
    VMAX = LMAX% / (C(5) * 3276)
    DIF1 = VMAX - VMIN1: DIF2 = VMAX - VMIN2
    VSAMP% = (POSS% + CMAX% / 2) - 1
4834 IF VIEW$ = "N" THEN 4838
    GOTO 4838
4835 LPRINT
    LPRINT "MAXIMUM VERTICAL DEFLECTION"
    LPRINT "        (before/after load)="; DIF1; "/"; DIF2; "FOR"; H; "CYCLE"
```

```
     LPRINT "MAXIMUM DEFLECTION OCCURED AT THE "; VSAMP%; "SAMPLE"
     LPRINT "THERE ARE "; CMAX%; "MAX VALUES"
     LPRINT "THE MIN VALUES WERE"; VMIN1; "/"; VMIN2
     LPRINT "THERE ARE"; CMIN1%; "/"; CMIN2%; "MIN SAMPLES"
4838 REM NOW STORE DATA FOR CREEP ANALYSIS
     VMAX(H, CP) = VMAX
     VMIN(H, CP) = VMIN2
     VDELTA%(H, CP) = VSAMP% - LDPOS%(H, CP)
     OFFSET% = BCNT%(H, CP) + (VDELTA%(H, CP) - 1) * 6'GET DISPLACEMENT @B(ADDRESS)
     IF OFFSET% > 1194 THEN OFFSET% = 1194
     VB(H, CP) = DATA1%(OFFSET% + K + J) / (C(5) * 3276)
     VC(H, CP) = VMIN2  'POST-LOAD MIN
     VAB(H, CP) = AAVG / (C(5) * 3276)'ABSOLUT POSITION OF SENSOR AFTER LOAD
4840 J = J + 1200
     NEXT H
     IF VIEW$ = "N" THEN 4950
4950 REM DETERMINE HORIZONTAL MOVEMENT
     PRINT " PROCESSING HORIZONTAL DEFLECTION"
4960 IF VIEW$ = "N" THEN 4970
     GOTO 4970
     LPRINT : LPRINT : LPRINT
     LPRINT "..........HORIZONTAL DEFLECTION.........."
     LPRINT "RESULTS FOR SAMPLE # ="; SAPNO$
     CCC = SKIPC&(test + 1)
     LPRINT "CYCLE COUNT="; CCC
4970 J = 0
     FOR H = 1 TO SP%
     K = 3      'FIRST XDUCER
     GOSUB 14000
     H1MAX = LMAX% / (C(3) * 3276)
     H1MIN = LMIN1% / (C(3) * 3276)       'PRE-LOAD MIN FOR 1ST XDUCER
     H2MIN = LMIN2% / (C(3) * 3276)       'POST-LOAD MIN FOR 1ST XDUCER
     H1AB = AAVG / (C(3) * 3276)
     POS1% = POSS%: C1MAX% = CMAX%
     C1MIN% = CMIN1%: C2MIN% = CMIN2%
     K = 4      'NOW SECOND XDUCER
     GOSUB 14000
     H2MAX = LMAX% / (C(4) * 3276)
     H12MIN = LMIN1% / (C(4) * 3276)        'PRE-LOAD MIN FOR 2ND XDUCER
     H22MIN = LMIN2% / (C(4) * 3276)      'POST-LOAD MIN FOR 2ND XDUCER
     H2AB = AAVG / (C(4) * 3276)
     POS2% = POSS%: C2MAX% = CMAX%
     C12MIN% = CMIN1%: C22MIN% = CMIN2%
     REM NOW COMBINE THE TWO XDUCER SIGNALS
     HOR1 = H1MAX - H1MIN + H2MAX - H12MIN'PRELOAD
     HOR2 = H1MAX - H2MIN + H2MAX - H22MIN'POST LOAD-(DE+EF)
     DIS3 = H1MAX - H1MIN 'Preload DISP SENSOR 3
     DIS4 = H2MAX - H12MIN'PreLOAD DISP SENSOR 4
     dis3p = H1MAX - H2MIN'postload disp sensor 3
     dis4p = H2MAX - H22MIN'postload disp sensor 4
     LPRINT "DIS3  "; DIS3; dis3p; "DIS4  "; DIS4; dis4p
4980 IF VIEW$ = "N" THEN 4990
     GOTO 4990
     LPRINT
     LPRINT "MAXIMUM HOR...DISP="; HOR1; "/"; HOR2; "FOR"; H; "CYCLE(before/after load)"
4990 POS1% = POS1% + C1MAX% / 2 - 1   'SHIFT TO MIDDLE OF PEAK
     POS2% = POS2% + C2MAX% / 2 - 1
     POSS% = (POS1% + POS2%) / 2  'GET AVERAGE
     IF VIEW$ = "N" THEN 5000
     GOTO 5000
     LPRINT "MAX HORZ DISP OCCURED AT "; POS1%; "/"; POS2%; "SAMPLES(SENSOR1/SENSOR2)"
     LPRINT "THERE ARE"; C1MAX%; "/"; C2MAX%; "MAX SAMPLES"
     LPRINT "THERE ARE"; C1MIN%; "/"; C12MIN%; "MIN SAP BEFORE LOAD"
     LPRINT "THERE ARE"; C2MIN%; "/"; C22MIN%; "MIN SAP AFTER LOAD"
5000 REM NOW STORE SAMPLES FOR CREEP ANALYSIS
     HMAX(H, CP) = H1MAX + H2MAX
     HMIN(H, CP) = H2MIN + H22MIN  'XDUCER OUTPUT
     HDELTA%(H, CP) = POSS% - LDPOS%(H, CP)
     OFFSET% = BCNT%(H, CP) + (HDELTA%(H, CP) - 1) * 6'GET DISP @ B
     IF OFFSET% > 1194 THEN OFFSET% = 1194
     HB1 = DATA1%(OFFSET% + 3 + J) / (C(3) * 3276)
```

```
     HB2 = DATA1%(OFFSET% + 4 + J) / (C(4) * 3276)
     HB(H, CP) = HB1 + HB2  'POINT B XDUCER OUTPUT
     HC(H, CP) = H2MIN + H22MIN 'POINT C XDUCER OUTPUT (TOTAL POST-LOAD MIN)
     H1AB(H, CP) = H1AB 'ABSOLUTE DISPLACEMENTS
     H2AB(H, CP) = H2AB 'FOR PLASTIC MODULUS
     J = J + 1200
     NEXT H
5130 REM GET LONGITUDINAL MOVEMENT
     PRINT " PROCESSING LONGITUDINAL DEFLECTION"
5140 IF VIEW$ = "N" THEN 5150
     GOTO 5150
     LPRINT : LPRINT : LPRINT
     LPRINT "..........LONGITUDINAL DEFLECTION.........."
     LPRINT "RESULTS FOR SAMPLE # = "; SAPNO$
     CCC = SKIPC&(test + 1)
     LPRINT "CYCLE COUNT= "; CCC
     LPRINT
5150 J = 0
     FOR H = 1 TO SP%
     K = 1   'FIRST XDUCER
     GOSUB 14000
     R1MAX = LMAX% / (C(1) * 3276)
     R1MIN = LMIN1% / (C(1) * 3276)   'PRE-LOAD MIN FOR 1ST XDUCER
     R2MIN = LMIN2% / (C(1) * 3276)   'POST-LOAD MIN FOR 1ST XDUCER
     R1AB = AAVG / (C(1) * 3276)
     POS1% = POSS%: C1MAX% = CMAX%
     C1MIN% = CMIN1%: C2MIN% = CMIN2%
     K = 2 'NOW SECOND XDUCER
     GOSUB 14000
     R2MAX = LMAX% / (C(2) * 3276)
     R12MIN = LMIN1% / (C(2) * 3276)       'PRE-LOAD MIN FOR 2ND XDUCER
     R22MIN = LMIN2% / (C(2) * 3276)    'POST-LOAD MIN FOR 2ND XDUCER
     R2AB = AAVG / (C(2) * 3276)
     POS2% = POSS%: C2MAX% = CMAX%
     C12MIN% = CMIN1%: C22MIN% = CMIN2%
     REM NOW COMBINE THE TWO XDUCERS
     RAD1 = R1MAX - R1MIN + R2MAX - R12MIN   'PRE LOAD
     RAD2 = R1MAX - R2MIN + R2MAX - R22MIN   'POST LOAD(DE+EF)
5160 IF VIEW$ = "N" THEN 5170
     GOTO 5170
     LPRINT "MAXIMUM RAD DISP="; RAD1; "/"; RAD2; "FOR"; H; "CYCLE(before/after load)"
5170 POS1% = POS1% + C1MAX% / 2 - 1   'SHIFT TO MIDDLE OF PEAK
     POS2% = POS2% + C2MAX% / 2 - 1
     POSS% = (POS1% + POS2%) / 2
     IF VIEW$ = "N" THEN 5180
     GOTO 5180
     LPRINT "MAX LONGITUDINAL DISP OCCURED AT"; POS1%; "/"; POS2%; "SAMPLES(SENSOR1/SENSOR2)"
     LPRINT "THERE ARE"; C1MAX%; "/"; C2MAX%; "MAX SAMPLES"
     LPRINT "THERE ARE"; C1MIN%; "/"; C12MIN%; "MIN SAMP BEFORE LOAD"
     LPRINT "THERE ARE"; C2MIN%; "/"; C22MIN%; "MIN SAMP AFTER LOAD"
5180 REM NOW STORE SAMPLES FOR CREEP ANALYSIS
     RMAX(H, CP) = R1MAX + R2MAX
     RMIN(H, CP) = R2MIN + R22MIN
     RDELTA%(H, CP) = POSS% - LDPOS%(H, CP)
     OFFSET% = BCNT%(H, CP) + (RDELTA%(H, CP) - 1) * 6
     IF OFFSET% > 1194 THEN OFFSET% = 1194
     RB1 = DATA1%(OFFSET% + 1 + J) / (C(1) * 3276)
     RB2 = DATA1%(OFFSET% + 2 + J) / (C(2) * 3276)
     RB(H, CP) = RB1 + RB2
     RC(H, CP) = R2MIN + R22MIN 'POINT C XDUCER OUTPUT (TOTAL POST-LOAD MIN)
     R1AB(H, CP) = R1AB 'ABSOLUTE LONGITUDINAL DISPLACEMENT
     R2AB(H, CP) = R2AB 'FOR PLASTIC DEFORMATION
     J = J + 1200
     NEXT H
     IF PLOT$ = "Y" THEN 5500
     REM DONE WITH TEST
     REM DETERMINE IF ANY MORE CREEP TESTS TO DO
5200 test = test + 1
     IF test = SAPER% THEN 5415
     IF POST = 1 THEN 15150 'POST PROCESS NEXT CREEP CYCLE
     IF VIEW$ = "N" THEN 5410
```

```
     PRINT
     PRINT "HIT ANY KEY TO START NEXT CREEP TEST"
     PRINT "AND START MTS"
     DUM$ = INPUT$(1)
5410 NEXT CP
5415 FOR K = 1 TO 5
     LOCATE 24, 30: COLOR 0, 7
     PRINT "CREEP TEST COMPLETE": COLOR 7, 0
     FOR L = 1 TO 1000: NEXT L
     LOCATE 24, 30: PRINT "CREEP TEST COMPLETE"
     FOR L = 1 TO 1000: NEXT L
     NEXT K
5420 CLS
     CLOSE 3     'DISK FILE COMPLETE
     REM PROCESS CREEP DATA
     DIM EL%(10)
     CLS
     PRINT "---- FINAL SPECIMEN RESULTS"
     PRINT
     FOR CP = 1 TO SAPER%  'SEE LINE 5426 +1 FOR NEXT
     PRINT "AVERAGES FOR #"; CP; "CREEP PERIOD"
     PRINT
     PRINT "MAX LOAD FOR EACH LOAD CYCLE FOLLOWS"
     FOR H = 1 TO SP%
     PRINT H, PMAX(H, CP)
     NEXT H
     FOR I = 1 TO SP%: EL%(I) = 0: NEXT I'ZERO ARRAY
     PRINT
     PRINT "HOW MANY CYCLES DO YOU WANT TO ELIMINATE?"
     INPUT R%
     DIV = SP% - R%'NUMB OF VAR IN AVG.
     IF R% = 0 THEN 5425
     PRINT "TYPE IN THE"; R%; "CYCLE NUMBERS"
     FOR I = 1 TO R%
     INPUT EL%(I)'ARRAY INDEX FOR CYCLE TO BE ELIMINATED FROM AVERAGE
     NEXT I
     REM NOW COMPLETE RESULTS
     REM COMPUTE AVERAGES OF LOAD CYCLE DATA FOR EACH CREEP TEST
5425 FOR H = 1 TO SP%
     FOR Z = 1 TO SP%
     IF EL%(Z) = H THEN 5426
     NEXT Z
     PMAXS(CP) = PMAXS(CP) + PMAX(H, CP) / DIV
     PMINS(CP) = PMINS(CP) + PMIN(H, CP) / DIV
     VMAXS(CP) = VMAXS(CP) + VMAX(H, CP) / DIV
     VMINS(CP) = VMINS(CP) + VMIN(H, CP) / DIV
     VDELTS%(CP) = VDELTS%(CP) + VDELTA%(H, CP) / DIV
     VBS(CP) = VBS(CP) + VB(H, CP) / DIV
     VCS(CP) = VCS(CP) + VC(H, CP) / DIV
     VABS(CP) = VABS(CP) + VAB(H, CP) / DIV
     HMAXS(CP) = HMAXS(CP) + HMAX(H, CP) / DIV
     HMINS(CP) = HMINS(CP) + HMIN(H, CP) / DIV
     HDELTS%(CP) = HDELTS%(CP) + HDELTA%(H, CP) / DIV
     HBS(CP) = HBS(CP) + HB(H, CP) / DIV
     HCS(CP) = HCS(CP) + HC(H, CP) / DIV
     H1ABS(CP) = H1ABS(CP) + H1AB(H, CP) / DIV
     H2ABS(CP) = H2ABS(CP) + H2AB(H, CP) / DIV
     RMAXS(CP) = RMAXS(CP) + RMAX(H, CP) / DIV
     RMINS(CP) = RMINS(CP) + RMIN(H, CP) / DIV
     RDELTS%(CP) = RDELTS%(CP) + RDELTA%(H, CP) / DIV
     RBS(CP) = RBS(CP) + RB(H, CP) / DIV
     RCS(CP) = RCS(CP) + RC(H, CP) / DIV
     R1ABS(CP) = R1ABS(CP) + R1AB(H, CP) / DIV
     R2ABS(CP) = R2ABS(CP) + R2AB(H, CP) / DIV
     DIV(CP) = DIV
5426 NEXT H
     NEXT CP
     REM NOW COMPLETE CREEP CALCULATIONS
     CLS
     LOCATE 14, 20: PRINT "PLACE PRINTER ON -LINE.....FONT 8"
     LOCATE 16, 20: PRINT "TYPE ANY KEY WHEN READY"
```

```
     DUM$ = INPUT$(1)
     DIV% = DIV(1)
     PLOAD = PMAXS(1) - PMINS(1)
5427 IF VIEW$ = "N" THEN 5428
     LPRINT : LPRINT : LPRINT : LPRINT
     DIV% = DIV(1)
     LPRINT "RESULTS OF CREEP TESTS"
     LPRINT
     PLOAD = PMAXS(1) - PMINS(1)
     LPRINT "INITIAL CONDITIONS"
     LPRINT "AVG CYCLIC LOAD WAS"; PLOAD
     LPRINT "PRELOAD WAS"; PMINS(1)
     LPRINT "NUMBER OF LOAD CYCLES FOR INITIAL DATA= 20"
     LPRINT "NUMBER OF USEABLE LOAD CYCLES ="; DIV%
     LPRINT
     LPRINT
     R1$ = "VERTICAL DEFORMATION"
     R2$ = "------DELTA="
     R3$ = "------RESILIENT DEFORMATION ="
     R4$ = "------VISCOELASTIC DEFORMATION ="
     R5$ = "------PLASTIC DEFORMATION ="
     R6$ = "HORIZONTAL DEFORMATION ="
     R7$ = "LONGITUDINAL DEFORMATION ="
     R8$ = "TOTAL DEFORMATION = "
5428 FOR CP = 2 TO SAPER%
     DIV% = DIV(CP): CRN% = CP - 1
     CCC(CP) = SKIPC&(CP)
     AVGLOAD(CP) = PMAXS(CP) - PMINS(CP)
5430 IF VIEW$ = "N" THEN 5431
     LPRINT "RESULTS FOR CREEP TEST"; CRN%; "  CYCLE COUNT="; CCC(CP)
     LPRINT "NUMBER OF LOAD CYCLES IN AVG="; DIV%
     LPRINT "AVERAGE CYCLIC LOAD = "; AVGLOAD(CP)
     LPRINT VMAXS(CP); VBS(CP); VCS(CP); VABS(1)
5431 DEV(CP) = ABS(VMAXS(CP) - VBS(CP)): VV(CP) = DEV(CP) * SPLNTH / AVGLOAD(CP)
     VV1(CP) = AVGLOAD(CP) / (SPLNTH * DEV(CP)) 'FOR MR CALCULATION USING VERT SENSOR ONLY
     EFV(CP) = ABS(VBS(CP) - VCS(CP)): VVV(CP) = EFV(CP) * SPLNTH / AVGLOAD(CP)
     TDEFV(CP) = DEV(CP) + EFV(CP)
     TDEFV1(CP) = AVGLOAD(CP) / (SPLNTH * TDEFV(CP))
     REM DETERMINE PLASTIC DEFOMATION
5437 FGV(CP) = ABS(VABS(1) - VABS(CP))   'VERTICAL PLASTIC DEFORMATION
5438 IF VIEW$ = "N" THEN 5439
     LPRINT R1$
     LPRINT R2$; VDELTS%(CP); "SAMPLES"
     LPRINT R3$; DEV(CP)
     LPRINT R4$; EFV(CP)
     LPRINT R5$; FGV(CP)
     LPRINT R8$; TDEFV(CP)
     LPRINT
5439 REM PRINT "TYPE ANY KEY TO CONTINUE"
     REM DUM$ = INPUT$(1)
     CLS  'NOW DO HORIZONTAL
     DEH(CP) = ABS(HMAXS(CP) - HBS(CP)): HH(CP) = DEH(CP) * SPLNTH / AVGLOAD(CP)
     EFH(CP) = ABS(HBS(CP) - HCS(CP)): HHH(CP) = EFH(CP) * SPLNTH / AVGLOAD(CP)
     REM DETERMINE HORIZONTAL PLASTIC DEFORMATION
5440 HFG1(CP) = (H1ABS(1) - H1ABS(CP))
5441 HFG2(CP) = (H2ABS(1) - H2ABS(CP))
     FGH(CP) = ABS(HFG1(CP) + HFG2(CP)) 'TOTAL HORIZONTAL PLASTIC DEFORMATION
     TDEFH(CP) = DEH(CP) + EFH(CP)
5442 IF VIEW$ = "N" THEN 5443
     LPRINT R6$
     LPRINT R2$; HDELTS%(CP)
     LPRINT HMAXS(CP); HBS(CP); HCS(CP)
     LPRINT R3$; DEH(CP)
     LPRINT R4$; EFH(CP)
     LPRINT R5$; FGH(CP)
     LPRINT R8$; TDEFH(CP)
     LPRINT
5443 REM PRINT "TYPE ANY KEY TO CONTINUE"
     REM DUM$ = INPUT$(1)
     CLS 'NOW DO LONGITUDINAL
     DER(CP) = ABS(RMAXS(CP) - RBS(CP)): AA(CP) = DER(CP) / AVGLOAD(CP)
```

```
     EFR(CP) = ABS(RBS(CP) - RCS(CP)): AAA(CP) = EFR(CP) / AVGLOAD(CP)
     REM DETERMINE LONGITUDINAL PLASTIC DEFORMATION
5444 RFG1(CP) = (R1ABS(1) - R1ABS(CP))
5445 RFG2(CP) = (R2ABS(1) - R2ABS(CP))
     FGR(CP) = ABS(RFG1(CP) + RFG2(CP))  'TOTAL LONGITUDINAL DEFORMATION
     TDEFR(CP) = DER(CP) + EFR(CP)
5446 IF VIEW$ = "N" THEN 5448
     LPRINT R7$
     LPRINT R2$; RDELTS%(CP)
     LPRINT RMAXS(CP); RBS(CP); RCS(CP)
     LPRINT R3$; DER(CP)
     LPRINT R4$; EFR(CP)
     LPRINT R5$; FGR(CP)
     LPRINT R8$; TDEFR(CP)
     LPRINT
     GOTO 5448
5447 REM PRINT "TYPE ANY KEY TO CONTINUE"
     REM DUM$ = INPUT$(1)
     dd(CP) = 1.105791 * (HH(CP) ^ 2 + VV(CP) ^ 2 + AA(CP) ^ 2) - (HH(CP) - 3.10979E-03 * VV(CP) +
.319145 * AA(CP)) ^ 2
     TDD(CP) = 1.105791 * ((HH(CP) + HHH(CP)) ^ 2 + (VV(CP) + VVV(CP)) ^ 2 + (AA(CP) + AAA(CP)) ^ 2)
- (HH(CP) + HHH(CP) - .0627461 * (VV(CP) + VVV(CP)) + .319145 * (AA(CP) + AAA(CP))) ^ 2
     TUU(CP) = (.225127 * (HH(CP) + HHH(CP)) ^ 2 - .269895 * (VV(CP) + VVV(CP)) ^ 2 - .0447676 *
(AA(CP) + AAA(CP)) ^ 2 + 3.570975 * (HH(CP) + HHH(CP)) * (VV(CP) + VVV(CP)) + .086136 * (AA(CP) +
AAA(CP)) * (HH(CP) + HHH(CP)) + 1.145064 * (AA(CP) +  _
AAA(CP)) * (VV(CP) + VVV(CP))) / TDD(CP)
     UU(CP) = (.225127 * HH(CP) ^ 2 - .269895 * VV(CP) ^ 2 - .0447676 * AA(CP) ^ 2 + 3.570975 * HH(CP)
* VV(CP) + .086136 * HH(CP) * AA(CP) + 1.145064 * AA(CP) * VV(CP)) / dd(CP)
     MR(CP) = (.25368 * HH(CP) + 3.9702876# * VV(CP) - .0142874 * AA(CP)) / dd(CP)
     EE(CP) = (3.8949E-04 * (HH(CP) + HHH(CP)) + 3.9702876# * (VV(CP) + VVV(CP)) - .0142874 * (AA(CP)
+ AAA(CP))) / TDD(CP)
5448 REM PRINT " TYPE ANY KEY TO CONTINUE"
     REM DUM$ = INPUT$(1)
     dd(CP) = 1.046878 * (HH(CP) ^ 2 + VV(CP) ^ 2 + AA(CP) ^ 2) - (HH(CP) - .0417333 * VV(CP) + .212453
* AA(CP)) ^ 2
     TDD(CP) = 1.046878 * ((HH(CP) + HHH(CP)) ^ 2 + (VV(CP) + VVV(CP)) ^ 2 + (AA(CP) + AAA(CP)) ^ 2)
- (HH(CP) + HHH(CP) - .0417333 * (VV(CP) + VVV(CP)) + .212453 * (AA(CP) + AAA(CP))) ^ 2
     TUU(CP) = (.170519 * (HH(CP) + HHH(CP)) ^ 2 - .271761 * (VV(CP) + VVV(CP)) ^ 2 - .101241 * (AA(CP)
+ AAA(CP)) ^ 2 + 4.08595 * (HH(CP) + HHH(CP)) * (VV(CP) + VVV(CP)) + .057736 * (AA(CP) + AAA(CP)) *
(HH(CP) + HHH(CP)) + .868072 * (AA(CP) + AAA( _
CP)) * (VV(CP) + VVV(CP))) / TDD(CP)
     UU(CP) = (.170519 * HH(CP) ^ 2 - .271716 * VV(CP) ^ 2 - .101241 * AA(CP) ^ 2 + 4.08595 * HH(CP)
* VV(CP) + .057736 * HH(CP) * AA(CP) + .868072 * AA(CP) * VV(CP)) / dd(CP)
     MR(CP) = (.1832585 * HH(CP) + 4.2817159# * VV(CP) - .0215089 * AA(CP)) / dd(CP)
     EE(CP) = (.1832585 * (HH(CP) + HHH(CP)) + 4.2817159# * (VV(CP) + VVV(CP)) - .0215089 * (AA(CP) +
AAA(CP))) / TDD(CP)
     MR1(CP) = VV1(CP) * 4.07343'POSSION'S RATIO 0.3
     EE1(CP) = TDEFV1(CP) * 4.07343'POSSION'S RATIO 0.3
     EEH(CP) = ((AVGLOAD(CP)) / (SPLNTH * TDEFH(CP))) * .57176' TOTAL MODULUS HOR.LVDT
5450 IF VIEW$ = "N" THEN 5460
     LPRINT "DD="; dd(CP); "HH="; HH(CP); "VV="; VV(CP); "AA="; AA(CP)
     LPRINT "RESILIENT MODULUS(PSI)= "; MR(CP); "RESILIENT MODULUS (VERT ONLY)="; MR(CP)
     LPRINT "TOTAL MODULUS(PSI)= "; EE(CP); "TOTAL MODULUS(VERT ONLY)= "; MR1(CP)
     LPRINT "RESILIENT POISSON'S RATIO = "; UU(CP); ""
     LPRINT "TOTAL POISSON'S RATIO = "; TUU(CP)
     LPRINT
     REM PRINT "TYPE ANY KEY TO CONTINUE"
     REM DUM$ = INPUT$(1)
     LPRINT : LPRINT
5460 NEXT CP
     WIDTH LPRINT 132
     LPRINT "
             DATE        :"; DATE1$
     LPRINT "
             SAMPLE NO.  :"; SAPNO$
     LPRINT "
             PROJECT NO. :"; PROJ$
     LPRINT "
             CHAMBER TEMP:"; TEMPF; " F"
     LPRINT : LPRINT : LPRINT
     LPRINT " NO. OF LOAD CYCLES         ";
```

```
CP = SAPER%
FOR TP = 2 TO CP
LPRINT USING "#########    "; CCC(TP);
NEXT TP
LPRINT
                                L       P       R       I       N       T               "
------------------------------------------------------------------------------------------
----------------------------"
LPRINT " AVG. CYCLE LOAD            ";
FOR TP = 2 TO CP
LPRINT USING "####.####    "; AVGLOAD(TP);
NEXT TP
LPRINT
LPRINT " RESILIENT MODULUS          ";
FOR TP = 2 TO CP
LPRINT USING "#######.#    "; MR(TP);
NEXT TP
LPRINT
LPRINT " RESILIENT MODULUSV(P=.30)  ";
FOR TP = 2 TO CP
LPRINT USING "#######.#    "; MR1(TP);
NEXT TP
LPRINT
LPRINT " TOTAL MODULUS              ";
FOR TP = 2 TO CP
LPRINT USING "#######.#    "; EE(TP);
NEXT TP
LPRINT
LPRINT " TOTAL MODULUSV(P=.30)      ";
FOR TP = 2 TO CP
LPRINT USING "#######.#    "; EE1(TP);
NEXT TP
LPRINT
LPRINT " TOTAL MODULUSH(P=.30)      ";
FOR TP = 2 TO CP
LPRINT USING "#######.#    "; EEH(TP);
NEXT TP
LPRINT
LPRINT " RESILIENT POISSON'S RATIO  ";
FOR TP = 2 TO CP
LPRINT USING "##.######    "; UU(TP);
NEXT TP
LPRINT
LPRINT " TOTAL POISSON'S RATIO      ";
FOR TP = 2 TO CP
LPRINT USING "##.######    "; TUU(TP);
NEXT TP
LPRINT
                                L       P       R       I       N       T               "
------------------------------------------------------------------------------------------
----------------------------"
LPRINT : LPRINT
LPRINT " VERTICAL DEFORMATION "
LPRINT " --------------------"
LPRINT " TIME LAG                   ";
FOR TP = 2 TO CP
LPRINT USING "#########   "; VDELTS%(TP);
NEXT TP
LPRINT
LPRINT " RESILIENT                 ";
FOR TP = 2 TO CP
LPRINT USING " ##.######   "; DEV(TP);
NEXT TP
LPRINT
LPRINT " VISCOELASTIC              ";
FOR TP = 2 TO CP
LPRINT USING " ##.######   "; EFV(TP);
NEXT TP
LPRINT
LPRINT " PLASTIC                   ";
FOR TP = 2 TO CP
```

```
    LPRINT USING " ##.######   "; FGV(TP);
    NEXT TP
    LPRINT
    LPRINT " TOTAL                    ";
    FOR TP = 2 TO CP
    LPRINT USING " ##.######   "; TDEFV(TP);
    NEXT TP
    LPRINT
                                     L       P       R       I       N       T              "
-----------------------------------------------------------------------------------------------
----------------------------"
    LPRINT : LPRINT
    LPRINT " HORIZONTAL DEFORMATION "
    LPRINT " ---------------------"
    LPRINT " TIME LAG                  ";
    FOR TP = 2 TO CP
    LPRINT USING "#########   "; HDELTS%(TP);
    NEXT TP
    LPRINT
    LPRINT " RESILIENT                ";
    FOR TP = 2 TO CP
    LPRINT USING " ##.######   "; DEH(TP);
    NEXT TP
    LPRINT
    LPRINT " VISCOELASTIC             ";
    FOR TP = 2 TO CP
    LPRINT USING " ##.######   "; EFH(TP);
    NEXT TP
    LPRINT
    LPRINT " PLASTIC                  ";
    FOR TP = 2 TO CP
    LPRINT USING " ##.######   "; FGH(TP);
    NEXT TP
    LPRINT
    LPRINT " TOTAL                    ";
    FOR TP = 2 TO CP
    LPRINT USING " ##.######   "; TDEFH(TP);
    NEXT TP
    LPRINT
    LPRINT
                                     L       P       R       I       N       T              "
-----------------------------------------------------------------------------------------------
----------------------------"
    LPRINT : LPRINT
    LPRINT " LONGITUDINAL DEFORMATION "
    LPRINT " -----------------"
    LPRINT " TIME LAG                  ";
    FOR TP = 2 TO CP
    LPRINT USING "#########   "; RDELTS%(TP);
    NEXT TP
    LPRINT
    LPRINT " RESILIENT                ";
    FOR TP = 2 TO CP
    LPRINT USING " ##.######   "; DER(TP);
    NEXT TP
    LPRINT
    LPRINT " VISCOELASTIC             ";
    FOR TP = 2 TO CP
    LPRINT USING " ##.######   "; EFR(TP);
    NEXT TP
    LPRINT
    LPRINT " PLASTIC                  ";
    FOR TP = 2 TO CP
    LPRINT USING " ##.######   "; FGR(TP);
    NEXT TP
    LPRINT
    LPRINT " TOTAL                    ";
    FOR TP = 2 TO CP
    LPRINT USING " ##.######   "; TDEFR(TP);
    NEXT TP
    LPRINT
```

```
                                     L     P     R     I     N     T                    "
-------------------------------------------------------------------------------------------
---------------------------"
     GOTO 100
     REM DISPLAY SIGNAL DURING TEST
5500 SP$ = "                                                        "
5550     CLS
     SCREEN 2, 0, 0, 0
     LOCATE 1, 1: PRINT "CYCLIC LOAD DATA FOR SAMPLE # "; SAPNO$
     LOCATE 2, 1: PRINT "THERE ARE"; SP%; "CYCLES OF DATA"
     LOCATE 3, 1: PRINT "WHICH CYCLE DO YOU WANT?"
     SCN% = VAL(INPUT$(1))
     IF SCN% = 0 THEN 5780
     LOCATE 2, 1: PRINT SP$
     LOCATE 2, 1: PRINT "SWEEP PERIOD = "; DIPY%; " CYCLE COUNT ="; SKIPC&(test + 1)
     LOCATE 3, 1: PRINT SP$
     LOCATE 3, 1:.PRINT "DATA CYCLE ="; SCN%
     LOCATE 4, 64: PRINT "LOAD(0)"
     LOCATE 6, 64: PRINT "VERTICAL(5)"
     LOCATE 8, 64: PRINT "HORIZONTAL(3)"
     LOCATE 10, 64: PRINT "HORIZONTAL(4)"
     LOCATE 12, 64: PRINT "LONGITUDINAL(1)"
     LOCATE 14, 64: PRINT "LONGITUDINAL(2)"
     J% = 1200 * (SCN% - 1) '200 SAMPLES PER SCAN
5600 FOR pp1 = 0 TO 5'PLOT ALL SIX SIGNALS
     PP2 = pp1 + 1    'NEED FOR COMPUTED GOTO STATEMENT
     V1 = 51 / C(pp1)
     FOR I = 0 TO 1194 STEP 6
     dz%(INT(I / 6)) = DATA1%(I + J% + pp1)
     NEXT I
     MAX = 0: MIN = 0 ' NORMALIZE AND SCALE PLOT
     FOR T = 0 TO 199
     IF dz%(T) > MAX THEN MAX = dz%(T)
     IF dz%(T) < MIN THEN MIN = dz%(T)
     NEXT T
     RANGE = MAX - MIN
     IF RANGE = 0 THEN RANGE = 1
     adpos = 100 / RANGE
     FOR T = 0 TO 199
     X1 = INT(T * 3)
     y1 = 190 - (INT(adpos * dz%(T)))
     IF pp1 = 0 THEN y1 = 50 + INT(adpos * (dz%(T) - MIN + 150))'FLOP LOAD SIGNAL
     PSET (X1, y1), 2
     IF T = 100 THEN 5800' DRAW LINE
5740 NEXT T
     NEXT pp1 'NEXT PLOT
5750 DUM$ = INKEY$ 'TEST IF DONE PLOTTING
     IF LEN(DUM$) = 0 THEN 5750
     GOTO 5550
5780 SCREEN 0, 0, 0, 0
     GOTO 5200
5800 ON PP2 GOTO 5801, 5802, 5803, 5804, 5805, 5806
5801 LINE (X1, y1)-(465, 28): GOTO 5740
5802 LINE (X1, y1)-(465, 92): GOTO 5740
5803 LINE (X1, y1)-(465, 108): GOTO 5740
5804 LINE (X1, y1)-(465, 60): GOTO 5740
5805 LINE (X1, y1)-(465, 76): GOTO 5740
5806 LINE (X1, y1)-(465, 44): GOTO 5740
     REM STORE DATA SUBROUTINE
6000 IF VIEW$ = "N" THEN 6070
     PRINT "DO YOU WANT TO STORE DATA ?(Y-N) "
     DUM$ = UCASE$(INPUT$(1))
     IF DUM$ = "Y" THEN 6040
     RETURN
6040 PRINT "WHEN THERE IS A FORMATTED DISK"
     PRINT "IN DRIVE B HIT ANY KEY"
     DUM$ = INPUT$(1)
6070 file$ = "c:\data\" + SAPNO$ + ".DAT"
6080 OPEN file$ FOR APPEND AS 3
     PRINT #3, PROJ$
     PRINT #3, MATD$
```

```
     PRINT #3, SPLNTH
     PRINT #3, TEMPF
     PRINT #3, DATE1$
     FOR I = 0 TO 5
     PRINT #3, C(I) 'CAL FACTORS
     NEXT I
     PRINT #3, SAPER%; SP%; N%
     FOR I = 1 TO SAPER%: PRINT #3, SKIPC&(I); : NEXT I
     FOR I = 0 TO N%
     PRINT #3, DATA1%(I)'STORE RAW DATA ON DISK
     NEXT I
     CLOSE 3
     RETURN
     REM INITIALIZE COUNTER
6500 OUT IOADR% + 10, 0'WRITE 0 TO ENABLE REG
     DIO%(0) = 0: MD% = 10
     CALL QBHRES(MD%, VARPTR(DIO%(0)), FLAG%)
     IF FLAG% > 0 THEN 7210
     DIO%(0) = NXTCNT% 'LOAD COUNTER VALUE
     MD% = 11
     CALL QBHRES(MD%, VARPTR(DIO%(0)), FLAG%)
     IF FLAG% > 0 THEN 7210
6520 RETURN
7000 REM INITIALIZE A/D MODULE
7010 MD% = 0'MODE
7015 FLAG% = 0
7020 DIO%(0) = IOADR%
7030 DIO%(1) = 7 ' INTERRUPT
7040 DIO%(2) = 3 'DMA LEVEL
7041 BACK%(1) = 0
7042 BACK%(2) = 0
7043 BACK%(3) = 0
7060 CALL QBHRES(MD%, VARPTR(DIO%(0)), FLAG%)
7070 IF FLAG% > 0 THEN 7210
7080 REM SET CHANNELS
7090 MD% = 1
7091 DIO%(0) = 0
7092 DIO%(1) = 5
7100 CALL QBHRES(MD%, VARPTR(DIO%(0)), FLAG%)
7110 IF FLAG% > 0 THEN 7210
     REM SET SAMPLE RATE FOR 1KHZ (CLOCK= 10MHZ)
     DIO%(0) = 100: DIO%(1) = 40
     MD% = 17
     CALL QBHRES(MD%, VARPTR(DIO%(0)), FLAG%)
     IF FLAG% > 0 THEN 7210
     RETURN
7210 PRINT "DAS-HRES ERROR"; FLAG%; "MODE"; MD%
7220 END
8990 REM ROUTINE TO EXIT PROGRAM
9000 CLS :
9005 LOCATE 10, 10:
9010 PRINT "TERMINATION OF CYCLIC LOAD TEST"
9020 'STOP
9030 END
      REM ROUTINE TO NORMALIZE DATA AND DETERMINE MAX-MIN-COUNT
      REM J,K ARE ARRAY OFFSETS
      REM K=SIG BEING PROCESSED
      REM 0=LOAD,1=LONGTTUDINAL-1,2=LONGITUDINAL-2,3=HORZ-1,4=HORZ-2,5=VERTICAL DISP.
      REM J=DATA OFFSET INDEX FOR BETWEEN EACH LOAD CYCLE
      REM I=DATA OFFSET FOR EACH SIGNAL
14000 I = 0
      FOR ID = 1 TO 50'INITIALIZE FILTER
      X = DATA1%(I + K + J)
      GOSUB 18000
      NEXT ID
      FOR I = 0 TO 1194 STEP 6'NOW FILTER DATA
      X = DATA1%(I + K + J)
      GOSUB 18000
      DATA1%(I + K + J) = y
      NEXT I
      REM DETERMINE ABSOLUTE POSITION OF SENSOR
```

```
      REM CALCULATE THE AVERAGE VALUE OF THE LAST 8 SAMPLES
      REM USED TO CALCULATE THE PLASTIC DEFORMATION
      ASUM = 0
      FOR I = 1152 TO 1194 STEP 6
      ASUM = ASUM + DATA1%(I + K + J)
      NEXT I
      AAVG = ASUM / 8'AVERAGE VALUE
      REM NOW PROCESS DATA FOR RELATIVE DISPLACEMENT
      REM DO ALL DATA HAVE SAME SIGN
      I = 0: NEG% = 0: POSS% = 0
      IF K = 0 THEN 14190'TREAT LOAD SEPARATELY
14020 FOR I = 0 TO 1194 STEP 6                  'look for neg
      IF DATA1%(I + K + J) > NEG% THEN 14030
      NEG% = DATA1%(I + K + J)' MOST NEG VALUE
14030 NEXT I
      IF NEG% = 0 THEN 14075'NO NEG VALUE
      REM 'MUST BE SOME NEG # IN ARRAY
      REM LOAD WILL NEVER HAVE POS #(COMPRESSION)
      REM REMOVE NEG OFFSET
      FOR I = 0 TO 1194 STEP 6
14035 DATA1%(I + K + J) = DATA1%(I + K + J) + ABS(NEG%)
14040 NEXT I
      REM OFFSET REMOVED
14075 REM SEE IF MIN VALUE IS ZERO IF NOT MAKE IT ZERO
14100 LMAX% = -32768: LMIN% = 32767
      FOR I = 0 TO 1194 STEP 6
      IF DATA1%(I + K + J) > LMAX% THEN 14102
      IF DATA1%(I + K + J) < LMIN% THEN 14104
      GOTO 14106
14102 LMAX% = DATA1%(I + K + J): GOTO 14106
14104 LMIN% = DATA1%(I + K + J)
14106 NEXT I
      IF LMIN% = 0 THEN 14108
      IF LMIN% < 0 THEN 14106
      FOR I = 0 TO 1194 STEP 6
      DATA1%(I + K + J) = DATA1%(I + K + J) - LMIN%
      NEXT I
      GOTO 14108
      FOR I = 0 TO 1194 STEP 6
      DATA1%(I + K + J) = DATA1%(I + K + J) + LMIN%
      NEXT I
14108 ON K GOTO 14111, 14111, 14111, 14111, 14110
14110 FOR I = 0 TO 1194 STEP 6
      DATA1%(I + K + J) = LMAX% - DATA1%(I + K + J)
      NEXT I
14111 REM NOW COMPUTE MAX-MIN-COUNT ETC
      LMAX% = -32768: CMIN1% = 0
      CMIN2% = 0: CMAX% = 0: POSS% = 0: PEAK% = 0
      LMIN1% = DATA1%(0 + K + J)
      LMIN2% = DATA1%(1194 + K + J)
      REM ALL DATA VALUES ARE POSITIVE AND + SLOPE
      REM FIND # OF MAX VALUES AND CENTER SAMPLE COUNT
      REM FIND # OF MIN VALUES (WITHIN-TOLERENCE)AND AVG VALUE
      REM LMIN1=INITIAL MIN LMIN2=MIN AFTER LOAD APPLIED
      FOR I = 0 TO 1194 STEP 6
      IF DATA1%(I + K + J) > LMAX% THEN 14170
      IF DATA1%(I + K + J) = LMAX% THEN 14180
14113 NEXT I
      PEAK% = POSS%'LOCATION OF 1ST MAX #
      FOR I = 0 TO 1194 STEP 6
      REM DEAL WITH DISP BEFORE-AFTER LOAD
14115 IF I >= PEAK% THEN 14140' AFTER PEAK
      IF DATA1%(I + K + J) > LMIN1% THEN 14130
      IF DATA1%(I + K + J) = LMIN1% THEN 14120
      LMIN1% = DATA1%(I + K + J)'NEW PRELOAD MIN
      CMIN1% = 1: MINP1% = I'MINIMUM POSITION BEFORE LOAD
      GOTO 14130
14120 CMIN1% = CMIN1% + 1
14130 NEXT I
      GOTO 14340
14140 IF DATA1%(I + K + J) > LMIN2% THEN 14142
```

```
      IF DATA1%(I + K + J) < LMIN2% THEN 14144
14141 CMIN2% = CMIN2% + 1
      GOTO 14130
14142 IF DATA1%(I + K + J) - 1 = LMIN2% THEN 14141
      GOTO 14130
14144 IF DATA1%(I + K + J) + 1 = LMIN2% THEN 14141
      LMIN2% = DATA1%(I + K + J)'NEW MIN
      CMIN2% = 1: MINP2% = I'MIN POSITION AFTER LOAD
      GOTO 14130
14170 LMAX% = DATA1%(I + K + J)
      POSS% = I: CMAX% = 1
14175 GOTO 14113
14180 CMAX% = CMAX% + 1
      GOTO 14113
      REM PROCESS LOAD SIGNAL- ALWAYS NEGATIVE-COMPRESSION
      FOR ID = 1 TO 20'INITIALIZE FILTER
      X = DATA1%(I + K + J)
      NEXT ID
      FOR I = 0 TO 1194' FILTER SIGNAL
      X = DATA1%(I + K + J) 'FILTER INPUT
      GOSUB 18000
      DATA1%(I + K + J) = y'FILTER OUTPUT
      NEXT I
14190 LMIN% = 32767: LMAX% = 0
      FOR I = 0 TO 1194 STEP 6
      IF ABS(DATA1%(I + J)) < LMIN% THEN 14192
14191 IF ABS(DATA1%(I + J)) > LMAX% THEN 14194
      IF ABS(DATA1%(I + J)) = LMAX% THEN 14196
      GOTO 14198
14192 LMIN% = ABS(DATA1%(I + J))'MIN NUMBER -MIN LOAD
      VALLY% = I'ADDRESS OF MIN LOAD
      GOTO 14191
14194 LMAX% = ABS(DATA1%(I + J))'MOST POS NUMBER  -MAX LOAD
      LPEAK% = I'ADDRESS OF PEAK LOAD
      CMAX% = 1: GOTO 14198
14196 CMAX% = CMAX% + 1
14198 NEXT I
      REM DETERMINE SAMPLE COUNT TO (B-DELTA ) TIME
      REM MIN LOAD DEVIATION=+/-3# 1000#/32767=1/2#(+/-6 COUNTS)
      I = 1194
      LMIN2% = ABS(DATA1%(I + J))'LAST VALUE
14310 IF ABS(ABS(DATA1%(I + J)) - LMIN2%) > 6 THEN 14320' TOLERENCE 3 LBS
      IF I < 20 THEN 14320'THATS ENOUGH OF SIGNAL TO LOOK AT
      I = I - 6: GOTO 14310
14320 BCNT% = I' SAMPLE ADDRESS FOR BEGINNING OF RELAXATION PERIOD OF LOAD
14330 POSS% = LPEAK% / 6 + 1     '  SAMPLE NUMB FOR MAX LOAD
      RETURN
      REM GET & STORE DATA FOR DEFORMATIONS
14340 POSS% = POSS% / 6 + 1'LOCATION RELATIVE TO 200 SAMPLES
      RETURN
15000 POST = 1'FLAG TO INDICATE POST PROCESSING DATA FROM DISK
      PRINT "WHAT IS THE NAME OF THE DATA FILE"
      INPUT file$
REM   SAPNO$ = file$
      INPUT "DO YOU WANT TO DISPLAY DATA(Y-N)"; DUM$
      VIEW$ = UCASE$(DUM$)
      INPUT "DO YOU WANT TO PLOT DATA ON CRT SCREEN ?"; DUM$
      PLOT$ = UCASE$(DUM$)
REM   file$ = " c:\data\" + file$ + ".DAT"
      CLS
      CLS
      OPEN file$ FOR INPUT AS 3
      GOSUB 15010
      GOTO 15100
15010 INPUT #3, PROJ$ 'READ DISK FILE
      INPUT #3, MATD$
      INPUT #3, SPLNTH
      INPUT #3, TEMPF
      INPUT #3, DATE1$
      FOR I = 0 TO 5
      INPUT #3, C(I)'CAL FACTORS
```

```
      NEXT I
      INPUT #3, SAPER%, SP%, N%
      FOR I = 1 TO SAPER%
      INPUT #3, SKIPC&(I)
      NEXT I
      FOR I = 1 TO SAPER%
      PRINT SKIPC&(I)
      NEXT I
      FOR I = 0 TO N%
      INPUT #3, DATA1%(I)
      NEXT I
      RETURN
15100 PRINT "THERE ARE"; SAPER%; "CREEP CYCLES"
      test = 0
      CP = 1
      GOTO 4672
      FOR CN = 2 TO SAPER%
15150 GOSUB 15010
      CP = CP + 1      ' FOR CREEP TEST
      GOSUB 16000
      GOTO 4672 'PROCESS DATA
      NEXT CN
15200 CLOSE 3
16000 FOR I = 1 TO 10
      PMAXS(I) = 0
      PMINS(I) = 0
      VMAXS(I) = 0
      VMINS(I) = 0
      VDELTS%(I) = 0
      VBS(I) = 0
      VCS(I) = 0
      VABS(I) = 0
      HMAXS(I) = 0
      HMINS(I) = 0
      HDELTS%(I) = 0
      HBS(I) = 0
      HCS(I) = 0
      H1ABS(I) = 0
      H2ABS(I) = 0
      RMAXS(I) = 0
      RMINS(I) = 0
      RDELTS%(I) = 0
      RBS(I) = 0
      RCS(I) = 0
      R1ABS(I) = 0
      R2ABS(I) = 0
      DIV(I) = 0
      NEXT I
      RETURN
      END
17000 FOR WW1 = 0 TO 1080 STEP 120
      FOR LL1 = 0 TO 114 STEP 6
      II1 = WW1 + LL1 + J
      D0% = DATA1%(II1): D1% = DATA1%(II1 + 1)
      D2% = DATA1%(II1 + 2): D3% = DATA1%(II1 + 3)
      D4% = DATA1%(II1 + 4): D5% = DATA1%(II1 + 5)
      PRINT D0%; D1%; D2%; D3%; D4%; D5%; K; J; NEG%
      NEXT LL1
      DUM$ = INPUT$(1)
      NEXT WW1
      RETURN
18000 W3 = X * Q - B1 * W2 - B2 * W1
      FILL = W3 + A1 * W2 + W1
      W1 = W2
      W2 = W3
      WW2 = FILL - BB1 * WW1
      y = WW2 + AA1 * WW1
      WW1 = WW2
      RETURN
      END
```

APPENDIX B

APPENDIX B

The layer thicknesses and deflection data for the indicated 563 pavement locations are presented in this appendix.

Table B.1 Layer thicknesses and deflection data for the indicated test designation number.

Line	Test Desig.	Thickness (inches)				ESAL	Rut	Sensor Deflection (mils)						
No.	Number	AC	Concrete	Base	S.Base	(mill)	(in.)	D1	D2	D3	D4	D5	D6	D7
1	7112011	6.70	0.00	4.00	24.00	1.25	0.19	8.26	6.67	5.61	4.35	3.35	2.12	1.16
2	7122411	6.34	0.00	4.00	24.00	1.25	0.19	7.56	6.23	5.39	4.32	3.40	2.23	1.18
3	7137022	6.29	0.00	4.00	24.00	1.25	0.44	10.35	8.47	7.19	5.61	4.28	2.57	1.23
4	7127721	6.55	0.00	4.00	24.00	1.25	0.19	6.85	5.72	4.92	3.91	3.01	1.89	0.98
5	7128332	6.84	0.00	4.00	24.00	1.25	0.25	5.56	4.43	3.86	3.23	2.63	1.84	1.02
6	7131211	6.24	0.00	4.00	24.00	1.25	0.31	7.12	5.52	4.74	3.77	2.98	1.98	1.06
7	7141211	5.12	0.00	4.00	24.00	1.25	0.50	12.24	9.85	8.08	6.02	4.45	2.58	1.19
8	13156621	3.93	0.00	12.00	12.00	1.51	0.19	10.78	7.01	5.50	4.01	3.02	1.95	1.09
9	13142311	4.02	0.00	12.00	12.00	1.51	0.13	8.96	6.14	4.80	3.57	2.76	1.86	1.12
10	13132911	3.44	0.00	12.00	12.00	1.51	0.31	9.42	6.43	4.90	3.58	2.82	1.97	1.22
11	13117121	4.77	0.00	12.00	12.00	1.51	0.13	10.55	7.11	5.57	4.10	3.18	2.14	1.19
12	13126311	3.36	0.00	12.00	12.00	1.51	0.25	10.46	7.06	5.41	4.04	3.16	2.14	1.25
13	13142922	4.07	0.00	12.00	12.00	1.51	0.13	8.31	5.62	4.50	3.35	2.65	1.85	1.13
14	13151511	3.99	0.00	12.00	12.00	1.51	0.19	9.90	7.21	5.75	4.30	3.29	2.15	1.18
15	13164311	3.75	0.00	12.00	12.00	1.51	0.19	10.57	7.52	5.88	4.40	3.27	2.11	1.24
16	29172711	12.89	0.00	12.00	0.00	0.76	0.13	9.17	6.52	5.46	4.20	3.06	1.58	0.50
17	29117721	14.56	0.00	12.00	0.00	0.76	0.13	6.45	5.22	4.74	4.25	3.71	2.93	1.85
18	29186711	13.15	0.00	12.00	0.00	0.76	0.13	8.32	6.35	5.62	4.86	4.07	2.86	1.39
19	29111711	13.81	0.00	12.00	0.00	0.76	0.13	5.99	4.94	4.47	3.93	3.38	2.59	1.57
20	29134511	14.13	0.00	12.00	0.00	0.76	0.06	6.51	5.67	5.32	4.88	4.36	3.56	2.28
21	29146911	14.19	0.00	12.00	0.00	0.76	0.00	5.66	4.79	4.46	4.04	3.57	2.84	1.80

Table B.1 Layer thicknesses and deflection data for the indicated test designation number (continued).

Line	Test Desig.	Thickness (inches)				ESAL	Rut	Sensor Deflection (mils)						
No.	Number	AC	Concrete	Base	S.Base	(mill)	(in.)	D1	D2	D3	D4	D5	D6	D7
22	29176321	13.43	0.00	12.00	0.00	0.76	0.13	7.95	5.62	4.78	3.92	3.04	1.78	0.59
23	29183321	13.88	0.00	12.00	0.00	0.76	0.13	8.02	6.04	5.33	4.56	3.71	2.50	1.11
24	19118331	6.30	0.00	12.00	12.00	1.58	0.23	7.28	4.71	3.62	2.55	1.88	1.20	0.77
25	19141811	6.40	0.00	12.00	12.00	1.58	0.25	7.79	4.90	3.71	2.69	2.02	1.37	0.87
26	19132322	6.60	0.00	12.00	12.00	1.58	0.23	7.01	4.90	3.71	2.26	2.02	1.37	0.87
27	19150911	6.40	0.00	12.00	12.00	1.58	0.20	7.81	4.95	3.73	2.66	2.04	1.40	0.93
28	19131111	6.20	0.00	12.00	12.00	1.58	0.20	7.16	4.29	3.27	2.31	1.75	1.17	0.72
29	19113011	6.20	0.00	12.00	12.00	1.58	0.20	6.93	4.58	3.41	2.43	1.81	1.18	0.75
30	19121611	5.60	0.00	12.00	12.00	1.58	0.20	7.32	4.85	3.68	2.64	1.96	1.28	0.79
31	19128221	6.30	0.00	12.00	12.00	1.58	0.25	7.19	4.47	3.30	2.34	1.73	1.17	0.74
32	19137431	5.30	0.00	12.00	12.00	1.58	0.20	7.19	4.56	3.47	2.39	1.78	1.16	0.75
33	19148131	5.10	0.00	12.00	12.00	1.58	0.20	7.99	5.07	3.84	2.72	2.09	1.42	0.94
34	19161211	7.50	0.00	12.00	12.00	1.58	0.28	7.82	4.90	3.79	2.75	2.13	1.45	0.97
35	19169131	8.50	0.00	12.00	12.00	1.58	0.22	8.15	5.34	3.96	2.89	2.20	1.48	0.91
36	11257021	2.48	9.10	12.00	0.00	0.12	0.06	7.19	6.89	6.74	6.41	5.73	4.77	3.04
37	11245021	2.41	9.30	12.00	0.00	0.12	0.06	7.09	7.09	6.93	6.50	5.87	4.90	3.02
38	11265911	2.32	8.80	12.00	0.00	0.12	0.06	9.38	8.20	7.65	6.92	6.12	4.95	2.94
39	11227022	2.30	8.60	12.00	0.00	0.12	0.19	8.37	7.65	7.15	6.35	5.44	4.12	2.45
40	11241012	2.39	9.20	12.00	0.00	0.12	0.06	13.71	10.94	9.75	8.07	6.53	4.40	2.22
41	11222311	2.19	7.70	12.00	0.00	0.12	0.19	8.65	8.05	7.58	6.85	5.91	4.42	2.44
42	4233011	2.48	8.10	6.00	0.00	0.31	0.00	6.03	5.93	6.02	5.80	5.22	4.26	2.31

Table B.1 Layer thicknesses and deflection data for the indicated test designation number (continued).

Line No.	Test Desig. Number	Thickness (inches) AC	Concrete	Base	S.Base	ESAL (mill)	Rut (in.)	Sensor Deflection (mils) D1	D2	D3	D4	D5	D6	D7
43	4227622	2.58	8.00	6.00	0.00	0.31	0.00	4.10	3.88	3.81	3.59	3.23	2.66	1.48
44	43148341	10.66	0.00	6.00	18.00	0.76	0.38	6.49	5.34	4.69	3.95	3.12	2.00	0.91
45	43141611	10.01	0.00	6.00	18.00	0.76	0.38	5.96	5.16	4.65	3.91	3.12	2.02	1.01
46	43131911	10.84	0.00	6.00	18.00	0.76	0.38	5.66	2.82	4.35	3.80	3.09	2.08	0.99
47	43178112	10.40	0.00	6.00	18.00	0.76	0.06	7.16	5.84	5.09	4.16	3.28	2.04	0.94
48	43152311	9.60	0.00	6.00	18.00	0.76	0.38	7.02	5.83	5.23	4.43	3.52	2.28	1.04
49	43111711	10.62	0.00	6.00	18.00	0.76	0.19	6.59	5.35	4.73	3.98	3.17	2.12	1.06
50	43121811	10.25	0.00	6.00	18.00	0.76	0.25	5.98	5.17	4.66	3.93	3.16	2.06	0.94
51	43148333	10.50	0.00	6.00	18.00	0.76	0.38	7.10	5.64	4.50	3.91	3.05	1.94	0.93
52	43161411	11.00	0.00	6.00	18.00	0.76	0.38	7.07	5.84	5.17	4.31	3.44	2.21	1.09
53	43178521	9.50	0.00	6.00	18.00	0.76	0.06	7.27	5.93	5.19	4.29	3.36	2.08	0.93
54	43188121	10.00	0.00	6.00	18.00	0.76	0.06	7.03	5.71	4.99	4.07	3.20	1.99	0.90
55	43191411	10.25	0.00	6.00	18.00	0.76	0.13	6.86	5.70	5.03	4.15	3.30	2.08	0.95
56	35136221	5.82	0.00	6.00	18.00	1.37	0.30	8.06	6.26	5.13	3.83	2.92	1.85	1.10
57	35118931	6.04	0.00	6.00	18.00	1.37	0.18	7.74	5.81	4.62	3.48	2.66	1.74	1.01
58	35114222	5.28	0.00	6.00	18.00	1.37	0.15	8.07	5.95	4.76	3.49	2.63	1.69	1.00
59	35123311	6.29	0.00	6.00	18.00	1.37	0.13	7.42	5.63	4.57	3.47	2.62	1.63	0.91
60	35128321	5.05	0.00	6.00	18.00	1.37	0.13	7.86	5.93	4.79	3.61	2.75	1.77	0.99
61	35132611	5.28	0.00	6.00	18.00	1.37	0.18	9.21	6.77	5.27	3.81	2.81	1.78	1.11
62	35112211	6.25	0.00	6.00	18.00	1.37	0.15	7.92	6.21	5.07	3.84	2.86	1.77	0.98
63	35143911	7.25	0.00	6.00	18.00	1.37	0.15	8.63	6.83	5.64	4.37	3.40	2.22	1.28

Table B.1 Layer thicknesses and deflection data for the indicated test designation number (continued).

Line No.	Test Desig. Number	Thickness (inches) AC	Concrete	Base	S.Base	ESAL (mill)	Rut (in.)	Sensor Deflection (mils) D1	D2	D3	D4	D5	D6	D7
64	35152311	6.00	0.00	6.00	18.00	1.37	0.23	9.55	7.13	5.67	4.20	3.26	2.12	1.19
65	35159121	6.75	0.00	6.00	18.00	1.37	0.20	9.14	6.95	5.70	4.36	3.40	2.28	1.41
66	35161411	6.50	0.00	6.00	18.00	1.37	0.13	9.61	7.45	6.21	4.92	3.96	2.81	1.70
67	35167331	5.03	0.00	6.00	18.00	1.37	0.18	9.88	7.46	6.09	4.66	3.70	2.66	1.72
68	10131011	5.45	0.00	6.00	18.00	0.22	0.13	12.40	9.32	7.41	5.49	4.02	2.46	1.49
69	10128121	5.02	0.00	6.00	18.00	0.22	0.18	12.71	9.76	7.85	5.86	4.38	2.72	1.57
70	10136641	4.87	0.00	6.00	18.00	0.22	0.05	12.69	9.76	7.86	5.77	4.24	2.60	1.50
71	10118731	2.33	0.00	6.00	18.00	0.22	0.43	12.55	9.61	7.67	5.70	4.21	2.64	1.50
72	10117322	2.30	0.00	6.00	18.00	0.22	0.40	12.42	9.15	7.16	5.27	3.93	2.50	1.46
73	10111711	2.38	0.00	6.00	18.00	0.22	0.35	13.57	10.41	8.35	6.18	4.61	2.88	1.69
74	10131821	4.25	0.00	6.00	18.00	0.22	0.13	12.86	9.60	7.53	5.48	4.04	2.48	1.48
75	8213022	4.35	8.00	0.00	14.00	1.74	0.25	4.24	3.88	3.78	3.58	3.26	2.78	1.84
76	8260911	4.33	8.20	0.00	14.00	1.74	0.06	4.87	4.33	4.31	4.15	3.78	3.23	2.02
77	8261622	4.48	8.20	0.00	14.00	1.74	0.06	4.04	3.50	3.42	3.30	2.99	2.54	1.66
78	8221011	3.61	8.10	0.00	14.00	1.74	0.13	5.91	5.68	5.60	5.64	5.24	4.74	3.33
79	8231511	3.96	8.30	0.00	14.00	1.74	0.13	5.70	5.30	5.22	4.98	4.64	4.03	2.78
80	8251811	3.99	8.60	0.00	14.00	1.74	0.06	5.71	4.99	4.91	4.75	4.37	3.79	2.54
81	8211211	3.78	7.90	0.00	14.00	1.74	0.25	6.96	6.48	6.33	6.20	5.96	4.92	3.30
82	8241011	4.10	8.20	0.00	14.00	1.74	0.06	4.42	3.91	3.83	3.63	3.29	2.83	1.86
83	5258321	2.69	7.80	0.00	6.00	0.31	0.20	4.04	3.83	3.72	3.64	3.32	2.84	1.90
84	5229221	4.19	7.80	0.00	6.00	0.31	0.45	2.72	2.41	2.32	2.21	2.00	1.70	1.11

Table B.1 Layer thicknesses and deflection data for the indicated test designation number (continued).

Line	Test Desig.	Thickness (inches)				ESAL	Rut	Sensor Deflection (mils)						
No.	Number	AC	Concrete	Base	S.Base	(mill)	(in.)	D1	D2	D3	D4	D5	D6	D7
85	5241411	2.79	7.90	0.00	6.00	0.31	0.15	3.12	2.86	2.73	2.62	2.33	1.90	1.14
86	5261712	3.04	7.80	0.00	6.00	0.31	0.20	3.86	3.80	3.65	3.41	3.03	2.42	1.42
87	5218631	4.59	7.80	0.00	6.00	0.31	0.55	2.90	2.56	2.48	2.37	2.19	1.88	1.26
88	1251611	8.81	8.50	0.00	16.00	3.11	0.63	5.63	4.07	3.87	3.63	3.34	2.90	1.99
89	1261611	8.42	8.20	0.00	16.00	3.11	0.44	5.00	3.44	3.17	2.98	2.70	2.35	1.64
90	1284611	8.52	8.10	0.00	16.00	3.11	0.31	5.55	4.15	3.99	3.87	3.60	3.20	2.21
91	1272411	8.52	8.70	0.00	16.00	3.11	0.31	5.67	4.16	3.97	3.77	3.48	3.01	1.98
92	1248931	10.61	8.90	0.00	16.00	3.11	0.56	3.87	3.25	3.04	2.85	2.54	2.11	1.49
93	1232611	9.82	9.10	0.00	16.00	3.11	0.19	3.52	2.82	2.67	2.59	2.40	2.14	1.56
94	1221711	10.62	8.90	0.00	16.00	3.11	0.38	3.37	2.54	2.42	2.31	2.15	1.93	1.40
95	1214111	10.10	9.00	0.00	16.00	3.11	0.31	4.80	3.80	3.55	3.34	3.06	2.64	1.87
96	14151513	3.05	0.00	18.00	6.00	0.18	0.40	16.09	11.86	9.10	6.23	4.48	2.66	1.47
97	14161813	3.13	0.00	18.00	6.00	0.18	0.18	14.77	10.93	8.28	5.85	4.28	2.71	1.45
98	14155123	2.83	0.00	18.00	6.00	0.18	0.40	17.11	12.60	9.67	6.72	4.76	2.77	1.50
99	14121713	2.54	0.00	18.00	6.00	0.18	0.18	17.91	13.37	10.31	7.27	4.96	2.75	1.47
100	14113023	2.69	0.00	18.00	6.00	0.18	0.50	18.18	13.24	9.88	6.52	4.50	2.57	1.47
101	14148233	2.80	0.00	18.00	6.00	0.18	0.00	15.09	11.64	9.18	6.68	5.04	3.28	1.81
102	14124223	2.50	0.00	18.00	6.00	0.18	0.40	25.31	18.11	13.39	8.66	5.59	2.81	1.62
103	14137831	2.44	0.00	18.00	6.00	0.18	0.10	18.86	14.15	11.02	8.32	6.51	4.29	2.22
104	14143711	2.32	0.00	18.00	6.00	0.18	0.10	18.21	13.57	10.47	7.63	5.90	3.92	2.18
105	111	2.25	0	8	3	0.76	1.07	12.36	8.62	6.41	4.37	3.25	2.19	1.35

Table B.1 Layer thicknesses and deflection data for the indicated test designation number (continued).

Line	Test Desig.	Thickness (inches)				ESAL	Rut	Sensor Deflection (mils)						
No.	Number	AC	Concrete	Base	S.Base	(mill)	(in.)	D1	D2	D3	D4	D5	D6	D7
106	20	2.25	0	8	3	0.76	1.07	13.71	8.76	6.48	4.40	3.27	2.19	1.33
107	40	2.25	0	8	3	0.76	0.92	13.30	8.16	5.82	4.14	3.16	2.14	1.36
108	60	2.25	0	8	3	0.76	0.77	13.37	9.00	6.58	4.46	3.39	2.26	1.38
109	80	2.25	0	8	3	0.76	0.77	15.14	10.17	7.27	4.80	3.53	2.35	1.46
110	112	2.25	0	8	3	0.76	0.92	12.54	8.55	6.02	3.86	2.92	1.95	1.21
111	20	2.25	0	8	3	0.76	0.92	12.43	8.15	5.76	3.92	2.98	2.05	1.26
112	40	2.25	0	8	3	0.76	0.98	13.56	8.71	6.10	4.06	2.99	2.01	1.22
113	60	2.25	0	8	3	0.76	1.05	14.79	9.60	6.58	4.32	3.17	2.14	1.34
114	80	2.25	0	8	3	0.76	1.05	14.35	8.99	6.40	4.38	3.20	2.22	1.38
115	113	2.25	0	8	3	0.76	1.10	12.81	8.62	6.34	4.36	3.14	2.86	2.02
116	20	2.25	0	8	3	0.76	1.10	12.55	8.57	6.09	4.13	3.07	2.14	1.37
117	40	2.25	0	8	3	0.76	1.07	14.63	9.98	7.16	4.82	3.55	2.40	1.45
118	60	2.25	0	8	3	0.76	1.05	14.26	9.06	6.38	4.13	3.09	2.11	1.37
119	80	2.25	0	8	3	0.76	1.05	13.72	9.16	6.40	4.25	3.16	2.14	1.35
120	411	2.25	0	4	14	2.03	0.20	10.65	7.71	6.16	4.80	3.93	2.97	1.95
121	20	2.25	0	4	14	2.03	0.20	10.46	7.72	6.17	4.73	3.85	2.84	1.86
122	40	2.25	0	4	14	2.03	0.30	10.43	7.39	5.95	4.73	3.75	2.85	1.99
123	60	2.25	0	4	14	2.03	0.40	10.51	7.58	6.09	4.64	3.79	2.84	1.89
124	80	2.25	0	4	14	2.03	0.40	11.09	8.09	6.53	5.05	4.13	3.08	2.00
125	412	2.25	0	4	14	2.03	0.35	12.03	9.30	7.69	6.02	4.97	3.66	2.26
126	20	2.25	0	4	14	2.03	0.35	12.00	9.18	7.52	5.88	4.76	3.40	2.06

Table B.1 Layer thicknesses and deflection data for the indicated test designation number (continued).

Line	Test Desig.	Thickness (inches)				ESAL	Rut	Sensor Deflection (mils)						
No.	Number	AC	Concrete	Base	S.Base	(mill)	(in.)	D1	D2	D3	D4	D5	D6	D7
127	40	2.25	0	4	14	2.03	0.35	10.93	8.28	6.75	5.18	4.23	3.11	2.00
128	60	2.25	0	4	14	2.03	0.35	10.20	7.58	6.10	4.62	3.74	2.77	1.84
129	80	2.25	0	4	14	2.03	0.35	9.85	7.43	6.05	4.72	3.91	2.97	1.96
130	413	2.25	0	4	14	2.03	0.18	9.76	6.85	5.59	4.13	3.48	2.61	1.76
131	20	2.25	0	4	14	2.03	0.18	9.69	7.02	5.50	4.10	3.25	2.38	1.68
132	40	2.25	0	4	14	2.03	0.27	10.04	7.11	5.56	4.19	3.93	2.52	1.67
133	60	2.25	0	4	14	2.03	0.35	9.33	6.81	5.39	4.11	3.36	2.54	1.74
134	80	2.25	0	4	14	2.03	0.35	10.12	7.33	5.85	4.40	3.49	2.62	1.73
135	511	2.25	0	12	12	0.64	0.22	16.95	13.68	11.21	8.74	6.86	4.54	2.40
136	20	2.25	0	12	12	0.64	0.22	16.07	13.11	10.81	8.41	6.64	4.47	2.43
137	40	2.25	0	12	12	0.64	0.18	15.59	12.66	10.44	8.18	6.51	4.37	2.42
138	60	2.25	0	12	12	0.64	0.15	15.98	12.98	10.55	8.23	6.56	4.43	2.42
139	80	2.25	0	12	12	0.64	0.15	16.21	13.18	10.78	8.49	6.69	4.57	2.46
140	512	2.25	0	12	12	0.64	0.12	15.28	12.54	10.09	7.79	6.18	4.22	2.33
141	20	2.25	0	12	12	0.64	0.12	15.29	12.16	9.61	7.28	5.74	3.90	2.08
142	40	2.25	0	12	12	0.64	0.12	14.72	11.80	9.42	7.29	5.76	3.91	2.13
143	60	2.25	0	12	12	0.64	0.12	15.93	12.64	9.96	7.63	6.05	4.10	2.23
144	80	2.25	0	12	12	0.64	0.12	15.67	12.88	10.20	7.73	6.21	4.20	2.32
145	513	2.25	0	12	12	0.64	0.15	15.52	12.49	10.18	7.95	6.32	4.33	2.40
146	20	2.25	0	12	12	0.64	0.15	15.53	12.75	10.49	8.17	6.54	4.45	2.43
147	40	2.25	0	12	12	0.64	0.17	15.23	12.39	10.18	8.00	6.37	4.35	2.40

Table B.1 Layer thicknesses and deflection data for the indicated test designation number (continued).

Line	Test Desig.	Thickness (inches)				ESAL	Rut	Sensor Deflection (mils)						
No.	Number	AC	Concrete	Base	S.Base	(mill)	(in.)	D1	D2	D3	D4	D5	D6	D7
148	60	2.25	0	12	12	0.64	0.18	15.60	12.73	10.75	8.48	6.75	4.56	2.46
149	80	2.25	0	12	12	0.64	0.18	15.80	12.76	10.44	8.22	6.59	4.51	2.50
150	1211	4.17	0	8	28	7.18	0.31	8.44	6.09	4.64	3.05	2.05	1.13	0.61
151	20	4.17	0	8	28	7.18	0.31	8.72	6.24	4.63	2.93	1.97	1.06	0.61
152	40	4.17	0	8	28	7.18	0.34	8.57	6.22	4.70	3.07	2.05	1.08	0.60
153	60	4.17	0	8	28	7.18	0.38	8.64	6.28	4.74	3.13	2.12	1.15	0.63
154	80	4.17	0	8	28	7.18	0.38	9.14	6.43	4.84	3.10	2.09	1.13	0.63
155	1212	4.17	0	8	28	7.18	0.25	10.68	6.57	4.90	3.18	2.13	1.16	0.66
156	20	4.17	0	8	28	7.18	0.25	8.51	6.14	4.58	2.99	2.00	1.11	0.67
157	40	4.17	0	8	28	7.18	0.28	8.06	5.68	4.25	2.80	1.93	1.10	0.65
158	60	4.17	0	8	28	7.18	0.31	8.28	5.86	4.41	2.89	1.94	1.09	0.64
159	80	4.17	0	8	28	7.18	0.31	8.58	6.03	4.48	2.87	1.94	1.05	0.63
160	1213	4.17	0	8	28	7.18	0.25	8.44	6.00	4.45	2.90	1.98	1.08	0.63
161	20	4.17	0	8	28	7.18	0.25	8.48	5.94	4.36	2.86	1.95	1.11	0.65
162	40	4.17	0	8	28	7.18	0.25	8.35	5.91	4.41	2.89	1.98	1.15	0.73
163	60	4.17	0	8	28	7.18	0.25	8.33	5.83	4.35	2.85	1.96	1.11	0.69
164	80	4.17	0	8	28	7.18	0.25	8.73	6.22	4.54	2.95	2.01	1.16	0.70
165	1214	4.17	0	8	28	7.18	0.38	9.71	7.26	5.68	4.03	2.92	1.82	1.12
166	20	4.17	0	8	28	7.18	0.38	8.97	6.63	5.03	3.44	2.47	1.54	0.96
167	40	4.17	0	8	28	7.18	0.31	9.35	6.82	5.20	3.57	2.54	1.58	0.98
168	60	4.17	0	8	28	7.18	0.25	9.67	7.13	5.61	3.97	2.93	1.85	1.07

Table B.1 Layer thicknesses and deflection data for the indicated test designation number (continued).

Line	Test Desig.	Thickness (inches)				ESAL	Rut	Sensor Deflection (mils)						
No.	Number	AC	Concrete	Base	S.Base	(mill)	(in.)	D1	D2	D3	D4	D5	D6	D7
169	80	4.17	0	8	28	7.18	0.25	9.32	6.86	5.24	3.65	2.59	1.58	0.95
170	1215	4.17	0	8	28	7.18	0.25	9.17	6.70	5.17	3.55	2.57	1.59	0.96
171	20	4.17	0	8	28	7.18	0.25	9.02	6.58	5.08	3.53	2.57	1.59	0.94
172	40	4.17	0	8	28	7.18	0.22	9.18	6.65	5.06	3.41	2.43	1.47	0.90
173	60	4.17	0	8	28	7.18	0.19	9.23	6.69	5.05	3.34	2.35	1.39	0.82
174	80	4.17	0	8	28	7.18	0.19	9.15	6.63	5.06	3.32	2.35	1.42	0.87
175	1216	4.17	0	8	28	7.18	0.25	9.18	6.73	5.11	3.43	2.45	1.54	0.96
176	20	4.17	0	8	28	7.18	0.25	9.26	6.77	5.11	3.41	2.42	1.46	0.91
177	40	4.17	0	8	28	7.18	0.11	9.05	6.47	4.90	3.23	2.24	1.31	0.78
178	60	4.17	0	8	28	7.18	0.19	9.25	6.65	5.02	3.35	2.36	1.38	0.78
179	80	4.17	0	8	28	7.18	0.19	9.34	6.77	5.12	3.40	2.35	1.37	0.77
180	1513	6.42	0	8	28	1.90	0.12	7.46	5.86	5.11	4.06	3.29	2.30	1.42
181	20	6.42	0	8	28	1.90	0.12	7.72	6.10	5.25	4.23	3.35	2.21	1.37
182	40	6.42	0	8	28	1.90	0.13	8.30	6.30	5.33	4.25	3.38	2.32	1.43
183	60	6.42	0	8	28	1.90	0.15	9.11	7.19	6.11	4.43	3.40	2.24	1.40
184	80	6.42	0	8	28	1.90	0.15	8.49	6.33	5.37	4.22	3.34	2.29	1.40
185	1512	6.42	0	8	28	1.90	0.12	7.66	6.03	5.23	4.26	3.34	2.25	1.39
186	20	6.42	0	8	28	1.90	0.12	8.10	6.48	5.65	4.65	3.78	2.61	1.40
187	40	6.42	0	8	28	1.90	0.11	8.07	6.12	4.96	3.82	2.96	2.00	1.28
188	60	6.42	0	8	28	1.90	0.10	8.06	5.97	5.06	3.84	3.01	2.08	1.31
189	80	6.42	0	8	28	1.90	0.10	7.77	5.86	4.99	3.93	3.12	2.16	1.38

Table B.1 Layer thicknesses and deflection data for the indicated test designation number (continued).

Line	Test Desig.	Thickness (inches)				ESAL	Rut	Sensor Deflection (mils)						
No.	Number	AC	Concrete	Base	S.Base	(mill)	(in.)	D1	D2	D3	D4	D5	D6	D7
190	1511	6.42	0	8	28	1.90	0.20	8.04	5.87	4.98	3.98	3.11	2.14	1.38
191	20	6.42	0	8	28	1.90	0.20	7.82	5.78	4.87	3.86	3.04	2.11	1.35
192	40	6.42	0	8	28	1.90	0.16	7.54	5.66	4.77	3.80	2.96	2.03	1.31
193	60	6.42	0	8	28	1.90	0.12	7.83	5.82	4.92	3.81	3.01	2.05	1.27
194	80	6.42	0	8	28	1.90	0.12	8.31	6.02	4.99	3.81	2.99	2.00	1.27
195	1611	4.18	0	8	28	1.97	0.06	11.31	9.08	7.18	5.06	3.78	2.46	1.47
196	20	4.18	0	8	28	1.97	0.06	11.06	8.49	6.90	5.14	3.89	2.56	1.51
197	40	4.18	0	8	28	1.97	0.13	12.71	9.48	7.17	4.97	3.80	2.58	1.57
198	60	4.18	0	8	28	1.97	0.19	11.87	9.07	7.21	5.37	4.14	2.77	1.61
199	80	4.18	0	8	28	1.97	0.19	12.23	9.63	7.74	5.64	4.34	2.78	1.58
200	1612	4.18	0	8	28	1.97	0.12	11.67	9.13	7.48	5.53	4.28	2.78	1.59
201	20	4.18	0	8	28	1.97	0.12	11.87	9.22	7.45	5.56	4.21	2.74	1.56
202	40	4.18	0	8	28	1.97	0.12	11.95	9.19	7.34	5.37	4.08	2.66	1.54
203	60	4.18	0	8	28	1.97	0.12	12.24	8.98	6.94	4.91	3.78	2.58	1.53
204	80	4.18	0	8	28	1.97	0.12	11.81	9.04	7.25	5.25	4.07	2.71	1.59
205	1613	4.18	0	8	28	1.97	0.19	12.26	9.36	7.52	5.53	4.22	2.78	1.61
206	20	4.18	0	8	28	1.97	0.19	12.83	9.68	7.46	5.03	3.77	2.51	1.52
207	40	4.18	0	8	28	1.97	0.16	12.44	9.10	6.91	4.97	3.91	2.75	1.64
208	60	4.18	0	8	28	1.97	0.12	11.94	8.70	6.56	4.45	3.43	2.34	1.45
209	80	4.18	0	8	28	1.97	0.12	11.10	8.08	6.25	4.50	3.47	2.39	1.49
210	1711	6.25	0	4	18	1.75	0.38	7.77	6.64	5.96	5.07	4.14	2.80	1.32

Table B.1 Layer thicknesses and deflection data for the indicated test designation number (continued).

Line No.	Test Desig. Number	Thickness (inches) AC	Concrete	Base	S.Base	ESAL (mill)	Rut (in.)	Sensor Deflection (mils) D1	D2	D3	D4	D5	D6	D7
211	20	6.25	0	4	18	1.75	0.38	7.34	6.34	5.71	4.84	3.97	2.70	1.30
212	40	6.25	0	4	18	1.75	0.41	7.43	6.38	5.71	4.83	4.02	2.74	1.33
213	60	6.25	0	4	18	1.75	0.44	7.76	6.66	6.00	5.07	4.14	2.80	1.37
214	80	6.25	0	4	18	1.75	0.44	7.94	6.82	6.17	5.24	4.31	2.92	1.45
215	1712	6.25	0	4	18	1.75	0.50	8.05	6.84	6.11	5.20	4.25	2.82	1.40
216	20	6.25	0	4	18	1.75	0.50	7.82	6.76	6.05	5.15	4.25	2.88	1.42
217	40	6.25	0	4	18	1.75	0.47	7.35	6.31	5.71	4.89	4.02	2.75	1.36
218	60	6.25	0	4	18	1.75	0.44	8.27	6.93	6.13	5.15	4.21	2.80	1.35
219	80	6.25	0	4	18	1.75	0.44	8.20	6.98	6.19	5.22	4.21	2.77	1.27
220	1713	6.25	0	4	18	1.75	0.25	8.03	6.91	6.13	5.14	4.16	2.74	1.26
221	20	6.25	0	4	18	1.75	0.25	7.59	6.48	5.75	4.77	3.87	2.54	1.19
222	40	6.25	0	4	18	1.75	0.37	7.17	6.09	5.38	4.50	3.62	2.38	1.15
223	60	6.25	0	4	18	1.75	0.50	7.32	6.09	5.43	4.53	3.68	2.48	1.24
224	80	6.25	0	4	18	1.75	0.50	6.88	5.73	5.13	4.32	3.51	2.39	1.27
225	1811	6.42	0	8	28	1.90	0.10	8.15	6.68	5.94	4.97	4.20	3.00	1.75
226	20	6.42	0	8	28	1.90	0.10	9.04	7.46	6.56	5.53	4.51	3.11	1.75
227	40	6.42	0	8	28	1.90	0.11	8.06	6.80	5.96	5.02	4.16	2.96	1.69
228	60	6.42	0	8	28	1.90	0.12	8.90	7.32	6.30	5.14	4.25	2.99	1.72
229	80	6.42	0	8	28	1.90	0.12	8.30	6.77	5.85	4.84	3.98	2.83	1.65
230	1812	6.42	0	8	28	1.90	0.10	8.15	6.65	5.81	4.78	3.98	2.78	1.52
231	20	6.42	0	8	28	1.90	0.10	7.85	6.46	5.68	4.71	3.88	2.68	1.54

Table B.1 Layer thicknesses and deflection data for the indicated test designation number (continued).

Line No.	Test Desig. Number	Thickness (inches)				ESAL (mill)	Rut (in.)	Sensor Deflection (mils)						
		AC	Concrete	Base	S.Base			D1	D2	D3	D4	D5	D6	D7
232	40	6.42	0	8	28	1.90	0.12	7.50	6.23	5.54	4.68	3.93	2.80	1.60
233	60	6.42	0	8	28	1.90	0.15	9.02	7.69	6.77	5.54	4.45	3.08	1.79
234	80	6.42	0	8	28	1.90	0.15	9.49	7.81	6.87	5.64	4.65	3.29	1.92
235	1813	6.42	0	8	28	1.90	0.15	9.85	8.16	7.13	5.88	4.88	3.50	2.01
236	20	6.42	0	8	28	1.90	0.15	12.60	9.64	8.27	6.78	5.49	3.73	2.01
237	40	6.42	0	8	28	1.90	0.13	9.30	7.67	6.75	5.69	4.74	3.44	2.03
238	60	6.42	0	8	28	1.90	0.10	9.82	8.24	7.26	5.69	4.60	3.16	1.77
239	80	6.42	0	8	28	1.90	0.10	9.42	7.79	6.92	5.84	4.89	3.54	1.76
240	2311	3.83	0	10	21	0.12	0.08	12.91	9.98	7.69	5.67	4.44	3.08	1.88
241	20	3.83	0	10	21	0.12	0.08	12.57	9.82	7.33	5.44	4.26	3.01	1.82
242	40	3.83	0	10	21	0.12	0.09	12.67	10.06	7.96	5.94	4.66	3.22	1.92
243	60	3.83	0	10	21	0.12	0.10	12.98	10.24	8.32	6.25	4.85	3.29	1.93
244	80	3.83	0	10	21	0.12	0.10	13.86	10.90	8.63	6.43	5.06	3.54	2.04
245	2312	3.83	0	10	21	0.12	0.08	12.75	9.78	7.81	5.79	4.53	3.13	1.84
246	20	3.83	0	10	21	0.12	0.08	14.58	11.27	9.12	6.91	5.46	3.75	2.13
247	40	3.83	0	10	21	0.12	0.08	13.04	9.40	7.30	5.19	4.01	2.77	1.66
248	60	3.83	0	10	21	0.12	0.08	15.69	12.29	9.90	7.45	5.78	3.85	2.18
249	2313	3.83	0	10	21	0.12	0.08	13.86	10.68	8.44	6.23	4.85	3.36	2.00
250	0	3.83	0	10	21	0.12	0.12	14.66	11.15	8.98	6.70	5.24	3.67	2.19
251	20	3.83	0	10	21	0.12	0.12	12.60	9.47	7.36	5.29	4.06	2.77	1.68
252	40	3.83	0	10	21	0.12	0.15	12.03	9.00	6.99	4.93	3.67	2.37	1.43

Table B.1 Layer thicknesses and deflection data for the indicated test designation number (continued).

Line	Test Desig.	Thickness (inches)				ESAL	Rut	Sensor Deflection (mils)						
No.	Number	AC	Concrete	Base	S.Base	(mill)	(in.)	D1	D2	D3	D4	D5	D6	D7
253	60	3.83	0	10	21	0.12	0.18	12.20	8.90	6.86	4.91	3.67	2.42	1.49
254	80	3.83	0	10	21	0.12	0.18	12.39	9.08	7.08	5.09	3.87	2.59	1.58
255	2411	10.36	0	6	10	3.97	0.06	7.03	5.54	4.93	4.19	3.47	2.30	1.06
256	20	10.36	0	6	10	3.97	0.06	6.57	5.58	5.12	4.53	3.88	2.92	1.52
257	40	10.36	0	6	10	3.97	0.06	5.92	5.05	4.65	4.10	3.51	2.60	1.36
258	60	10.36	0	6	10	3.97	0.06	5.86	4.75	4.25	3.69	3.04	2.11	0.97
259	80	10.36	0	6	10	3.97	0.06	6.60	5.12	4.55	3.91	3.17	2.12	0.87
260	2412	10.36	0	6	10	3.97	0.06	6.14	4.88	4.34	3.67	2.98	1.98	0.84
261	20	10.36	0	6	10	3.97	0.06	5.56	4.69	4.24	3.62	2.98	2.03	0.89
262	40	10.36	0	6	10	3.97	0.06	5.66	4.77	4.29	3.67	2.98	2.03	0.88
263	60	10.36	0	6	10	3.97	0.06	7.05	5.64	4.97	4.21	3.39	2.20	0.94
264	80	10.36	0	6	10	3.97	0.06	9.33	6.78	5.41	4.21	3.30	2.03	0.84
265	2413	10.36	0	6	10	3.97	0.12	9.66	6.53	5.25	4.04	3.12	1.87	0.73
266	20	10.36	0	6	10	3.97	0.12	6.67	5.19	4.50	3.70	2.92	1.86	0.78
267	40	10.36	0	6	10	3.97	0.12	6.22	5.05	4.46	3.77	3.04	1.99	0.88
268	60	10.36	0	6	10	3.97	0.12	6.07	4.95	4.42	3.83	3.16	2.17	1.04
269	80	10.36	0	6	10	3.97	0.12	5.38	4.34	3.90	3.41	2.84	2.02	1.04
270	2514	4.18	0	8	28	1.97	0.12	6.48	5.18	4.55	3.74	3.04	2.04	0.97
271	20	4.18	0	8	28	1.97	0.12	6.43	5.02	4.38	3.58	2.92	1.97	0.96
272	40	4.18	0	8	28	1.97	0.09	6.99	5.45	4.72	3.81	3.12	2.12	1.13
273	60	4.18	0	8	28	1.97	0.06	6.30	5.08	4.45	3.66	3.05	2.12	1.20

Table B.1 Layer thicknesses and deflection data for the indicated test designation number (continued).

Line	Test Desig.	Thickness (inches)				ESAL	Rut	Sensor Deflection (mils)						
No.	Number	AC	Concrete	Base	S.Base	(mill)	(in.)	D1	D2	D3	D4	D5	D6	D7
274	80	4.18	0	8	28	1.97	0.06	6.41	5.20	4.57	3.79	3.15	2.21	1.20
275	2513	4.18	0	8	28	1.97	0.12	7.49	6.19	5.27	3.88	2.99	2.01	1.14
276	20	4.18	0	8	28	1.97	0.12	9.45	6.76	5.66	4.38	3.47	2.29	1.26
277	40	4.18	0	8	28	1.97	0.09	11.30	7.91	6.30	4.63	3.68	2.49	1.46
278	60	4.18	0	8	28	1.97	0.06	8.23	6.64	5.81	4.72	3.88	2.69	1.52
279	80	4.18	0	8	28	1.97	0.06	8.40	7.05	6.07	4.72	3.56	2.38	1.40
280	2512	4.18	0	8	28	1.97	0	7.88	6.41	5.58	4.57	3.71	2.54	1.38
281	20	4.18	0	8	28	1.97	0	10.36	7.21	5.70	4.22	3.37	2.30	1.34
282	40	4.18	0	8	28	1.97	0.03	7.95	6.52	5.72	4.73	3.93	2.75	1.52
283	60	4.18	0	8	28	1.97	0.06	9.62	7.80	6.85	5.57	4.55	3.14	1.72
284	80	4.18	0	8	28	1.97	0.06	10.87	8.19	7.07	5.65	4.61	3.15	1.69
285	2511	4.18	0	8	28	1.97	0.06	8.56	6.69	5.94	4.78	3.95	2.79	1.65
286	20	4.18	0	8	28	1.97	0.06	8.44	6.75	5.84	4.74	3.87	2.69	1.61
287	40	4.18	0	8	28	1.97	0.06	10.33	7.24	5.97	4.51	3.61	2.45	1.44
288	60	4.18	0	8	28	1.97	0.06	9.03	7.07	5.99	4.69	3.74	2.53	1.44
289	80	4.18	0	8	28	1.97	0.06	9.60	7.40	6.29	4.93	3.88	2.53	1.38
290	2711	5.68	0	4	18	0.93	0.45	6.69	5.08	4.29	3.37	2.61	1.69	0.93
291	20	5.68	0	4	18	0.93	0.45	6.93	5.09	4.24	3.39	2.59	1.66	0.92
292	40	5.68	0	4	18	0.93	0.45	6.93	5.08	4.30	3.33	2.57	1.63	0.90
293	60	5.68	0	4	18	0.93	0.45	7.14	5.37	4.52	3.51	2.68	1.70	0.95
294	80	5.68	0	4	18	0.93	0.45	7.21	5.28	4.48	3.49	2.70	1.71	0.99

Table B.1 Layer thicknesses and deflection data for the indicated test designation number (continued).

Line	Test Desig.	Thickness (inches)				ESAL	Rut	Sensor Deflection (mils)						
No.	Number	AC	Concrete	Base	S.Base	(mill)	(in.)	D1	D2	D3	D4	D5	D6	D7
295	2712	5.68	0	4	18	0.93	0.4	7.33	5.31	4.41	3.44	2.64	1.66	0.94
296	20	5.68	0	4	18	0.93	0.4	6.94	4.96	4.15	3.23	2.50	1.61	0.92
297	40	5.68	0	4	18	0.93	0.38	6.85	5.11	4.39	3.51	2.75	1.75	0.92
298	60	5.68	0	4	18	0.93	0.35	6.62	4.86	4.08	3.19	2.46	1.57	0.86
299	80	5.68	0	4	18	0.93	0.35	7.01	5.31	4.52	3.58	2.71	1.73	0.93
300	2713	5.68	0	4	18	0.93	0.45	6.78	5.00	4.26	3.40	2.61	1.67	0.92
301	20	5.68	0	4	18	0.93	0.45	6.90	5.16	4.36	3.39	2.60	1.68	0.94
302	40	5.68	0	4	18	0.93	0.37	7.21	5.50	4.75	3.72	2.95	1.86	0.90
303	60	5.68	0	4	18	0.93	0.28	6.72	5.03	4.26	3.31	2.57	1.68	0.96
304	80	5.68	0	4	18	0.93	0.28	7.00	5.21	4.43	3.49	2.72	1.80	1.03
305	3011	7.92	0	8	4	1.62	0.18	7.68	5.39	4.12	2.91	2.14	1.30	0.76
306	20	7.92	0	8	4	1.62	0.18	7.69	5.12	3.98	2.80	2.07	1.31	0.75
307	40	7.92	0	8	4	1.62	0.17	7.66	5.16	4.02	2.79	2.05	1.23	0.72
308	60	7.92	0	8	4	1.62	0.15	7.78	5.38	4.11	2.82	2.11	1.28	0.74
309	80	7.92	0	8	4	1.62	0.15	7.83	5.42	4.18	2.90	2.13	1.31	0.75
310	3012	7.92	0	8	4	1.62	0.15	7.96	5.37	4.10	2.88	2.10	1.31	0.78
311	20	7.92	0	8	4	1.62	0.15	8.20	5.43	4.18	2.94	2.16	1.37	0.83
312	40	7.92	0	8	4	1.62	0.18	8.00	5.64	4.32	3.09	2.24	1.43	0.85
313	60	7.92	0	8	4	1.62	0.2	8.01	5.62	4.30	3.06	2.26	1.43	0.87
314	80	7.92	0	8	4	1.62	0.2	8.16	5.50	4.21	2.90	2.16	1.38	0.81
315	3013	7.92	0	8	4	1.62	0.2	8.04	5.27	3.98	2.77	2.03	1.27	0.77

Table B.1 Layer thicknesses and deflection data for the indicated test designation number (continued).

Line No.	Test Desig. Number	Thickness (inches)				ESAL (mill)	Rut (in.)	Sensor Deflection (mils)						
		AC	Concrete	Base	S.Base			D1	D2	D3	D4	D5	D6	D7
316	20	7.92	0	8	4	1.62	0.2	8.11	5.57	4.29	3.04	2.23	1.34	0.77
317	40	7.92	0	8	4	1.62	0.16	8.24	5.51	4.28	2.97	2.13	1.28	0.73
318	60	7.92	0	8	4	1.62	0.12	7.88	5.23	3.91	2.72	1.95	1.19	0.71
319	80	7.92	0	8	4	1.62	0.12	8.17	5.38	4.10	2.84	2.02	1.27	0.71
320	3211	7.25	0	4	18	1.81	0.02	8.93	6.74	5.79	4.70	3.71	2.46	1.36
321	20	7.25	0	4	18	1.81	0.02	8.92	6.61	5.82	4.68	3.68	2.40	1.31
322	40	7.25	0	4	18	1.81	0.02	8.43	6.46	5.77	4.55	3.54	2.37	1.29
323	60	7.25	0	4	18	1.81	0.02	9.04	6.86	6.02	4.82	3.77	2.47	1.37
324	80	7.25	0	4	18	1.81	0.02	9.12	6.73	5.78	4.71	3.75	2.48	1.40
325	3212	7.25	0	4	18	1.81	0.08	8.90	6.61	5.69	4.55	3.52	2.32	1.33
326	20	7.25	0	4	18	1.81	0.08	8.41	5.86	5.81	4.62	3.61	2.30	1.25
327	40	7.25	0	4	18	1.81	0.09	9.75	7.08	6.10	4.84	3.72	2.37	1.25
328	60	7.25	0	4	18	1.81	0.1	7.46	5.60	5.05	4.33	3.55	2.49	1.35
329	80	7.25	0	4	18	1.81	0.1	7.14	5.10	4.56	4.04	3.38	2.44	1.34
330	3213	7.25	0	4	18	1.81	0.05	8.28	6.02	5.18	4.27	3.36	2.25	1.26
331	20	7.25	0	4	18	1.81	0.05	8.64	6.19	5.27	4.25	3.36	2.22	1.24
332	40	7.25	0	4	18	1.81	0.065	8.54	6.06	5.12	4.23	3.33	2.24	1.25
333	60	7.25	0	4	18	1.81	0.08	7.49	5.82	5.11	4.20	3.34	2.26	1.28
334	80	7.25	0	4	18	1.81	0.08	8.29	5.92	5.22	4.26	3.40	2.28	1.27
335	3214	7.25	0	4	18	1.81	0.08	7.56	5.68	4.91	4.05	3.27	2.23	1.25
336	20	7.25	0	4	18	1.81	0.08	8.29	5.97	5.15	4.26	3.37	2.25	1.21

Table B.1 Layer thicknesses and deflection data for the indicated test designation number (continued).

Line No.	Test Desig. Number	Thickness (inches) AC	Concrete	Base	S.Base	ESAL (mill)	Rut (in.)	Sensor Deflection (mils) D1	D2	D3	D4	D5	D6	D7
337	40	7.25	0	4	18	1.81	0.1	9.22	6.74	5.66	4.55	3.56	2.31	1.19
338	60	7.25	0	4	18	1.81	0.12	9.11	6.58	5.42	4.41	3.41	2.19	1.15
339	80	7.25	0	4	18	1.81	0.12	8.95	6.56	5.53	4.38	3.38	2.15	1.12
340	3215	7.25	0	4	18	1.81	0.1	8.56	6.08	5.19	4.13	3.18	2.07	1.14
341	20	7.25	0	4	18	1.81	0.1	8.98	6.22	5.22	4.18	3.22	2.07	1.12
342	40	7.25	0	4	18	1.81	0.1	9.10	6.25	5.12	4.04	3.15	2.05	1.12
343	60	7.25	0	4	18	1.81	0.1	9.05	6.34	5.11	4.00	3.15	2.06	1.12
344	80	7.25	0	4	18	1.81	0.1	9.28	6.50	5.39	4.18	3.25	2.05	1.09
345	3315	6.00	0	4	18	1.25	0.19	7.30	5.65	4.76	3.64	2.77	1.80	1.07
346	20	6.00	0	4	18	1.25	0.19	7.79	6.07	5.03	3.86	2.96	1.95	1.18
347	40	6.00	0	4	18	1.25	0.19	7.56	6.17	5.32	4.21	3.32	2.24	1.31
348	60	6.00	0	4	18	1.25	0.19	8.12	6.62	5.68	4.54	3.52	2.33	1.31
349	80	6.00	0	4	18	1.25	0.19	7.86	6.32	5.41	4.30	3.39	2.25	1.30
350	3314	6.00	0	4	18	1.25	0.25	7.60	6.32	5.51	4.43	3.51	2.29	1.25
351	20	6.00	0	4	18	1.25	0.25	7.35	6.06	5.26	4.18	3.32	2.23	1.28
352	40	6.00	0	4	18	1.25	0.32	7.52	6.25	5.33	4.23	3.30	2.20	1.30
353	60	6.00	0	4	18	1.25	0.38	7.98	6.46	5.52	4.36	3.37	2.25	1.35
354	80	6.00	0	4	18	1.25	0.38	7.86	6.54	5.61	4.45	3.49	2.33	1.35
355	3313	6.00	0	4	18	1.25	0.19	9.11	7.26	6.15	4.78	3.73	2.45	1.43
356	20	6.00	0	4	18	1.25	0.19	9.51	7.31	6.17	4.78	3.70	2.41	1.45
357	40	6.00	0	4	18	1.25	0.19	7.98	6.51	5.60	4.41	3.45	2.31	1.37

Table B.1 Layer thicknesses and deflection data for the indicated test designation number (continued).

Line	Test Desig.	Thickness (inches)				ESAL	Rut	Sensor Deflection (mils)						
No.	Number	AC	Concrete	Base	S.Base	(mill)	(in.)	D1	D2	D3	D4	D5	D6	D7
358	60	6.00	0	4	18	1.25	0.19	8.54	7.01	6.01	4.72	3.65	2.34	1.31
359	80	6.00	0	4	18	1.25	0.19	7.98	6.74	5.68	4.41	3.33	2.11	1.20
360	3312	6.00	0	4	18	1.25	0.22	8.76	7.04	6.00	4.72	3.65	2.35	1.30
361	20	6.00	0	4	18	1.25	0.22	8.54	6.81	5.91	4.70	3.66	2.42	1.33
362	40	6.00	0	4	18	1.25	0.22	7.99	6.22	5.28	4.06	3.13	2.03	1.19
363	60	6.00	0	4	18	1.25	0.22	7.75	6.09	5.14	4.04	3.11	2.05	1.20
364	80	6.00	0	4	18	1.25	0.22	8.06	6.30	5.30	4.06	3.09	1.96	1.12
365	3311	6.00	0	4	18	1.25	0.22	8.33	6.85	5.61	4.41	3.36	2.09	1.15
366	20	6.00	0	4	18	1.25	0.22	8.17	6.50	5.63	4.43	3.45	2.29	1.30
367	40	6.00	0	4	18	1.25	0.22	8.70	6.75	5.62	4.30	3.32	2.17	1.26
368	60	6.00	0	4	18	1.25	0.22	8.22	6.55	5.66	4.49	3.54	2.34	1.34
369	80	6.00	0	4	18	1.25	0.22	8.40	6.77	5.78	4.65	3.68	2.48	1.51
370	3411	6.00	0	4	18	1.25	0.05	17.19	14.16	12.13	9.55	7.40	4.84	2.66
371	20	6.00	0	4	18	1.25	0.05	16.30	13.54	11.72	9.30	7.34	4.83	2.70
372	40	6.00	0	4	18	1.25	0.066	17.01	14.07	12.26	9.96	7.89	5.20	2.80
373	60	6.00	0	4	18	1.25	0.08	15.81	13.44	11.86	9.62	7.73	5.10	2.70
374	80	6.00	0	4	18	1.25	0.08	16.82	14.11	12.32	10.01	7.77	5.09	2.69
375	3412	5.00	0	7	3	0.43	0.05	17.64	14.49	12.40	9.76	7.54	4.93	2.70
376	20	5.00	0	7	3	0.43	0.05	18.21	14.93	12.63	9.84	7.63	4.92	2.78
377	40	5.00	0	7	3	0.43	0.035	17.02	14.17	12.24	9.78	7.73	5.05	2.80
378	60	5.00	0	7	3	0.43	0.02	17.84	15.39	13.46	10.71	7.49	4.74	2.74

Table B.1 Layer thicknesses and deflection data for the indicated test designation number (continued).

Line No.	Test Desig. Number	Thickness (inches) AC	Concrete	Base	S.Base	ESAL (mill)	Rut (in.)	Sensor Deflection (mils) D1	D2	D3	D4	D5	D6	D7
379	80	5.00	0	7	3	0.43	0.02	16.80	14.11	12.31	9.93	7.78	5.10	2.79
380	3413	5.00	0	7	3	0.43	0.02	16.67	14.02	12.31	9.85	7.81	5.18	2.83
381	20	5.00	0	7	3	0.43	0.02	16.05	13.38	11.60	9.31	7.27	4.79	2.67
382	40	5.00	0	7	3	0.43	0.02	16.71	13.82	12.01	9.50	7.41	4.82	2.72
383	60	5.00	0	7	3	0.43	0.02	18.59	14.85	12.49	9.75	7.53	4.91	2.79
384	80	5.00	0	7	3	0.43	0.02	19.49	15.47	13.09	10.07	7.76	5.04	2.88
385	3614	5.68	0	4	18	0.93	0.15	6.44	5.26	4.63	3.78	3.04	2.03	1.14
386	20	5.68	0	4	18	0.93	0.15	6.59	5.29	4.66	3.80	3.02	2.01	1.13
387	40	5.68	0	4	18	0.93	0.17	7.65	6.43	5.17	4.10	3.15	2.04	1.12
388	60	5.68	0	4	18	0.93	0.18	6.79	5.51	4.84	3.94	3.13	2.05	1.12
389	80	5.68	0	4	18	0.93	0.18	6.55	5.36	4.76	3.91	3.11	2.09	1.13
390	3613	5.68	0	4	18	0.93	0.18	7.81	6.05	5.22	4.18	3.27	2.12	1.16
391	20	5.68	0	4	18	0.93	0.18	6.93	5.66	4.99	4.06	3.22	2.18	1.18
392	40	5.68	0	4	18	0.93	0.2	7.36	5.81	5.06	4.14	3.33	2.20	1.21
393	60	5.68	0	4	18	0.93	0.22	8.94	6.79	5.79	4.70	3.68	2.43	1.31
394	80	5.68	0	4	18	0.93	0.22	7.56	6.12	5.36	4.37	3.49	2.33	1.27
395	3612	5.68	0	4	18	0.93	0.22	7.77	6.47	5.66	4.36	3.34	2.13	1.16
396	20	5.68	0	4	18	0.93	0.22	7.06	5.73	5.03	4.14	3.28	2.17	1.19
397	40	5.68	0	4	18	0.93	0.22	7.35	5.89	5.11	4.10	3.24	2.11	1.17
398	60	5.68	0	4	18	0.93	0.22	7.13	5.67	4.97	4.07	3.16	2.06	1.16
399	80	5.68	0	4	18	0.93	0.22	6.90	5.57	4.90	3.97	3.13	2.04	1.11

Table B.1 Layer thicknesses and deflection data for the indicated test designation number (continued).

Line	Test Desig.	Thickness (inches)				ESAL	Rut	Sensor Deflection (mils)						
No.	Number	AC	Concrete	Base	S.Base	(mill)	(in.)	D1	D2	D3	D4	D5	D6	D7
400	3611	5.68	0	4	18	0.93	0.22	6.71	5.43	4.78	3.89	3.08	2.04	1.12
401	20	5.68	0	4	18	0.93	0.22	7.08	5.65	4.99	4.08	3.23	2.12	1.15
402	40	5.68	0	4	18	0.93	0.2	7.07	5.81	5.20	4.31	3.46	2.32	1.25
403	60	5.68	0	4	18	0.93	0.18	7.98	6.45	5.74	4.74	3.83	2.61	1.45
404	80	5.68	0	4	18	0.93	0.18	7.24	5.76	5.07	4.16	3.26	2.14	1.17
405	3711	5.67	0	8	28	0.89	0.08	6.90	5.71	5.14	4.35	3.56	2.49	1.34
406	20	5.67	0	8	28	0.89	0.08	8.68	6.88	6.11	5.15	4.23	2.99	1.62
407	40	5.67	0	8	28	0.89	0.08	6.84	5.52	4.92	4.13	3.43	2.29	1.16
408	60	5.67	0	8	28	0.89	0.08	7.23	5.77	5.13	4.31	3.48	2.34	1.19
409	80	5.67	0	8	28	0.89	0.08	6.87	5.52	4.92	4.14	3.41	2.38	1.28
410	3712	5.67	0	8	28	0.89	0.1	7.47	6.19	5.55	4.68	3.71	2.46	1.23
411	20	5.67	0	8	28	0.89	0.1	7.95	6.56	5.71	4.75	3.74	2.33	1.23
412	40	5.67	0	8	28	0.89	0.1	6.60	5.32	4.76	3.97	3.23	2.23	1.22
413	60	5.67	0	8	28	0.89	0.1	7.17	5.94	5.35	4.52	3.68	2.49	1.19
414	80	5.67	0	8	28	0.89	0.1	6.36	5.18	4.66	3.92	3.16	2.21	1.26
415	3713	5.67	0	8	28	0.89	0.12	6.65	5.49	4.91	4.13	3.33	2.29	1.30
416	20	5.67	0	8	28	0.89	0.12	6.89	5.44	4.76	3.94	3.19	2.21	1.28
417	40	5.67	0	8	28	0.89	0.1	6.49	5.33	4.76	4.00	3.35	2.37	1.40
418	60	5.67	0	8	28	0.89	0.08	7.21	5.80	5.13	4.39	3.59	2.54	1.47
419	80	5.67	0	8	28	0.89	0.08	6.90	5.73	5.11	4.31	3.54	2.51	1.43
420	3811	7.25	0	10	0	0.30	0.08	5.65	4.63	4.00	3.24	2.54	1.65	0.90

Table B.1 Layer thicknesses and deflection data for the indicated test designation number (continued).

Line	Test Desig.	Thickness (inches)				ESAL	Rut	Sensor Deflection (mils)						
No.	Number	AC	Concrete	Base	S.Base	(mill)	(in.)	D1	D2	D3	D4	D5	D6	D7
421	20	7.25	0	10	0	0.30	0.06	5.80	4.72	4.06	3.21	2.54	1.66	0.91
422	40	7.25	0	10	0	0.30	0.06	5.51	4.53	3.92	3.12	2.49	1.61	0.87
423	60	7.25	0	10	0	0.30	0.06	5.76	4.60	4.01	3.19	2.54	1.66	0.88
424	80	7.25	0	10	0	0.30	0.06	5.82	4.62	4.05	3.19	2.55	1.64	0.88
425	3812	7.25	0	10	0	0.30	0.08	7.76	6.80	6.14	5.17	3.04	1.97	0.91
426	20	7.25	0	10	0	0.30	0.08	5.99	4.85	4.23	3.40	2.66	1.75	0.94
427	40	7.25	0	10	0	0.30	0.066	5.65	4.67	4.12	3.33	2.67	1.74	0.92
428	60	7.25	0	10	0	0.30	0.05	5.75	4.71	4.16	3.30	2.60	1.69	0.90
429	80	7.25	0	10	0	0.30	0.05	5.61	4.60	4.01	3.20	2.57	1.68	0.91
430	3813	7.25	0	10	0	0.30	0	5.64	4.67	4.07	3.28	2.59	1.68	0.90
431	20	7.25	0	10	0	0.30	0	5.61	4.71	4.13	3.33	2.61	1.68	0.89
432	40	7.25	0	10	0	0.30	0.025	5.32	4.54	4.01	3.29	2.61	1.70	0.90
433	60	7.25	0	10	0	0.30	0.05	5.67	4.63	4.08	3.30	2.63	1.73	0.92
434	80	7.25	0	10	0	0.30	0.05	5.85	4.78	4.18	3.34	2.61	1.71	0.91
435	3911	5.00	0	9	15	1.13	0.08	7.58	6.20	5.26	4.14	3.25	2.15	1.30
436	20	5.00	0	9	15	1.13	0.08	8.31	6.77	5.73	4.48	3.50	2.34	1.42
437	40	5.00	0	9	15	1.13	0.09	8.38	6.86	5.82	4.59	3.63	2.45	1.54
438	60	5.00	0	9	15	1.13	0.1	8.71	7.36	6.34	5.02	3.83	2.03	1.29
439	80	5.00	0	9	15	1.13	0.1	8.12	6.60	5.58	4.39	3.43	2.29	1.40
440	3912	5.00	0	9	15	1.13	0.1	7.81	6.34	5.34	4.18	3.22	2.12	1.30
441	20	5.00	0	9	15	1.13	0.1	7.54	6.23	5.29	4.13	3.23	2.10	1.25

Table B.1 Layer thicknesses and deflection data for the indicated test designation number (continued).

Line	Test Desig.	Thickness (inches)				ESAL	Rut	Sensor Deflection (mils)						
No.	Number	AC	Concrete	Base	S.Base	(mill)	(in.)	D1	D2	D3	D4	D5	D6	D7
442	40	5.00	0	9	15	1.13	0.1	7.18	5.81	4.83	3.74	2.84	1.80	1.10
443	60	5.00	0	9	15	1.13	0.1	7.17	5.84	4.90	3.86	3.00	2.00	1.24
444	80	5.00	0	9	15	1.13	0.1	7.46	6.03	5.03	3.91	3.07	2.01	1.24
445	3913	5.00	0	9	15	1.13	0.1	7.57	6.10	5.16	4.07	3.21	2.15	1.31
446	20	5.00	0	9	15	1.13	0.1	7.68	6.46	5.64	4.59	3.72	2.51	1.46
447	40	5.00	0	9	15	1.13	0.1	7.96	6.59	5.67	4.56	3.62	2.47	1.54
448	60	5.00	0	9	15	1.13	0.15	8.06	6.68	5.73	4.57	3.59	2.38	1.44
449	80	5.00	0	9	15	1.13	0.15	8.43	6.83	5.73	4.54	3.53	2.38	1.46
450	4011	7.92	0	8	3	1.67	0	5.77	4.31	3.59	2.78	2.15	1.41	0.86
451	20	7.92	0	8	3	1.67	0	5.52	4.15	3.45	2.69	2.06	1.37	0.83
452	40	7.92	0	8	3	1.67	0.025	5.40	4.10	3.41	2.65	2.03	1.33	0.84
453	60	7.92	0	8	3	1.67	0.05	5.50	4.10	3.37	2.58	1.98	1.29	0.81
454	80	7.92	0	8	3	1.67	0.05	5.67	4.29	3.51	2.69	2.05	1.30	0.79
455	4012	7.92	0	8	3	1.67	0.08	5.57	4.18	3.43	2.65	2.01	1.27	0.76
456	20	7.92	0	8	3	1.67	0.08	5.64	4.22	3.42	2.59	1.98	1.25	0.78
457	40	7.92	0	8	3	1.67	0.08	5.26	3.98	3.33	2.53	1.93	1.21	0.72
458	60	7.92	0	8	3	1.67	0.08	5.77	4.22	3.45	2.65	1.99	1.24	0.73
459	80	7.92	0	8	3	1.67	0.08	5.72	4.20	3.44	2.60	1.96	1.23	0.74
460	4013	7.92	0	8	3	1.67	0	5.78	4.26	3.50	2.67	2.03	1.29	0.76
461	20	7.92	0	8	3	1.67	0	5.68	4.26	3.47	2.64	2.00	1.27	0.76
462	40	7.92	0	8	3	1.67	0	6.03	4.42	3.58	2.68	2.00	1.26	0.77

Table B.1 Layer thicknesses and deflection data for the indicated test designation number (continued).

Line No.	Test Desig. Number	Thickness (inches) AC	Concrete	Base	S.Base	ESAL (mill)	Rut (in.)	Sensor Deflection (mils) D1	D2	D3	D4	D5	D6	D7
463	60	7.92	0	8	3	1.67	0	6.15	4.55	3.65	2.78	2.07	1.29	0.75
464	80	7.92	0	8	3	1.67	0	5.88	4.39	3.61	2.70	2.02	1.28	0.75
465	4111	7.92	0	8	3	1.70	0.08	6.75	4.87	3.87	2.76	1.99	1.15	0.58
466	20	7.92	0	8	3	1.70	0.08	6.55	4.66	3.77	2.67	1.92	1.14	0.58
467	40	7.92	0	8	3	1.70	0.05	6.37	4.77	3.87	2.83	2.04	1.19	0.61
468	60	7.92	0	8	3	1.70	0.02	6.32	4.71	3.82	2.77	2.00	1.15	0.57
469	80	7.92	0	8	3	1.70	0.02	6.70	4.94	3.96	2.81	2.02	1.16	0.56
470	4112	7.92	0	8	3	1.70	0.05	6.64	4.83	3.84	2.76	1.95	1.12	0.57
471	20	7.92	0	8	3	1.70	0.05	6.88	4.90	3.86	2.78	2.00	1.18	0.60
472	40	7.92	0	8	3	1.70	0.035	6.83	4.92	3.92	2.81	2.04	1.23	0.64
473	60	7.92	0	8	3	1.70	0.02	6.81	4.96	4.05	2.94	2.16	1.29	0.70
474	80	7.92	0	8	3	1.70	0.02	6.80	4.94	3.98	2.86	2.07	1.23	0.64
475	4113	7.92	0	8	3	1.70	0.05	7.03	5.19	4.16	3.01	2.21	1.34	0.71
476	20	7.92	0	8	3	1.70	0.05	6.84	5.18	4.24	3.15	2.34	1.41	0.75
477	40	7.92	0	8	3	1.70	0.05	7.34	5.40	4.32	3.17	2.34	1.44	0.77
478	60	7.92	0	8	3	1.70	0.05	7.28	5.47	4.41	3.22	2.38	1.48	0.80
479	80	7.92	0	8	3	1.70	0.05	8.04	5.91	4.70	3.44	2.58	1.66	0.91
480	4211	10.00	0	4	29	8.48	0.12	6.24	4.36	3.75	3.16	2.63	1.93	1.19
481	20	10.00	0	4	29	8.48	0.12	5.81	4.26	3.84	3.41	2.83	2.12	1.24
482	40	10.00	0	4	29	8.48	0.155	7.21	5.07	4.32	3.68	2.96	2.11	1.20
483	60	10.00	0	4	29	8.48	0.19	8.26	5.34	4.23	3.47	2.83	2.02	1.20

Table B.1 Layer thicknesses and deflection data for the indicated test designation number (continued).

Line No.	Test Desig. Number	Thickness (inches)				ESAL (mill)	Rut (in.)	Sensor Deflection (mils)						
		AC	Concrete	Base	S.Base			D1	D2	D3	D4	D5	D6	D7
484	80	10.00	0	4	29	8.48	0.19	9.11	5.86	4.54	3.68	3.00	2.12	1.28
485	4212	10.00	0	4	29	8.48	0.12	8.75	5.72	4.44	3.68	2.97	2.09	1.23
486	20	10.00	0	4	29	8.48	0.12	8.39	5.44	4.24	3.54	2.87	2.11	1.22
487	40	10.00	0	4	29	8.48	0.156	7.63	5.39	4.41	3.61	2.95	2.06	1.22
488	60	10.00	0	4	29	8.48	0.19	6.24	4.67	4.08	3.46	2.86	2.06	1.24
489	80	10.00	0	4	29	8.48	0.19	6.83	4.77	4.04	3.32	2.74	2.00	1.23
490	4213	10.00	0	4	29	8.48	0.12	6.83	4.76	4.06	3.42	2.83	2.07	1.27
491	20	10.00	0	4	29	8.48	0.12	6.31	4.70	4.02	3.38	2.81	2.02	1.19
492	40	10.00	0	4	29	8.48	0.156	6.45	4.67	3.87	3.28	2.63	1.90	1.12
493	60	10.00	0	4	29	8.48	0.19	6.51	4.48	3.78	3.18	2.61	1.84	1.10
494	80	10.00	0	4	29	8.48	0.19	7.17	5.47	4.62	3.88	3.25	2.30	1.33
495	4611	7.25	0	10	0	0.27	0.12	8.23	6.72	5.82	4.59	3.58	2.45	1.49
496	20	7.25	0	10	0	0.27	0.12	8.31	6.57	5.62	4.29	3.41	2.27	1.39
497	40	7.25	0	10	0	0.27	0.11	8.26	6.40	5.51	4.25	3.31	2.12	1.25
498	60	7.25	0	10	0	0.27	0.1	7.29	5.84	5.15	4.12	3.25	2.21	1.27
499	80	7.25	0	10	0	0.27	0.1	6.47	5.31	4.77	3.85	3.03	2.05	1.22
500	4612	7.25	0	10	0	0.27	0.1	9.42	8.02	7.04	5.22	3.80	2.34	1.25
501	20	7.25	0	10	0	0.27	0.1	5.67	4.72	4.13	3.24	2.60	1.81	1.60
502	40	7.25	0	10	0	0.27	0.1	6.38	4.90	4.18	3.13	2.47	1.68	1.04
503	60	7.25	0	10	0	0.27	0.1	6.22	4.96	4.28	3.39	2.64	1.76	1.04
504	80	7.25	0	10	0	0.27	0.1	6.20	4.89	4.27	3.31	2.60	1.73	1.01

Table B.1 Layer thicknesses and deflection data for the indicated test designation number (continued).

Line No.	Test Desig. Number	Thickness (inches) AC	Concrete	Base	S.Base	ESAL (mill)	Rut (in.)	Sensor Deflection (mils) D1	D2	D3	D4	D5	D6	D7
505	4613	7.25	0	10	0	0.27	0.12	6.27	4.76	4.21	3.35	2.61	1.76	1.04
506	20	7.25	0	10	0	0.27	0.12	6.67	4.80	4.21	3.36	2.65	1.80	1.07
507	40	7.25	0	10	0	0.27	0.1	6.05	4.84	4.33	3.49	2.77	1.86	1.07
508	60	7.25	0	10	0	0.27	0.08	7.10	5.40	4.63	3.66	2.69	1.91	1.09
509	80	7.25	0	10	0	0.27	0.08	7.34	5.90	5.11	4.13	3.18	2.05	1.16
510	4711	2.25	0	10	15	0.40	0.12	9.88	7.08	5.30	3.55	2.57	1.60	0.92
511	20	2.25	0	10	15	0.40	0.12	9.55	7.00	5.42	3.72	2.74	1.72	0.93
512	40	2.25	0	10	15	0.40	0.12	10.41	7.66	5.98	4.21	3.18	1.98	1.04
513	60	2.25	0	10	15	0.40	0.12	11.04	8.11	6.23	4.48	3.31	2.05	1.08
514	80	2.25	0	10	15	0.40	0.12	11.10	8.12	6.27	4.49	3.30	2.07	1.09
515	4712	2.25	0	10	15	0.40	0.06	10.88	8.00	6.03	4.22	3.14	1.97	1.06
516	20	2.25	0	10	15	0.40	0.06	10.95	8.00	5.91	4.13	3.05	1.91	1.01
517	40	2.25	0	10	15	0.40	0.09	11.72	8.53	6.40	4.44	3.28	1.99	1.04
518	60	2.25	0	10	15	0.40	0.12	11.34	8.32	6.37	4.41	3.24	1.97	1.04
519	80	2.25	0	10	15	0.40	0.12	11.26	8.10	6.06	4.22	3.09	1.92	1.05
520	4713	2.25	0	10	15	0.40	0.19	11.74	8.50	6.54	4.65	3.49	2.23	1.22
521	20	2.25	0	10	15	0.40	0.19	11.53	8.35	6.37	4.47	3.33	2.12	1.16
522	40	2.25	0	10	15	0.40	0.19	11.53	8.22	6.07	4.23	3.13	2.03	1.13
523	60	2.25	0	10	15	0.40	0.19	11.31	8.01	6.06	4.17	3.14	2.03	1.13
524	80	2.25	0	10	15	0.40	0.19	11.74	8.51	6.36	4.54	3.35	2.12	1.16
525	4714	2.25	0	10	15	0.40	0.19	12.00	8.73	6.63	4.63	3.42	2.14	1.14

Table B.1 Layer thicknesses and deflection data for the indicated test designation number (continued).

Line	Test Desig.	Thickness (inches)				ESAL	Rut	Sensor Deflection (mils)						
No.	Number	AC	Concrete	Base	S.Base	(mill)	(in.)	D1	D2	D3	D4	D5	D6	D7
526	20	2.25	0	10	15	0.40	0.19	12.59	9.15	6.77	4.77	3.55	2.25	1.18
527	40	2.25	0	10	15	0.40	0.156	12.85	9.43	7.05	4.86	3.61	2.24	1.14
528	60	2.25	0	10	15	0.40	0.12	12.42	9.01	6.70	4.78	3.51	2.17	1.08
529	80	2.25	0	10	15	0.40	0.12	12.28	8.93	6.63	4.78	3.56	2.21	1.08
530	4715	2.25	0	10	15	0.40	0.19	12.59	9.02	6.77	4.67	3.45	2.11	1.09
531	20	2.25	0	10	15	0.40	0.19	12.34	8.99	6.78	4.71	3.47	2.14	1.10
532	40	2.25	0	10	15	0.40	0.19	12.18	8.85	6.58	4.67	3.47	2.14	1.09
533	60	2.25	0	10	15	0.40	0.19	12.24	8.83	6.56	4.64	3.47	2.17	1.09
534	80	2.25	0	10	15	0.40	0.19	12.57	9.51	6.86	4.83	3.58	2.23	1.10
535	1021	2.75	8	0	6	0.62	0.06	4.60	3.59	3.65	3.26	2.79	2.31	1.46
536	20	2.75	8	0	6	0.62	0.06	4.34	3.51	3.47	3.25	2.89	2.36	1.52
537	40	2.75	8	0	6	0.62	0.06	6.41	4.33	3.64	3.07	2.70	2.23	1.48
538	60	2.75	8	0	6	0.62	0.12	5.08	4.01	3.88	3.32	2.94	2.40	1.62
539	80	2.75	8	0	6	0.62	0.12	6.04	5.52	5.11	4.23	3.40	2.57	1.77
540	1022	2.75	8	0	6	0.62	0.06	4.77	3.90	3.81	3.66	3.23	2.66	1.72
541	20	2.75	8	0	6	0.62	0.06	4.58	3.68	3.64	3.43	3.04	2.44	1.54
542	40	2.75	8	0	6	0.62	0.09	5.24	4.07	3.96	3.69	3.24	2.58	1.59
543	60	2.75	8	0	6	0.62	0.12	5.80	4.38	4.28	4.09	3.66	2.92	1.75
544	80	2.75	8	0	6	0.62	0.12	5.94	4.39	4.26	4.06	3.58	2.84	1.65
545	1023	2.75	8	0	6	0.62	0.12	11.25	9.64	7.03	4.53	3.38	2.43	1.27
546	20	2.75	8	0	6	0.62	0.12	5.59	4.18	4.10	3.82	2.88	2.24	1.14

Table B.1 Layer thicknesses and deflection data for the indicated test designation number (continued).

Line	Test Desig.	Thickness (inches)				ESAL	Rut	Sensor Deflection (mils)						
No.	Number	AC	Concrete	Base	S.Base	(mill)	(in.)	D1	D2	D3	D4	D5	D6	D7
547	40	2.75	8	0	6	0.62	0.09	5.73	4.16	3.91	3.66	3.08	2.32	1.21
548	60	2.75	8	0	6	0.62	0.06	6.07	4.36	4.13	3.67	3.26	2.63	1.55
549	80	2.75	8	0	6	0.62	0.06	6.52	4.79	4.21	4.00	3.56	2.90	1.76
550	1221	3.00	9	0	6	0.22	0.06	9.76	7.65	7.63	7.46	6.74	5.71	3.59
551	20	3.00	9	0	6	0.22	0.06	8.89	7.05	7.01	6.80	6.16	5.27	3.32
552	40	3.00	9	0	6	0.22	0.045	15.05	13.34	13.17	12.36	11.11	9.14	5.35
553	60	3.00	9	0	6	0.22	0.03	9.16	7.73	7.68	7.27	6.57	5.42	3.23
554	80	3.00	9	0	6	0.22	0.03	9.46	8.51	8.55	8.48	8.10	7.46	5.72
555	1222	3.00	9	0	6	0.22	0.06	11.18	9.85	9.81	9.32	8.34	6.97	4.12
556	20	3.00	9	0	6	0.22	0.06	8.89	7.52	7.36	7.08	6.35	5.24	3.17
557	40	3.00	9	0	6	0.22	0.06	7.99	6.80	6.60	6.37	5.84	5.06	3.34
558	60	3.00	9	0	6	0.22	0.06	8.33	7.55	7.28	6.91	6.24	5.27	3.36
559	80	3.00	9	0	6	0.22	0.06	8.32	7.55	7.39	7.04	6.43	5.47	3.55
560	1223	3.00	9	0	6	0.22	0.03	8.32	7.51	7.29	6.90	6.28	5.34	3.47
561	20	3.00	9	0	6	0.22	0.03	9.52	8.56	8.24	7.85	7.11	5.92	3.64
562	40	3.00	9	0	6	0.22	0.03	10.09	9.53	9.36	8.99	8.14	6.85	4.00
563	60	3.00	9	0	6	0.22	0.03	8.22	7.72	7.23	6.65	5.94	4.82	2.82